Topics in Safety, Risk, Reliability and Quality

Michael Ochs
Dirk Mallants
Lian Wang

Radionuclide and Metal Sorption on Cement and Concrete

Springer

Topics in Safety, Risk, Reliability and Quality

Volume 29

Series editor

Adrian V. Gheorghe, Old Dominion University, Norfolk, VA, USA

Editorial Advisory Board

Hirokazu Tatano, Kyoto University, Kyoto, Japan
Enrico Zio, Ecole Centrale Paris, France and Politecnico di Milano, Milan, Italy
Andres Sousa-Poza, Old Dominion University, Norfolk, VA, USA

More information about this series at http://www.springer.com/series/6653

Michael Ochs · Dirk Mallants · Lian Wang

Radionuclide and Metal Sorption on Cement and Concrete

Springer

Michael Ochs
BMG Engineering Ltd
Schlieren
Switzerland

Dirk Mallants
CSIRO Land and Water
Adelaide, SA
Australia

Lian Wang
Waste and Disposal Unit
Belgian Nuclear Research Centre
SCK•CEN
Mol
Belgium

ISSN 1566-0443 ISSN 2215-0285 (electronic)
Topics in Safety, Risk, Reliability and Quality
ISBN 978-3-319-23650-6 ISBN 978-3-319-23651-3 (eBook)
DOI 10.1007/978-3-319-23651-3

Library of Congress Control Number: 2015948731

Springer Cham Heidelberg New York Dordrecht London
© Springer International Publishing Switzerland 2016
This work is subject to copyright. All rights are reserved by the Publisher, whether the whole or part of the material is concerned, specifically the rights of translation, reprinting, reuse of illustrations, recitation, broadcasting, reproduction on microfilms or in any other physical way, and transmission or information storage and retrieval, electronic adaptation, computer software, or by similar or dissimilar methodology now known or hereafter developed.
The use of general descriptive names, registered names, trademarks, service marks, etc. in this publication does not imply, even in the absence of a specific statement, that such names are exempt from the relevant protective laws and regulations and therefore free for general use.
The publisher, the authors and the editors are safe to assume that the advice and information in this book are believed to be true and accurate at the date of publication. Neither the publisher nor the authors or the editors give a warranty, express or implied, with respect to the material contained herein or for any errors or omissions that may have been made.

Printed on acid-free paper

Springer International Publishing AG Switzerland is part of Springer Science+Business Media (www.springer.com)

Preface

This book presents a full state-of-the-art review and critical evaluation of the type and magnitude of the various sorption and incorporation processes in hydrated cement systems that are responsible for the retention properties of cementitious materials towards radionuclides and metals from a variety of radioactive and industrial wastes.

The book is triggered by and based on two reports commissioned by the Belgian Agency for Radioactive Waste and Enriched Fissile Materials ONDRAF/NIRAS, which are both authored or co-authored by the authors of this book. While these reports were ultimately aimed at providing key sorption values for the safety analysis of a planned repository for short-lived low- and medium-level radioactive waste, it is emphasised throughout both the original reports and the present book that selected sorption values should be underpinned, to the greatest extent possible, by scientific arguments and process understanding. Accordingly, an international panel of experts, including the authors of this book, had been involved in a peer review process of data evaluation, selection of recommended values, and development of the scientific state of the art.

There are a number of people to be greatly acknowledged for their important role in providing critical data, argumentation, and advice regarding completion of this book. Chiefly among them are Robert Gens and Wim Cool representing ONDRAF/NIRAS, for initiating the entire project and providing guidance as well as funding, the further members of the expert panel (John Berry, Virginie Blin, Pierre de Cannière, Christoph Gallé, Fred Glasser, Eric Giffaut, Alan Hooper, Diederik Jacques, David Lever, Evelien Martens, Bernhard Schwyn, Ludovic Vielle-Petit, Erich Wieland, Steve Williams) for their contributions in developing the presented material, and Cynthia Feenstra from Springer for her support in questions of publication.

Schlieren, Switzerland — Michael Ochs
Adelaide, Australia — Dirk Mallants
Mol, Belgium — Lian Wang
July 2015

Contents

Acronyms

ACW	Artificial cement water
AES	Altered evolution scenario
ALB	High alumina cement
BFS	Blast furnace slag
BP	Belgoprocess
BZM	Selected concrete admixtures
CASH	Calcium aluminium silicate hydrate
CEC	Cation exchange capacity
CEM I	Portland cement type I
CEM V	Portland cement type V
CILVA	Centrale Infrastructuur voor Laagactief Vast Afval
CNT	Tihange nuclear power plant
CSH	Calcium silicate hydrate
DOPC	Degraded ordinary Portland cement
DVB	Divinylbenzene
EC	Evence-Coppée oven
EXAFS	Extended X-ray absorption fine structure
FAB	Fly ash cement
FCPW	Fresh cement pore water
FPB	Standard Portland cement French mixture
HCP	Hardened cement paste
HIS	Human intrusion scenario
HSR	High sulphate resistant
HTO	Tritiated water
HTS	Haute Teneur en Silice
ISA	Isosaccarinic acid
KCD	Doel nuclear power plant
LDH	Layered double hydroxides
LILW-SL	Low and intermediate level waste—short lived
LS	Ligno-sulphonate

MB	Blast furnace slag cement
MS	Melamine sulphonate
MWCO	Molecular weight cut-off
NPP	Nuclear power plant
NRVB	Nirex reference vault backfill
NS	Napthalene sulphonate
OPC	Ordinary Portland cement
PB	65-years-old concrete
PFA	Pulverised fuel ash
PWR	Pressurized water reactor
SA	Safety assessment
SCM	Surface complexation model
SG	Sodium gluconate
SIB	Silica cement
SMF	Sulphonated melamine formaldehyde
SNF	Sulphonated naphtalene formaldehyde
SPB	Standard Portland cement
SRB	Sulphate resistant cement
SRPC	Sulphate resisting Portland cement
TB	74-years-old concrete
TSM	Thermodynamic sorption models
WPC	White Portland cement
XAFS	X-ray absorption fine-structure spectroscopy

Symbols

$A_{l,m}$	Minimum measurable activity (Bq)
A_m	Sorption capacity Langmuir constant (M/M)
A_{susp}	Total initial activity in the suspension (Bq)
C_{con}	Total concentration in a unit volume of concrete (M/L^3)
C_{eq}	Equilibrium concentration in solution (M/L^3)
C_l	Liquid phase concentration (M/L^3)
C_s	Adsorbed concentration (M/M)
C_s^0	Stable element in cement (mol/M)
D	Hydrodynamic dispersion coefficient (L^2/T)
D_o	Diffusion coefficient in free water (L^2/T)
D_p	Pore water diffusion constant of the porous medium (L^2/T)
F	Fraction of cellulose converted to ISA (–)
f	Fugacity (–)
f_{Fe}	Fraction of iron in carbon steel (–)
I	Mass of organic material (M)
K	Thermodynamic mass action constant (–)
K_d	Distribution coefficient (L^3/M)
K_F	Freundlich constant (L^{3n}/M^n)
K_L	Langmuir sorption constant (L^3/M)
M	Mass (M)
M_X	Molar mass of chemical species X (M/mol)
m	Mass of (crushed) sorbing solid (M)
m_{sf}	Stoichiometric factor (mol/mol)
n	Freundlich constant (–)
P	Partial gas pressure (atm)
q	Water flux (L/T)
R	Retardation factor (–)
R_C	Corrosion rate (L/T)
R_d	Distribution ratio (L^3/M)
$R_{d,max}$	Maximum distribution ratio (L^3/M)

$R_{d,min}$	Minimum distribution ratio (L^3/M)
$R_{d,M}$	Distribution ratio of non-radioactive element (L^3/M)
$R_{d,M*}$	Distribution ratio of radioactive element (L^3/M)
$R_{d,max}$	Maximum distribution ratio (L^3/M)
S	Reactive surface (L^2)
S	Solubility of element (mol/L^3)
t	Time (T)
$T_{1/2}$	Radionuclide half-life (T)
v	Pore water velocity (L/T)
V	Volume of solution (L^3)
V_p	Volume of porous material (L^3)
x	Distance (L)
Z	Amount of cement (M/L^3)
α_L	Longitudinal dispersivity (L)
α	Accessibility factor for isotopic exchange (–)
αp	Partition coefficient for isotopic exchange (–)
Φ	Grain diameter for aggregates (L)
η	Porosity (L^3/L^3)
η_D	Diffusion accessible porosity (L^3/L^3)
η_e	Effective porosity (L^3/L^3)
μ	First order decay coefficient (T^{-1})
ρ	Density (M/L^3)
ρ_b	Dry bulk density (M/L^3)
θ	Water content (L^3/L^3)
τ	Tortuosity (–)

List of Figures

List of Tables

Chapter 1
Introduction and Objective

Abstract Cementitious materials are being widely used as solidification/stabilisation and barrier materials for a variety of chemical and radioactive wastes, due to their favourable retention properties for metals and other inorganic contaminants. These result from mineral phases in hydrated cement that (i) possess a high density of sites for the fixation of contaminants through a variety of sorption and incorporation reactions and that (ii) buffer pH in the range 10–13, depending on composition, which tends to limit the solubility of many metal ions. The present book represents a state-of-the-art review and evaluation of the type and magnitude of the various sorption and incorporation processes in hydrated cement systems for twenty-five elements. It is aimed at describing the interaction of dissolved constituents with hydrated cementitious materials (i.e. already set or hardened). While the immobilisation of contaminants by mixing with dry cement clinker before hydration is not explicitly addressed, many underlying processes will be similar. On the basis of a consistent review and re-evaluation of the literature data, we established a quantitative database on the solid/liquid distribution behaviour ("sorption database") for radionuclides and other elements in hydrated cement systems. This database is closely tied to the safety analysis of the near-surface disposal of radioactive waste in Belgium, which is reflected in the focus on radioelements. However, the book addresses also a number of stable elements and heavy metals, which makes it relevant for the interaction of conventional contaminants with cement-based barriers.

Cementitious materials have been widely used as solidification/stabilisation (s/s) agents for industrial and civil wastes (Chen et al. 2008; Glasser 1993), as well as for radioactive waste (Glasser 1989, 2006; Atkins and Glasser 1992). It is generally accepted that the retention potential of cementitious materials for many contaminants is very high due to the high sorption or uptake capacity of these materials. This is linked to the presence of several minerals in hydrated cement possessing a high density of sorption sites for both cations and anions, especially in the pH range 10–13 (Glasser 1993). In addition to surface sorption, hydrated cement minerals can immobilise many contaminants through incorporation

© Springer International Publishing Switzerland 2016

M. Ochs et al., *Radionuclide and Metal Sorption on Cement and Concrete*,
Topics in Safety, Risk, Reliability and Quality 29,
DOI 10.1007/978-3-319-23651-3_1

reactions and the formation of solid solutions. In addition, under the alkaline conditions characteristic for cement systems, many contaminants become much less soluble than under the less alkaline pH values of typical near-surface or geological environments.

The present book represents a state-of-the-art review and evaluation of the type and magnitude of the various sorption processes in hydrated cement systems for twenty-five elements. It is thus aimed at describing the interaction of dissolved constituents with cementitious materials that are already hydrated (set or hardened). While many underlying processes may be similar, the immobilisation of contaminants by mixing with dry cement clinker before hydration is not the subject of this book.

On the basis of a consistent review and re-evaluation of the literature data, we established a sorption database for radionuclides and some environmentally relevant elements. Such a database and the scientific underpinning of its derived sorption values will be of use to support the safe disposal of radioactive waste and other cemented industrial wastes. Specifically, this book is based on several reports developed by the Belgian agency for radioactive waste and enriched fissile materials ONDRAF/NIRAS and its partner technical support organisations, more in particular the Belgian Nuclear Research Centre SCK•CEN. The sorption database forms an integral part of the documentation that supports the safety analysis of the near-surface disposal of low- and intermediate-level radioactive waste at Dessel, Belgium.

This is reflected in the selection of elements treated in this book, with a focus on radioelements. However, the book addresses also a number of stable elements and heavy metals, which makes it also relevant for many types of conventional waste in landfills or for cement-based barriers used at contaminated sites.

While well-accepted compilations and databases of sorption values for cementitious materials have been prepared in the context of radioactive waste disposal (such as Wieland and van Loon 2002; Andra 2005), it was felt that a new data compilation and derivation of recommended values is needed, for the following reasons:

- The majority of the existing databases deal with situations typical for deep geological disposal of radioactive waste where redox conditions are likely to be reducing, while conditions are expected to be oxidising in case of near-surface disposal. Similarly, slow groundwater flow in a deep-disposal situation normally leads to an extremely low rate of cement degradation. Because of this, most existing databases consider sorption for intact or slightly degraded cement. For near-surface disposal, cement degradation would proceed much faster; therefore, sorption in highly degraded cementitious materials would also be relevant in the long term.
- Significant progress in the understanding of sorption in cementitious systems has been made in recent years, and it is necessary to include these state-of-the-art data and information in the current database.

- Distinct from the majority of existing databases, an international panel of experts has been involved in the process of data review, selection of recommended values, and development of scientific arguments supporting the selections.

The treatment of the various elements in this book is organised into separate, dedicated chapters. For each element, relevant background information is provided, followed by a discussion of the expected chemical form, speciation, and solubility. Each chapter then presents a detailed literature survey and review of experimental observations relevant for evaluating sorption processes, pertaining to fresh and degraded cementitious material. Finally, the likely sorption processes are identified, and key sorption values (distribution coefficients) for fresh and degraded cementitious material are recommended. Beforehand, an overview of hydrated cementitious materials and related degradation processes is presented.

For some elements, supplemental key sorption values are presented, which are based on chemical analogies with other elements or similar approximations. This was done mainly in cases where no or only very few recommended values could be given for an element, due to a limited experimental database. However, supplemental values were not systematically derived for all elements where, e.g., only an upper limit value is missing.

References

Andra, Référentiel de comportement des radionucléides et des toxiques chimiques d'un stockage dans le Callovo-Oxfordien jusqu'à l'homme, Site de Meuse/Haute-Marne, Tome 1/2: Chapitres 1 à 4, Dossier 2005 Argile, 2005

M. Atkins, F.P. Glasser, Application of portland cement-based materials to radioactive waste immobilization. Waste Manag **12**, 105–131 (1992)

Q.Y. Chen, M. Tyrer, C.D. Hills, X.M. Yang and P. Carey, Immobilisation of heavy metal in cement-based solidification/stabilisation: a review. Waste Manag. (2008). doi:10.1016/j.wasman.2008.01.019

F.P. Glasser, Immobilization of radwaste in cement based matrices, DoE/RW/89.133 (Aberdeen University, Scotland, 1989)

F.P. Glasser, Chemistry of cement-solidified waste forms, in *Chemistry and Microstructure of Solidified Waste Forms*, ed. by R.D. Spence (Lewis Publishers, New York, 1993)

F.P. Glasser, *Cement conditioning of nuclear wastes—where do we go?* (DoE Workshop, Savannah River, 2006)

E. Wieland, L. Van Loon, Cementitious near-field sorption data base for performance assessment of an ILW repository in Opalinus Clay, PSI Bericht Nr. 03–06 (2002)

Chapter 2
Cementitious Materials and Their Sorption Properties

Abstract The cementitious materials considered here include hydrated cement grout, concrete, and mortar. These materials may be used for waste conditioning, as waste container, and for backfilling. Dry cement (clinker) is a hydraulic binder; concrete is a mixture of hydrated cement, water, and coarse and fine aggregates; mortar and grout are a mixture of water, hydrated cement, and fine aggregates. Clinker is a mixture of several anhydrous minerals, mainly calcium silicates. Ordinary Portland cement (OPC) consists of finely ground clinker plus a small amount of gypsum. Hydration results in the formation of portlandite $Ca(OH)_2$, largely amorphous calcium silicate hydrates (CSHs), and minor crystalline phases containing aluminium, iron, and sulphate (e.g. ettringite, monosulphate, hydrogarnet, and hydrotalcite). Solutions in equilibrium with fresh hydrated cement are hyperalkaline (pH $\geq$ 13.2) with correspondingly high Na- and K-concentrations. It follows that hydrated cement systems are not in equilibrium with infiltrating water, which leads to dissolution and re-precipitation reactions. It is well established that the degradation of hydrated cement follows a pattern of several different, more or less distinct states, characterised by progressively lower pore water pH and Ca/Si ratio. Hydrated cement solid phases provide a variety of potential sites for different uptake reactions for dissolved elements, ranging from surface adsorption to incorporation and solid-solution formation (these processes are termed sorption henceforth). At low sorbate concentration (below the respective solubility limit), use of a single distribution coefficient for quantifying uptake under a defined set of conditions (e.g. a specific degradation state) is a defensible approach.

2.1 Cementitious Materials

The cementitious materials considered here include hydrated cement grout, concrete, and mortar. These materials may be used for conditioning the waste, as waste container and for backfilling containers in the repository. Cement is a hydraulic binder and can bind other materials together through hydration reaction

© Springer International Publishing Switzerland 2016

M. Ochs et al., *Radionuclide and Metal Sorption on Cement and Concrete*,
Topics in Safety, Risk, Reliability and Quality 29,
DOI 10.1007/978-3-319-23651-3_2

with water (see below). Concrete is a mixture of hydrated cement, water, and coarse and fine aggregates. Mortar is a mixture of water, hydrated cement, and fine aggregates. There are excellent textbooks on the chemistry of hydrated cement and concrete (e.g. Taylor 1997); the respective background information is therefore only briefly summarised below.

2.2 Cement

Cement itself is a mixture of several anhydrous minerals, mainly calcium silicates, which form in the reaction of calcium carbonate with silica-bearing minerals. Cement is normally produced by heating limestone with clay to about 1450 °C in a kiln. The resulting hard cement clinker is then ground with a small amount of gypsum into a powder to make ordinary Portland cement (OPC), the most common cement type. Portland cements normally comprise four main components: 50–70 % alite, 20–30 % belite, 5–12 % aluminates, 5–12 % ferrite, and small amounts (~2 %) of the added gypsum (Chen et al. 2008; Taylor 1997).

- Alite is tricalcium silicate, C_3S (where C = CaO and S = SiO_2) or Ca_3SiO_5, which reacts with water to form calcium silicate hydrate (CSH) gel and portlandite ($Ca(OH)_2$). Alite is considered to be the most significant constituent phase with respect to strength development at the early stage of cement hydration up to 28 days.
- Belite is dicalcium silicate, C_2S or β-Ca_2SiO_4. Belite reacts with water to produce also CSH and portlandite but at a slower rate. The strength development by belite hydration is only fully attained after about 1 year.
- Aluminate in unhydrated cement is present partly as ferrite and tricalcium aluminate C_3A (where A = Al_2O_3) or $Ca_3Al_2O_6$. C_3A reacts with water in the presence of sufficient amount of gypsum to yield AFt (calcium aluminosulphate, F = Fe_2O_3), e.g., ettringite or AFm (calcium monosulphoaluminate) if the availability of gypsum is limited.
- Ferrite is a calcium aluminoferrite, $C_2(F,A)_5$ with high substitution of Fe for Al; it reacts with water in a similar way as aluminate C_3A.
- Finally, gypsum is added to slow the setting time and permit a period of workability. A too rapid setting is caused by an immediate hydration of aluminates and because of that, the subsequent strength development of cement becomes poor.

To produce concrete or mortar, the cement clinker is mixed with the appropriate amount of water and aggregate material (Taylor 1997). Aggregate material typically consists of sand (quartz) and gravel form silicate or calcareous rocks. In the present case (near-surface disposal of low- and intermediate-level radioactive wastes at Dessel, Belgium), it is specified that all aggregate material consists of calcite grains.

2.3 Cement Hydration

Upon interacting with water, the anhydrous cement clinker undergoes hydration reactions and develops binding properties and strength. Hydration results in the formation of portlandite $Ca(OH)_2$, CSHs, and other minor phases containing aluminium, iron, and sulphate:

- calcium hydroxide $Ca(OH)_2$, or portlandite;
- amorphous (or microcrystalline) CSH phases with an initial Ca to Si molar ratio (C/S) at around 1.8 (this ratio will decrease as cement degrades);
- AFt phases (aluminoferrite trisulphate)—a group of calcium sulphoaluminate hydrates, such as ettringite with $[Ca_3(Al,Fe)(OH)_6{\cdot}12H_2O]X_3{\cdot}H_2O$ as general formula, where X denotes a double-charged anion (typically sulphate) or two units of a single-charged anion; and AFm phases (aluminoferrite monosulphate)—with $[Ca_2(Al,Fe)(OH)_6]X{\cdot}H_2O$ as general formula;
- Hydrogarnet $(3CaO{\cdot}Al_2O_3{\cdot}6H_2O)$; and
- Hydrotalcite, a layered double hydroxide of the general formula $(Mg_6Al_2(CO_3)(OH)_{16}{\cdot}4(H_2O)$.

2.4 Sorbing Minerals in Cementitious Materials

The concrete to be used for the ONDRAF/NIRAS disposal facility in the municipality of Dessel is mainly a mixture of Portland cement (slag-free for CEM I and slag-containing for CEM III), and calcareous aggregates of different grain sizes (Tables 2.1 and 2.2). Solid phases in the concrete therefore comprise hydrated cement solids and calcite aggregates. The major cement solid phases

Table 2.1 Concrete composition for the modules and the containers, Gens (2008). CEM I defined according to EN 197-1:2000 (2000)

Component	Content (kg/m^3)	Content (weight %)
CEM I 42.5 N LA HSR LH[a]	350	15
Calcitec™ 2001 MS (ground calcium carbonate)	50	2.1
Sand 0/4 (limestone)	708	30
Calcareous aggregates (2/6)	414	17.5
Calcareous aggregates (6/14)	191	8
Calcareous aggregates (6/20)	465	19.7
Water	175	7.4
Water/cement ratio	0.50	
Superplasticiser (Rheobuild™ 1100 conc. 30 %, NS type)	6.46	0.3

[a]*LA* low alkali, *HSR* High sulphate resisting, *LH* low heat (hydration). Values in () are size range in mm. *NS* napthalene sulphonate

Table 2.2 Proposed composition of backfilling mortar for use in containers, Gens (2008)

Component	Content (kg/m^3)	Content (weight %)
CEM III/C 32.5 LA HSR LH	510	23.3
Silica fume	52	2.4
Calcareous aggregates (0/4)	1392	63.7
Water	223	10.2
Water/cement ratio	0.437	
Superplasticiser (Rheobuild 1100 conc. 30 %, NS[b] type)	8.9 maximum[a]	0.406

[a]Could be adjusted downwards, depending on seasonal conditions
[b]Naphtalene sulphonate

are crystalline portlandite ($Ca(OH)_2$) and amorphous CSH. Minor phases include ettringite (aluminoferrite trisulphate, AFt), monosulphate (aluminoferrite monosulphate, AFm), hydrogarnet, and hydrotalcite. All these solids provide potential sorbing surfaces for dissolved radionuclides. CSH phases display non-specific sorption; that is, both cations and anions can be sorbed although the mechanism may not always be known. Examples for anion immobilisation onto hydrotalcite, AFm, and AFt phases may be obtained from Wieland and Van Loon (2002) Calcite, initially present as aggregates and/or generated as a newly formed phase owing to cement carbonation, may also sorb radionuclides (Zachara et al. 1991). Although co-precipitation of radionuclides with calcite has been considered in the literature as a particularly relevant sorption process (Curti 1997; Meece and Benninger 1993; Komarneni and Roy 1981), in this review clear distinction is to be made between true sorption and solubility control leading to precipitation. Therefore, data on precipitation and co-precipitation associated with calcite will not be considered as true sorption.

Different sorbing cement minerals have a characteristically high surface area (m^2/g solid); for example, hardened cement paste (HCP) has a surface area >50 m^2/g, portlandite had a surface area of ~6 m^2/g, while CSH phases were reported to have a surface area of 148 m^2/g (Tits et al. 2006a, b). Large surface area combined with high-sorption data (mol/g) results in high surface densities of sorption sites (mol/m^2 or sites/nm^2). Therefore, large masses of cement result in a large sorption capacity for radionuclides and other contaminants. Also, under such circumstances, use of a single K_d or R_d to represent sorption at low radionuclide concentration is a defensible approach. From a qualitative point of view, differences in sorption values for different cement or natural minerals such as calcite may be related to differences in surface area and nature (intrinsic charge) of the surface. From a more quantitative point of view, surface area information may also be used in calculating sorption values, for example by means of surface complexation models (Apello and Postma 2006) or ion exchange models (Tits et al. 2008).

Portlandite ($Ca(OH)_2$)

Portlandite is rarely studied as a sorbing solid. The hydroxyl functional groups on the surface of portlandite have potential to bind strongly sorbing metal ions, in addition to Ni, or sorb anions such as the halogens Cl^- and I^- through substitution with hydroxyl (Gougar et al. 1996). One of the few experimental studies identified in this review is that of Noshita et al. (2001) which demonstrated that portlandite does not sorb Cs and iodide to a significant extent, but it binds Ni as strongly as CSH phases. The observed Ni sorption was interpreted as being due to surface complexation and co-precipitation. Binding of anions and oxyanions is presumably weak, although it has been reported that some oxyanions may have some affinity to portlandite (Cornelis et al. 2008).

CSH Phases

The CSH phase refers to a CSH, as defined previously. CSH is nearly amorphous to X-ray diffraction and, on that account, is often referred to as "cement gel". Its low crystallinity suggests a structural resemblance to two crystalline CSH, tobermorite, and jennite. The structures of both are known—they occur in nature and can be made synthetically—and consist of corrugated sheets or layers of alternating (Ca–OH) and silicate units. In tobermorite, the silicate sheets are incomplete and much of the silica is dimeric, whereas in jennite, the dimeric units are bridged by additional silicate tetrahedra forming pentameric or higher molecular weight units. From NMR (nuclear magnetic resonance), it appears that these polymer units are organised into platelets, each with typical maximum dimensions of a few tens of nanometres. The individual platelets adhere strongly giving rise to nanoporous bulk gel. The high surface area measured by gas sorption (e.g. 148 m^2/g reported by Tits et al. 2006b) arises from the poor packing of platelet substructures. This nanometre-scale substructure is responsible for the low crystallinity reported by XRD: sharp diffractions typical of a "crystal" are only obtained from crystals bigger than approximately 100 nm. Therefore, the low crystallinity and imperfect "structure" of CSH can be expected to give rise to a high density of sorption sites for both cations and anions (Glasser 1993). The "structure" of CSH also makes it impossible to distinguish in any fundamental way between "surface" and "bulk" processes. No doubt operational criteria could be developed to distinguish "surface" from "bulk" but at present, there are no agreed criteria.

There is also controversy about the limits of composition of CSH. For example, Al can substitute in CSH. But the role of aluminium appears to be twofold: as a genuine substituent and in occluded phases. For example, tetrahedral Al occurs in CSH and there is general agreement from NMR that it preferentially substitutes in bridging positions between adjacent silicate dimmers. However, NMR also records penta- and octrahedrally coordinated Al, the structural role of which is less clear. It is probable that octahedral Al is, at least in part, presented as occluded AFm, i.e. a second phase is present (F. Glasser, personal communication).

These complex structural considerations and the possible presence of an occluded second phase or phases cannot, at present, be resolved. But the precursors of CSH, alite and belite, incorporate 1–2 wt% alumina and, since their hydration gives rise to CSH, it is likely that all Portland cements give rise to similar CSH. It is an open question to what extent alumina-free synthetic preparations, as for example those frequently made in the laboratory, will reflect the sorption properties of "real" CSH, i.e. CSH from commercial cements containing Al. Also, the extent to which intercalated phases (if present) will affect the properties is variable. Tentatively, differences between synthetic CSH and the product from commercial cement may occur but are unlikely to be large. This is because in many cases, also some data on the sorption properties of phases are likely to be present as intercalates (AFm and AFt). The main feature, which seems to dominate CSH sorptive properties, is the presence of a relatively high volume fraction, several %, of nanopores.

In this context, CSH also exhibits a zeta potential which affects the balance between "surface" and "bulk" sorption. The zeta potential is dependent on the C/S ratio: CSH with high Ca/Si molar ratio has a positive charge and thus tends to sorb anions. Atkins and Glasser (1992) demonstrated that CSH of high C/S ratio is a better scavenger for I than CSH of lower C/S ratio. As the C/S ratio decreases as a result of cement degradation, the surface charge becomes less positive, passing through the point of zero charge at C/S of about 1.2 and turns to negative at lower C/S ratio. Thus, in terms of electrostatic sorption, CSH with a low C/S ratio is a better sorbent for cationic species.

AFt

AFt is calcium aluminosulphate hydrate with some iron substituted for aluminium, with ettringite being the most important AFt phase. It has a very open structure and presents several possibilities for crystal chemical incorporation. Many contaminant ions may substitute for the essential ionic components of ettringite—calcium, aluminium, and sulphate. Gougar et al. (1996) summarised sorption mechanisms on ettringite: divalent cations such as Sr^{2+} and Ni^{2+} may substitute calcium; trivalent metal ions replace aluminium, and anions such as CO_3^{2-}, Cl^-, IO_3^- exchange with sulphates. Ettringite surfaces exhibit a net negative charge, so incorporation of anions in the bulk is probably more important than surface adsorption (Cornelis et al. 2008). Although our definition of sorption was based on an exclusion rule, i.e. all processes other than precipitation, co-precipitation, and solid solutions are considered as sorption, ettringite is included as a relevant solid phase for selecting sorption values.

AFm

This phase forms in the presence of limited sulphate availability or an elevated temperature. Its structure is tolerant of substitution and can sorb many contaminants through ion substitution. AFm is known to sorb di- and trivalent heavy

metal ions and diverse anions. The formation of solid solution with AFm may cause a stronger sorption of oxyanions on AFm as compared to ettringite. AFm phases bind iodide, I^-, better than AFt phase (Atkins and Glasser 1992). Based on anticipated chemically similar behaviour between Cl^- and I^-, AFm phase should have the potential to sorb Cl^- as shown by formation of Friedel's salt ($3CaO{\cdot}Al_2O_3{\cdot}CaCl_2{\cdot}10H_2O$), a chloride-containing AFm phase.

Hydrogarnet
Sorption may happen on hydrogarnet through ion substitution, e.g., Cr(III) may replace Al in hydrogarnet (Glasser 2002).

Hydrotalcite
Hydrotalcite has a layer structure and can incorporate many di- and trivalent cations, e.g. Ni^{2+}, and Co^{2+} in place of Mg^{2+}, Cr^{3+} in place of Al, etc. Anions such as CO_3^{2-}, Cl^-, and NO_3^- may also substitute for OH^- and SO_4^{2-}.

Calcite
Calcite will be present as aggregate and newly generated by cement carbonation. Calcite is highly crystalline and has a much smaller reactive surface area [e.g. between 0.2 and 1 m^2/g (Jacques 2003)] and much simpler structure than the sorbing cement materials. It therefore exhibits lower sorption potential than most other cement phases.

2.5 Degradation of Hydrated Cement

2.5.1 Degradation States

Solutions in equilibrium with hydrated cement are hyperalkaline, featuring pH values of about 13.2 or higher, and correspondingly high Na- and K-concentrations. It follows that hydrated cement minerals are not in equilibrium with infiltrating water and will dissolve partly upon contact. Moreover, in particular the amorphous CSH phases are not thermodynamic ally stable in contact with infiltrating water and tend to degrade over time. Depending on the conditions, cement degradation may arise from a number of processes, but the principal degradation mechanism expected for a near-surface waste disposal facility is leaching of HCP components by infiltrating water.

It is well established in the literature that degradation of hydrated cement follows a pattern of several different, more or less distinct states that are characterised by progressively lower pore water pH (Berner 1992; Neall 1994; Atkinson et al. 1989a). Figure 2.1 shows schematically the degradation of hydrated cement with the corresponding pH decrease as a function of time (or more

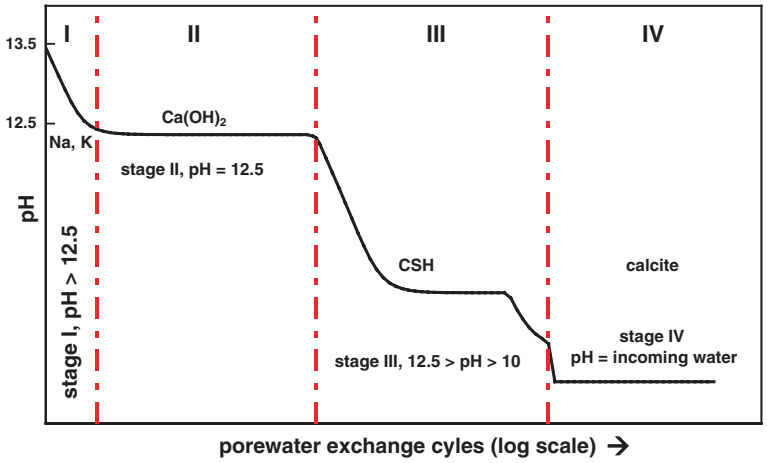

Fig. 2.1 Schematic diagram illustrating the evolution of pH at 25 °C in hydrated cement pore fluid as a result of cement degradation. The scales of pH and pore water exchange cycles (time) are indicative and depend on many factors such as rate of pore fluid replacement, aggressiveness of the environment, and temperature. The solution composition in State I is controlled by soluble sodium (Na) and potassium (K) salts, in State II by portlandite ($Ca(OH)_2$), in State III by calcium silica hydrate (CSH), and in State IV by residual minerals (in the present case, calcite). Modified from Berner (1992) and Andra (2005)

specifically, with the number of pore water exchanges). A representative illustration of a detailed modelling analysis of the degradation sequence of cement is given below for the Dessel disposal facility (Jacques 2008; Jacques et al. 2008).

According to scheme shown in Fig. 2.1, four states of cement degradation are typically distinguished.

State I (13.5 > pH > 12.5)
Pore fluids in hydrated cement contain high concentrations of free alkali metal ions resulting from the initial dissolution of alkali metal sulphates (and the subsequent uptake of sulphate by AFt and AFm phases). In charge balancing the system, equivalent concentrations of hydroxyl ions are produced. Thus, HCP pore fluid in State I has a very high pH in a range of >12.5–13.5 at 25 °C. The pore fluid composition of this state is dominated by Na, K, and OH. As the solubility of portlandite is low at such pH values, only small amounts of Ca are released from the solids and the C/S ratio is high.

State II (pH = 12.5)
When all alkali ions are removed at the end of State I, the pH of the pore fluid will be controlled by the solubility of portlandite at 12.5 (25 °C). The composition of

the pore fluid at this state is essentially a 20 mM calcium hydroxide solution. The duration of this state is proportional to the amount of portlandite in the hydrated cement.

State III (12.5 > pH > 10)
This state follows the complete dissolution of portlandite at the end of State II. The pH in this state is regulated by the incongruent dissolution of CSH phases. CSH phases of high Ca/Si ratio (C/S > 1.5) coexist with portlandite at States I and II. The dissolution of CSH with high Ca/Si ratio begins at the end of State II, and the Ca/Si ratio as well as pH begins to decrease. Atkins and Glasser (1992) reported that the pH of the pore fluid controlled by the solubility of CSH phases with a C/S of 0.8–1.5 should be in a range of 11–12.4. Tits et al. (2008) found that the pH of the pore fluid in equilibrium with synthetic CSH phases (C/S of 0.82–1.65) is in a range of 10–12.5. At the end of State III, CSH phases dissolve congruently, fixing the pH at a constant value of about 10 (Jacques et al. 2008). The lower-bound pH is thus set at 10.

State IV (pH < 10)
CSH phases and other hydrated cement components are completely dissolved and the pH drops below pH 10. The composition of the pore fluid is governed by the remaining aggregate minerals (only calcite in the present case) and the incoming water.

2.5.2 Illustrative Example

As an illustration, the changes in solid phase and pore water composition of the concrete envisaged for the surface disposal facility at Dessel, Belgium, are shown in Fig. 2.2 for the infiltration of typical soil water. The four states of cement/concrete degradation are clearly visible:

- State I: The pH is controlled by the dissolution of alkalies. This state ends after approximately 0.35 kg of cumulative leached water. This amount of water correspond to approximately 5 pore volumes assuming a porosity of 7 % (or about 3 years under the assumptions specific for the Dessel site, cf. Jacques et al. 2008).
- State II: The pH is controlled mainly by the dissolution of portlandite. The concentrations of all other elements (except Na and K) are controlled by cement phases and remain constant due to the constant pH. This state ends after approximately 3500 years for the same assumptions (Jacques et al. 2008).

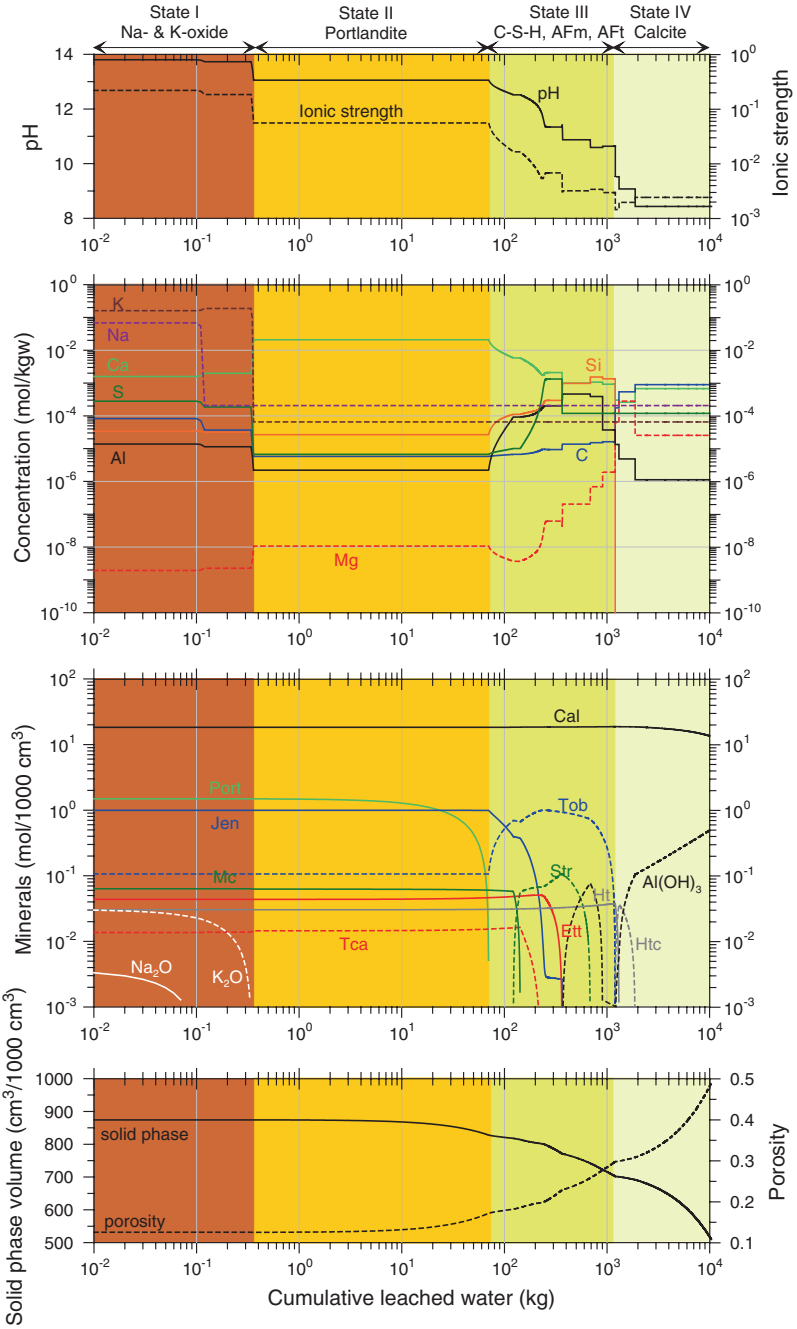
State I
Na- & K-oxide
State II
Portlandite
State III
C-S-H, AFm, AFt
State IV
Calcite
pH
Ionic strength
Concentration (mol/kgw)
K
Na
Ca
S
Al
Si
C
Mg
Minerals (mol/1000 cm3)
Cal
Port
Jen
Mc
Tob
Str
Ht
Ett
Tca
Htc
Al(OH)3
Na2O
K2O
Solid phase volume (cm3/1000 cm3)
solid phase
porosity
Porosity
Cumulative leached water (kg)

Fig. 2.2 Geochemical changes during leaching of 1000 cm^3 concrete with typical soil water (pH = 3.73, Al = 4.48 × 10^{-5} mol/L, C = 2.70 × 10^{-4} mol/L, Ca = 5.71 × 10^{-5} mol/L, Cl = 1.82 × 10^{-4} mol/L, K = 6.53 × 10^{-5} mol/L, Mg = 2.53 × 10^{-5} mol/L, N(V) = 3.54 × 10^{-4} mol/L, Na = 2.05 × 10^{-4} mol/L, S(VI) = 1.19 × 10^{-4} mol/L) About 21 % of the 1000 cm^3 is occupied by cement and 67 % by the concrete aggregates. *Port* portlandite, *Jen* jennite-like endmember, *Mc* monocarboaluminate, *Tca* tricarboaluminate, *Tob* tobermorite-like endmember, *Str* strätlingite, *Ett* ettringite, *Htc* CO_2-hydrotalcite, *Ht* OHhydrotalcite, *Cal* calcite (from Jacques et al. 2008)

- State III is the most complex. The pH and element concentrations (except Na and K) are controlled by a sequence of dissolution and precipitation reactions of the CSH, AFm, and AFt phases. This state ends when these phases are no longer present, i.e. after depletion of the last phase characteristic for hydrated cement, the tobermorite-like endmember of the CSH phases. This state ends after approximately 36,400 years for the same assumptions (Jacques et al. 2008).
- State IV: After depletion of the hydrotalcite phases, pH is partly buffered by calcite dissolution.

References

Andra, Référentiel de comportement des radionucléides et des toxiques chimiques d'un stockage dans le Callovo-Oxfordien jusqu'à l'homme, Site de Meuse/Haute-Marne, Tome 1/2: Chapitres 1 à 4, Dossier 2005 Argile (2005)

C.A.J. Apello, D. Postma, *Geochemistry, Groundwater and Pollution*, 2nd edn. (A.A. Balkema Publishers, Amsterdam, 2006)

M. Atkins, F.P. Glasser, Application of portland cement-based materials to radioactive waste immobilization. Waste Manage. **12**, 105–131 (1992)

A. Atkinson, N.M. Everitt, R. Guppy, *Evolution of pH in a Radwaste Repository: Experimental Simulation of Cement Leaching: Part 1*, DOE/RW/89/025 (1989a)

U. Berner, Evolution of pore water chemistry during degradation of cement in a radioactive waste repository environment. Waste Manage. **12**, 201–219 (1992)

Q.Y. Chen, M. Tyrer, C.D. Hills, X.M. Yang, P. Carey, Immobilisation of heavy metal in cement-based solidification/stabilisation: a review. Waste Manage. (2008). doi:10.1016/j.wasman.2008.01.019

G. Cornelis, C.A. Johnson, T. Van Gerven, C. Vandecasteele, Leaching mechanisms of oxyanionic metalloid and metal species in alkaline solid wastes: a review. Appl. Geochem. **23**, 955–976 (2008)

E. Curti, *Coprecipitation of Radionuclides: Basic Concepts, Literature Review and First Applications*. (PSI Bericht Nr., Villigen, 1997)

R. Gens, Formulation of the concrete for the modules, concrete containers and the cementitious backfill. NIROND 2007–1876 (rev. 0) (2008)

F.P. Glasser, Chemistry of cement-solidified waste forms, in *Chemistry and Microstructure of Solidified Waste Forms*, ed. by R.D. Spence (Lewis Publishers, Boca Raton, 1993)

F.P. Glasser, Characterization of the barrier performance of cements, in *Proceedings of the Material Research Society Symposium*, vol. 713–732 (2002)

M.L.D. Gougar, B.E. Scheetz, D.M. Roy, Ettringite and CSH portland cement phases for waste ion immobilization: a review. Waste Manage. **16**, 295–303 (1996)

D. Jacques, Geochemical model for boom clay pore water, mineralogy and solution-mineral-surface interactions. SCKCEN R-3747 (2003)

D. Jacques, Benchmarking of the cement model and detrimental chemical reactions including temperature dependent parameters, project near surface disposal of category: a waste at Dessel. NIROND-TR 2008-0X E (2008)

D. Jacques, D. Mallants, Modelling of the potential and actual evaporation and drainage at the nuclear zone Mol-Dessel, project near surface disposal of category: a waste at Dessel. NIRAS-MPXX-XX Version X, NIROND-TR 2008-0X E (2008)

D. Jacques, L. Wang, E. Martens, D. Mallants, Time dependency of the geochemical boundary conditions for the cementitious engineered barriers of the Belgian surface disposal facility, project near surface disposal of category: a waste at Dessel. NIRAS-MP5 DATA-LT(NF) Version 1, NIROND-TR 2008-24 E (2008)

S. Komarneni, D.M. Roy, Mechanisms of immobilization of nuclear waste elements by cement minerals, cement and mortar. Cem. Concr. Res. **11**, 789–794 (1981)

D.E. Meece, L.K. Benninger, The coprecipitation of Pu and other radionuclides with $CaCO_3$. Geochim. Cosmochim. Acta **57**, 1447–1458 (1993)

F.B. Neall, *Modelling of the Near-Field Chemistry of the SMA Repository at the Wellenberg Site*. (PSI-Bericht Nr., Villigen, 1994)

K. Noshita, T. Nishi, T. Yoshida, H. Fujihara, N. Saito, S. Tanaka, Categorization of cement hydrates by radionuclide sorption mechanism, in *Proceedings of the Material Research Society Symposium*, vol. 663 (2001), pp. 115–121

H.F.W. Taylor, in *Cement Chemistry*, 2nd edn. (Thomas Telford Publishing, London, 1997) 465 pp (ISBN:0-7277-2592-0)

J. Tits, K. Iijima, E. Wieland, G. Kamei, The uptake of radium by calcium silicate hydrates and hardened cement paste. Radiochim. Acta **94**, 637–643 (2006a)

J. Tits, E. Wieland, C.J. Muller, C. Landesmann, M.H. Bradbury, A wet chemistry study of the strontium binding by calcium silicate hydrates. J. Colloid Interface Sci. **300**, 78–87 (2006b)

J. Tits, T. Fujita, M. Tsukamoto, E. Wieland, Uranium(VI) uptake by synthetic calcium silicate hydrates, in *Proceedings of the Material Research Society Symposium*, vol. 1107 (2008), pp. 467–474

E. Wieland, L. Van Loon, *Cementitious Near-Field Sorption Data Base for Performance Assessment of an ILW Repository in Opalinus Clay*. (PSI Bericht Nr., Villigen, 2002), pp. 03–06

J.M. Zachara, C.E. Cowan, C.T. Resch, Sorption of divalent metals on calcite. Geochim. Cosmochim. Acta **55**, 1549–1562 (1991)

Chapter 3
Sorption Values for Chlorine and Iodine

Abstract This chapter addresses the behaviour of halside anions in cementitious environments. In any typical aqueous environmental setting, chlorine exists exclusively in the form of chloride (Cl^-). Inorganic iodine may be present as iodate (IO_3^-) and iodide (I^-), with the latter being typical for cementitious environments. Radioactive isotopes of both elements (^{36}Cl, ^{125}I, ^{131}I, ^{129}I) are relevant constituents of different types of radioactive waste. The most influential factor on sorption values for radioactive chloride is aqueous total chloride concentration, including stable chloride present in cement solid phases and infiltrating water. All available studies indicate a decrease of chloride sorption with increasing total chloride (stable chloride and ^{36}Cl) aqueous concentration. Close examination of available data indicates different chloride behaviour within two distinct concentration ranges, namely the predominance of surface versus incorporation processes. At aqueous chloride concentrations well below millimolal level, the magnitude of Cl sorption can be directly related to the surface charge of CSH phases. At higher total Cl concentrations, ^{36}Cl behaviour is probably controlled by the formation of Friedel's salt (a chloride-containing calcium aluminate hydrate) or solid solution formation with alumino-sulphate phases. Isotopic dilution may also play a role in these cases. Data obtained for dilute suspensions show that the behaviour of iodide is analogous to that of chloride in qualitative terms. A comparison with data for intact hydrated cement paste suggests that the solid/liquid ratio has a significant effect in case of iodide, but not in case of chloride. Until this issue is resolved, data from dilute systems should not be used for quantifying iodide sorption.

3.1 Chlorine

3.1.1 Chemical Form, Speciation, and Solubility

In any typical aqueous environmental setting (water, soils, aquifers, etc.), chlorine exists exclusively in the form of chloride (Cl^-). Chloride is ubiquitous in

© Springer International Publishing Switzerland 2016

M. Ochs et al., *Radionuclide and Metal Sorption on Cement and Concrete*,
Topics in Safety, Risk, Reliability and Quality 29,
DOI 10.1007/978-3-319-23651-3_3

the environment, mostly in low concentrations, but also at high concentrations in saline soils and groundwater as well as in the ocean. In that sense, stable (non-radioactive) chloride is not a typical contaminant. It is included in this volume mainly because the radioactive isotope ^{36}Cl is very relevant in many disposal scenarios of radioactive waste. In addition, the interaction of chloride with hydrated cement is of interest because many types of conventional wastes contain salts which contain chloride.

LILW typically contains ^{36}Cl. However, the behaviour of ^{36}Cl sorption in a cementitious material may be influenced by the presence of stable chloride. Several sources of stable chloride are distinguished that may influence ^{36}Cl sorption: (i) chloride associated with the production of concrete (usually very low and regulated, see further), (ii) stable chloride originating from particular radioactive waste streams (e.g. evaporator concentrates generated from NPP operation), and (iii) chloride originating from external sources such as soil solutions or groundwater.

- *Chloride associated with cement production*: Background chloride concentration in cement pore water is generally low. Stable chloride is present in commercial cements up to 0.01 wt%. The chloride amount in commercial cement is kept at a low level to reduce the risk of rebar corrosion. Chloride concentrations up to 0.4 % (by weight of cement) can be taken as a conservative value below which steel corrosion will not be significantly alterated (Alonso et al. 2002; Izquierdo et al. 2004). Only part of total chloride in cement remains in the pore water under soluble form because of sorption and/or formation of a solid solution (Nielsen et al. 2005). The pore water concentration of chlorine originated from cement itself is in the range of millimolal to a few tenth of millimolal. Calculated chloride concentration was shown to be 0.64 mmol for evolved concrete at pH 12.5 (Savage 1999). Friedel's salt ($3CaO{\cdot}Al_2O_3{\cdot}CaCl_2{\cdot}10H_2O$) may be formed as a solid solution if the pore water chloride concentration increases to somewhat above a few millimolal (Bothe and Brown 2004). Friedel's salt, a chloride-containing calcium aluminate hydrate, is known to play an important role as a diffusion barrier against chloride migration (Bothe and Brown 2004). Based on this information, chloride in LILW is likely to be present as dissolved Cl^- anion in most of waste types except in the evaporator concentrates where Friedel's salt may be present and associated with different cement phases (see further).
- *Chloride associated with infiltrating soil water*: chloride concentrations in the range of a fraction of a millimol/L are expected from soil water potentially getting into contact with the conditioned waste when engineered barriers preventing soil water infiltration have become ineffective (e.g. Jacques et al. 2008). The concentration will depend in part on wet/dry deposition rates and in part on the rate of chloride dissolution from soil material overlying the repository. Depending on the geographical setting, saline groundwater may also be relevant.
- *Chloride associated with particular wastes*: The amount of stable chlorides in radioactive waste is the highest in the evaporator concentrates which can be up to 150 g/L for the concentrates of the Doel nuclear power plant and 4 g/L for the concentrates of the Tihange nuclear power plant (note that 1 L of concentrate is assumed to correspond to ~2 L of conditioned waste). Evaporator

concentrates that contain high chloride concentrations (and associated counter ions such as sodium) may negatively impact the long-term safety of a facility. Possible effects include (i) accelerated corrosion of reinforcement steel used in the monolith, (ii) reduction of the sorption of ^{36}Cl (see Sect. 3.1.3.1), and (iii) reduction of the sorption of other radionuclides.

Chloride does not form low-soluble solid phases in a cementitious environment so that the dissolved Cl concentration is normally considered as being "not limited" (Berner 2002). It is however well known that chloride may form readily soluble Friedel's salts or calcium oxychlorides in cement and concrete when chloride concentration in the pore fluid exceeds millimol level (Nielsen et al. 2005; Glasser et al. 2008). Berner (1999) referred to the work of Gunkel (1992) in which up to 2×10^{-3} mol/L of dissolved Cl was measured in commercial cements. This is an indication that a background chloride concentration in the pore fluid of a benchmark cement may reach millimolal levels. Chloride exists in cement normally through sorption or binding to aluminate phases as solid solutions.

Bradbury and Sarott (1995) observed from a diffusion experiment on hardened cement samples previously carried out by Sarott et al. (1992) that a steady-state diffusion condition was established at a total dissolved Cl concentration below 3×10^{-5} mol/L. They therefore suggested to consider sorption as the dominant binding mechanism below this concentration. To the authors' observation, the concentration of 3×10^{-5} mol/L Cl was added to the diffusion experiment without accounting for possible Cl leached from cement samples. The actual Cl concentration therefore might have been higher than the value of 3×10^{-5} mol/L.

Bothe and Brown (2004) determined the solubility of a laboratory prepared Friedel's salt by mixing Cl with AFm and other cement components and derived the solubility product:

$$\text{Friedel's - salt} + 12H^{+} = 4Ca^{2+} + 2Cl^{-} + 16H_2O + 2Al^{3+}, \text{Log}K = 73 - 74.2(23\,^{\circ}\text{C}) \tag{3.1}$$

Using the above equilibrium and the solubility product, a scoping calculation using *The Geochemist's Workbench®* (Bethke 2006) demonstrated that Friedel's salt will not form with the concrete composition and total chloride concentration considered in this review. Furthermore, Glasser et al. (2008) pointed out that a chloride bearing AFm phase proved stable over a wide range of Cl concentrations: from a few millimolal to over 3 m.

Based on the above, it seems difficult to assign a single solubility limit for Cl in a cement system. Many studies observed a threshold concentration above which Cl bearing solid phases may form, but these phases are more likely of a solid solution nature, so the calculated solubility limit will vary as the composition varies. There seems a consistent trend, however, that Cl may start to form a solid phase on cement when the total dissolved concentration of Cl becomes higher than a few millimolal. In case of Friedel's salts, ion exchange kinetics are important too. Typically, these are rapid (days, weeks), so chloride in Freidel's salt is still "available"—it is not permanently locked away. Thus for many purposes—mainly kinetics—there is a single Cl reservoir, and one need not to distinguish between mechanisms whereby Cl is bound.

3.1.2 Sorption Values from the Literature for the Benchmark Cement

Figure 3.1 summarises the reviewed R_d values for chloride as a function of pH for different states of cement degradation. A summary of experimental conditions under which these sorption values are determined is given in Table A.1 (Annex).

Two groups (A and B) are identified in Fig. 3.1. The sorption mechanisms are probably controlled by different processes. Group A R_d values might be governed by sorption associated with surface processes, while group B data are probably controlled by the formation of Friedel's salt or solid solutions with cement phases such as AFm. This distinction is made based on arguments provided by Glasser et al. (2008) (discussed further on).

Baker et al. (1994) and Bayliss et al. (1996) reported R_d values for chloride on NRVB determined from batch experiments. Sorption value R_d increased linearly with decreasing initial chloride concentration introduced in the system. Total chloride concentration thus seems to influence R_d.

Sorption of ^{36}Cl on hardened cement pastes was determined by Pointeau et al. (2008) as a function of pH in pore waters derived from leaching of cement paste at States I, II, and a part of III of cement degradation (see reproduced plot in Fig. 3.2). These authors demonstrated that the sorption of chloride (similar to other anionic species included in the experiments) is strongest at pH around 12.6 where the solubility of portlandite controls the pH and the Ca concentration is at its highest value.

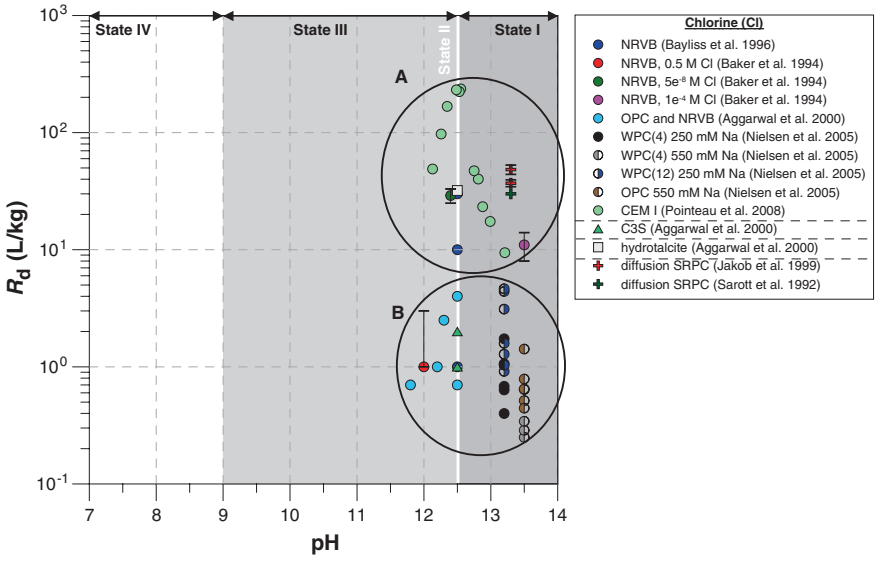

Fig. 3.1 Distribution ratio (R_d) of chloride in cementitious systems as a function of pH. Groups A (<millimolal level) and B (>millimolal level) are based on total aqueous chloride concentration. *NRVB* Nirex reference vault backfill; *HCP* hardened cement paste; *WPC* white Portland cement; *OPC* ordinary Portland cement; *SRPC* sulphate-resisting Portland cement

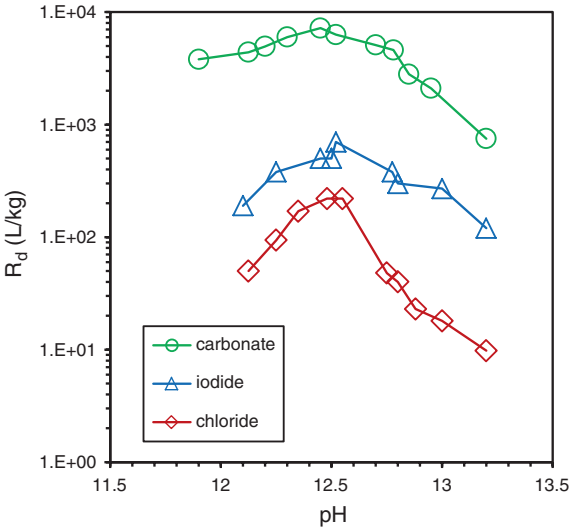

Fig. 3.2 Sorption of anionic radionuclides ($^{36}Cl^-$, $^{125}I^-$, $^{14}CO_3^{2-}$) as a function of cement degradation. Data from Pointeau et al. (2008)

R_d seems positively correlated to the dissolved Ca concentration in pore water and negatively correlated to the dissolved SO_4^{2-} concentration. The observed dependency of R_d on Ca concentration was considered to be related to the variation of surface potential of cement materials as Ca concentration changes: when its concentration is sufficiently high, a global positive charge near the surface exists. Pointeau et al. (2008) reported a difference between the R_d evolution of pure anionic radionuclides including Cl with that of U(VI), which suggests different uptake mechanisms. The authors further concluded that chloride sorption is more likely through an outer-sphere surface complex on HCP surfaces, while U(VI) may chiefly bond to CSH by inner-sphere surface complexes. Finally, Pointeau et al. (2008) also observed a higher HCP affinity for I^- than for Cl^-. It was also noticed by the authors of the study that up to a tenth of a millimolal of stable chloride existed in the pore fluid and that might have had an impact on the overall removal of ^{36}Cl added as the tracer. However, the content of stable Cl on the cement paste was not reported. The ratio of the dissolved Cl in the pore fluid and the Cl content in cement paste may have affected the observed R_d for ^{36}Cl via isotopic dilution.

Nielsen et al. 2005 studied binding of chloride and alkali metal ions on white Portland cements and OPC with different content of C_3A. Figure 3.3 shows the chloride sorption isotherms determined through batch experiments by adding $CaCl_2$ to cement–water systems (8.3 g/12 ml). The results of the study suggest that alkali metal ions have a negative impact on the binding of chloride, so chloride sorption at State I should be weaker than at State II. This agrees with the findings from Pointeau et al. (2008), as shown in Fig. 3.2. Comparison between the sorption of chloride on white Portland cement (low iron content) and on OPC indicates that the absence of iron is beneficial to chloride binding (for white cements, more chloride is bound to CSH phases compared to conventional Portland cement). A model based on the phase rule and the formation of a solid solution including Friedel's salt and monocarbonate was developed to explain the observed relationship between the quantity of binding and solution compositions (Nielsen et al. 2005).

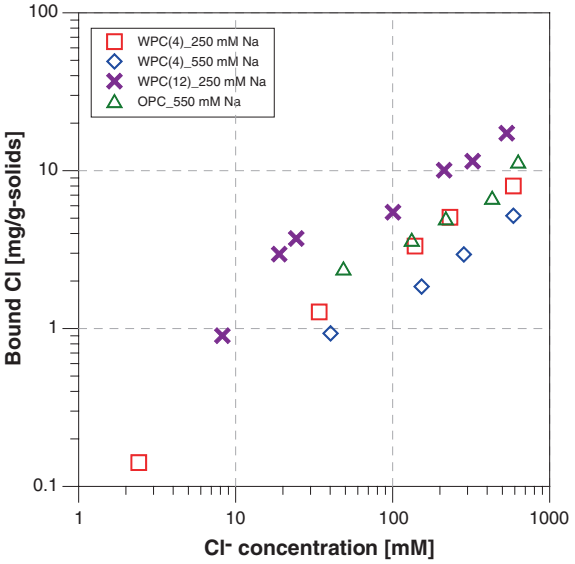

Fig. 3.3 Sorption isotherms for white Portland cements (*WPC*) and grey Portland cement (*OPC*) in the presence of high alkali concentrations (*source* Nielsen et al. 2005). WPC(4) and WPC(12) contain, respectively, 4 and 12 % of Bogue-C_3A

Aggarwal et al. (2000) determined R_d for ^{36}Cl on cement blends, NRVB materials, CSH, and minor phases such as hydrotalcite, C_3A, and chloroaluminates. In general, sorption of ^{36}Cl on cement materials is very weak, especially on CSH (almost no sorption was observed). Sorption of ^{36}Cl is relatively high on minor phases such as chloroaluminate and hydrotalcite. X-ray analysis suggested that upon interaction between chloride and C_3A phases, $C_3A{\cdot}CaCl_2{\cdot}H_2O$ solids formed. The authors presumed that isotopic exchange of ^{36}Cl with the sorbed chloride in aluminate components in cement might be the main sorption mechanism in the experiments.

Sorption values may also be derived from diffusion experiments, as was demonstrated for HCP by Sarott et al. (1992) and Jakob et al. (1999). By fitting the diffusion profiles from through-diffusion experiments and assuming a linear sorption and reversible sorption as the retardation mechanism, K_d values were obtained as 30 (Sarott et al. 1992) and 50 L/kg (Jakob et al. 1999), respectively. The latter value was found about a factor of two too high as compared to the batch K_d of 24 L/kg measured in the same laboratory. The earlier Sarott et al. (1992) study concluded that the assumed linear sorption K_d explained adequately the observed diffusion profiles, while the more detailed modelling on the newer through-diffusion experiments demonstrated that none of the models including linear sorption isotherm, nonlinear (Freundlich) isotherm, first-order sorption kinetics, and nonlinear sorption kinetics is able to describe all available data with consistent parameter values (Jakob et al. 1999). These studies were based on very well-controlled experiments, both batch tests on crushed cement and diffusion experiments in cement discs, combined with consistent modelling accounting for several retardation mechanisms. Still, they illustrated that although diffusion-type experiments have a S/L ratio more representative

of the real repository[1] conditions, and therefore may produce more appropriate sorption values, there are difficulties in determining reliable sorption values from inverse optimisation of experimental diffusion profiles. These lead to a conclusion that at the present stage, the uptake mechanism of Cl by cement in a core diffusion experiment is not identified and thus subject to uncertainties in the K_d or R_d definition. A linear and reversible K_d may be used to quantify the retardation of Cl in cement to an approximate extent but is too simple to account for real sorption mechanisms which might be at work, such as formation of solid solution and/or a kinetically controlled sorption and desorption processes. An important point to note is that none of the above discussed diffusion studies has accounted for cement-based Cl leached from cement samples that may have interacted with the Cl tracer. As the initial Cl tracer, concentration was lower than 10^{-5} mol/L in those diffusion experiments, one might suspect, based on the discussions till now, that the actual total Cl concentrations in the experiments were likely to have been higher and that this may have been an important influence on the derived R_d values.

3.1.3 Sorption Mechanisms and Selected Sorption Values

Based on the literature reviewed, the most influential factor on chloride sorption values is aqueous total chloride concentration, including stable chloride present in cement solid phases and leached into the pore fluid, while pH becomes important only after the effect of total chloride concentration has been accounted for.

3.1.3.1 Influence of Chloride Concentration on Chloride Sorption Values

A commercial cement normally has a chlorine content lower than 0.01–0.012 wt% (Glasser et al. 2008, personal communication). The aqueous Cl concentration seems low in the pore fluid of cementitious materials according to the studies of Pointeau et al. (2008) and Bayliss et al. (1996). These authors report in their batch sorption experiments a background Cl aqueous concentration around 0.1–0.2 mmol.

Relevant data from Fig. 3.1 are replotted in Fig. 3.4 to show the R_d evolution as a function of total chloride pore water concentration. All studies indicate a decrease of chloride sorption with increasing total chloride (stable chloride and ^{36}Cl) aqueous concentration.

The data from Pointeau et al. (2008) are plotted according to their sorption values measured by ^{36}Cl removal from solutions which contain also 0.01–0.2 mmol of stable chloride leached from cement paste (see Wang et al. (2009) for details on data treatment).

[1]The solid/liquid ratio for a concrete block with density 2.3 kg/L, porosity = 0.1, and a fraction of hardened cement paste of 0.19 is 4.37.

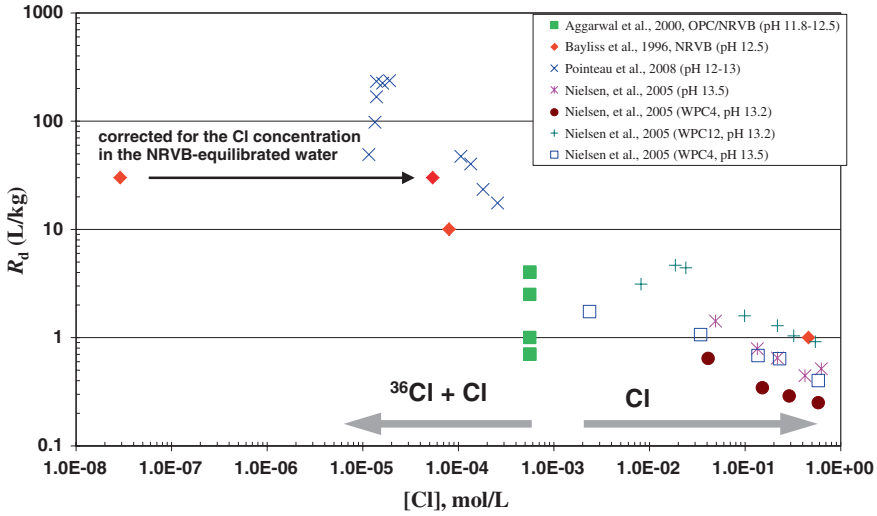

Fig. 3.4 Observed R_d versus aqueous stable chloride (Cl) or radioactive and stable chloride (^{36}Cl + Cl) concentration in cement pore water

The original data of Bayliss et al. (1996) presented the influence of chloride concentration on R_d with the lowest chloride concentration of 2.9×10^{-8} mol/L (Table 5 from their original report), but were corrected here to account for the stable chloride background concentration in the NRVB-equilibrated water, i.e. 5.4×10^{-5} mol/L. The proper total (^{36}Cl and stable Cl) chloride concentration of 5.4×10^{-5} mol/L has been used in Fig. 3.4. Note that except the study of Nielsen et al. (2005), all other data presented in Fig. 3.4 were measured with ^{36}Cl tracer in the presence of stable chloride released from cementitious materials.

NRVB contains little cement and is mainly composed of inactive components (from the sorption point of view), making its place in Fig. 3.4 uncertain. The remaining data cover several orders of magnitude so it is not surprising that no single mechanism controls the entire range of concentrations. But we can conclude that in the low concentration range, a single trend exists. But at 1–10 mM, approximately, a separate event—i.e. formation of Friedels salt—creates a break in the data. But once this capacity is saturated, the data resume a linear trend, not necessarily having the same slope. The magnitude of the break arising from Friedel's salt will depend on the cement type/chemistry, mainly on the availability of alumina to form Friedels salt and competition from other anions, e.g. carbonate and sulphate.

3.1.3.2 Grouping of R_d Values as a Function of Total Aqueous Chloride Concentration

Based on the above discussions, the reviewed R_d values seem to be governed predominantly by total aqueous chloride concentration in cement pore fluid and to a lesser extent by pH. Replotting Fig. 3.4 using a linear y-axis reveals that the

R_d–[Cl] relationship has very different slopes at [Cl] concentrations below and above a few millimolal (Fig. 3.5). In general, R_d decreases with increasing [Cl] concentration, but the slope is flatter at higher [Cl]. The formation of Friedel's salt occurs across a range of concentrations, and this may well be reflected in the blue data points which increasingly deviate form a straight line trend as the critical minimum concentration necessary to form Friedel's salt is approached.

As pH also has an influence on Cl sorption, it cannot be demonstrated that the observed variation in R_d–[Cl] slope shown in Fig. 3.5 is due only to the effect of aqueous Cl concentration. To further evaluate the effect of [Cl], only R_d values measured at pH > 12.8, i.e., for State I, are plotted in Fig. 3.6. The presumed R_d–[Cl] relationship is confirmed and independent of pH, with a change in slope at [Cl] approximately 1 mmol. In other words, the effect of pH becomes important only after the division of the data into low/high Cl groups.

Based on observations from Figs. 3.5 and 3.6, two groups of R_d values are distinguished, i.e. R_d at aqueous Cl concentration below and above millimolal, indicated as group A and B in Fig. 3.1. Group A represents R_d values measured in low aqueous chloride concentration well below millimolal level (Pointeau et al. 2008; Baker et al. 1994; Bayliss et al. 1996; Jakob et al. 1999). The dissolved concentration of stable chloride in the Pointeau et al. (2008) sorption tests was below millimolal level (0.01–0.2 mmol) in the pH range 12–13. The background chloride concentration in the NRVB pore fluid was reported as 5.4×10^{-5} mol/L (Bayliss et al. 1996). Group B R_d values are lower than the group A values and were measured in a Cl concentration around millimolal level (Aggarwal et al. 2000) or higher (Nielsen et al. 2005). Data for the latter study were derived from experiments

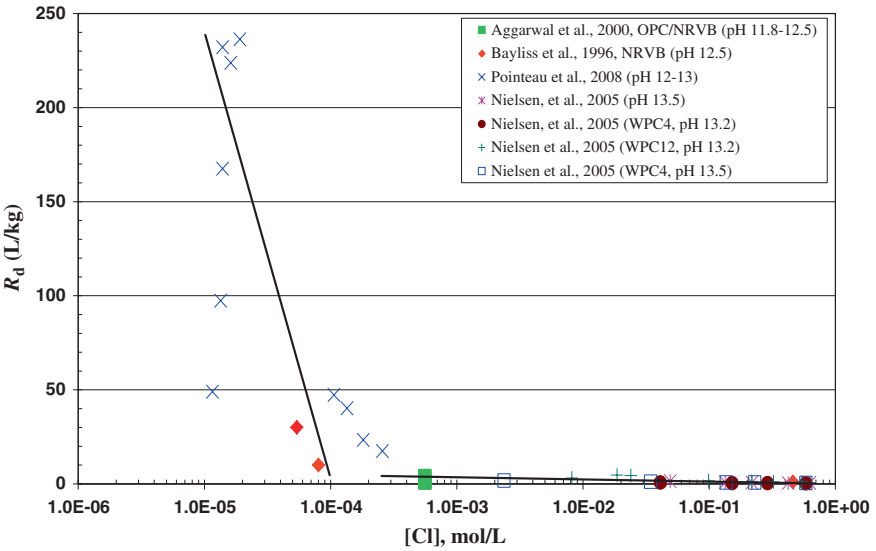

Fig. 3.5 Replotting of Fig. 3.4 with a linear y-axis. Observed R_d versus aqueous stable chloride (Cl) or radioactive and stable chloride (^{36}Cl + Cl) concentration in cement pore water. The two *solid lines* are added to indicate the slopes and are not mathematical regressions

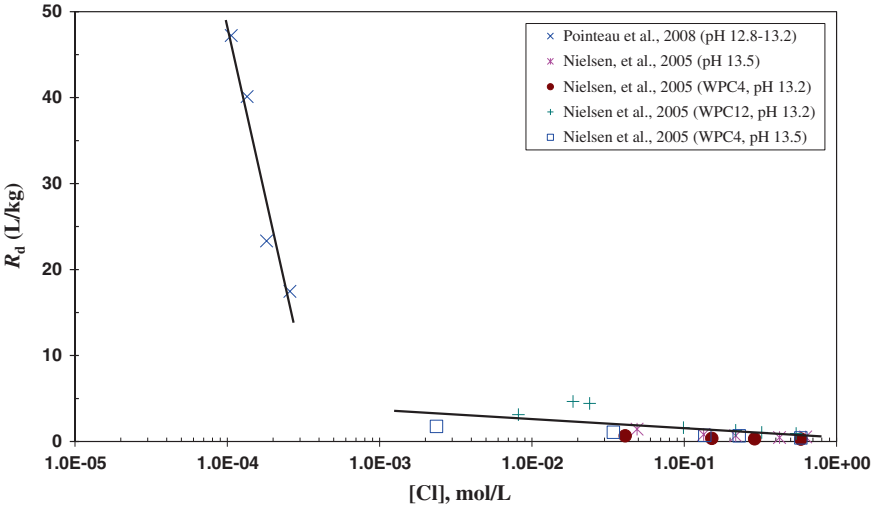

Fig. 3.6 Observed R_d versus aqueous stable chloride (Cl) or radioactive and stable chloride (^{36}Cl + Cl) concentration in cement pore water. All data points were determined at pH > 12.8, i.e. relevant for State I. The two *solid lines* are added to indicate the slopes and are not mathematical regressions

using stable chloride tracer. Chloride concentrations used by Nielsen et al. (2005) ranged between 1 and 1000 mmol.

A possible explanation for a variation of sorption slope as demonstrated in Figs. 3.5 and 3.6 is that sorption may have occurred on different sorbing sites on solid surfaces. For example, Baeyens and Bradbury (1997) used experimentally derived sorption isotherms to quantify sorption site densities of two different sorption sites on montmorillonite. At a low concentration of the sorbing element, sorption was found to be linear and controlled by sorption sites of strong affinity, i.e. the strong sites. When the concentration of sorbing element increased, the sorption isotherm changed its slope at a certain concentration indicating that strong sites were saturated. Further increase of the concentration of the sorbing element will lead to sorption on weak sorption sites, which results in a sorption isotherm of different slope as compared to the sorption isotherm on strong sites. For such interpretation to be true, one needs to demonstrate that sorption on both sites is dominated by surface processes only. Furthermore, processes for clays may not directly translate to cements. Clays are well crystallised, and uptake is actually dominated by defined surface adsorption. Cement paste is an evolving matrix where surface sorption may be only one of several processes. In the case of Cl uptake by cement as shown in Fig. 3.4, sorption mechanisms are not known so the observed difference in sorption slopes cannot, at present, be attributed to sorption on different sorbing sites.

Glasser et al. (2008) summarised that common binding mechanisms for Cl in cementitious materials are the formation of Friedel's salt, ion exchange of Cl ions in pore water to hydroxyl and/or sulphate species on solid phases, and physical sorption. The same review concludes that the formation of Friedel's salt normally

occurs only at Cl concentrations above a few millimolal. Chemical binding such as ion exchange and physical sorption takes place at lower Cl concentrations, but the former normally dominates the latter in terms of sorbed Cl concentration. These arguments are the bases for defining the sorption mechanisms in group A (surface processes) and B (formation of Friedel's salt or solid solutions) as stated previously. Pointeau et al. (2008) argue that their R_d values are regulated by electrostatic sorption and can therefore be correlated to zeta potential of cement suspensions studied. In the present document, data for group B are considered to be still the result of sorption processes, even though other processes may be at work. Further work is needed to determine whether a solubility limit is more appropriate under those conditions.

Another important uptake mechanism that might be at work for group A R_d values is isotope dilution since all data in this group were determined by the removal of ^{36}Cl tracer. Adding low concentrations of Cl radiotracer to cement systems originally containing stable Cl will result in diluting the radiotracer into stable Cl present on solid (sorption) and in pore water (dilution). Isotope dilution of Cl as an uptake mechanism has rarely been discussed in the literature, but is a relevant process in the ONDRAF/NIRAS near-surface disposal project. As this study deals with radioactive waste, relevant R_d values should be in general isotope specific rather than element specific, except when chemical toxicity of non-radioactive substances is concerned. While stable chloride concentrations in OPC pore waters generally are low [~0.003–0.004 % (m/m)], some LILW waste streams such as evaporator concentrates contain elevated chloride levels and could thus have an impact on the ^{36}Cl R_d values and/or have an impact on R_d of other elements (see Sect. 3.1.1).

3.1.3.3 Influence of pH on Chloride Sorption Values

Among the reviewed data presented in Fig. 3.1, Pointeau et al. (2008) studied particularly the pH influence on chloride sorption as a result of cement degradation. They found that R_d is the highest at pH around 12.5 (State II). Sorption of chloride increases from State I to II with decreasing pH from 13.2 to 12.5 and decreases from State II to part of State III with decreasing pH from about 12.5 to around 12. This typical evolution of R_d with pH is found to be related to the change of zeta potential of cement suspension and is also associated with dissolved calcium concentration (see further).

Nielsen et al. (2005) studied the effect of alkali metal (sodium) concentration on chloride binding using 250 and 550 mmol NaOH. These authors did not report the equilibrium pH in their experiments. Therefore, a supporting equilibrium calculation was performed using *The Geochemist's Workbench*® (Bethke 2006) for 250 and 550 mmol/L NaOH solutions, and the resulting pH was found to be 13.2 and 13.5, respectively. These pH values are used for plotting the data of Nielsen et al. (2005) in Fig. 3.1. This study found that the presence of alkali metal affects chloride binding negatively, i.e. higher NaOH concentration resulted in lower R_d values. As a higher NaOH concentration is related to a higher pH, this study

demonstrated that R_d decreases with increasing pH from 13.2 to 13.5. Although the authors explained the finding by a solid-solution model involving sodium, i.e. sorption is affected by sodium not directly by pH, the observed decrease in sorption of chloride with increasing pH is in line with the result of Pointeau et al. (2008).

Other studies mentioned in Fig. 3.1 did not investigate in particular the effect of pH on chloride sorption. It must be noted that the observed R_d variation with pH may relate to other system variables also. For example, pH decrease associated with cement degradation may cause a change of Cl concentration in pore fluid which in turn could have an impact on R_d as well. In other words, pH and other system variables are correlated and cannot be separated from the experiments discussed above.

3.1.3.4 R_d Values at a Low Aqueous Cl Concentration

Based on group A data, R_d for State I is about 10 L/kg (lower range of values), considering the recent data (Fig. 3.2) from Pointeau et al. (2008) on HCP as the most representative of group A. Experiments done at PSI indicate values of 30–50 L/kg obtained from diffusion experiments, while values obtained from batch experiments are a factor of 2 lower, i.e. 15–25 L/kg (Sarott et al. 1992; Jakob et al. 1999). The latter values are in good agreement with the data from Pointeau et al. (2008). Lower and upper limits are, respectively, 5 and 50 L/kg.

The available data indicate sorption of Cl increases when pH decreases, at least in the range above pH 13–12.5. State II R_d ranges from 10 to 30 L/kg (Bayliss et al. 1996) to about 200 L/kg (Pointeau et al. 2008). At pH 12.5, the Pointeau et al. data are well above 100 L/kg. The experts select thus conservatively the lower limit and upper limit for R_d as 10 and 200 L/kg, respectively, and the best estimate is 50 L/kg.

State III R_d for Cl decreases with decreasing pH as indicated by the data of Pointeau et al. and is interpreted as being due to the decrease in zeta potential on cement surfaces. If sorption of Cl is indeed controlled by electrostatic interactions as suggested by Pointeau et al., one should expect that the evolution of R_d for Cl resembles that of the evolution of zeta potential of cement systems. Figure 3.7 reproduces the plot representing measured and calculated (expressed in terms of silanol ($\equiv SiO^-$) groups) evolution of zeta potential as a function of pH from Pointeau et al. (2006). It is seen that the zeta potential of cement paste decreases from pH 12.5 to 11 and R_d for Cl should follow the same trend. As the zeta potential at pH 11 is a little higher than at pH > 13, one can reasonably assume that R_d for Cl at pH 11 should be at least as high as the R_d at pH > 13, i.e. about 10 L/kg as a minimum. Pointeau et al. (2008) also suggest using the R_d for State I as the conservative value for degraded cement systems in safety assessments. Therefore, in the absence of measured sorption data for State III, the experts agreed to use the same best estimate R_d value as for State I (20 L/kg) but to increase the range

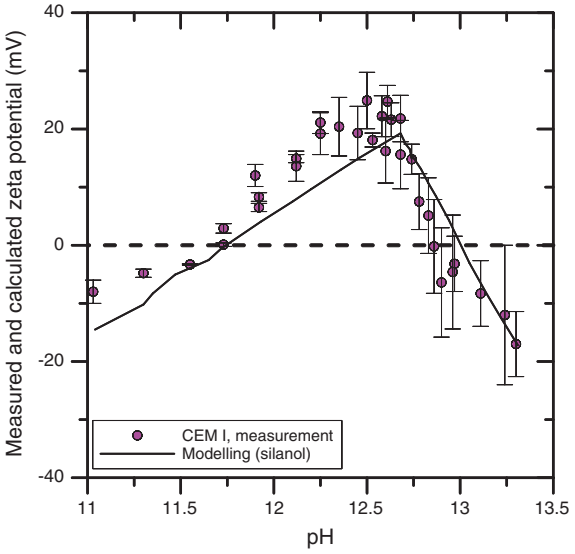

Fig. 3.7 Zeta potential of CEM I cement paste as a function of pH (replotted from Pointeau et al. 2006)

of values. Upper and lower bounds of 200 and 2 L/kg were selected to reflect the uncertainty arising from the lack of data.

No R_d on calcite has been found from the literature; hence, a value of zero is assigned for State IV [the same as in Barbury and Bayens (2003)].

3.1.3.5 R_d Values at a High Aqueous Cl Concentration

At a Cl aqueous concentration higher than one millimolal, group B R_d is in the range of 0.2–10 L/kg (Fig. 3.1). The experts therefore select the best estimate R_d for States I to III as 1 L/kg with a lower and upper limit values of 0.2 and 10, respectively. For State IV, a zero value of R_d is chosen.

3.1.3.6 Sorption Mechanisms

Chloride sorption values can be separated into two groups, and these two groups represent different mechanisms. In the high Cl group, uptake is controlled by the formation of Friedel's salt at a dissolved Cl concentration higher than a few millimolal. At a lower dissolved Cl concentration (the low Cl group), uptake of Cl is controlled by sorption which is likely regulated by mechanisms such as electrostatic interaction and/or anion exchange. As sorption values and mechanisms are different at different dissolved Cl concentrations, R_d cannot be assigned as a constant when Cl concentration varies in cement pore fluid. Further details on sorption/uptake mechanisms are discussed in the following sections.

Evans (2008) reviewed literature and listed several possible mechanisms for chloride uptake in cement systems:

- Chloride can react with unhydrated aluminate phases to form Friedel's salt;
- Chloride may be removed from the solution by sorption or secondary phase formation depending on cation composition in the aqueous phase, i.e. binding is found stronger if chloride is added as $CaCl_2$ rather than NaCl. A possible mechanism for this is the formation of the $CaO–CaCl_2–H_2O$ salt when $CaCl_2$ interacts with $Ca(OH)_2$ in cement;
- Chloride may sorb on CSH and the binding capacity may depend on the content of CSH gel;
- Chemisorption may occur also on the surface of hydrated C_3S; and
- Chloride removal by the formation of surface complexes of ion pairs.

Ion exchange is another mechanism for chloride binding in cement (Glasser et al. 2008). Chloride may exchange with surface hydroxyl groups on hydrated cement. Ion exchange may also occur on the surfaces of AFm and Friedel's salt. In this case, chloride in pore solution exchanges sulphate on the surface. Apart from chemisorption, physical binding of chloride to cement surfaces takes place through electrostatic interactions, e.g. on CSH surfaces. Chemical reactions contribute, however, much more than physical interaction to the total amount of chloride bound by hydrated cement systems.

Zibara et al. (2008) found that chloride retention is high at a low C/A (calcium to aluminium) ratio when the formation of monocarboaluminate is favoured. Such condition promotes the formation of Friedel's salt at relatively low chloride concentration (<0.1 mol/L). CSH phases bind chloride also but with a significantly lower capacity than aluminate phases. It was also found that a higher C/S ratio promotes greater chloride binding.

Kinetic sorption studies for chloride have not been carried out to date, although Bonhoure et al. (2002) mention kinetic uptake studies for iodide. After 180 days of equilibration time, R_d values for iodide were still increasing. This suggests that, in addition to sorption onto mineral surfaces, much slower diffusion into the cement mineral structure may also occur. A similar mechanism may occur for chloride, as both anions are expected to behave in a similar manner. However, the diffusion and sorption data for chloride were not in disagreement, whereas this was not the case for iodine (see Sect. 3.2.2). Because a normal contact time used in a sorption experiment is typically from a few days to a month or so, e.g. Pointeau et al. (2008) did their sorption test for 30 days, R_d values under repository conditions will probably be higher owing to the long time available for equilibration before any considerable concrete degradation occurs.

Based on the reviewed literature, sorption of chloride on cementitious materials is likely controlled by several possible mechanisms including physical sorption via electrostatic interactions, anion exchange, and formation of solid solutions and in particular the formation of Freidel's salt on alumina phases. Processes that lead to formation of Friedel's salt obviously represent an uptake process, which is

expressed in this review as R_d. Although sorption mechanisms are not well understood, it is demonstrated that the key factors affecting sorption of Cl on cement are the chloride concentration in cement pore fluid and pH. The influence of pH is via its control on the solution composition and the surface charge and surface potential of the cement particles. It is generally found that sorption of Cl by cement at low Cl concentration is relatively lower at State I than at State II where sorption of Cl is the strongest. Sorption of Cl at State III is also lower as compared to the sorption at State II. The observed trend is mainly based on data from Pointeau et al. (2008) (Fig. 3.2). The Pointeau et al. data agreed quite well with the PSI diffusion data at State I (the diffusion data are not contradicted by the data of Pointeau).

The cement to be used in the ONDRAF/NIRAS LILW repository has a background Cl concentration in the pore fluid of a few millimolal (except waste from evaporator concentrates). The authors therefore consider sorption values based on group A data to be relevant for the reference cement and for the Dessel facility. Note that such selection should only be applicable to the case where Cl concentration is low and sorption is the dominant process responsible for Cl removal from cement pore water. For evaporator concentrates, sorption values based on group B data are more appropriate, as the expected chloride background concentration in the pore water will be higher than one millimolal (refer to concentrates data).

Besides the Cl present in cement materials and conditioned waste, Cl concentration in infiltrating waters from the overlying soils at the Dessel site has been demonstrated to be low (~0.1 mmol) and will therefore unlikely impose extra influences on Cl distribution in cement (Jacques et al. 2008).

Following the reasoning presented in this section, we propose to select two sets of R_d values: (i) group A data for cements with normal background Cl concentrations (less than one millimolal) that will not be negatively affected by high Cl waste streams such as evaporator concentrates; (ii) group B data for cements that will most likely experience high Cl concentrations, for example, as the result of Cl-rich waste streams such as evaporator concentrates. Both groups of data are indicated in Fig. 3.1. The proposed best estimates R_d (L/kg) for both group A and B are provided in Table 3.1.

Table 3.1 Selected best estimate, upper and lower limit chloride R_d values for total chloride concentrations $\leq$1 mmol

pH state	Best estimate (L/kg)	Upper limit (L/kg)	Lower limit (L/kg)
State I	2×10^1 (1)	5×10^1 (10)	5×10^0 (0.2)
State II	5×10^1 (1)	2×10^2 (10)	1×10^1 (0.2)
State III	2×10^1 (1)	2×10^2 (10)	2×10^0 (0.2)
State IV	0 (0)	0 (0)	0 (0)

Values between parentheses are for total background concentrations >1 mmol

3.1.3.7 Sorption at State I

New data from Pointeau et al. (2008) on HCP were regarded as high quality and were weighted accordingly; nevertheless, they were for dilute suspensions which are different from the real disposal system, which is a compacted material. Therefore, best estimate values are selected that are lower to account for the uncertainty associated with the transferability to a real compacted system. The increasing Cl uptake with decreasing pH, at least in the range above 13–12.5, was interpreted in terms of surface charge. At a low aqueous Cl concentration, the experts agreed that a best estimate of 20 L/kg was acceptable, considering these recent data (Fig. 3.2) as the most representative of group A. Experiments done at PSI indicate values of 30–50 L/kg obtained from diffusion experiments, while values obtained from batch experiments are a factor of 2 lower. The new Pointeau et al. data agreed quite well with the PSI diffusion data (the diffusion data give credibility to the data of Pointeau et al.). Lower and upper limits were agreed as 50 and 5 L/kg, respectively. The spread of limits was relatively small reflecting the fact that there were many data with modest scatter.

At a Cl aqueous concentration higher than 1 mmol (group B), R_d is in the range of 0.2–10 L/kg for sorption onto cement pastes. A best estimate R_d for States I to III as 1 L/kg was selected by the experts, with an upper and lower value of 10 and 0.2 L/kg, respectively. Any experimental trend between states was lost in the experimental "noise". It was recognised that the group B data do not represent a "true" sorption process.

3.1.3.8 Sorption at State II

At low Cl concentrations, the Pointeau et al. data show State II R_d values (which range from 10 to 30 L/kg to about 200 L/kg) to be slightly higher than those for State I. The experts selected the upper and lower limits for R_d as 200 and 10 L/kg, respectively, and the best estimate as 50 L/kg (for chloride background concentrations $\leq$1 mmol).

As stated above in Sect. 3.1.3.7, with no detectable trend at higher Cl concentrations (i.e. group B data), a best estimate R_d for States I to III as 1 L/kg was selected by the experts, with an upper and lower value of 10 and 0.2 L/kg, respectively. Note that the absence of a trend at higher Cl concentrations is not unexpected because higher chloride leads to the formation of Friedl's salt, which is a different process than sorption according to the K_d concept.

3.1.3.9 Sorption at State III

State III R_d values for Cl at low overall Cl concentrations are limited. Pointeau et al. (2008) suggest using the R_d for State I as the conservative value for degraded cement systems in safety assessments. The experts agreed to keep the same best

estimate as for State I (20 L/kg), but to increase the range of upper and lower limits and to go one order of magnitude each way to broaden uncertainty in the absence of data (for chloride background concentrations $\leq$1 mmol).

As stated above in Sect. 3.1.3.7, at higher Cl concentrations (background chloride >1 mmol), a best estimate R_d for States I to III as 1 L/kg was selected by the experts, with an upper and lower value of 10 and 0.2 L/kg, respectively.

3.1.3.10 Sorption at State IV

No sorption data for calcite were found in the literature; hence, a value of zero is assigned for State IV.

3.2 Iodine

3.2.1 Chemical Form, Speciation, and Solubility

Similar to chlorine, mainly radioactive isotopes of iodine are important in the present context. Stable iodine is also present in many environments, but only at comparatively low (trace) concentrations. As discussed in the following, the aqueous chemistry of iodine is also somewhat more complex than that of chlorine.

Radioactive isotopes of iodine typical of low and intermediate level waste include ^{125}I, ^{131}I, and ^{129}I (ONDRAF/NIRAS 2011). The long-lived radionuclide ^{129}I (half-life 1.6×10^7 years) is produced by uranium fission primarily in nuclear power reactors. Significant amounts were released into the atmosphere as a result of nuclear weapons testing in the 1950s and 1960s. It is also naturally produced in very small quantities, (1) due to the spontaneous fission of natural uranium, (2) by cosmic ray spallation of trace levels of xenon in the atmosphere, and (3) by cosmic ray muons striking tellurium-130 (Edwards 1962; Fabryka-Martin et al. 1985). LILW may contain ^{129}I from ion exchange resins (treatment of primary effluents), concentrated fluids obtained from evaporating boric acid containing effluents, filter sludge, and cartridge filters, and from operation of research facilities.

The Eh–pH diagram for iodine is shown in Fig. 3.8 and is based on the reaction:

$$I^- + 1.5\,O_2(aq) = IO_3^-, \mathrm{Log}\,K = -17.68\left(25\,^\circ C\right) \tag{3.2}$$

Within the stability field of water, inorganic iodine is present as iodate (IO_3^-) and iodide (I^-) as the oxidised and the reduced form, respectively. Both species may persist in a cementitious environment depending on the speciation of iodine in the

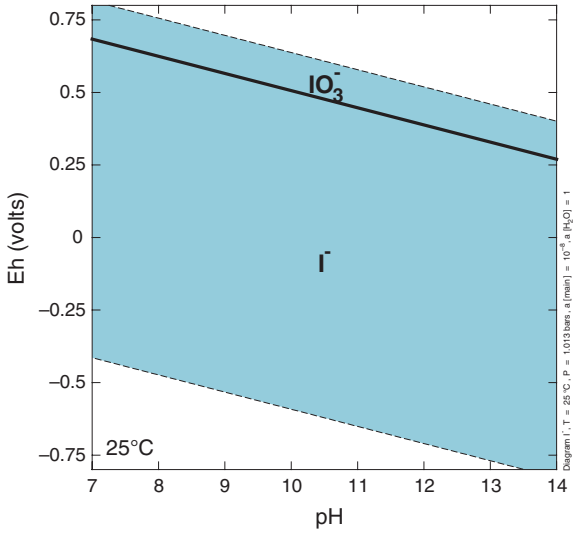

Fig. 3.8 Eh–pH diagram of iodine calculated with *The Geochemist's Workbench®*. Iodine activity is 10^{-8}

waste and the redox potential of the concrete. The boundary between IO_3^- and I^- in Fig. 3.8 has a slope of −0.059 and intersects the Eh axis at 1.09, i.e.:

$$E_h = 1.09 - 0.059\ pH \tag{3.3}$$

In natural waters, iodine speciation is usually indicated as the reduced anion iodide (I^-), although thermodynamic considerations predict that the more probable stable species is the oxidised iodate anion IO_3^- (see Hem 1985 and also below).

In the absence of active reductants, the redox potential in an aerated cementitious system is controlled by the oxygen partial pressure through the following reaction:

$$O_2(g) + 4e^- + 4H^+ = 2H_2O, \text{Log } K(25\,^\circ C) = 83.1056 \tag{3.4}$$

Taking the partial pressure of O_2 (g) in air as 0.2, the redox potential can be expressed as follows:

$$E_h = 1.22 - 0.059\,pH \tag{3.5}$$

Comparing this with the redox expression for the IO_3^-/I^- boundary, the latter has a lower intersect value (1.09 compared to 1.22). This means that the redox potential controlled by oxygen is higher than that controlled by the IO_3^-/I^- couple so that IO_3^- should be the dominant species existing in an oxidising cementitious system. However, I^- may prevail if the O_2 partial pressure decreases, e.g. due to the depletion of O_2 downwards into soil or repository or the reduction of O_2 by reductants present in cement. Bonhoure et al. (2002) illustrated spectroscopically that both I^- and IO_3^- may be sorbed on cement and CSH phases and the iodine

speciation does not change during sorption processes. Atkins and Glasser (1992) suggest that the likely speciation of iodine in a cementitious system is I^- because:

- oxidation of I^- to IO_3^- by molecular oxygen occurs through a slow reaction rate; even in an oxygenated aqueous waste stream, I^- may persist owing to slow kinetics; and
- the presence of reductants such as BFS in cement (in slag-rich cement blends, the redox condition is dominated and buffered by reduced S species, mainly S^{2-}, resulting in strongly reducing conditions). Reducing conditions will likely develop within a year in slag-rich cement owing to release of sulphides from the hydrating slag (Atkins and Glasser 1992). Even in Portland cement, reducing conditions will develop after approximately 100 years owing to corrosion of steel (Atkins and Glasser 1992).

Iodine salts are highly soluble except AgI (NEA 2007); therefore, precipitation as a simple iodide solid phase (salt) in cement is unlikely (see also the recent review of Evans (2008) and earlier work of Glasser (1989). The incorporation of iodine into cement phases is however possible. Brown and Grutzeck (1985) studied the leaching of the iodine equivalent of Friedel's salt (the AFm iodine analogue is $3CaO{\cdot}Al_2O_3{\cdot}Ca(IO_3)_2{\cdot}12H_2O$) and found the equilibrium soluble concentration of iodine to be about 0.03 mmol. Note that this is about two orders of magnitude lower than the chloride concentration controlled by the solubility of Friedel's salt reported by others (Bothe and Brown 2004). Leaching rates measured for the AFm iodine analogue compare well to the ones measured for $Ba(IO_3)_2$, $Ca(IO_3)_2$, and $Hg(IO_3)_2$ encapsulated in cement (Potgieter and Marjanoric 2007) suggesting similar binding mechanism.

3.2.2 Sorption Values from the Literature for the Benchmark Cement

Reviewed R_d values for iodine in a cementitious system are presented in Fig. 3.9 and Table A.2 (see Annex). The pH values for the data of Andra (2005) were reinterpreted according to the cement phases present in the system, i.e. the pH in a system containing pure $Ca(OH)_2$ has a pH of 12.5, while the pH of a calcite system is set at 8. The pH value in a system containing one of the CSH phases is in between pH 8 and 12.5 and decreases with decreasing C/S ratio.

From Fig. 3.9 and the literature reviewed, the following observations can be made:

- The major sink for iodine in a cementitious system seems to be cement phase(s), whereas geologic materials used as aggregate or filler materials do not seem to contribute to the sorption capacity of cementitious materials (Atkins and Glasser 1992);

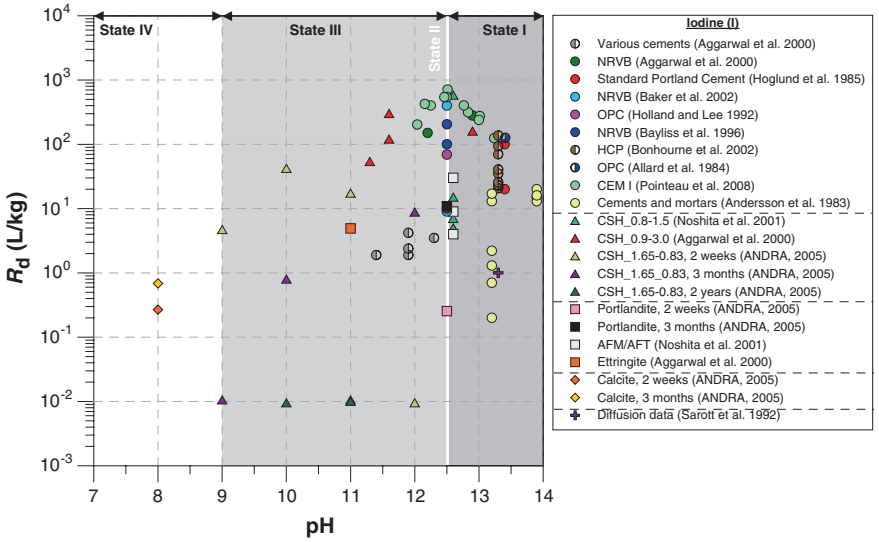

Fig. 3.9 Distribution ratio (R_d) of iodine in cementitious systems. Values are presented as a function of pH in terms of different states of cement evolution. For data where no information about pH was available from the original source (e.g. Andra 2005), pH is interpreted based on the mineral phase(s) present in the system (see text). Various cements (Aggarwal et al. 2000) include BFS/OPC (3/1 and 9/1), PFA/OPC (3/1 and 10/1), and limestone/OPC (6/1)

- Several studies illustrate a strong sorption of iodine on CSH phases, and the sorption increases with increasing C/S ratio (Aggarwal et al. 2000). This suggests that a higher R_d is expected at the States I and II compared to the States III and IV of cement degradation;
- One data set indicates a significant decrease in sorption as a function of time (Andra 2005). R_d for CSH phases dropped about 4 orders of magnitudes to an insignificant value after 2 years of contact time. Note that most of the other sorption experiments reviewed here were run for several days or months only;
- Sorption of iodine may decrease significantly as the initial iodine concentration increases (Anderson et al. 1983). This behaviour resembles that of chlorine (Baker et al. 2002);
- Although AFm and AFt phases have been shown to be probably the strongest iodine sorbent, Noshita et al. (2001) found lower R_d values on these phases than on CSH phases;
- There seems a tendency that R_d decreases as the cement system degrades and pH drops. This does not contradict experimental data where R_d decreases with decreasing C/S ratio in CSH (Aggarwal et al. 2000);
- Iodine sorption on calcite is weak, in agreement with findings from studies using geologic materials as sorbent (Badbury and Bayens 1997a);
- Studies suggest that the sorption of iodine depends on its speciation. Evans (2008) concludes (based on his literature survey) that CSH phases sorb

IO_3^- stronger than I^-, while Allard et al. (1984) suspected that the high sorption of iodine on cements is probably due to the sorption of IO_3^- which is the oxidation product of I^- initially introduced in the system. Bonhoure et al. (2002) however illustrated that neither I^- nor IO_3^- changes its initial speciation during sorption. In any case, as the majority of experiments use I^- as the initial sorbing species, the reported R_d values are normally reported as R_d for I^-. Note that in the majority of the studies, iodine speciation is assumed to be I^- with no knowledge if I^- is oxidised to IO_3^- or not; and

- R_d derived from diffusion experiments performed on hardened cement paste (Sarott et al. 1992) is about an order of magnitude lower than that from a batch test (Wieland and Van Loon 2002). However, in view of the difficulties in determining reliable values from inverse optimisation of experimental breakthrough curves, a lower weight was assigned to the diffusion data (Sarott et al. 1992). The difficulty to obtain reliable and consistent R_d values from diffusion tests was further confirmed by Jakob et al. (1999). In the latter study, sorption values ranged from ~10 to 50 L/kg when a simple linear sorption model was invoked. Use of a first-order kinetic model combined with linear sorption resulted in a best-fit sorption value in the range ~15–110 L/kg. For the same reason as for the Sarott et al. diffusion data, values from the Jakob et al. study are also given a lower weight. Nevertheless, the use of diffusion-type experiments to infer uptake values merits further consideration because the experimental conditions (e.g. S/L ratio) are much closer to the ones prevailing under repository conditions.

3.2.3 Sorption Mechanisms and Selected Sorption Values

Because of the similarity in chemical behaviour between halogens, the sorption mechanism of iodine on cement is expected to be alike to that of chlorine. This implies that chlorine may compete with iodine for sorption sites on cement and vice versa. Experimental evidence shows, however, that such competition is not very important for low-level waste disposal because of a generally relative low background Cl concentration (see Sect. 3.2.3.2). Based on the observation from chlorine data, the important factors influencing iodine sorption on cement are likely to be pH and the aqueous concentrations of iodine, other halogens and sulphate in pore water (competing for sorption sites).

3.2.3.1 Influence of pH on Iodine Sorption

As shown by the Pointeau et al. (2008) data in Fig. 3.2 (Sect. 3.1.2), the R_d evolution for iodine as a function of pH looks similar to that of chlorine although R_d for iodine is systematically higher. A possible explanation for the higher affinity for I^- compared to Cl^- could be the much lower initial total I^- concentration compared

to that of Cl^-. While initial I^- concentration was 1.4×10^{-8} m, the total Cl^- concentration was between 2×10^{-4}–10^{-5} m, mainly due to stable Cl^-. Although the amount of stable I^- in solution was not determined, it is expected to be much lower than the stable Cl^-. Linking these observations with the notion that increasing background concentration decreases R_d may explain the difference. To be consistent with the behaviour of chlorine, one may expect the highest R_d for iodine at State II and a lower R_d at States I and III as demonstrated by the data of Pointeau et al. (2008). The R_d data reviewed (Fig. 3.9) agree with the expected pH influence on R_d for iodine.

3.2.3.2 Influence of Aqueous Concentration of Chlorine

The chlorine data (Sect. 3.1.3.1) demonstrated that a high concentration of dissolved Cl in pore water reduces R_d. One could expect the same to be true for iodine tracers, because an elevated Cl concentration in pore water may result in high coverage of sorption sites on cement by Cl so that iodine sorption might be hindered. Atkins and Glasser (1992) demonstrated that the addition of a 0.1 mol/L chloride solution (1000 fold excess over iodide) causes iodide desorption (13–8 or 8–5 %) from CSH phases. However, for AFm and AFt, addition of Cl^-concentrations similar to those of I^- had a negligible effect on I^- sorption. The effect of Cl on I sorption was thus considered to be minor. One must note that the I concentration in the experiments of Atkins and Glasser was about 10^{-4} mol/L which is much higher than most of the I concentrations used for sorption experiments listed in Table A.2. Sorption mechanisms might be different at lower I concentrations, and so the effect of competing anions like Cl may be smaller too. On the other hand, these authors stated that salt-rich waste streams that contain almost molar levels of NO_3^-, NO_2^-, or SO_4^{2-}, etc., may provide considerable competition for sorption sites. The quantification of these potential effects can be done on the basis of data on the chemical inventory (salt-rich waste streams) of LILW streams.

Because of similar chemical behaviours between iodine and chlorine, the selection of R_d values for iodide should account for competing ions available in high concentrations, including Cl: at Cl concentration higher than 1 mmol, i.e. for waste streams containing evaporator concentrates, R_d values could be reduced by the same factor as was assigned for chlorine. Data for evaporator concentrates illustrated that 86.5 % of concentrates have an estimated mean chloride concentration of 0.07–0.21 m, 9.7 % have a mean concentration of 0.38 m, and 3.2 % have a concentration of 0.45 mol/L (Wang et al. 2009). These concentration ranges are similar in magnitude to the 0.1 mol/L Cl^- used by Atkins and Glasser (1992) in their analysis of competing effects between I^- and Cl^- on CSH. Although the effect was shown to be small, the best estimate values for I^- sorption onto benchmark cement were cautiously reduced using a similar sorption reduction factor as for Cl^-. In this way, potential competing effects from other anions are accounted for. A conservative approach would be to have the same best estimate for I^- as for Cl^-, i.e. 1 L/kg (sorption reduction factor for I^- would range from 10 to 30).

3.2.3.3 Sorption Mechanisms

Most of the literature reviewed in this work demonstrates that iodine species (I^-/IO_3^-) sorb stronger on cement materials than on most geologic materials in groundwater systems. Probable sorption mechanisms onto hardened cement and CSH mentioned in the literature include sorption and/or incorporation (Atkins and Glasser 1992), electrostatic interactions which implies opposite charge on the sorbate (Bonhoure et al. 2002), and surface complexation (Heath et al. 1996). Precipitation as an iodide salt on the other hand is a very unlikely uptake process (see above).

Evans (2008) recently summarised literature data and concluded that I^- retention on cement can be defined as sorption through surface processes or incorporation of I^- in cement structures. Possible sorption sinks in cement are as follows (ranked in decreasing order of sorption potential): AFm, high C/S ratio CSH phases, AFt, low C/S ratio CSH phases, and hydrotalcite (Atkins and Glasser 1992). AFm seems the strongest scavenger for I^- in cement (Brown and Grutzeck 1985; Atkins and Glasser 1990). For sorption onto AFm and AFt, substitution of SO_4^{2-} by I^- is considered to be the predominant process (Atkins and Glasser 1990, 1992). Batch sorption experiments using pure CSH phases illustrated that (1) sorption increases with increasing C/S ratio in spite of increased competition with OH^-, and (2) CSH has a much stronger affinity (at least five times higher) for iodate than iodide (Atkins and Glasser 1992). The latter observation is important for safety assessment because iodide is the most probable iodine species under near-surface repository conditions, although iodate could possibly form in the very long run when most reductants (e.g. BFS in CEM III) have been neutralised away. Therefore, using iodide sorption values for the entire lifetime of a near-surface disposal facility is conservative in view of the higher values for iodate (Atkins and Glasser 1992).

X-ray absorption spectroscopic data indicated, however, that CSH is not the uptake-controlling phase for IO_3^- in a hardened cement paste (Bonhoure et al. 2002). This confirms earlier observations that AFm is a much more efficient scavenger for I^- than CSH (Atkins and Glasser 1992). Sorption on CSH is not the major uptake phase. It seems that the uptake process for IO_3^- is immobilisation into a solid similar to $Ca(IO_3)_2$ or KIO_3. The same study also demonstrates that no changes in the formal oxidation state of iodine (I^- or IO_3^-) upon uptake by cement paste and CSH occurs. Bonhoure et al. (2002) found that although I^- sorption was significant, the intensity of the I^- EXAFS signals was very weak which hindered a more detailed interpretation of the chemical environment of I^- in these systems.

Toyohara et al. (2000, 2002) proposed that the AFm phase ($4CaO{\cdot}Al_2O_3{\cdot}13H_2O$) controls the uptake of iodine by forming a new hydrate ($3CaO{\cdot}Al_2O_3{\cdot}CaI_2{\cdot}12H_2O$); also, I^- sorption was shown to be reversible up to a concentration of 10^{-2} m.

Atkinson and Nickerson (1988) found that the uptake of iodine on cements is nonlinear. R_d values were found to decrease when the initial iodine concentration

Table 3.2 Selected best estimate, upper and lower limit R_d values for iodide

pH state	Best estimate (L/kg)	Upper limit (L/kg)	Lower limit (L/kg)
State I	1×10^0 (1)	3×10^2 (10)	0 (0)
State II	1×10^1 (1)	1×10^3 (10)	0 (0)
State III	1×10^0 (1)	5×10^2 (10)	0 (0)
State IV	4×10^{-1} (0)	4×10^0 (0)	0 (0)

Values in parentheses are high chloride background concentrations

increases (Bayliss et al. 1996), which was similar to chlorine uptake observed in the same work. Heath et al. (1996) interpreted the sorption of I^- on CSH phases of different C/S ratio using the diffuse-double-layer surface complexation model developed by Dzombak and Morel (1990).

Proposed best estimate R_d (L/kg) values are provided in Table 3.2. These values are supported by the experimental data from Table A.2 and Fig. 3.9 and are broadly similar to those from chloride, since at low background concentrations similar sorption mechanisms would be expected to be at work for both chloride and iodide (electrostatic interactions, incorporation into AFm phases, etc.). There was, however, a significant spread of data, and this spread is reflected in the range of upper and lower limits. In order to be consistent with the treatment of chloride results (where reliable diffusion data gave a consistent picture with batch sorption data), earlier estimates of R_d were reduced to take account of diffusion experiment data from Sarott et al. (1992), even though these values were of low reliability. Nevertheless, the central anchor point for data selection was placed in the vicinity of the diffusion data because it was obtained at a S/L ratio close to real compacted materials [the issue of apparent dependency of R_d on S/L was raised by Wieland and Van Loon (2002)]. By analogy with chloride, values of R_d appropriate to evaporator concentrates (chloride at millimolal levels) are also given; the same numerical values as for chloride were selected. The following R_d selections in Sects. 3.2.3.4–3.2.3.7 apply to low chloride concentrations.

3.2.3.4 Sorption at State I

Although there are many data points at the higher end of the range of values (10–100 L/kg), 1 L/kg was selected as best estimate in order to be consistent with the approach adopted for chloride in terms of diffusion data: because there are uncertainties about the effect of S/L ratio, R_d was placed in the range of diffusion data. Unlike chloride, the R_d values from diffusion tests were much lower than the batch sorption data of Pointeau et al. (2008). In other words, the comparison of batch and diffusion-derived data suggests that the S/L ratio has a significant effect in case of iodide, but not in case of chloride. Overall, sorption at State I appeared to be lower than State II, a trend consistent with chloride although the data were spread over a wider range. The experts agreed on a best estimate of 1 L/kg with

upper and lower limits of 300 and 0 L/kg, respectively. Given the very low R_d values measured for State III after long experimental times (Andra 2005), the experts felt that they had to assign a 0 L/kg value for the lower bound for all states.

For the remaining states, the trends between states were again based on batch data, after the overall magnitude was anchored to low values based on that from State I.

3.2.3.5 Sorption at State II

As stated above in Sect. 3.2.3.4, sorption appeared to be stronger at State II than State I. The experts assigned values of 10 L/kg as the best estimate, 1000 L/kg as the upper limit and 0 L/kg for the lower limit, based on the observation that the Pointeau et al. (2008) data increase by an order of magnitude when moving from State I to II. The trend from the Pointeau et al. data were followed, but the absolute values are based on State I, increased by a factor of 10.

3.2.3.6 Sorption at State III

Sorption was observed to be lower at State III than at State II, and with a wider spread. The experts agreed on a best estimate of 1 L/kg (the same as for State I) with upper and lower limits of 500 and 0 L/kg, respectively. The experts noted that they were deriving a single value for State III which covered a range of pH values and this would affect sorption. This was taken as a further reason to put forward a conservative value. Also during State III, there could be infiltration of anions from the overlying soil which would cause competition with I^-.

3.2.3.7 Sorption at State IV

The experts noted that there is very little information directly relevant to State IV. However, data for sorption onto geological materials showed very weak sorption. To be conservative, the experts selected a best estimate of 0.4 L/kg, an upper limit of 4 L/kg and again a lower limit of 0 L/kg.

References

S. Aggarwal, M.J. Angus, J. Ketchen, Sorption of radionuclides onto specific mineral phases present in repository cements. NSS/R312, AEA-DandR-0395, 2000

B. Allard, L. Eliasson, S. Hoglund, K. Andersson, Sorption of Cs, I and actinides in concrete systems, SKB Technical Report 84–15, 1984

C. Alonso, M. Castellote, C. Andrade, Chloride threshold dependence of pitting potential of reinforcement. Electrochim. Acta **47**, 3469–3481 (2002)

Andra, Référentiel de comportement des radionucléides et des toxiques chimiques d'un stockage dans le Callovo-Oxfordien jusqu'à l'homme, Site de Meuse/Haute-Marne, Tome 1/2: Chapitres 1 à 4, Dossier 2005 Argile, 2005

K. Andersson, B. Torstenfelt, B. Allard, Sorption and diffusion studies of Cs and I in concrete. SKB Technical Report (1983), pp. 83–13

M. Atkins, F.P. Glasser, Encapsulation of radioiodine in cementitious waste forms, in *Proceedings of the Material Research Society Symposium*, vol. 176 (1990), p. 15

M. Atkins, F.P. Glasser, Application of portland cement-based materials to radioactive waste immobilization. Waste Manag. **12**, 105–131 (1992)

A. Atkinson, A. Nickerson, Diffusion and sorption of caesium, strontium, and iodine in water-saturated cement. Nucl. Technol. **81**, 100–113 (1988)

B. Baeyens, M.H. Bradbury, A mechanistic description of Ni and Zn sorption on Na-montmorillonite, 1: Titration and sorption measurements. J. Contam. Hydrol. **27**, 199–222 (1997)

S. Baker, R. McCrohon, P. Oliver, N.J. Pilkington, The sorption of niobium, tin, iodine and chlorine onto NIREX reference vault backfill, in *Proceedings of the Material Research Society Symposium*, vol. 333 (1994), pp. 719–724

S. Baker, P. Oliver, R. McCrohon, Near-field batch sorption studies—1992 to 1998, AEAT/ERRA-0345 (2002)

S. Bayliss, R. McCrohon, P. Oliver, N.J. Pilkington, HP. Thomason, Near-field sorption studies: January 1989–June 1991, NSS/R277, AEA-ESD-0353 (1996)

U. Berner, *Concentration Limits in the Cement Based SWISS Repository for Long-Lived, Intermediate-Level Radioactive Wastes (LMA)*. (PSI Bericht Nr., Villigen, 1999), pp. 99–10

U. Berner, *Project Opalinus Clay: Radionuclide Concentration Limits in the Cementitious Near-Field of an ILW Repository*. (PSI Bericht, Villigen, 2002), pp. 02–26

C.M. Bethke, *The Geochemist's Workbench, Release 6.0, GWB Reference Manual, Hydrogeology Program*. (University of Illinois, Illinois, May 2006)

I. Bonhoure, A.M. Scheidegger, E. Wieland, R. Dahn, Iodine species uptake by cement and CSH studied by I K-edge X-ray absorption spectroscopy. Radiochim. Acta **90**, 647–651 (2002)

J. Bothe Jr., P. Brown, PhreeqC modelling of Friedel's salt equilibria at 23 ± 1 °C. Cem. Concr. Res. **34**, 1057–1063 (2004)

M.H. Bradbury, B. Baeyens, *Far-Field Sorption Data Bases for Performance Assessment of a L/ILW Repository in an Undisturbed Palfris Marl Host Rock*. (PSI Bericht, Villigen, 1997a), pp. 97–15

M.H. Bradbury, B. Baeyens, *Far-Field Sorption Data Base for Performance Assessment of a HLW Repository in an Undisturbed Opalinuss Clay Host Rock*. (PSI Bericht Nr., Villigen, 2003), pp. 03–08 (Nagra NTB 02–19)

M.H. Bradbury, F. Sarott, *Sorption Databases for the Cementitious Near-Field of a L/ILW Repository for Performance Assessment*. (PSI Bericht, Villaign, 1995), pp. 95–06

D.R. Brown, M.W. Grutzeck, Iodine waste forms: calcium aluminate hydrate analogues, *in Proceedings of the Material Research Society Symposium*, vol. 44 (1985), pp. 911–918

D.A. Dzombak 1, F.F.M. Morel, *Surface Complexation Modelling*. (Wiley, New York, 1990)

R.R. Edwards, Iodine-129: its occurrence in nature and its utility as a tracer. Science **137**(3533), 851–853 (1962)

N.D.M. Evans, Binding mechanisms of radionuclides to cement. Cem. Concr. Res. **38**, 543–553 (2008)

J. Fabryka-Martin, H. Bentley, D. Elmore, P.L. Airey, Natural iodine-129 as an environmental tracer. Geochim. et. Cosmochim. Acta **49**, 337–347 (1985)

F.P. Glasser, *Immobilization of Radwaste in Cement Based Matrices*. (Aberdeen University, Scotland, 1989) (DoE/RW/89.133)

F.P. Glasser, J. Marchand, E. Samson, Durability of concrete- Degradation phenomena involving detrimental chemical reactions. Cem. Concr. Res **38**, 226–246 (2008)

H.P. Gunkel, Die Bindung des Chlorids im Zementstein und die Zusammensetzung chloridhaltiger Porenlösungen, Dissertation Universität Dortmund (1992)

T. G. Heath, D. J. Ilett, C. J. Tweed, Thermodynamic modelling of the sorption of radioelements onto cementitious materials, in *Proceedings of the Material Research Society Symposium*, vol. 412 (1996), pp. 443–449

J.D. Hem, *Study and Interpretation of the Chemical Characteristics of Natural Water*, 3rd edn. (U.S Geological Survey Water-supply Paper 2254, 1985)

S. Hoglund, L. Eliasson, B. Allard, K. Andersson, B. Torstenfelt, Sorption of some fission products and actinides in concrete systems, in *Proceedings of the Material Research Society Symposium*, vol. 50 (1985), pp. 683–690

T.R. Holland, D.J. Lee, Radionuclide Getters in Cement. Cem. Concr. Res. **22**, 247–258 (1992)

D. Izquierdo, C. Alonso, C. Andrade, M. Castellote, Potentiostatic determination of chloride threshold values for rebar depassivation: experimental and statistical study. Electrochim. Acta. **49**, 2731–2739 (2004)

D. Jacques, L. Wang, E. Martens, D. Mallants, Time dependency of the geochemical boundary conditions for the cementitious engineered barriers of the Belgian surface disposal facility, Project near surface disposal of category A waste at Dessel, NIRAS-MP5 DATA-LT(NF) Version 1, NIROND-TR 2008-24 E (2008)

A. Jakob, F. Sarott, P. Spieler, Diffusion and sorption on hardened cement pastes—experimental and modelling results. Nagra Techncial Report (1999), pp. 99–06

E.P. Nielsen, D. Herfort, M.R. Geiker, Binding of chloride and alkalis in Portland cement systems. Cem. Concr. Res. **35**, 117–123 (2005)

K. Noshita, T. Nishi, T. Yoshida, H. Fujihara, N. Saito, S. Tanaka, Categorization of cement hydrates by radionuclide sorption mechanism, in *Proceedings of the Material Research Society Symposium*, vol. 663 (2001), pp. 115–121

Nuclear Energy Agency (NEA-OECD), State of the art report on iodine chemistry, NEA/CSNI/R(2007)1 (2007)

ONDRAF/NIRAS, Identification of critical radionuclides through a screening of the ondraf/niras 2003/2004 radiological inventory for category A waste, Nirond-tr 2007-05e, Apr 2011

I. Pointeau, P. Reiller, N. Macé, C. Landesmann, N. Coreau, Measurement and modelling of the surface potential evolution of hydrated cement pastes as a function of degradation. J. Colloid. Interface. Sci. **300**, 33–44 (2006)

I. Pointeau, N. Coreau, P.E. Reiller, Uptake of anionic radionuclides onto degraded cement pastes and competing effect of organic ligands. Radiochim. Acta **96**, 367–374 (2008)

S.S. Potgieter, L. Marjanoric, A further method for chloride analysis of cement and cementitious materials—ICP-OES. Cem. Concr. Res. **37**, 1172–1175 (2007)

F. Sarott, M.H. Bradbury, P. Pandolfo, P. Spieler, Diffusion and adsorption studies on hardened cement paste and the effect of carbonation on diffusion rates. Cem. Concr. Res. **22**, 439–444 (1992)

D. Savage, *Alteration of Boom Clay by Hyperalkaline Fluids: a Review of Potential Processes and Input Data for Reaction-Diffusion Simulations*. (QuantiSci, Leicestershire, UK, 1999)

M. Toyohara, M. Kaneko, S. Ueta, N. Mitsutsuka, H. Fujihara, T. Murase, N. Saito, Iodine sorption onto mixed solid alumina cement and calcium compounds. J. Nucl. Sci. Technol. **37**, 970–978 (2000)

M. Toyohara, M. Kaneko, N. Mitsutsuka, H. Fujihara, N. Saito, T. Murase, Contribution to understanding iodine sorption mechanism onto mixed solid alumina cement and calcium compounds. J. Nucl. Sci. Technol **39**, 950–956 (2002)

L. Wang, E. Martens, D. Jacques, P. De Canniere, J. Berry, D. Mallants, Review of sorption values for the cementitious near field of a near surface radioactive waste disposal facility, NIROND-TR 2008-23E, Apr 2009

E. Wieland, L. Van Loon, *Cementitious Near-Field Sorption Data Base for Performance Assessment of an ILW Repository in Opalinus Clay*. (PSI Bericht Nr., Villigen, 2002), pp. 03–06

H. Zibara, R.D. Hooton, M.D.A. Thomas, K. Stanish, Influence of the C/S and C/A ratios of hydration products on the chloride ion binding capacity of lime-SF and lime-MK mixtures. Cem. Concr. Res. **38**, 422–426 (2008)

Chapter 4
Sorption Values for Caesium, Strontium, Radium, and Silver

Abstract This chapter discusses the sorption behaviour of several elements—caesium (Cs), strontium (Sr), radium (Ra), and silver (Ag)—that tend to form simple aqueous ions and typically interact with minerals mainly by ion exchange reactions. In contrast, these elements show only a very weak tendency towards the formation of coordinative bonds. Many types of radioactive waste contain a range of radioactive isotopes of these four elements. The main sorption process of Cs on hardened cement pastes (HCP) is an exchange-type process on the CSH phases. Therefore, Cs sorption is controlled by the concentration of competing ions (Na, K, and Ca) and by the charge of the interlayer CSH surface, which in turn are a function of the C/S ratio. Cs sorption increases with increasing HCP degradation and decreasing C/S ratio. This is directly related to the decreasing concentration of competing cations. Dissolved Na and K reach high concentrations in fresh hydrated cement (State I) but are largely leached in the following HCP degradation states. In degraded HCP (State II and following), aqueous Ca concentrations decrease with decreasing C/S ratio of the CSH phases. In case of Cs, aggregate material containing phyllosilicates (such as micas and clay minerals) used in mortar or concrete may influence Cs behaviour, as Cs sorbs particularly strong to these minerals. For radium and strontium, essentially a similar behaviour as for Cs is observed, with the difference that competition by Ca is more important in comparison with competition by Na and K. In case of silver, no reliable sorption values on cementitious materials are available to date. However, there are several independent indications that Ag sorption on cementitious materials is different from zero, and that Ag may show sorption behaviour analogous to alkali earth elements.

4.1 Caesium

4.1.1 Chemical Form, Speciation, and Solubility

The relevance of caesium in the context of waste disposal is entirely associated with radioactive isotopes of this element. Caesium exists in the environment in the +1 oxidation state. There is little, if any, tendency for caesium to form aqueous

© Springer International Publishing Switzerland 2016

M. Ochs et al., *Radionuclide and Metal Sorption on Cement and Concrete*,
Topics in Safety, Risk, Reliability and Quality 29,
DOI 10.1007/978-3-319-23651-3_4

complexes in soil/water environments. Baes and Mesmer (1986) report that caesium may be associated with OH^- ions in solution, but that the extent of this association cannot be estimated accurately. The uncomplexed Cs^+ ion forms extremely weak aqueous complexes with sulphate, chloride, and nitrate.

^{137}Cs (half-life 30.0 years) is produced by the fission of uranium in nuclear reactors and is not a naturally occurring radionuclide. The largest source of ^{137}Cs and potential waste material is from nuclear reactor operations. The quantity of ^{137}Cs waste material generated in medical, academic, or commercial facilities is small compared to the quantity of ^{137}Cs waste produced as a result in nuclear reactor operations. Ion exchange resins used to purify coolant water in a nuclear power plant frequently contain large amounts of ^{137}Cs (IAEA 2002) and are typically part of LILW. Approximately 62 % of the total ^{137}Cs inventory for the Belgian LILW is generated by nuclear reactors: 55 % of total inventory occurs in resins. An additional 35 % exists in waste from decommissioning and remediation associated with former research activities (Wang et al. 2009). Resins are partly grouted in drums grouted in monoliths, and partly polymerised with subsequent grouting in monoliths. Waste from nuclear research facilities is either bituminized or grouted in drums grouted in monoliths.

4.1.2 Sorption Values from the Literature for the Benchmark Cement

Table A.3 summarises the main experimental conditions of the available R_d values, whereas the selected data (see below) are shown in Fig. 4.1 grouped according to various cementitious materials (concrete, cement pastes, and CSH phases). Values show a very large variability of several orders of magnitude. A similar variation was found in the literature review reported by Andra (2005). Overall, Cs sorption on all cement systems is relatively weak (e.g. Aggarwal et al. 2000; Andra 2005).

Some authors found higher sorption of caesium in concretes than in cement (e.g. Andersson et al. 1983) which was attributed to preferential adsorption of caesium by the aggregates in the crushed concrete (Hietanen et al. 1984, 1985). Because of the possible role of the aggregates in influencing sorption on concrete, only data measured on concrete with calcareous aggregates are shown (only such aggregates are to be used for concrete and backfill in the Dessel repository). Therefore, some data of Allard (1984), Andersson et al. (1983), and all data of Hietanen et al. (1984) and Idemitsu et al. (1991) are not further discussed here. No information was available on the aggregates used in the study by Hietanen et al. (1985). Figure 4.1a shows the retained data for concrete. Most data are within two orders of magnitude with exception of the data from Hietanen et al. (1985) and from Andersson et al. (1983). The data point of Hietanen et al. (1985) was measured on crushed concrete, whereas the experimental data of Jakubick et al. (1987), for example, used concrete coupons ($4 \times 4 \times 0.2$ cm^3) which may explain the difference. The high value of Andersson et al. (1983) was obtained with a solution with a low ionic strength (~5×10^{-2} M, artificial ground water).

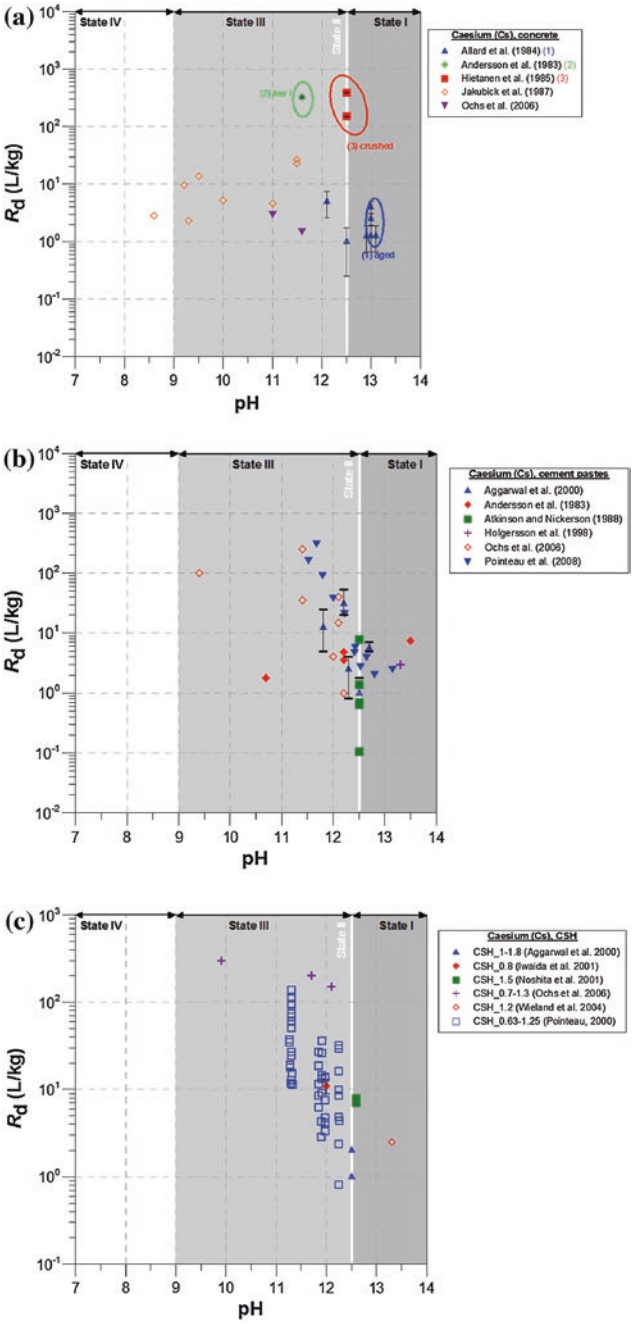

Fig. 4.1 **a** Caesium sorption on concrete (*vertical lines with bars* indicate minimum and maximum). **b** Caesium sorption on cement pastes (*vertical lines with bars* indicate minimum and maximum). **c** Caesium sorption on CSH phases

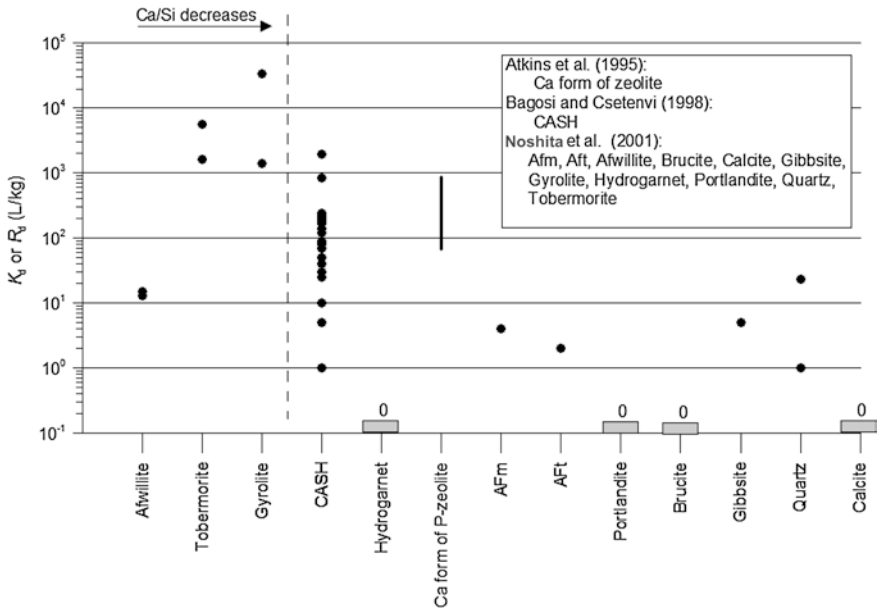

Fig. 4.2 Sorption of caesium on pure cement phases. *Long dashed line* differentiates between the CSH phases (*left*) and the other cement minerals. The range of R_d values as reported in Atkins et al. (1995) is indicated by the *vertical solid line*

The calcareous aggregates probably contribute only slightly to Cs sorption. Bradbury and Baeyens (1997) assumed on the basis of literature review that Cs was not sorbed onto calcite in the presence of two site-specific groundwater types. Bradbury and Baeyens (1997) considered Cs to be non-sorbing at high pH values on pure limestone (based on Tits et al. 1998). The sorption experiments of Noshita et al. (2001) on pure calcite also revealed no sorption on calcite (Fig. 4.2). Jakubick et al. (1987) also found very low sorption of Cs on carbonate aggregates (by α-autoradiographs). On the other hand, if the limestone contains some illite, as is the case for marl (an impure limestone) which in this case contained 22 % illite (known to be a strong sorber for Cs), Cs sorption has been shown to be considerable (~600 L/kg at S/L 0.5 kg/L, Cornell 1992).

4.1.2.1 Cement Pastes R_d Values

Figure 4.1b shows the results from the literature review on R_d values in pure cement systems, i.e. hardened cement paste without ballast or additional aggregates. All experimental data mentioned in Table A.3 (see Annex) are shown with the exception of two data points from Ochs et al. (2006) because they were measured on a peculiar system (CEM I and V HCP reacted with 0.5 M NH_4NO_3 solution to produce a 0.7 C/S ratio system). There is a slight trend of increasing R_d with decreasing pH which can be related to a decreasing C/S ratio with decreasing pH (see further). The data points are quite consistent.

4.1.2.2 CSH Phases R_d Values

The main phase in cement pastes responsible for Cs sorption is CSH (e.g. Aggarwal et al. 2000; Ochs et al. 2006). The CSH of cement pastes is amorphous and contains some Al, presumably substituting for Si in tetrahedral sites. Therefore, data for calcium aluminium silicate hydrate (CASH), for example as reported by Noshita et al. (2001) and shown in Fig. 4.2, may be considered to be representative. But a number of crystalline CASH phases are also known and although unlikely to be encountered in the present scenario, are also shown. Data for the crystalline substances scatter widely because the sorption potential is related to structure type, with open framework and layer-lattice types having the highest uptakes. Here, emphasis is placed on CSH, as reflected by data for the alumina-substituted CASH composition. Figure 4.1c shows the R_d values on CSH phases. Since sorption of Cs increases with decreasing C/S ratio of the CSH phases and because the C/S ratio decreases with chemical cement degradation (i.e. decreasing pH), it is important to interpret only the experimental data for which the CSH phase is in the appropriate pH range. CSH phases with C/S ratios of 1.5 and larger are representative for States I and II (coexisting with portlandite), whereas CSH phases with C/S ratios smaller than 1.5 are representative for State III. Figure 4.1c, showing the R_d values as a function of pH, retains only the data points measured on CSH phases representative for a given cement degradation stage. As such, some data points of Aggarwal et al. (2000), Noshita et al. (2001) and the data point of Iwaida et al. (2001) are not shown.

Figure 4.1c reveals an increase in R_d with decreasing pH, related to a decrease in the C/S ratio of the CSH phases. This is further illustrated in Fig. 4.3 displaying R_d as a function of the CSH phase C/S ratio, and it includes all data of Aggarwal et al. (2000), Noshita et al. (2001), and Iwaida et al. (2001). The variability in the data of Pointeau (2000) in Figs. 4.1c and 4.3 is due to different initial Cs

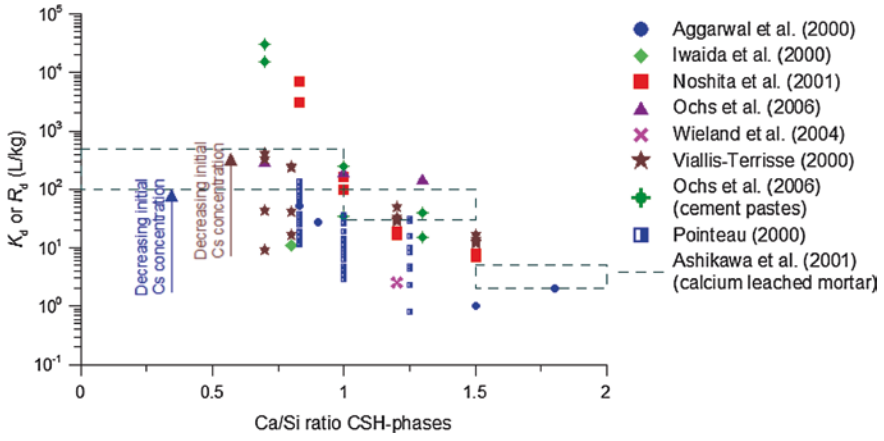

Fig. 4.3 Cs sorption as a function of the CSH phase C/S ratio

concentrations ranging from 3.42×10^{-6} to 8.50×10^{-4} mol/L (see further). The data of Viallis-Terrisse (2000) in Fig. 4.3 show a large variability, especially at low C/S ratio. This variability is due to different initial Cs concentrations used, ranging from 1 to 1×10^{-6} to 10^{-2} mol/L with highest sorption for lowest initial Cs concentration (see further). The effect of decreasing C/S ratio is more important than the composition of the solution, at least for the data for Noshita et al. (2001), who measured R_d for different C/S ratios in the same solution.

4.1.3 Sorption Mechanisms and Selected Sorption Values

4.1.3.1 Sorption Mechanisms

The main sorption process of Cs on hardened cement pastes (HCP) is ion exchange on the CSH phases (Aggarwal et al. 2000; Allard 1984; Andersson et al. 1983; Ochs et al. 2006). Therefore, ionic strength and competing ions (Na, K, and Ca, Hoglund et al. 1985) also influence Cs sorption. Cs sorption increases with decreasing C/S ratio due to the condition of the interlayer CSH surface which changes sign as a function of C/S ratio. At a high C/S ratio, the Ca concentration in the solution is high and the surface is positively charged by adsorption of Ca on the silanol groups resulting in limited Cs sorption. At a low C/S ratio, Ca concentrations in solutions are smaller and the surface is deprotonated at high pH (higher than 9) and therefore negatively charged resulting in an increase in surface sites with high affinity for Cs and thus in higher Cs sorption (Ochs et al. 2006). A similar behaviour was observed for radium (see Sect. 4.3.3) and strontium (see Sect. 4.2.3).

In contrast to CSH phases, other cement phases are less crucial in Cs sorption by ion exchange, although they can play a role in Cs incorporation. Since aggregates are the most abundant component of concrete, impurities present in nominally pure limestones, e.g. montmorillonite or illite, could contribute significantly to the sorption potential. For concretes, ballast material such as sand will contribute only minimally to Cs sorption. In case of limestone or calcite aggregates, the role of the ballast in Cs sorption is not negligible. First of all, caesium sorption on marl (42 % calcite, 22 % illite) has been shown to be considerable (~600 L/kg at S/L 0.5 kg/L Cornell 1992). Secondly, the amount of calcite (in the form of calcareous aggregates) for the ONDRAF/NIRAS LILW backfill grout is large, approximately 1390 kg (64 wt%) versus 510 kg CEM III (23 wt%).

Sorption is further governed by the exchange capacity of the cement. The cation exchange capacity (CEC) of CSH is ~1.2 eq/kg (Tits et al. 2006b). Cs sorption increases with decreasing C/S ratio (Pointeau 2000; Pointeau et al. 2001; Ashikawa et al. 2001; Faucon et al. 1998). This is especially pronounced at tracer concentrations (Heath et al. 1996; Viallis-Terrisse 2000). The increasing sorption is related to the decreasing concentration of competing cations, since the aqueous Ca concentration decreases with decreasing C/S ratio of the CSH phases. A

similar behaviour was observed for radium (see Sect. 4.3.3) and strontium (see Sect. 4.2.3). As pointed out by Ochs et al. (2006), the concentration of sorption sites associated with the CSH phases is also a critical factor.

Sorption in State IV on the remaining cement phases and the ballast material is expected to be rather low because sorption on calcite is negligible. However, the presence of small quantities of silica gel in the cement paste and/or e.g. clay minerals in limestone and calcareous aggregates may have a large effect on Cs sorption in State IV.

Taking account of the above information, relatively lower sorption is expected in States I and II due to competition with Na^+ and K^+ in State I and competition with Ca^{2+} for negatively charged CSH surfaces in State II. As degradation of the concrete proceeds during State III (decreasing pH, with lower Ca^{2+} concentration in the aqueous phase and a decreasing C/S ratio of the CSH phases), Cs sorption is expected to increase owing to the reduced aqueous calcium concentration. In State IV, sorption is determined by the remaining ballast material, which is calcite in case of the ONDRAF/NIRAS LILW concrete.

Since the main sorption process for Cs on cementitious materials is ion exchange (Allard 1984; Anderson et al. 1983), caesium sorption is expected to depend on the ionic strength. Several studies have shown that Cs sorption increases with decreasing ionic strength or salinity (Allard 1984; Andersson et al. 1983; Hietanen et al. 1984; Ochs et al. 2006). Similar observations were made by Pointeau et al. (2001) for pure CSH phases.

Some other factors that could potentially influence Cs sorption have been investigated:

- Andersson et al. (1983) observed increased caesium sorption when sulphate and magnesium are added or in case of carbonation (the latter condition reflects a decreasing pH and decreasing ionic strength).
- The sorption of Cs on cement and concrete is not influenced by the presence of gluco-isosaccharinic acid (ISA) (Holgersson et al. 1998).
- Atkinson and Nickerson (1988) found an effect of the S/L ratio: increasing sorption with decreasing S/L ratio which might be due to dilution of the competing ions (Na and K).

Some studies found sorption to be independent of time (Atkinson and Nickerson 1988; Holland and Lee 1992), and others found a time-dependency (e.g. Hietanen et al. 1984). A difference in sorption was also found between crushed samples and concrete coupons (Hietanen et al. 1984). The crushed samples showed mainly sorption on sand ballast (grain size <2 or <4 mm) which was optimally exposed to the Cs-containing test solution.

Figure 4.4 shows the dependency of R_d on the initial concentration. For concrete, R_d shows an increasing trend with increasing initial concentration (at least until ~10^{-7} M). R_d values of about 1–3 L/kg pertaining to the Hietanen et al. (1984) data were obtained on concrete coupons and are less representative because of the relatively small surface area available for sorption. Jakubick et al. (1987) observed linear isotherms for Cs sorption on normal and high-density concretes

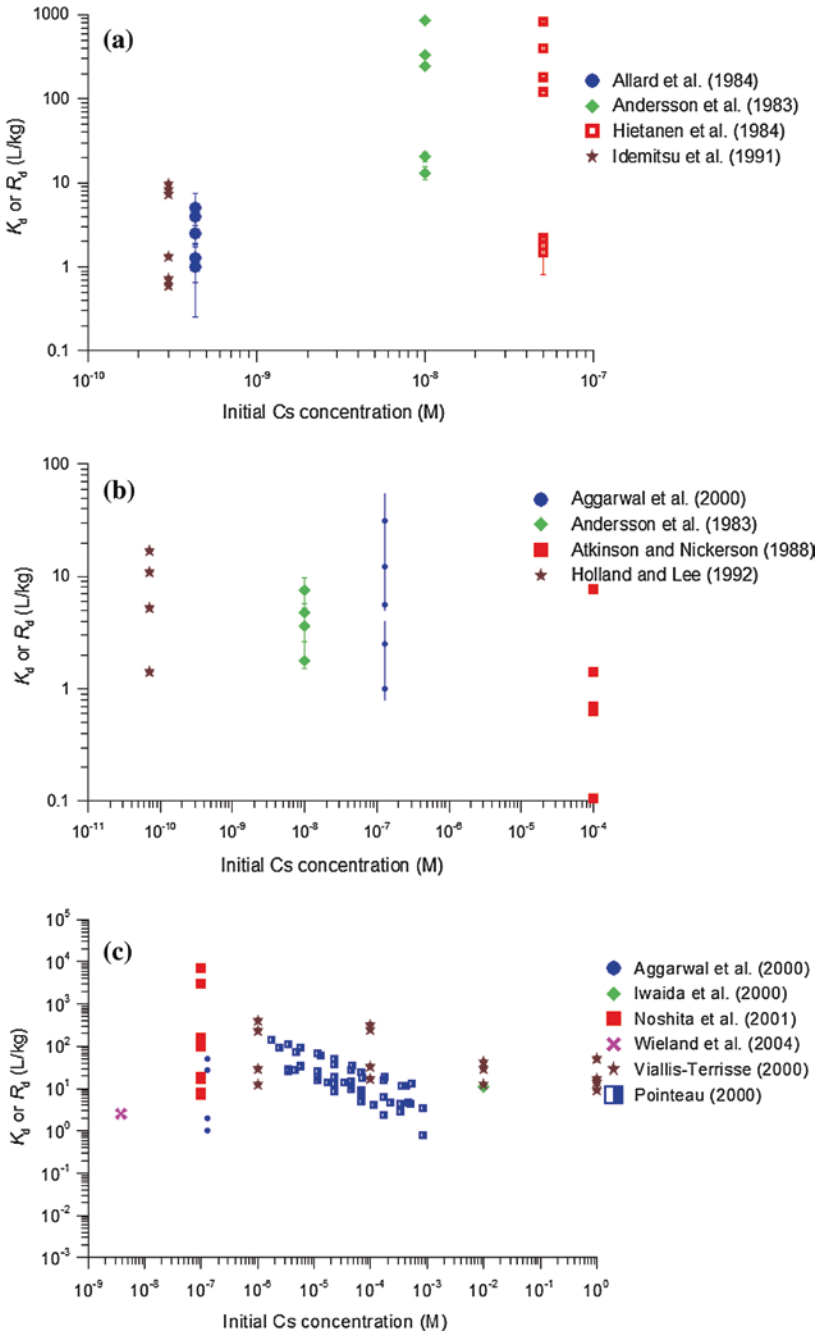

Fig. 4.4 Caesium sorption as a function initial concentration on concrete (*top*), cement paste (*middle*), and CSH phases (*bottom*) (*vertical lines with bars* error; *vertical line* minimum and maximum as given in Allard (1984), Aggarwall et al. (2000), respectively)

for initial Cs concentrations ranging between 6.4×10^{-7} and 1.0×10^{-3} M. The latter would suggest R_d to be independent of initial Cs concentration (i.e. reflecting real sorption). Note that the Cs concentration range of Jakubick et al. is considerably higher than the range displayed for all other data sets.

For cement pastes, there does not seem to be any trend provided the Atkinson and Nickerson (1988) data are given less weight. This would be justified because the background Cs concentration was fairly large (10^{-4} mol/L stable Cs) and because the data are from several experimental approaches with considerable uncertainty in parameter estimation. Atkinson et al. (1984) described the experimental sorption data on hardened OPC with the Langmuir isotherm. When the liquid concentration of Cs is much smaller than ~10^{-4} M, the relation between liquid and sorbed Cs concentration is approximately linear. This is consistent with the observation in Fig. 4.4 that R_d shows no trend between 10^{-11} and 10^{-7} M.

The data of Pointeau (2001) for CSH phases show a decrease in R_d values with increasing (initial or equilibrium) Cs concentration for all C/S ratios. In contrast, Viallis-Terresse (2000) observed that the effect of decreasing R_d with increasing Cs concentration depends on the C/S concentration: the effect is almost negligible at high C/S ratios (1.5 and 1.2), but large at low C/S ratios (0.8 and 0.7). The other data points provided only information on a single initial concentration and are not very useful for detecting a trend with changing initial concentration.

Besides the role of Ca and other competing ions for Cs sorption on the CSH phases, some other factors contribute to the sorption of Cs to cementitious systems. Ochs et al. (2006) indicated that the concentration of sorption sites on the CSH phases plays a role.

Sorption or the leachability of Cs from cement-based waste forms is also dependent on the bulk composition, particularly Al content and its distribution. Hoyle and Grutzeck (1989) reported that in States III and IV, co-crystallisation of Cs with other cement components could yield low soluble phases such as pollucite, caesium herschelite, or related zeolite phases and their precursors. However, while these phases are known from natural occurrences, they were not directly observed to form in the course of experiments and this outcome remains speculative. Bagosi and Csetenyi (1998) studied Cs sorption in Ca–Al–Si systems (concentrations of Cs between 1 and 100 ppm). They found that sorption of Cs is promoted by the decrease of Al_2O_3/SiO_2 ratios, and the increase of CaO/Al_2O_3 molar ratios. In contrast to earlier studies (mainly in the Ca–Si system), they found that Cs sorption decreases when the C/S ratio decreases. They also observed that for one particular case, sorption increased to an unexpectedly high level after one year which may be due to the formation of gismondine that has an excellent Cs binding potential. However, they were not able to unequivocally identify the mineral by X-ray diffraction.

The experts agreed to use data for cement pastes and CSH phases only, due to the large amount of available data and uncertainty associated with the contribution to sorption of caesium from the aggregate in concrete. In other words, aggregates in concrete would have a beneficial effect on Cs sorption. A further reason would be that the aggregates may contribute to the dissolved Na/K/Ca in a way not to be expected from cement alone. Data for CSH phases not at their natural pH value

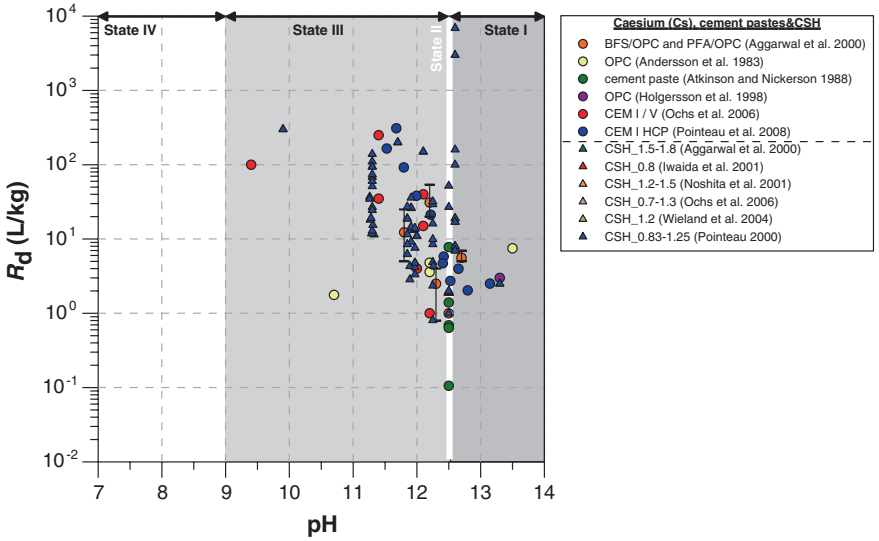

Fig. 4.5 Cs sorption on cement pastes and CSH. For Aggarwal et al. (2000) and Noshita et al. (2001) data R_d values for C/S smaller than 1.2 were omitted because such values are not relevant for State II

were also excluded for directly selecting sorption values (but they were clearly included for showing the systematic relation between R_d and C/S).

By combining the sorption data for cement pastes and CSH phases, a trend becomes apparent from State II into State III (Fig. 4.5): R_d increases as pH decreases (or decreasing C/S ratio). In addition, R_d should also increase when moving from State I into State II owing to decreased competition with other alkali metal ions (K, Na) in State I (ions that have leached out by States II and III). This trend from States I to II is more or less confirmed by the data, although the number of data in State I is very limited; especially the data from Pointeau et al. (2008) (the only data that have data for State I through State III) show a more or less continuous trend. This trend should be reflected in the best estimate R_d values, i.e. lowest in State I and highest in State III.

In conclusion, sorption increases from Stage I to Stage III (effect of C/S and competing cations). Because of the amount of data available, values were first fixed for State II, then chosen for the other States to reflect (1) trends of sorption versus C/S and competing cation concentration from selected systematic experiments and (2) the actual data situations for the other stages. This will be broadly reflected in lower/upper and best estimates.

4.1.3.2 Sorption at State I

For State I, only limited data are available, and the scatter is relatively small. Note that the scatter is small because the variability of conditions is small, i.e. there are very few data sets. Although this is reflected in a relatively small data range (upper

Table 4.1 Selected best estimate, upper and lower limit R_d values for Cs

pH state	Best estimate (L/kg)	Upper limit (L/kg)	Lower limit (L/kg)
State I	i.d.	10^1	1×10^{-1}
State II	2×10^0	5×10^1	1×10^{-1}
State III	2×10^1	3×10^2	1×10^0
State IV	i.d.	i.d.	i.d.

i.d. insufficient data

and lower limits span two orders of magnitude), this gives a false impression that uncertainty is small, while in principle it is the reverse owing to limited data. R_d values range from 2 to 10 L/kg. The best estimate should be smaller than that for State II owing to increased competition from other alkali metal ions (K, Na) in State I. This trend from States I to II is confirmed by the data, especially those from Pointeau et al. (2008), the only data that cover States I through III, and show a more or less continuous increasing trend. However, because of the limitations in the data, the experts agreed to give a range but not a best estimate (Table 4.1). Upper and lower limits of 10 and 0.1 L/kg were selected, being the extreme measured value for the upper limit and a conservative estimate for the lower limit.

4.1.3.3 Sorption at State II

For State II, the range is somewhat larger, from 0.1 to ~50 L/kg, with most of the data lying between 1 and 10 L/kg. In State II, the sodium and potassium ions will have been leached, so caesium R_d values would be expected to increase as the repository evolves from State I to State II. The experts agreed on a best estimate of 2 L/kg, with an upper bound of 50 L/kg and a lower bound of 0.1 L/kg, which is consistent with the expected increase in sorption from State I to State II (Table 4.1). By comparison with the bounds for State I, the upper bound for State II was increased while the lower bound was left at the same value as State I in order to reflect the greater spread of data.

4.1.3.4 Sorption at State III

In State III, the R_d values seem to increase from those of State II. Two very high points at pH 9.8 were not included as they were considered to be exceptionally high as a result of solid phases being prepared in an unusual way. The highest measured points were thus about 300 L/kg for cement pastes and 200 L/kg for CSH. The experts acknowledged that the chemistry of State III changes significantly with time and that there appears to be a relatively steep slope of R_d values across State III, with sorption increasing with decreasing pH. It was agreed to take 20 L/kg as the best estimate as the increase from Stages II to III is by an order of magnitude, with 300 L/kg as the upper bound and a lower bound of 1 L/kg. It was felt that 20 L/kg was a realistic value, yet lying on the conservative side of the

range of State III values—almost all measured values are higher below pH 12. The upper and lower bounds again reflected the range of measured values.

4.1.3.5 Sorption at State IV

For State IV, there is one calcite point which shows an R_d value of 0 L/kg. The experts were reluctant to rely on this one point, as silica gel may be present in State IV and this can increase R_d. It was noted that data on cement pastes contain residual CSH phases, so are not applicable to State IV conditions. State IV was defined by the presence of calcite controlling pH. Bradbury and Baeyens (1997) stated that "Cs is not considered to be sorbing at high pH measured on pure limestone". However, as noted above there may be silica gel present in State IV, depending on the composition of the infiltrating water. It was agreed that R_d values could be variable in State IV depending on the solids present. Higher calcite composition will give lower R_d values, and higher silica will give higher R_d values for caesium. It was noted that even with silica present the values could be very low. When silica hydrates it is a very good absorber, but when it reacts with the rest of the cement the sorption decreases. Furthermore, it could be anticipated that generally speaking the short-lived caesium-137 will have decayed before State IV is reached. The experts therefore agreed to assign no R_d values to State IV.

4.2 Strontium

4.2.1 Chemical Form, Speciation, and Solubility

In the context of waste disposal, strontium is relevant due to the existence of different radioactive isotopes of this element. Stable strontium occurs in the environment at low concentration levels, but is typically not important in conventional waste types.

^{90}Sr (half-life 28.8 years) is not a naturally occurring radionuclide. It is produced in nuclear reactions as a fission product, and the largest source of ^{90}Sr and potential waste material is from nuclear reactor operations. Most of the LILW-SL generated at nuclear power plants (NPP) will contain some ^{90}Sr; however, other radionuclides such ^{137}Cs are usually more prevalent and generally determine the waste characterisation. Wastes that contain ^{90}Sr include wet and dry wastes such as spent ion exchange resins, filter sludge, filter cartridges, evaporator bottoms, compactable and non-compactable trash, and irradiated components. A smaller fraction of wastes containing ^{90}Sr are generated from industrial, institutional, and medical applications. Based on the Belgian LILW inventory (Wang et al. 2009), about 86 % of the total ^{90}Sr inventory exists in waste from decommissioning and remediation associated with former research activities, and approximately 13 % is generated by the operation and decommissioning of NPP. ^{90}Sr in NPP operational waste exists mainly in resins (12 %).

Thermodynamic data from Table 4.2 were used to construct the Eh–pH and solubility diagrams for strontium shown in Fig. 4.6. Strontium speciation is similar to

Table 4.2 Thermodynamic data of strontium

Reaction	log K (25 °C)
$SrOH^+ + H^+ = Sr^{++} + H_2O$	13.2900
Celestite $= Sr^{++} + SO_4^-$	−6.6372
Strontianite $= Sr^{++} + CO_3^-$	−9.2705

Source LLNL v8r6 (1996)

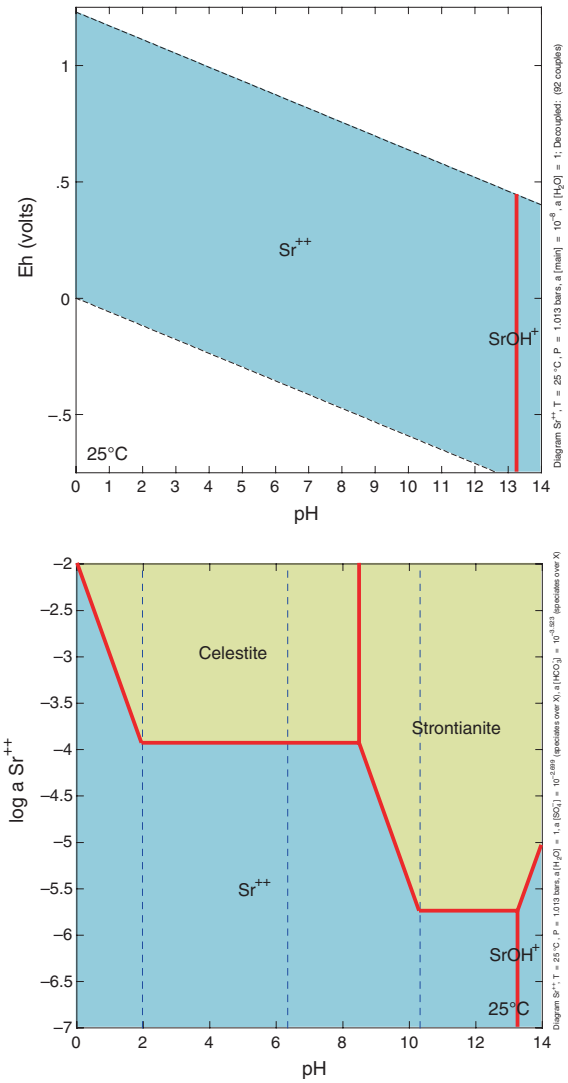

Fig. 4.6 Eh–pH (*top*) and solubility (*bottom*) diagrams of strontium calculated with *The Geochemist's Workbench*®. Strontium activity is 10^{-8}, activity of $HCO_3^- = 10^{-3.523}$, activity of $SO_4^{2-} = 10^{-2.699}$ ($T = 25$ °C)

that of Ra^{2+} where Sr^{2+} dominates almost the entire pH range, while $SrOH^{+}$ species dominate at very high pH (>13).

Possible pure phases controlling the solubility of Sr are celestite ($SrSO_4$) and strontianite ($SrCO_3$) with a solubility of around 10^{-4} and 10^{-6} mol/L, respectively, under the considered conditions. Ochs et al. (1998) measured a total dissolved concentration of Sr of around 10^{-4} mol/L in a cement system at pH 13.2, which is a value close to the calculated solubility of celestite.

4.2.2 Sorption Values from the Literature for the Benchmark Cement

Figure 4.7 and Table A.4 (see Annex) present the reviewed R_d values and the experimental conditions based on Wieland et al. (2008), Tits et al. (2004), Zachara et al. (1991), Sugiyama and Fujita (1999), Ewart et al. (1985), Atkinson and Nickerson (1988), Hietanen et al. (1985), Iwaida et al. (2001), Johnston and Wilmot (1992). A warning is added here when interpreting the data of Sugiyama and Fujita (1999) and Johnston and Wilmot (1992), because geochemical calculations with *The Geochemist's Workbench*® (Bethke 2006) carried out in the current study showed that the initial solutions are over saturated with respect to strontianite (results not shown). However, this does not mean that this phase was effectively formed during the experiments, partly because of the complex geochemistry of cement and its buffering capacities and partly because it is related to the question of the fastest process (sorption or precipitation).

Iwaida et al. (2001) suggested that sorption of Sr on cement takes place on the deprotonated-specific siliceous surface sites or silanol groups ($\equiv SiO^{-}$) and the concentration of such sites decreases with increasing C/S ratio. The observed R_d evolution was related to the zeta potential of the CSH phases at different C/S ratios. At low C/S ratios, the zeta potential was negative (CSH carries deprotonated silanol groups), and the potential increased with increasing C/S ratio (surface of CSH carries $\equiv SiOCa^{+}$ or $\equiv SiOCaOH_2^{+}$ groups). The negative potential changed to positive at C/S ~1.3. A maximum K_d of ~680 L/kg was obtained at C/S = 0.8, and a minimum K_d of 25 L/kg at C/S = 1.6.

Wieland et al. (2008) demonstrated with X-ray absorption fine-structure spectroscopy (XAFS) data that the uptake sink for strontium in cement is CSH and Sr binding is via cation exchange on the deprotonated edge and planar silanol groups of the CSH. The same study revealed that the presence of calcite (4–5 wt%) does not seem to influence the uptake of Sr on cement suggesting that calcite is not the major sink (pore water pH = 13.3). Also the ageing of cement does not seem to affect the extent of Sr uptake illustrated by a similar R_d on either 15-year-old cement samples or newly prepared cement pastes. Sorption tests done with either radiostrontium (^{85}Sr, initial concentration 2×10^{-9} M) or stable strontium (so-called pristine strontium, equilibrium Sr concentrations from 10^{-4} to 3×10^{-3} M) revealed:

- Sorption was linear and reversible for both ^{85}Sr and pristine strontium, resulting in a K_d rather than an R_d. This was confirmed by varying the S/L ratio between 10^{-6} and 0.13 kg/L: K_d remained nearly constant;
- K_d values obtained for ^{85}Sr and pristine strontium were nearly identical, i.e. 80–110 L/kg for ^{85}Sr and 100–120 L/kg for pristine strontium;
- ^{85}Sr replaces pristine Sr in HCP by means of an isotopic exchange process. Based on the ratio of radiostrontium-K_d versus pristine Sr-K_d, it was shown that 80 % of pristine Sr is subject to reversible sorption and isotopic exchange with ^{85}Sr. This is an important observation because commercial cements contain considerable amounts of pristine Sr (~between 100 and a few 1000 ppm, also see Table 5.4). Pore water in equilibrium with HCP was shown to have pristine Sr concentrations of about 10^{-4} M. The ^{85}Sr K_d was not influenced by the much higher pristine "background" Sr concentration compared to the initial ^{85}Sr concentration (2×10^{-9} M).

Several studies further reveal that the uptake of Sr in cement is closely related to the calcium concentration on solid and in solution phases. R_d decreases as calcium concentration in solution increases (Tits et al. 2006b). Batch sorption experiments performed at PSI repeatedly illustrate that Sr and Ra sorption on cement and CSH phases can be explained by ion exchange theory (Wieland et al. 2008; Tits et al. 2004, 2006b). Other exchangeable cations may also compete with Sr^{2+} for sorbing sites on the surface of CSH and lower the sorption, e.g. Na^+ in a saline water at pH 12.5 (Johnston and Wilmot 1992). In the latter study, the very high aqueous calcium concentrations (~3.6 M) used explain the low R_d (0.18 L/kg). The normal equilibrium calcium concentration at pH 12.5 is ~0.02 M, about 180 times lower. Based on the inverse proportionality between Sr R_d and calcium concentration, the R_d from Johnston and Wilmot (1992) may be corrected for calcium concentration under non-saline conditions, which would then yield an R_d of $180 \times 0.18 = 32.4$ L/kg, fully in agreement with other values shown in the review (Fig. 4.7).

In contradiction to most studies, Serne et al. (1996) found no removal of Sr by cement in a CO_2-free system although the study was meant to measure the solubility of Sr in cement. These authors performed batch leaching experiments on $SrCl_2$ doped "Portland Type I cement" in pH 7–12.5. After only two days of leaching (the longest duration of leaching was 17 days), soluble Sr concentrations approximate the total amount of Sr added to the cement during cement sample preparation. According to these results, it was concluded that Sr does not enter appreciably into the solid matrix of cement and does not form insoluble compounds in carbonate-free environments.

Strontium sorption on calcite seems low (Zachara et al. 1991) at about $R_d = 1$ L/kg at pH around 8. In a cement system open to atmospheric CO_2, Sr coprecipitation or a formation of solid solution may keep the total dissolved concentration of Sr at a level lower than the solubility of strontianite (10^{-6} M). These observations are in line with the conclusion from Wieland et al. (2008) that calcite in cements is not a major sink for uptake of strontium.

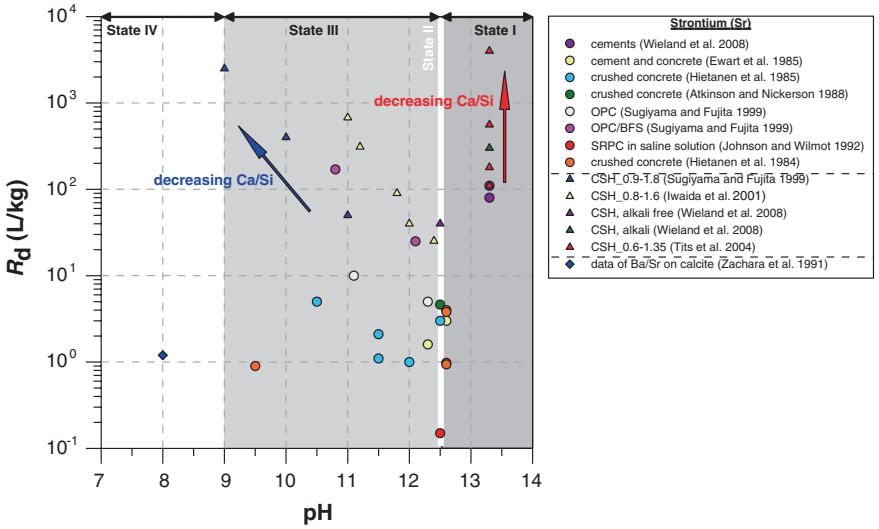

Fig. 4.7 Distribution ratio (R_d) of strontium in cementitious systems. *SRPC* sulphate resisting Portland cement; *OPC/BFS* ordinary Portland cement/blast furnace slag; *CSH* calcium silica hydrates. *Arrows* indicate effect of decreasing C/S ratio for Tits et al. (2004) data and Sugiyama and Fujita (1999) data

In some cases, high calcium concentrations can result in higher Sr immobilisation, as was demonstrated by Fuhrmann and Colombo (1989). These authors determined leaching rate of Sr from cemented waste in seawater and found a decreased leaching compared to distilled water. The positive effect of seawater on immobilisation was due to the coprecipitation of Sr with calcite.

A detailed study of Sr uptake by CSH revealed that R_d depends on the Ca concentration in the pore fluid, which in turn is controlled by the solubility of CSH phases at different states of cement degradation (Tits et al. 2004). A cation exchange model based on CSH data was proposed and demonstrated to be applicable in explaining the R_d values measured on cement paste. Following these findings, R_d for Sr on cement is expected to be lowest in State II of cement degradation because aqueous Ca concentration is the highest, where Ca is the most important competing ion with Sr for sorption sites.

4.2.3 Sorption Mechanisms and Selected Sorption Values

4.2.3.1 Sorption Mechanisms

A summary of cement solid phases responsible for Sr uptake was provided by Evans (2008). Solid phases responsible for Sr uptake include:

- OPC, considered a very efficient scavenger for Sr, especially the hydration products of C_4AF and C_3A (probably C_3AH_{13}) are known to accommodate low Sr levels;

- CSH gels of high C/S ratio (1.7) and $Ca(OH)_2$ are less efficient sorbers than OPC and the hydration products of C_4AF and $C_3A{\cdot}(C_4AH_{13})$;
- CSH gels of low C/S ratio are expected to be more efficient sorbers;
- AFt and C_3AH_6.

Substitution of Sr for Ca in the cement hydration products has been demonstrated as a sorption mechanism; cements high in Al and Ca should have the best sorption capacity. Coprecipitation of $SrCO_3$ during the carbonation of cement has also been identified as a solubility-limiting process for release, although coprecipitation is not among one of the processes that were qualified here as true sorption.

In addition, retention studies at PSI suggest that Sr^{2+} is sorbed on the CSH fraction in HCP (Tits et al. 2006b). It appears that the process governing Sr^{2+} sorption by CSH is cation exchange via a stoichiometric replacement of Ca^{2+} by Sr^{2+} at the surface sites of the CSH (Tits et al. 2006b), involving Ca–Sr replacements and Na/K–Sr replacements (Wieland et al. 2008).

For HCP, strontium is typically cation exchangeable and has similar cation exchange selectivity as calcium (the selectivity coefficient for the Sr^{2+}–Ca^{2+} exchange reaction, ${}^{Sr}_{Ca}K_C$ is nearly one (Tits et al. 2006b)). A selectivity coefficient of ~1 implies that the CSH phases exhibit equal affinities for Ca^{2+} and Sr^{2+} regardless of the CSH composition and the concentration of Sr^{2+}. Sorption of strontium is therefore controlled by cation exchange and the extent of uptake by cement has been shown to be closely related to the calcium concentration in cement pore water (Tits et al. 2006b).

For calcite, several sorption mechanisms have been identified, mostly depending on the concentration of the divalent metallic cations. At low aqueous concentrations, divalent cations associate with the calcite surface via an adsorption process, possibly via exchange with Ca in exposed structural sites. In more concentrated metal solutions, metal carbonate precipitates may form on the calcite surface (Zachara et al. 1991).

The experts agreed that they would not use data obtained from crushed concrete or from experiments with saline solutions so that these values, while shown in Fig. 4.7, were not used in the data estimation procedure. Selection of sorption values for strontium for all degradation states should be consistent with those selected for radium (Sect. 4.3), given their chemical analogy. Analogous behaviour in the presence of HCP was confirmed by Wieland et al. (2008). Both strontium and radium exhibit a clear dependency on aqueous calcium concentration across State I through State III, while in State I an additional dependency on alkali metal ions (K^+, Na^+) is observed (Tits et al. 2004, 2006b). Also for sorption onto calcite, similar mechanisms are assumed (Zachara et al. 1991).

Further evidence for similarity in Sr–Ra R_d is obtained from Fig. 4.8, where all R_d values for strontium and radium are combined. Both elements display the same trend in R_d: a decrease from States I to II, followed by an increase from States II to III. Within State III, the increase is present throughout the entire pH range (12.5–9). The R_d values for radium are consistently higher than those for strontium. In State I, the difference is less than one order of magnitude, whereas in States II

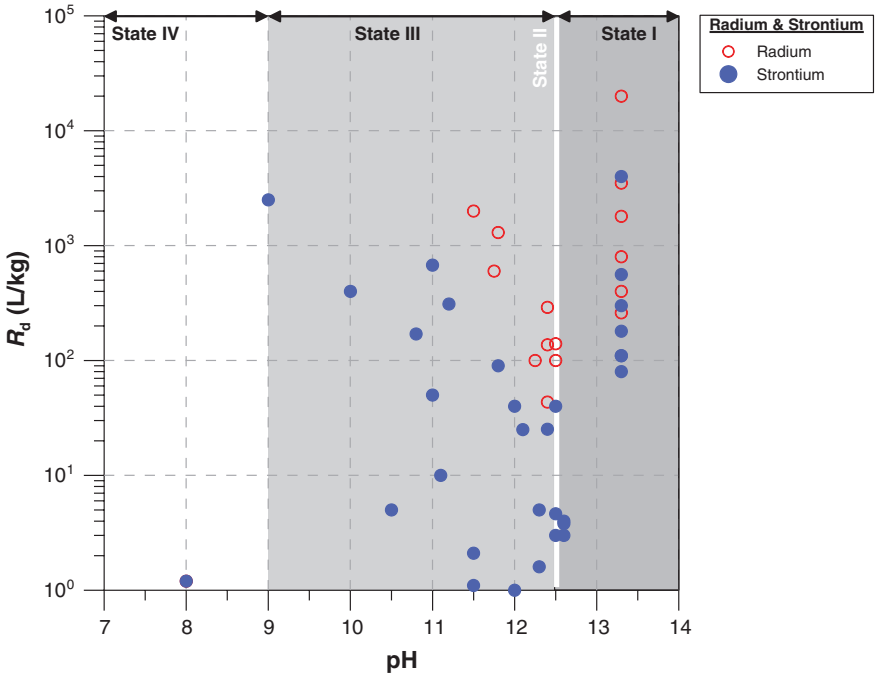

Fig. 4.8 Distribution ratio (R_d) of radium and strontium in cementitious systems (based on Figs. 4.7 and 4.10). Data from Johnston and Wilmot (1992) have been omitted because of saline water used. *Error bars* have been omitted for plotting purposes

and III (where only aqueous calcium is the dominant factor influencing R_d), the difference is at least one order of magnitude. It was previously shown that Ra^{2+} sorbs more strongly onto CSH than Sr^{2+}, because the selectivity coefficient for Ra^{2+}–Ca^{2+} exchange reaction is about 5 times larger than that for the Sr^{2+}–Ca^{2+} exchange (Tits et al. 2004). The data shown in Fig. 4.8 are consistent with the difference in selectivity coefficient. Best estimate values for strontium should reflect this difference.

The most important factor influencing strontium R_d on cement is dissolved calcium concentration (in States II and III), while for State I alkalis are competing for sorption sites. The expected trend in R_d across States I, II, and III is as follows: R_d decreases from I to II, but increases from II to III.

The selected best estimate R_d values for States I, II, and III reflect the presumed theoretical behaviour, the observed data, and are consistent with the values derived for radium (Fig. 4.10). A decrease from 100 (State I) to 30 L/kg (State II) and then an increase from 30 to 100 L/kg (State III) were selected (Table 4.3).

Table 4.3 Selected best estimate, upper and lower limit R_d values for Sr

pH state	Best estimate (L/kg)	Upper limit (L/kg)	Lower limit (L/kg)
State I	1×10^2	3×10^2	3×10^1
State II	3×10^1	1×10^2	5×10^0
State III	1×10^2	3×10^3	1×10^1
State IV	1×10^0	3×10^1	1×10^{-1}

4.2.3.2 Sorption at State I

The range for State I was around 100–200 L/kg, on the basis of limited experimental data. Data for mineral phases not at their natural pH were not used. The experts agreed on a best estimate of 100 L/kg (based on the range of reliable experimental data), an upper bound of 300 L/kg and a lower bound of 30 L/kg. It was agreed, as discussed above, that values for State I would be higher than those for State II and similar to State III.

4.2.3.3 Sorption at State II

After omitting data for crushed concrete and saline solutions, the range for State II appeared to be generally 5–50 L/kg with one data point at 90 L/kg (Iwaida et al. 2001). The experts agreed that a best estimate of 30 L/kg with bounds of 100 and 5 L/kg captured the data and could be justified.

4.2.3.4 Sorption at State III

The range for State III was agreed to be 10–1000 L/kg. There was a concern that the data from Sugiyama and Fujita (1999) came from experiments that used a high initial strontium concentration (10^{-3} M) and that there might have been precipitation of strontianite (oversaturation was demonstrated here based on geochemical calculations). The data were given a low weighting with this uncertainty. The experts agreed that the range spread suggested 100 L/kg as the best estimate. It was noted that there is a definite trend of R_d values increasing as the system evolves from State II to State III conditions at lower pH. It was agreed to include the isolated point at pH 9 (Sugiyama and Fujita 1999) in State III as it was CSH-based, the definition of State III. It was also agreed to increase the upper bound to 3000 L/kg to include this point. However, there are few data in the pH range 9–10, and there is a lack of information on the amount of CSH in the same pH range. The best estimate and bounds were regarded as conservative values.

4.2.3.5 Sorption at State IV

There was only one data point for State IV [for Ba/Sr on calcite (Zachara et al. 1991)]. It was suggested and agreed that the experts accept this value as a best

estimate, with a note highlighting that it was based on only one data source. The best estimate at 1 L/kg is the same value as for radium, and we suggest upper and lower bounds of 30 and 0.1 L/kg, respectively.

4.3 Radium

4.3.1 Chemical Form, Speciation, and Solubility

All isotopes of radium are radioactive. Radium is one of the radioactive elements found in nature; it is the daughter of other naturally occurring radioactive elements. For example, ^{224}Ra results from ^{232}Th decay and ^{226}Ra from ^{238}U decay. Other than ^{226}Ra (half-life 1600 years), all are short-lived and uncommon. ^{226}Ra is a typical radionuclide in LILW, though present only at low levels (Wang et al. 2009). As a daughter of Th and U and because of its much higher mobility, Ra can also be a relevant contaminant where U- or Th-containing conventional waste (such as mineral waste with a natural U/Th background) is concerned.

The Eh–pH diagram for radium is shown in Fig. 4.9 and is based on the thermodynamic data given in Table 4.4. The expected aqueous species for radium under high pH is Ra^{2+} and $RaOH^{+}$ (pH > 13.5). $RaSO_4$(aq) may also prevail if SO_4^{2-} concentration is higher than ~2 millimolal.

A shortcoming of the available data is the lack of information on the threshold for precipitation of radium sulphate and carbonate. Unlike for strontium, where the possible precipitation of the sulphate and carbonate is well examined and the data integrated into the data assessment, such an analysis has not been made for radium so far.

The radium inventory is generally negligibly low in conditioned LILW meant for near-surface disposal; therefore, solubility-limiting solids will probably not be

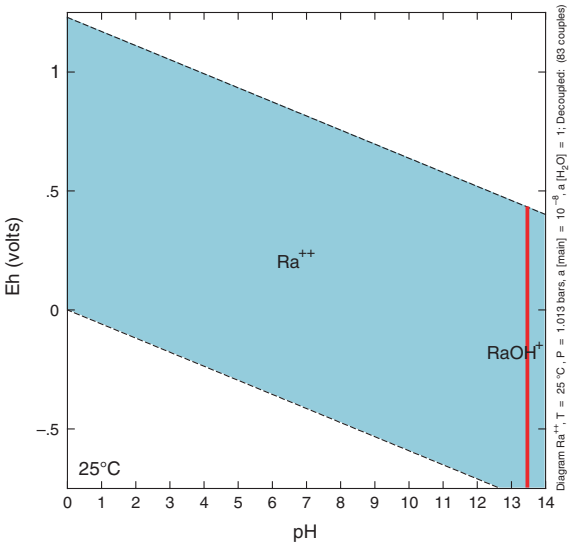

Fig. 4.9 Eh–pH diagram of radium calculated with *The Geochemist's Workbench®*. Radium activity 10^{-8}

Table 4.4 Thermodynamic data of radium

Reaction	log K (25 °C)
$RaOH^+ + H^+ = Ra^{++} + H_2O$	13.4915
$RaSO_4(aq) = Ra^{++} + SO_4^-$	−2.7500

Source LLNL v8r6 (1996) and PSI/NAGRA 01/01 Hummel et al. (2002)

present under the considered disposal conditions. The same can be assumed for Ra resulting from the U- or Th-decay chains in natural materials.

4.3.2 Sorption Values from the Literature for the Benchmark Cement

Reviewed R_d values for radium in a cementitious system are presented in Fig. 4.10 based on the literature data from Holland and Lee (1992), Bayliss et al. (2000), Tits et al. (2006a), Zachara et al. (1991). Experimental details are given in Table A.5 (see Annex).

Experimental R_d values for radium on cementitious materials are scarce. However, the few existing data seem to be of good quality. There is good evidence that Ra sorption increases as the C/S ratio decreases on CSH (Fig. 4.10).

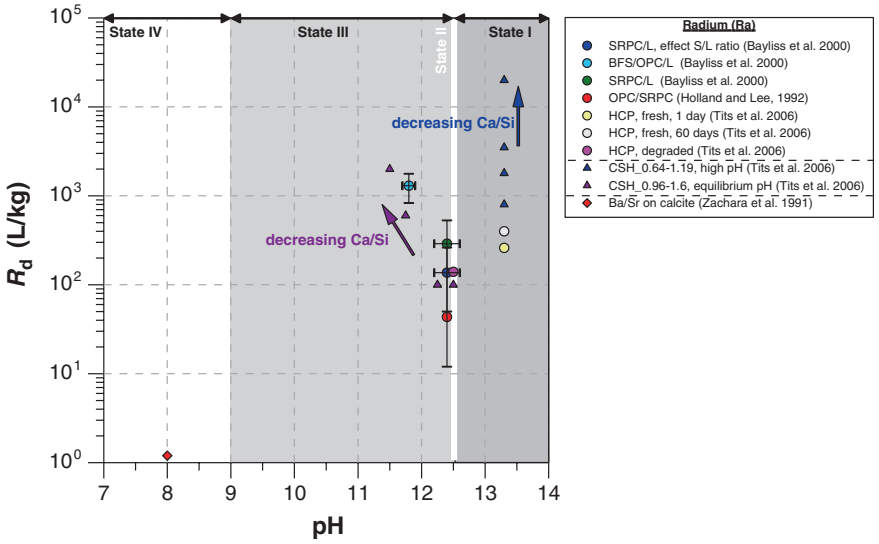

Fig. 4.10 Distribution ratio (R_d) of radium in cementitious systems. *SRPC/L* sulphate resisting Portland cement/fine limestone aggregate; *BFS/OPC/L* blast furnace slag/ordinary Portland cement/fine limestone aggregate; *CSH* calcium silica hydrates. *Arrows* indicate effect of decreasing C/S ratio for Tits et al. (2006a) data. Variation in R_d for all Bayliss et al. (2000) data due to different initial concentrations

This is generally interpreted as being due to the decrease in pore water concentration of the competing Ca ions. Sorption of Ra is thought to be controlled by cation exchange on CSH. As Ca concentration in pore water decreases, more cation exchange sites are available for sorbing Ra (and other cations such as Sr). These sites are fully occupied by Ca when the Ca concentration is at its maximum, the latter being controlled by the solubility of portlandite at State II. Therefore, the R_d evolution as cement degrades (decreasing C/S ratio) is regulated by the competition between Ca and Ra for cation exchange sites on CSH.

An effect of the S/L ratio was found by Bayliss et al. (2000) but not by the more recent work of Tits et al. (2006a), where R_d was constant as a function of S/L ratio. R_d values reported by Bayliss et al. (2000) also vary with the cement type. Values for BFS/OPC/L are of the order of 1000 L/kg compared to 100 L/kg for SRPC/L and 50 L/kg for 9:1 BFS/OPC. The presence of chloride, on the other hand, appears to have no effect on radium sorption.

Tits et al. (2006a) also studied CSH phases of different C/S ratios at a single pH (about 13.3) and found a very high R_d value (20,000 L/kg) for a CSH phase with a low C/S ratio of 0.64. However, this high R_d value may not be relevant for the State I because at pH > 13 the CSH in cement should have a C/S ratio probably larger than 1.5. A more representative R_d for the State I should be the one measured for cement paste systems (R_d of a few hundred). Results further showed that radium sorption onto CSH in absence of alkalis (pH = 11.5–12.5) was linear and reversible, at least in the Ra^{2+} equilibrium range of the experiments (1.5×10^{-10} to 1.4×10^{-8} M). For degraded cement, uptake was fast, i.e. equilibrium was obtained within one day (same as for CSH phases). For fresh HCP, a two-step uptake occurred. Tits et al. further demonstrated a trend similar to that previously observed for Sr^{2+} (Tits et al. 2006b), i.e. R_d values are inversely proportional to the equilibrium Ca^{2+} concentration in solution. Based on the analogy with Sr^{2+}, sorption on CSH is by means of cation exchange, with Ra^{2+} sorption causing an equal amount of Ca^{2+} release into solution (Tits et al. 2006b). Finally, a cation exchange model was presented that successfully predicted R_d for Ra^{2+} in alkali-free systems. In the presence of alkali ions (State I), sorption displays a similar change in R_d with changing equilibrium concentration of Ca^{2+}, but there is competition with alkalis resulting in 3 times lower sorption values compared to the alkali-free system.

Radium sorption onto Carboniferous limestone (96 % calcite, 3 % dolomite) at pH 7 using saline groundwater (~1 mol/L sodium, 5×10^{-2} mol/L calcium) resulted in R_d values less than 7 L/kg (Berry et al. 2001). Varying calcium concentrations from 10^{-2} to 5×10^{-2} mol/L did not affect R_d (at an initial radium concentration of ~10^{-8} mol/L at a S/L ratio of 0.02 kg/L). The relatively low R_d value may be influenced by the high sodium concentration, as Na^+ and K^+ are the known competitors for sorption sites under the assumption that cation exchange is the relevant sorption mechanism. The latter cannot be confirmed at present, because other sorption mechanisms such as formation of surface complexes were identified for Ba and Sr sorption onto calcite (Zachara et al. 1991). More general, at low trace metal concentrations uptake onto calcium seems governed by sorption (adsorption via exchange with Ca), while at higher concentrations solid solution formation may become dominant (Apello and Postma 2006).

4.3.3 Sorption Mechanisms and Selected Sorption Values

4.3.3.1 Sorption Mechanisms

In his review of binding mechanisms of radionuclides to cement, Evans (2008) provided information for strontium, which, given its chemical analogy to radium, may be useful to consider as a first approximation (also see Sect. 4.2.3). For example, for both Sr and Ra, sorption behaviour is expected to mirror that of calcium. CSH gels of low C/S ratio are expected to be more efficient sorbers (an increase in sorption with decreasing C/S ratio has also been observed for Ra, see Fig. 4.10). Although there is a strong analogy in sorption mechanism between Sr^{2+} and Ra^{2+}, Ra^{2+} sorbs more strongly onto CSH than Sr^{2+}; the selectivity coefficient for the Ra^{2+}–Ca^{2+} exchange reaction is about 5 times larger than that for the Sr^{2+}–Ca^{2+} exchange (Tits et al. 2006a). It was shown that R_d values are inversely proportional to the equilibrium Ca^{2+} concentration in solution in alkali metal ion-free systems (States II and III), with Ra^{2+} sorption causing an equal amount of Ca^{2+} release into solution. In the presence of alkali metals (State I), sorption displays a similar dependency on equilibrium Ca^{2+}, but there is also competition with alkali metals resulting in 3 times lower sorption values (based on a theoretical model calculation of Tits et al. 2006a). Our calculations predicted a 2×10^{-3} mol/L Ca concentration in State I, which then increases to 2×10^{-2} mol/L in State II, followed by a decrease to ~7–9 $\times 10^{-4}$ mol/L at the end of State III (for one particular calculation case). Because Ra sorption was shown to be inversely proportional to Ca concentration (plus alkali metals in State I), a ten times higher R_d value is expected in State I compared to State II, while in State III R_d might be up to 25 times higher than in State II. However, in State I the competition with alkali metals will reduce the increase in sorption owing to lower Ca concentration compared to State II; therefore, the expected theoretical difference between State I and II would be reduced by ~1/3 of the value expected from the calcium concentration only (Tits et al. 2006a). Judging from the summary R_d graph (Fig. 4.10), the theoretical difference between States I and II seems to be confirmed. Note that the CSH data for State I with low C/S ratio should be less weighted than the high C/S ratio, as the latter are more appropriate than the former for State I. The data points for State I are then on average less than a factor of 10 larger than those for State II, which is consistent with the theory and observations of Tits et al. (2006a). From States II and III, R_d values increase at least an order of magnitude (although the data are scarce, the two data sets show a consistent trend), which is again in agreement with the theory and observations of Tits et al. (2006a).

There are no data between pH 9–11.5. As the calcium concentration further decreases (our calculations show that at the beginning of State III (high pH) [Ca] = 7×10^{-3} mol/L while at the final state (low pH) it dropped to 8×10^{-4} M), sorption values are expected to further increase. Thus at most a factor of 10 increases in R_d is expected between the beginning and the end of State III. However, the theoretical model of Tits et al. (2006a) also includes the amount of CSH available for sorption (expressed as weight% CSH). The model further

assumed that the CEC of the CSH phase was independent from C/S ratio. As cement degrades, the amount of CSH decreases and thus the increase in R_d owing to a decrease in calcium concentration is counterbalanced by a decrease in CSH (total CEC remains unchanged). A low CSH phase was simulated to be present during State III (Fig. 4.10). Predictions for the pH range 9–11.5 can only be made if both the amount of CSH and the amount of calcium concentration are known.

Based on wet chemistry sorption data, radium uptake on cement and CSH phases was explained as being controlled by ion exchange (Tits et al. 2006a). This was supported by experimental evidence showing that Ra sorption on CSH strongly decreases at State II due to the competition with calcium for the cation exchange sites on cement materials. The uptake sink for Ra in cement is likely to be the CSH phases.

Also in terms of sorption mechanisms, Wieland et al. (2008) demonstrated with XAFS data that the uptake sink for strontium in cement is CSH and that Sr is sorbed as partly hydrated species via two bridging oxygen atoms. Considering the similarity in chemical behaviour of Ra^{2+} and Sr^{2+}, the uptake mechanisms could be similar as well. However, the wet chemistry data were interpreted well with the classical ion exchange theory neglecting the specific uptake mechanisms in the CSH phase.

Based on the above arguments, Ra^{2+} is expected to sorb on cement through ion exchange with Ca^{2+}; hence, R_d is expected to vary as a function of calcium concentration in different states of cement degradation. Calcium should compete with Ra for sorption sites on cement. Alkali metals may also have a negative impact on Ra sorption if present in high concentrations. Therefore, competition with calcium will be lower in State I compared to States II and III, but in State I competition with alkalis will be higher. The sorption mechanism is very similar to that observed by Sr^{2+} (Tits et al. 2006b). Both Sr and Ra show an increase in R_d as C/S ratio decreases (and Ca in solution decreases). The decrease in Ca in solution from 2×10^{-2} mol/L at State II to ~7–9 $\times$ 10^{-4} mol/L at the end of State III will give rise to an increase in R_d. In terms of speciation, the experts noted that the aqueous speciation of radium would be the same throughout all the states, as Ra^{2+}, although some speciation change may occur in State I, with Ra being speciated as $Ra(OH)^+$ at very high pH. Sorption behaviour across State I through State III could therefore depend solely on competition with Ca^{2+}. Radium sorption on calcite is most probably similar to barium and strontium and is regulated by a formation of surface complexes as shown by Zachara et al. (1991).

The summary graph with Ra R_d values (Fig. 4.10) displays a clear trend across degradation states: in State I R_d values are clearly higher than in State II, while R_d increases again when the pH further decreases from States II to III. This is in agreement with the presumed mechanism controlling Ra^{2+} sorption. Finally, in State IV, R_d values are considerably lower than in State III. It was noted that there was some uncertainty over solubility limits given high calcium and strontium levels. The experts agreed to reflect this by allowing a reasonably large spread between upper and lower bounds. Best estimates, upper and lower bounds, are available from Table 4.5.

Table 4.5 Selected best estimate, upper and lower limit R_d values for Ra

pH state	Best estimate (L/kg)	Upper limit (L/kg)	Lower limit (L/kg)
State I	3×10^2	1×10^3	1×10^2
State II	1×10^2	1×10^3	1×10^0
State III	8×10^2	8×10^3	8×10^1
State IV	1×10^0	3×10^1	1×10^{-1}

Radium sorption is primarily influenced by the dissolved calcium concentration, i.e. R_d values are inversely proportional to the equilibrium Ca^{2+} concentration in solution. S/L ratio did not have any effect based on Tits et al. (2006a), although Bayliss et al. (2000) reported the opposite. The latter may be the result of increased Ca concentrations in solution as S/L ratio increased. At higher calcium concentrations, competition with Ra would be higher (see the cation exchange mechanism discussed above).

4.3.3.2 Sorption at State I

Most data came from Tits et al. (2006a), and these were considered reliable. The experts agreed on a best estimate R_d value for State I of 300 L/kg, with an upper bound of 1000 L/kg and a lower bound of 100 L/kg.

4.3.3.3 Sorption at State II

The experts had data for CSH and also evidence that real cement systems with additional components might potentially allow further sorption processes to operate. The experts agreed on a best estimate of 100 L/kg with upper and lower bounds of 1000 and 10 L/kg, respectively. The reduction from State I was attributed to higher calcium concentrations. Tits et al. (2006a) had evidence for reversibility of sorption giving confidence in the use of the data as genuine sorption.

4.3.3.4 Sorption at State III

There were few data available for this state, and they tended to be towards the high pH end of the range. Given the resulting uncertainty and the fact that CSH 1.1 would be stable, agreement was reached on a best estimate of 800 L/kg with upper and lower bounds of 8000 and 80 L/kg, respectively.

4.3.3.5 Sorption at State IV

Sorption onto calcite is low, and with few data available for Ra (radium sorption onto limestone (96 % calcite) and of these data, some were for saline waters), analogue data[1] (Ba and Sr) have been added. The experts agreed on a best estimate of 1 L/kg, with an upper bound of 30 L/kg and lower bound of 0.1 L/kg. The upper bound value reflected the fact that these saline sorption values could be higher in the absence of saline conditions.

4.4 Silver

4.4.1 Chemical Form, Speciation and Solubility

Silver is a noble metal. It can occur in certain waste types, but is not a common contaminant. Radioactive isotopes are part of the waste generated in NPP. In a natural environment, ^{107}Ag and ^{109}Ag are the most prevailing stable isotopes, with respective relative abundances of 51.35 and 48.65 %. Silver has 48 radioisotopes, from which only ^{110m}Ag, with a half-life of 250 days (NEA 2006), can be detected in the environment (Calmon et al. 2002). In a nuclear reactor, ^{108m}Ag and ^{110m}Ag are both produced due to activation of, respectively, ^{107}Ag and ^{109}Ag present in the silver in the control rods (these are made of elements with high neutron absorption cross sections, such as Ag, In, Cd, B, and others) used for controlling the nuclear reaction rate.

In LILW radioactive waste, typical silver isotopes are: ^{105}Ag (half-life 1.31×10^{-1} year), ^{108}Ag (half-life 4.56×10^{-6} year), ^{108m}Ag (half-life 4.18×10^{2} year), ^{110}Ag (half-life 7.78×10^{-7} year), and ^{110m}Ag (half-life 6.84×10^{-1} year) (ONDRAF/NIRAS 2011).

Due to its reactivity, it can form complexes in solution. With the exception of nitrate ($AgNO_3$), perchlorate ($AgClO_4$), fluoride (AgF), acetate ($AgCH_3COO$), and chlorate ($AgClO_3$), the salts of silver are very insoluble. Following Charlot (1983), Ag_2S is the least soluble solid. The stable oxidation state of silver in water is +I. Ag^+ forms aqueous anion and cation complexes which are very stable as well as numerous minerals and organic compounds (Sposito 1989).

Figure 4.11 plots the Eh–pH diagram of a Ag–H_2O system showing that silver metal is stable under most of Eh–pH conditions and that oxidising conditions are required to form soluble silver.

Aqueous silver species existing in a Ag–H_2O system are Ag^+ and the hydrolysis species AgOH and $Ag(OH)_2^-$ (see Fig. 4.12). When chloride is present, silver may form aqueous complexes with chloride or precipitate as AgCl (s) as shown in Fig. 4.15.

[1]Radium and barium are adjacent to each other in the alkaline earth group. Due to the similarity of their ionic radii (3.98 and 4.04 Å for, respectively, hydrated Ra^{2+} and Ba^{2+}), the chemical behaviour of radium is similar to that of barium.

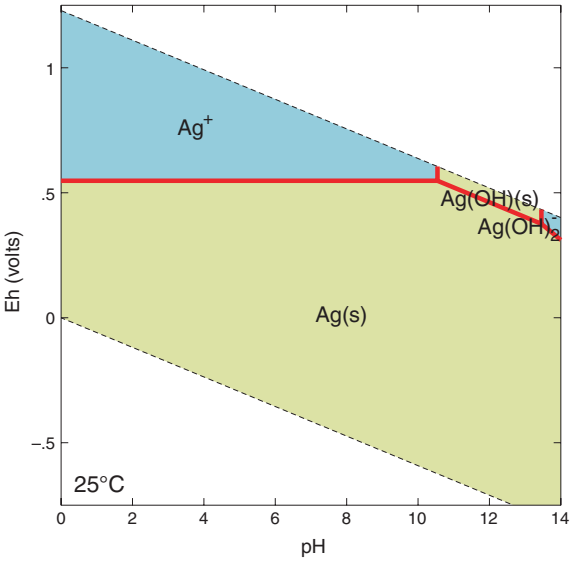

Fig. 4.11 Eh–pH diagram of silver in a Ag–H_2O system, assumed Ag activity is 5.7×10^{-5} Thermodynamic database: ThermoChimie 7b

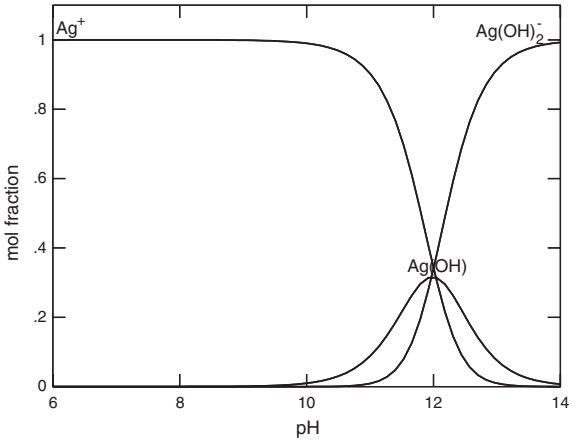

Fig. 4.12 Speciation diagram of silver in a Ag–H_2O system, Ag concentration 10^{-8} mol/L. Thermodynamic database: ThermoChimie 7b

Based on thermodynamic calculations considering the estimated LILW inventory Ag activity (Fig. 4.13), relevant solubility controlling phases of silver that are worthwhile considering include AgOH (s), AgCl (cr), and metallic Ag (s). Solubilities of these phases are given in Figs. 4.14, 4.15, and 4.16. Silver sulphide (Ag_2S) and carbonate (Ag_2CO_3) are also sparingly soluble phases but not relevant in the current context. Silver sulphide is only stable at an Eh much lower than −230 mV (results not shown).

Yousuf et al. (1998) have identified by means of XRD and FT-IR analysis that in a high Ag loading (2.6 mol/L Ag) cement sample under oxidising conditions, relevant solid phases are AgCl, Ag_2CO_3, and Ag_2O (which is similar to AgOH).

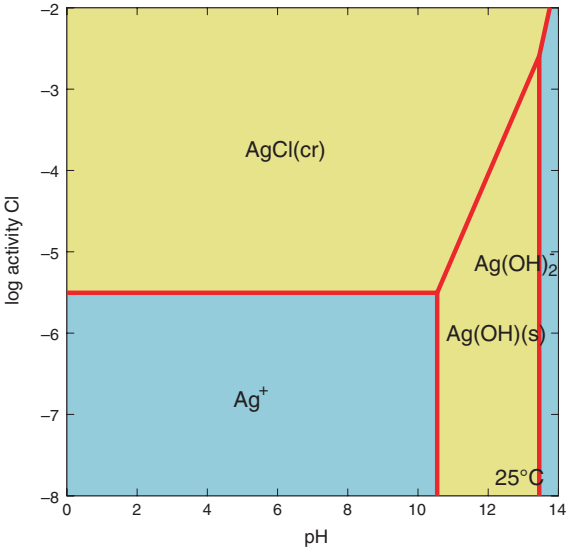

Fig. 4.13 Solubility of silver as a function of chloride activity in a Ag–Cl–H_2O system. Ag activity is 5.7×10^{-5}. Thermodynamic database: ThermoChimie 7b

However, these authors underlined that Ag_2CO_3 is less relevant in a real system because of the limited amount of CO_3^{2-} in cement. The presence of Ag_2CO_3 in their samples was probably due to the unusually high loading of Ag. Ag_2S was considered not to be formed because of the lack of sulphide (S^-) in the pore water.

Silver speciation is sensitive to the dissolved chloride concentration in pore water. Figure 4.11 indicates that precipitation of chlorargyrite (AgCl solid) starts at Cl activity of 3×10^{-6} when pH is below about 10. At higher pH, the Cl activity needed to precipitate AgCl (cr) is higher because of the competition of Ag hydrolysis. Since higher chloride concentrations may be obtained for specific waste streams including evaporator concentrates (Wang et al. 2009), some scoping calculations are done to show the effect of higher Cl on the speciation and solubility of Ag (Section "Impact assessment by thermodynamic modelling").

Both Figs. 4.14 and 4.15 suggest that in State I, AgOH (s) is the solubility controlling phase and the solubility can be estimated from the following equilibrium:

$$\mathrm{Ag(OH)(s) + H_2O = Ag(OH)_2^- + H^+} \quad \log K = -17.7 \tag{4.1}$$

At pH 13.5 representing the start of State I, the solubility of AgOH (s) in a water system in the absence of chloride is about 6×10^{-5} mol/L (see Fig. 4.14). A minimum solubility of 6.4×10^{-6} mol/L occurs at about pH 12. In States II to IV, the solubility of AgOH (s) increases with decreasing pH. In a cement system containing chloride as impurities, however, the pore water concentration of Ag may not be related to the solubility of AgOH (s), as suggested by Fig. 4.15, but be controlled by the solubility of AgCl (s) as suggested by Fig. 4.15.

In State II (i.e. at pH 12.5), the following solubility equilibrium will likely determine the total dissolved Ag concentration in cementitious pore water:

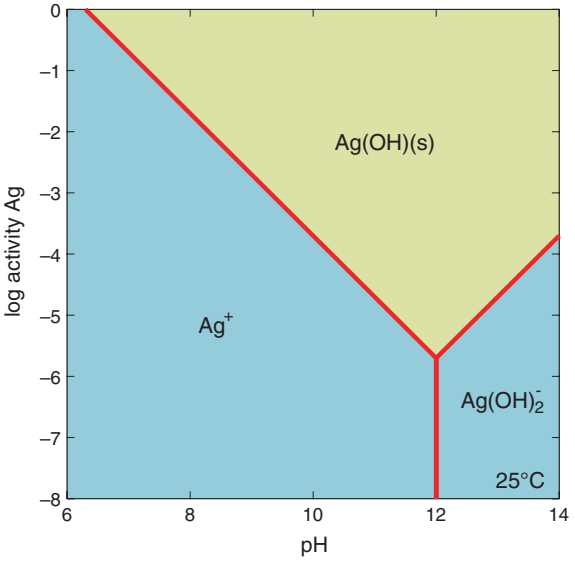

Fig. 4.14 Solubility of AgOH (s) in a Ag–H_2O system. Thermodynamic database: ThermoChimie 7b

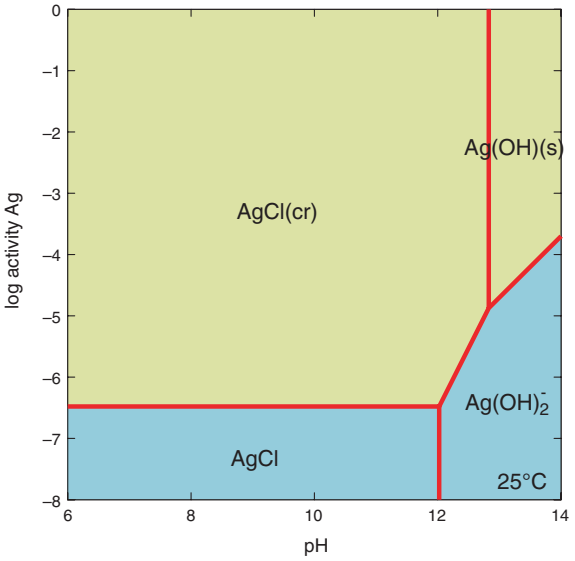

Fig. 4.15 Solubility of AgCl (cr) and AgOH (s) with dissolved chloride activity of 6×10^{-4}. Thermodynamic database: ThermoChimie 7b

$$AgCl(cr) + 2H_2O = Ag(OH)_2{}^- + Cl^- + 2H^+ \log K = -33.7 \quad (4.2)$$

When chloride concentration is at 0.2 mmol/L [characteristic of a low chloride content in a benchmark cement (Jacques et al. 2008)] and 0.6 mmol/kg [characteristic of normal chloride content in a benchmark cement (Jacques et al. 2008)], the

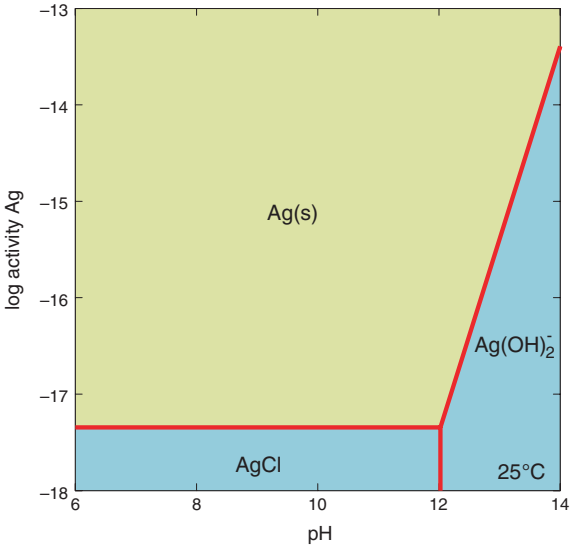

Fig. 4.16 Solubility of Ag (s) at Eh −230 mV with dissolved Cl activity 6×10^{-4} Thermodynamic database: ThermoChimie 7b

activities of $Ag(OH)_2^-$ are 9×10^{-6} and 3×10^{-6}, respectively. This suggests a maximum solubility around 10^{-5} mol/kg in State II.

For the large part of State III and State IV, Fig. 4.15 indicates that the solubility of Ag is independent of pH and is at about 10^{-6} mol/kg (for chloride ~0.2 mmol/L).

Under reducing conditions, silver may also be reduced to metallic Ag^0 (s) and so its solubility may control the dissolved Ag concentration. Figure 4.16 displays the solubility diagrams for Ag^0 (s), from which it is seen that the solubility is extremely low (~10^{-17} mol/kg).

In conclusion, the most likely solubility of silver in benchmark cementitious pore water with expected levels of chloride might be in the range of 10^{-6} to 10^{-4} mol/kg. The Ag solubility tends to increase with increasing pH and is highest at State I.

4.4.2 Sorption Values from the Literature for the Benchmark Cement

No reliable sorption values for silver on cementitious materials could be found. Ochs et al. (2001) observed significant removal of Ag in the presence of various cement mineral phases (corresponding to apparent R_d values of at least 1500 L/kg in case of CSH). However, it cannot be completely excluded that the apparent sorption may be due to the precipitation of Ag phases (see also Andra 2005), although Ag appeared not to be in oversaturation in blank solutions.

In the absence of any sorption data on cementitious materials, possible analogies could be used to derive sorption values; and it may also be helpful to consider the sorption behaviour of Ag on other minerals:

- In terms of basic chemical properties, the charge/M–O bond distance ratio and hydrolysis behaviour of Ag seem to be similar to that of alkaline elements (Baes and Mesmer 1986). As Ag^+ is a very soft metal ion, it also forms very strong chloride complexes.
- Curti (1997) lists a partitioning coefficient (calculated from mean seawater/solid carbonate concentrations) for solid solution formation in calcite of Ag that is similar to that of Cs, Cd, and Sr.
- Sorption data on minerals for Ag are generally extremely scarce. To our knowledge, only Legoux et al. (1992) measured Ag sorption on quartz-rich soil samples at slightly acidic to slightly alkaline pH. Some R_d values (at pH 6.6–8) are very high and may be due to precipitation. One value obtained at pH 6 appears to be reasonable and is of the same magnitude as observed for Cs and Ra under similar conditions.

4.4.3 Sorption Mechanisms and Selected Sorption Values

No reliable sorption data for Ag on cementitious materials or other minerals were found. However, there are several independent indications that Ag sorption is generally different from zero, and that Ag may show sorption values in the same order of magnitude as alkali and maybe alkaline earth elements. At least in terms of hydrolysis, Ag appears to be closer to alkali than to alkaline earth elements.

Together, the above evidence is taken to propose a nominal R_d value for Ag that is different from zero. Most evidence for the definition of a minimal value may be available for calcite; State IV is a calcite-dominated system and thus relatively well controlled (i.e., geochemically stable). In Wang et al. (2009), a value of 1 L/kg is selected for the sorption of Ra and Sr in State IV on calcite, whereas a value of zero is chosen (conservatively) for Cs. Based on the data discussed in Bradbury and Baeyens (1997) (and in the references therein) for sorption on calcite at elevated pH, the value of 1 L/kg is estimated to be representative for alkali and alkaline earth elements. This value is accepted for Ag sorption in State IV as a best estimate. Upper/lower limits cannot be selected on the basis of experimental data. However, it is proposed to use the value of 0 L/kg as a lower limit, because conditions leading to a null sorption cannot be excluded.

For States I–III, no values are proposed for best estimate and upper/lower limits because of insufficient data. Also, States I and III are less well defined in terms of cement chemistry and mineralogy (Table 4.6).

Table 4.6 Selected best estimate, upper and lower limit R_d values for silver

pH state	Best estimate (L/kg)	Upper limit (L/kg)	Lower limit (L/kg)
State I	i.d.[a]	i.d.	i.d.
State II	i.d.	i.d.	i.d.
State III	i.d.	i.d.	i.d.
State IV	1	i.d.	0

[a]*i.d.* insufficient data

Table 4.7 Supplemental R_d values for silver

pH state	Best estimate (L/kg)	Upper limit (L/kg)	Lower limit (L/kg)
State I	1	n.v.p.[a]	0
State II	1	n.v.p.	0
State III	1	n.v.p.	0
State IV	1	n.v.p.	0

[a]No value provided

4.4.4 Supplemental Values for Safety Assessment Calculations

For the provision of supplemental values, the best estimate of 1 L/kg given for State IV is accepted for all states. This is based on the reasoning that this value is derived from experimental data for calcite and the presence of calcareous aggregates in all states. Similarly, the lower limit of 0 L/kg is accepted for all states, while supplemental values for the upper limit are not provided. Note that these data are of a lesser quality than the best estimates (Table 4.7).

References

S. Aggarwal, M.J. Angus, J. Ketchen, Sorption of radionuclides onto specific mineral phases present in repository cements. NSS/R312, AEA-DandR-0395 (2000)

B. Allard, Mechanisms for the interaction of americium(III) and neptunium(V) with geologic media, in *Proceedings of the Material Research Society Symposium*, vol. 26 (1984), pp. 899–906

K. Andersson, B. Torstenfelt, B. Allard, Sorption and diffusion studies of Cs and I in concrete, SKB Technical Report (1983), pp. 83–13

Andra, Référentiel de comportement des radionucléides et des toxiques chimiques d'un stockage dans le Callovo-Oxfordien jusqu'à l'homme, Site de Meuse/Haute-Marne, Tome 1/2: Chapitres 1 à 4, Dossier 2005 Argile (2005)

C.A.J. Apello, D. Postma, *Geochemistry, Groundwater and Pollution*, 2nd edn. (A.A. Balkema Publishers, Amsterdam, 2006)

N. Ashikawa, T. Tajima, H. Saito, A. Fujiwara, Sorption behavior of radionuclides on calcium-leached mortar, in *Proceedings of the Material Research Society Symposium*, vol. 663 (2001) pp. 97–104

M. Atkins, F.P. Glasser, J.J. Jack, Zeolite P in cements: its potential for immobilizing toxic and radioactive waste species. Waste Manage. **15**(2), 127–135 (1995)
A. Atkinson, A. Nickerson, Diffusion and sorption of caesium, strontium, and iodine in water-saturated cement. Nucl. Technol. **81**, 100–113 (1988)
A. Atkinson, A.K. Nickerson, T.M. Valentine, The mechanism of leaching from some cement-base nuclear wasteforms. Radioact. Waste Manage. Nucl. Fuel Cycle **4**, 357–378 (1984)
C.F. Baes, R.E. Mesmer, *The Hydrolysis of Cations*, 2nd edn, ed. by R.E. Krieger (Wiley, New York, 1986)
S. Bagosi, L.J. Csetenyi, Caesium immobilisation in hydrated calcium-silicate-aluminate systems. Cem. Concr. Res. **28**, 1753–1759 (1998)
S. Bayliss, R.M. Howse, R. McCrohon, P. Oliver, Near-field sorption studies. AEAT/ERRA-0073 (2000)
J.A. Berry, K.A. Bond, K.A. Boult, M. Brownsword, A. Green, C.M. Linklater, Sorption onto samples of Permo-Triassic and Carboniferous sedimentary rock from boreholes 1, 2, and 10 at Sellafield. NSS/R383 (Oct 2001)
C.M. Bethke, *The Geochemist's Workbench, Release 6.0, GWB Reference Manual, Hydrogeology Program*. (University of Illinois, Illinois, May 2006)
M.H. Bradbury, B. Baeyens, *Far-field Sorption Data Bases for Performance Assessment of a L/ILW Repository in an Undisturbed Palfris Marl Host Rock* (PSI Bericht, Villigen, 1997), pp. 97–15
P. Calmon, J. Gamier-Laplace, C. Fortin, Fiche radionucléide: Argent 110 m et environnement (rév. 08/01/2002), Institut de Radioprotection et de Sûreté Nucléaire (2002)
G. Charlot, Les réactions chimiques en solution. L'analyse quantitative minérale. Masson, Cie, Paris, 7ème éd., (1983), 413 pp
R.M. Cornell, Adsorption behaviour of caesium on marl. Clay Miner. **27**, 363–371 (1992)
E. Curti, *Coprecipitation of Radionuclides: Basic Concepts, Literature Review and First Applications*. (PSI Bericht Nr., Villigen, 1997), pp. 97–10
N.D.M. Evans, Binding mechanisms of radionuclides to cement. Cem. Concr. Res. **38**, 543–553 (2008)
F.T. Ewart, S. Terry, S.J. Williams, Near field sorption data for caesium and strontium. AERE-M 3452 (1985)
P. Faucon, T. Charpentier, P. Henocq, J.C. Petit, J. Virlet, F. Adenot, Interactions of alkalis (Cs) with calcium silicates hydrates. in *Proceedings of the Material Research Society Symposium*, vol. 506 (1998), pp. 551–559
M. Fuhrmann, P. Colombo, Radionuclide release from cement waste forms in seawater. Radioact. Waste Manage. Nucl. Fuel Cycle **11**, 365–380 (1989)
T.G. Heath, D.J. Ilett, C.J. Tweed, Thermodynamic modelling of the sorption of radioelements onto cementitious materials, in *Proceedings of the Material Research Society Symposium*, vol. 412 (1996), pp. 443–449
R. Hietanen, E.-L. Kamarainen, M. Alaluusua, Sorption of strontium, caesium, nickel, iodine and carbon in concrete. Report YJT-84–04 (1984)
R. Hietanen, M. Alaluusua, T. Jaakkola, Sorption of caesium, strontium, iodine, nickel and carbon in mixtures of concrete, crushed rock and bitumen. Report YJT-85-38 (University of Helsinki, Department of Radiochemistry, Sept 1985)
S. Hoglund, L. Eliasson, B. Allard, K. Andersson, B. Torstenfelt, Sorption of some fission products and actinides in concrete systems, in *Proceedings of the Material Research Society Symposium*, vol. 50 (1985), pp. 683–690
S. Holgersson, Y. Albinsson, B. Allard, H. Boren, I. Pavasars, I. Engkvist, Effects of Gluco-isosaccharinate on Cs, Ni, Pm, and Th sorption onto, and diffusion into cement. Radiochim. Acta **82**, 393–398 (1998)
T.R. Holland, D.J. Lee, Radionuclide getters in cement. Cem. Concr. Res. **22**, 247–258 (1992)
S.L. Hoyle, M.W. Grutzeck, Incorporation of caesium by hydrating calcium aluminosilicates. J. Am. Ceram. Soc. **72**, 1938–1947 (1989)

W. Hummel, U. Berner, E. Curti, F.J. Pearson, T. Thoenen, *Nagra/PSI Chemical Thermodynamic Data Base 01/01* (Universal publishers, Parkland, 2002)

K. Idemitsu, H. Furuya, R. Tsutsumi, S. Yonezawa, Y. Inagaki, S. Sato, Migration of caesium, strontium and cobalt in water-saturated concretes. in *Proceedings of the Material Research Society Symposium*, vol. 212 (1991), pp. 427–432

International Atomic Energy Agency (IAEA), Application of ion exchange processes for the treatment of radioactive waste and management of spent ion exhangers, Technical Reports Series no. 408, Vienna, June 2002

T. Iwaida, S. Nagasaki, S. Tanaka, T. Yaita, Sorption of alkaline metal ions onto CSH (Calcium silicate hydrated phases). Cem. Sci. Concr. Technol. **55**, 21–25 (2001)

D. Jacques, L. Wang, E. Martens, D. Mallants, Time dependency of the geochemical boundary conditions for the cementitious engineered barriers of the Belgian surface disposal facility, project near surface disposal of category: a waste at Dessel. NIRAS-MP5 DATA-LT(NF) Version 1, NIROND-TR 2008-24 E (2008)

T. Jakubick, R.W. Gillham, I. Kahl, M. Robin, Attenuation of Pu, Am, Cs, and Sr mobility in concrete, in *Proceedings of the Material Research Society Symposium*, vol. 84 (1987), pp. 355–368

H.M. Johnston, D.J. Wilmot, Sorption and diffusion studies in cementitious grouts. Waste Manage. **12**, 289–297 (1992)

Lawrence Livermore National Laboratory, version 8 release 6 (LLNL v8r6). Extended Thermodynamic Database (1996)

Y. Legoux, G. Blain, R. Guillaumont, G. Ouzounian, L. Brillard, M. Hussonnois, Kd measurements of activation, fission and heavy elements in water/solid phase systems. Radiochim. Acta **58**(59), 211–218 (1992)

Nuclear Energy Agency (NEA-OECD), The jeff-3.1 nuclear data library, jeff report 21, oecd/nea, Paris, France (2006)

K. Noshita, T. Nishi, T. Yoshida, H. Fujihara, N. Saito, S. Tanaka, Categorization of cement hydrates by radionuclide sorption mechanism, in *Proceedings of the Material Research Society Symposium*, vol. 663 (2001), pp. 115–121

M. Ochs, D. Hager, S. Helfer, B. Lothenbach, Solubility of radionuclides in fresh and leached cementitious systems at 22 °C and 50 °C, in *Proceedings of the Material Research Society Symposium*, vol. 506 (1998), pp. 773–780

M. Ochs, B. Lothenbach, C. Talerico, Support of Kd models and datasets for the retention of radionuclides in cementitious repositories. Andra 2005 Report C.RP.0BMG.01-001, Andra 2005, France (2001)

M. Ochs, I. Pointeau, E. Giffaut, Caesium sorption by hydrated cement as a function of degradation state: experiments and modelling. Waste Manage. **26**, 725–732 (2006)

ONDRAF/NIRAS, Identification of critical radionuclides through a screening of the ondraf/niras 2003/2004 radiological inventory for category: a waste. Nirond-tr 2007-05 e (Apr 2011)

I. Pointeau, *Etude mécanistique et modélisation de la retention de radionucléides par les phases de silicate de calcium des ciments hydrates* (Thèse de l'Université de Reims-Champagne-Ardennes, France, 2000)

I. Pointeau, N. Marmier, F. Fromage, M. Fedoroff, E. Giffaut, Caesium and lead uptake by CSH phases of hydrated cement. in *Proceedings of the Material Research Society Symposium*, vol. 663 (2001), pp. 105–113

I. Pointeau, N. Coreau, P.E. Reiller, Uptake of anionic radionuclides onto degraded cement pastes and competing effect of organic ligands. Radiochim. Acta **96**, 367–374 (2008)

R.J. Serne, D. Rai, P.F. Martin, A.R. Felmy, L. Rao, S. Ueta, Leachability of Nd, U, Th, and Sr from cements in a CO_2 free atmosphere, in *Proceedings of the Material Research Society Symposium*, vol. 412 (1996), pp. 459–467

G. Sposito, *The Chemistry of Soils* (Oxford University Press, New York, 1989)

D. Sugiyama, T. Fujita, Sorption of radionuclides onto cement materials altered by hydrothermal reaction, in *Proceedings of the Material Research Society Symposium*, vol. 556 (1999), pp. 1123–1130

J. Tits, M.H. Bradbury, P. Eckert, A. Schaible, The uptake of some key-radionuclides by calcite under high pH cement pore water conditions. PSI TM-44-98-02 (1998)
J. Tits, E. Wieland, J.-P. Dobler, D. Kunz, The uptake of strontium by calcium silicate hydrates under high pH conditions: an experimental approach to distinguish adsorption from co-precipitation processes, in *Proceedings of the Material Research Society Symposium*, vol. 807 (2004), pp. 689–694
J. Tits, K. Iijima, E. Wieland, G. Kamei, The uptake of radium by calcium silicate hydrates and hardened cement paste. Radiochim. Acta **94**, 637–643 (2006a)
J. Tits, E. Wieland, C.J. Muller, C. Landesmann, M.H. Bradbury, A wet chemistry study of the strontium binding by calcium silicate hydrates. J. Colloid Interface Sci. **300**, 78–87 (2006b)
H. Viallis-Terrisse, Interactions des silicates de calcium hydratés, principaux constituants du ciment, avec let chlorures d'alcalins. Analogies avec les argile. Thèse de l'Université de Bourgogne, Dijon, France (2000), 255 p
L Wang, E. Martens, D. Jacques, P. De Canniere, J. Berry, D. Mallants, Review of sorption values for the cementitious near field of a near surface radioactive waste disposal facility. NIROND-TR 2008-23E (Apr 2009)
E. Wieland, J. Tits, M.H. Bradbury, The potential effect of cementitious colloids on radionuclide mobilisation in a repository for radioactive waste. Appl. Geochem. **19**, 119–135 (2004)
E. Wieland, J. Tits, D. Kunz, R. Dahn, Strontium uptake by cementitious materials. Environ. Sci. Technol. **42**, 403–409 (2008)
M. Yousuf, A. Mollah, J. Liang, D.L. Cocke, Speciation of silver in cementitious environment. J. Hazard. Mater. **63**(2–3), 163–177 (1998)
J.M. Zachara, C.E. Cowan, C.T. Resch, Sorption of divalent metals on calcite. Geochim. Cosmochim. Acta **55**, 1549–1562 (1991)

Chapter 5
Sorption Values for Calcium, Nickel, and Carbon

Abstract These elements are grouped together because, despite their differences in chemistry, their radioactive isotopes are taken up in cementitious materials by isotopic exchange, a physical process, rather than by some chemical sorption process. ^{41}Ca, ^{14}C, and ^{59}Ni plus ^{63}Ni are relevant constituents of radioactive wastes. For any radioactive isotope of a given element, isotopic exchange becomes important when the pore solution in the hydrated cement is already saturated with respect to some solubility-limiting phase of this element. In the case of Ca and C, this does not appear as a surprise, since both elements occur at high concentration levels in different HCP minerals as well as in the pore solution. In case of Ni, the formation of layered double hydroxides leads to a very low aqueous solubility in cementitious systems. Therefore, the comparatively low content of stable Ni in hydrated cement paste (stemming mainly from clinker production) is sufficient to reach the solubility limit for Ni in cementitious pore solutions.

5.1 Calcium

5.1.1 Chemical Form, Speciation, and Solubility

Calcium is not naturally found in its elemental state but occurs most commonly in sedimentary rocks in the minerals calcite ($CaCO_3$), dolomite ($CaMg(CO_3)_2$), and gypsum ($CaSO_4{\cdot}2H_2O$). It also occurs in igneous and metamorphic rocks chiefly in the silicate minerals: plagioclase, amphiboles, pyroxenes, and garnets (Deer et al. 2004; Hurlbut and Klein 1985). Its oxidation state is +II (Hein and Arena 2006).

Calcium has four stable isotopes (^{40}Ca, ^{42}Ca, ^{43}Ca, and ^{44}Ca), plus two more isotopes that, due to their long half-lives, can be considered stable (e.g. ^{46}Ca and ^{48}Ca). 97 % of naturally occurring calcium is ^{40}Ca, one of the daughter products

© Springer International Publishing Switzerland 2016

M. Ochs et al., *Radionuclide and Metal Sorption on Cement and Concrete*,
Topics in Safety, Risk, Reliability and Quality 29,
DOI 10.1007/978-3-319-23651-3_5

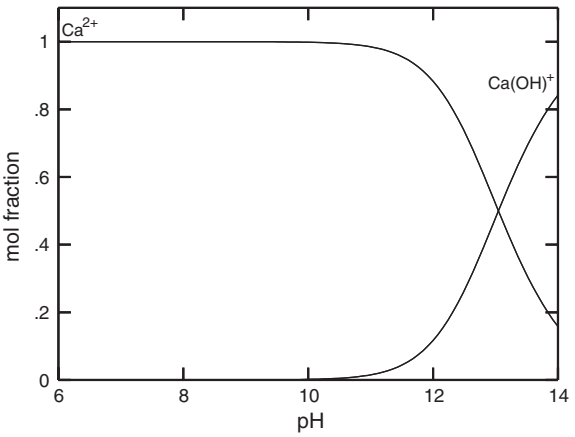

Fig. 5.1 Dissolved calcium speciation as mol fraction versus pH. Ca concentration is 10^{-8} mol/L. Thermodynamic database: ThermoChimie 7b

of ^{40}K decay, along with ^{40}Ar. Calcium also has a cosmogony isotope,[1] the radioactive ^{41}Ca, which has a half-life of 1.03×10^5 years (NEA 2006; Audi et al. 2003). This ^{41}Ca is predominantly produced by cosmic ray secondary thermal neutrons, captured by the stable isotope ^{40}Ca (Wieser 2006; Henning et al. 1987; Fink et al. 1990).

^{41}Ca is also produced anthropogenically by neutron capture in nuclear reactors and during nuclear tests. In nuclear reactors, ^{41}Ca is produced within the biological shield that surrounds the reactor core, which largely consists of calcium-rich concrete (Muller et al. 2000; Itoh et al. 2002). Furthermore, the extremely low natural abundance and the low specific activity of ^{41}Ca make it an ideal isotopic tracer for biomedical research (Freeman et al. 1997). In LILW, the following radionuclides may be present: ^{41}Ca (half-life 1.03×10^5 years) and ^{45}Ca (half-life 0.446 years) (ONDRAF/NIRAS 2011).

Calcium is not redox sensitive, and Ca^{2+} is the dominating dissolved species over a large pH range. The hydrolysis species $CaOH^+$ is significant only at pH > 12 (Fig. 5.1). $CaOH^+$ becomes more abundant than Ca^{2+} above pH ~ 13. In States I and II, calcium concentration is controlled by the solubility of portlandite as shown in Fig. 1.2 (Fig. 5.2 shows the solubility of portlandite in pure water). In State III, at a pH significantly lower than 12, Ca concentration in a cement system should be determined by the solubility calculated from log K of a given stoichiometric phase, or from solid solutions within a continuous evolution of CSH versus Ca content. The dissolved Ca concentration controlled by the dissolution of CSH phases is lower than the solubility of portlandite at around 20 mmol/kg and decreases with pH as shown in Fig. 1.2.

[1]Rare isotope created when a high-energy cosmic ray interacts with the nucleus of an in situ atom.

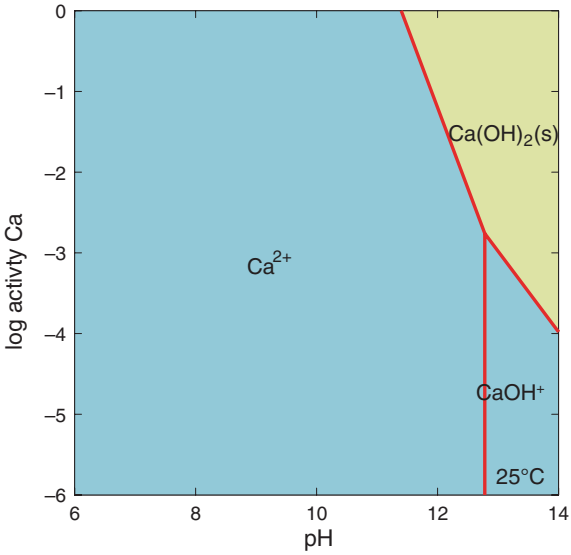

Fig. 5.2 Solubility and speciation of portlandite in a Ca–H_2O system. Thermodynamic database: ThermoChimie 7b

5.1.2 Literature Information, Mechanisms, and Selected Sorption Values

Ca is one of the main elements of various mineral phases in HCP, and the respective equilibrium solutions are saturated with respect to dissolved Ca. Under such conditions, it can be expected that any removal of radioactive Ca from solution will take place by isotopic exchange with stable Ca in the HCP matrix.

Nominal R_d values for radioactive Ca can then be calculated from the (accessible) amount of stable Ca in HCP and the solubility of Ca in the corresponding equilibrium solutions. This approach was used by Wang et al. (2009) for calculating $R_{d,\,M^*}$ values for radioactive Ni (see Sect. 5.2) and C (see Sect. 5.3), where $R_{d,\,M^*}$ is the distribution ratio of the radioactive isotope of a given element and is calculated as follows (Wieland and Van Loon 2002):

$$R_{d,M^*} = \left(M_c^*/M_{aq}^*\right) \times (v/m) = (M_c \times a/M_{aq}) \times (v/m) \tag{5.1}$$

where M_c and M_c* are the number of moles of the stable and radioactive isotopes of a given element in the HCP matrix (mol); M_{aq} and M_{aq}* are the number of moles of the stable and radioactive isotopes of a given element in the corresponding volume of pore solution (mol); m is the mass of HCP (kg), and v is the volume of the corresponding pore solution (L); and α is the accessibility factor, i.e. the fraction of the amount of stable isotope accessible to isotopic exchange (dimensionless).

The concentration of Ca in the HCP matrix and the solubility limit of Ca in the corresponding pore solutions are shown in Fig. 1.2, respectively. The accessibility factor α needs to be estimated for the three different mineral phases controlling dissolved Ca in States I–IV. According to Fig. 1.2, these are portlandite for States I and II, CSH for State III, and calcite (as calcareous aggregates) for State IV. Note that the largest uncertainty about estimating α for these minerals is for State III, because of the broad Ca domain in equilibrium (various Ca/Si ratios).

In case of calcite, it may be assumed that the accessibility (fraction of stable isotope accessible to isotopic exchange) of Ca and that of carbonate in $CaCO_3$ are numerically equal. For the accessibility of carbonate in finely distributed calcite, Bradbury and Sarott (1995) proposed a value of 10 %, based on an examination of data by Bayliss et al. (1992). Total calcite content was considered in their assessment. Pointeau et al. (2002) determined a value of ≈0.5 % on the basis of uptake experiments with radioactive carbonate. For accessibility determinations on calcite, time is a less important parameter, with Ca exchange being mainly a function of the available surface. Short-term laboratory determinations will provide most of the Ca uptake, while diffusive uptake by the matrix is a long-term process and accounts only for a small fraction of total uptake. Pointeau et al. used calcite solid for accessibility determination neglecting[2] any carbonate in cement minerals with different grain sizes and developed a simple relation between solid carbonate grain size and accessibility. Note that surface reactivity, and hence accessibility, is likely to depend on the type of calcite solids. Based on this relation and the expected grain size distribution of the ONDRAF/NIRAS backfill mortar, Wang et al. (2009) calculated a mean accessibility factor α of 0.23 %. It appeared that this value allowed the calculation of distribution values for radioactive carbonate that are in reasonable agreement with literature data (see Sect. 5.3). Based on this evidence, the value of 0.23 % is proposed as best estimate for the accessibility of stable isotopes in calcite contained in HPC or mortar.

Mandaliev et al. (2010) measured the accessibility of Ca in tobermorite and xonotlite by following the removal of ^{45}Ca from solution. After one year, about 35 % of the ^{45}Ca was removed, which corresponds to a replacement of about 50–60 % of the Ca in the CSH phases. This indicates that the values considered for the present data selection, which are based on short-term experiments (up to 140 days for the Pointeau et al.'s data), may be very conservative for situations where long time frames are relevant. Note, however, that accessibility is (1) a function of the type of solid system, and (2) also structurally sensitive; i.e., the exchange characteristics of crystalline tobermorite are not necessarily applicable to gel-like CSH.

In the absence of systematic data regarding the accessibility of stable Ca in calcite, portlandite, and CSH phases embedded in a HCP matrix at relevant solid/

[2]Neglecting carbonate in cement is conservative in view of determining sorption values. Also, the related model is independent of cement composition and avoids the need to account for difficult to estimate atmospheric/aqueous carbonation processes.

solution ratios, it is proposed to consider in a first and cautious approximation only calcite and neglect the contribution of CSH and portlandite. One particular source of uncertainty is the impact of cement degradation on accessibility, especially for portlandite and CSH. In the current approach, α was considered constant for all degradation States and based on calcareous granulates only. Any exchange with other calcium-bearing minerals, also those newly formed from infiltrating soil water, is conservatively ignored. Another source of uncertainty relates to the kinetics of dissolution/precipitation of CSH versus portlandite and calcite. At present, uncertainties regarding the accessibility factor cannot be evaluated on the basis of reliable quantitative information. An arbitrary lower limit of 0.1 % and upper limit of 10 % were considered by Bradbury and Sarott (1995). A ten times smaller uncertainty range is considered in this review (see further), because the calcareous aggregates are likely to behave in a similar manner as the calcite used by Pointeau et al. (2002) in their derivation of the accessibility factor.

As the amount of Ca-bearing solid and the aqueous concentrations of stable Ca are variable within each degradation State, the following approach was used (Fig. 5.3):

- For the calculation of best estimates, the values representing the mid-point of each State were used (note that in State II a fixed value exists);
- For upper/lower limit, an uncertainty range for the accessibility factor was used, in line with the concept of uncertainty used for upper/lower limit estimation for R_d values, i.e. half an order of magnitude up and down. An uncertainty range of one order of magnitude was used for each State, which is equal to an uncertainty factor (UF[3]) of 3.3, where lower limit = best estimate/UF and upper limit = best estimate × UF. This uncertainty includes, among others, the potential impact of coating of grains with a wide range of reaction products and particulate material on accessibility, which is currently difficult to quantify.

In view of this situation, it is proposed not to assign uncertainties to the concentration of stable Ca in the respective solids and to the solubility limit and to base these on the values given in Fig. 1.2. Formal R_d values for radioactive Ca can then be calculated for each state on the basis of the following considerations (also see Fig. 5.3):

- the concentration of stable Ca in the HCP matrix and the solubility limit of Ca in the corresponding pore solutions as shown in Fig. 1.2 (see also Fig. 5.3); the evolution in R_d values is inversely related to the evolution in the Ca pore water concentration;
- the accessibility factor discussed above: best estimate = 0.0023 (or 0.23 %); lower limit = 0.0008 (or 0.08 %); and upper limit = 0.008 (or 0.8 %). Although the same uncertainty is assumed throughout all States of cement degradation, R_d values in State III are given for several discrete pH values to account for the

[3]An uncertainty factor (UF) is defined for x such that the range of possible x values is defined by the limits best estimate/UF $\leq x \leq$ BE × UF.

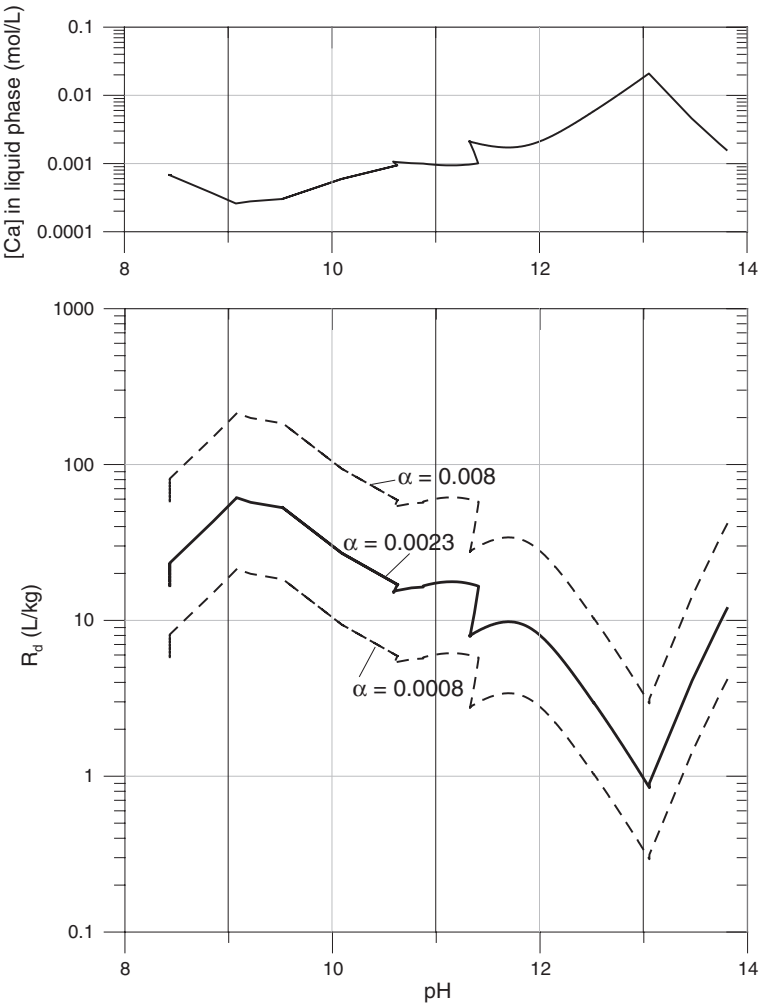

Fig. 5.3 *Top* Calcium concentration in pore water as function of pH. *Bottom* Calculated distribution ratio (R_d) values for calcium (Eq. 5.2) as function of pH for the degradation of category A cement in contact with soil water at 10 °C (based on calculation case 7, Jacques et al. 2008). The accessibility factor has a best estimate of 0.0023 (0.23 %), with 0.0008 (0.08 %) as lower limit and 0.008 (0.8 %) as upper limit based on uncertainty factor of 3.3 (uncertainty range of one order of magnitude)

variation in accessible CSH. Indeed, owing to sequential dissolution of several CSH phases in State III, variation in accessible amount of (solid) calcium, and hence calculated R_d values, is larger than that in other States. Therefore, R_d values for discrete pH values are obtained (best estimate $\alpha = 0.23$ %): $R_d = 0.97$, 30.7, 8.02, 9.15, and 17.30 L/kg at pH of 13, 12.5, 12, 11.5, and 11 (at 10 °C). Best estimate R_d values and upper and lower limits are summarised in Table 5.1.

Table 5.1 Selected best estimate, upper and lower limit R_d values for calcium

pH state	Best estimate (L/kg)	Upper limit (L/kg)	Lower limit (L/kg)
State I	7	23	2
State II	1	3	0.3
State III	10	30	3
State IV	40	130	13

5.2 Nickel

5.2.1 Chemical Form, Speciation, and Solubility

LILW contains both ^{59}Ni (half-life 76,000 years) and ^{63}Ni (half-life 101 years). Neither ^{59}Ni nor ^{63}Ni is a naturally occurring radionuclide. They are produced by neutron activation of, respectively, ^{58}Ni and ^{62}Ni, both naturally occurring and stable isotopes of nickel in the structural steels and internal components of nuclear reactor vessels. Nickel is resistant to attack by water or air and, therefore, is often used as a protective coating for other metals or as an alloy to create a corrosion-resistant metal such as stainless steel and Inconel. Limited amounts of these nickel isotopes can enter the operational waste from a nuclear reactor by corrosion of stainless steel surfaces and accompanying release of nickel into the primary cooling circuit. Both radionuclides also enter the dismantling waste from nuclear reactors.

The Eh–pH and solubility diagrams for nickel are produced with the thermodynamic data given in Table 5.2 and are shown in Fig. 5.4. How different aqueous nickel species vary with pH is summarised in Fig. 5.5 [based on calculations with *The Geochemist's Workbench*® (Bethke 2006)].

Most abundant aqueous nickel species at high pH relevant to cement systems is $Ni(OH)_3^-$ as predicted by the speciation diagram produced with the recent NEA thermodynamic data (Gamsjager et al. 2005) (Fig. 5.5). A significant point is that the NEA (2005) review did not select the neutral species $Ni(OH)_2(aq)$ which is normally considered to be present in an aqueous cement environment (e.g., see Berner 2002; Pilkington and Stone 1990; Cross et al. 1995). The NEA review argues that there is no evidence for the existence of $Ni(OH)_2(aq)$ species from the reviewed experiments. In all cases, the presence of $Ni(OH)_3^-$ explains experimental data equally as well as the alternative, assuming the presence of two hydrolysis species $Ni(OH)_2(aq)$ and $Ni(OH)_3^-$. Hummel and Curti (2003) argue that despite

Table 5.2 Thermodynamic data for nickel

Reaction	log K (25 °C)
$NiOH^+ = Ni^{2+} + OH^-$	−4.4614
$Ni(OH)_3^- = Ni^{2+} + 3\ OH^-$	−12.8043
$Ni(OH)_2(beta) + OH^- = Ni(OH)_3^-$	−4.1699

Source NEA database (Gamsjager et al. 2005)

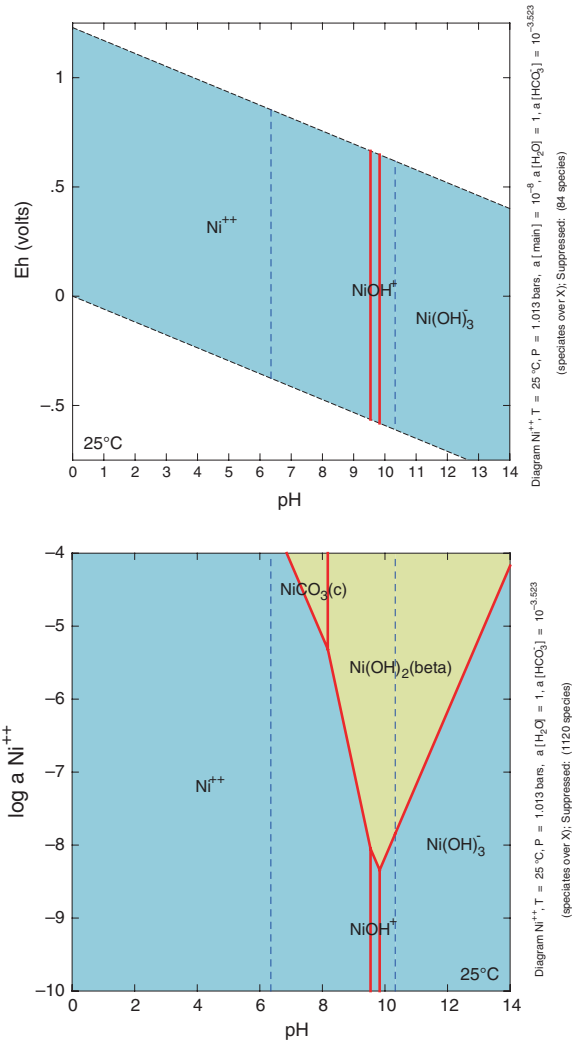

Fig. 5.4 Eh–pH (*top*) and solubility (*bottom*) diagrams of nickel calculated with *The Geochemist's Workbench*®. Nickel activity is 10^{-8}, and HCO_3^- is $10^{-3.523}$

the uncertainty associated with the stability constants of high hydrolysis Ni species, chemistry of carbonate complexes of Ni is even less known.

In terms of Ni solubility in a cement system, most studies consider nickel hydroxide $Ni(OH)_2(s)$ as a relevant solubility-controlling phase (see Fig. 5.4 for the solubility diagram of $Ni(OH)_2$). A detailed experiment on determination of $Ni(OH)_2(s)$ solubility in a wide range of pH was presented by Mattigod et al. (1997), and a typical result from the study is shown in Fig. 5.6. Mattigod et al. (1997), however, emphasised that determination of stability constants of different hydrolysis species present at pH higher than 11.3 was not possible because the solubility measurements were at or below the instrumental detection limit.

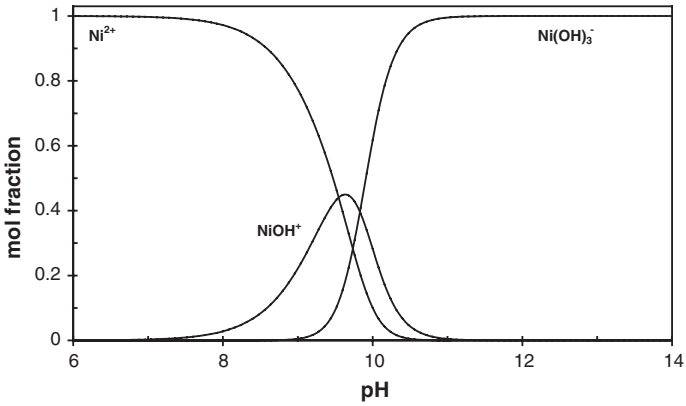

Fig. 5.5 Dissolved nickel speciation (total dissolved Ni = 1×10^{-8} molal, no precipitation of solids)

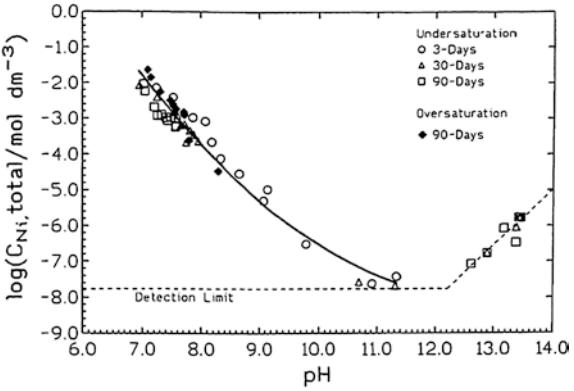

Fig. 5.6 Solubility of $Ni(OH)_2$ (s) as a function of pH. With kind permission from Springer Science + Business Media: Mattigod et al. (1997), Fig. 2)

We notice that for cement environments, the solubility curve shown in Fig. 5.4 is probably too simplified, as it does not account for other elements such as aluminium, magnesium, andfor calculating an apparent iron. Also, nickel hydroxide is not stable and reacts with other cement components to form layered double hydroxides, with lower solubilities than nickel hydroxide (Wieland and Van Loon 2002).

With the NEA data as shown in Fig. 5.4, the solubility of $Ni(OH)_2$ (beta) is related to pH by the following relationship:

$$\text{Log}\left\{Ni(OH)_3^-\right\} = \text{pH} - 18.17 \tag{5.2}$$

where { } denotes activity (dimensionless). If the solubility of $Ni(OH)_2$ (beta) (i.e. pure $Ni(OH)_2$) is determined by the aqueous activity of $Ni(OH)_3^-$ as predicted, the solubility of $Ni(OH)_2$ (beta) at pH 12.5 and 13.5 should be about 2×10^{-6} and 2×10^{-5} M, respectively. These values are somewhat higher than the experimental data shown in Fig. 5.6 (~6×10^{-8}–2×10^{-6} M), the latter being representative

of mixed nickel phases. Note that in the Mattigod et al.'s (1997) data (Fig. 5.6), the solubility is shown versus detection limit, and the rising detection limit as pH increases reflects difficulties with the experimental matrix. Therefore, solubility values at pH 12.5 and higher are at the detection limit.

Note that the PSI-NAGRA database assigns a solubility constant for the reaction $Ni(OH)_2 + OH^- = Ni(OH)_3^-$ as $\log K = -6.48$ which is more than two orders of magnitudes lower than the log K from the NEA (2005) review (Table 5.2). That explains the observation that the PSI-NAGRA database predicts Ni solubility two orders of magnitudes lower than that predicted by the NEA (2005) database.

Although the $Ni(OH)_2$(s) phase has been studied as a relevant solubility-controlling phase in cement waters, Hummel and Curti (2003) consider that the phase is not relevant for most of geological environments because it is too soluble. Other more stable phases such as magnesium clay minerals and layered double hydroxides are more likely to precipitate with Ni and regulate the solubility. Based on wet chemistry data and spectroscopic evidences, Wieland and Van Loon (2002) concluded that the Ni solubility in a fresh cement system at pH 13.3 is 2×10^{-7} mol/L and is probably controlled by the solubility of mixed Ni–Al layered double hydroxides (LDHs) which is formed in cement.

There is consistency in the observations that all solubility experiments performed under cementitious conditions resulted in a solubility or total dissolved Ni concentration significantly lower (range 10^{-8}–10^{-7} M) than the solubility predicted (range 2×10^{-6}–2×10^{-5}) with a pure phase of nickel hydroxide as the controlling phase. The solubility of the pure phase $Ni(OH)_2$ (s) can thus only be taken as the conservative upper limit to indicate the soluble Ni concentration in a cement system.

Furthermore, based on geochemical calculations (see Fig. 1.2), aluminium and magnesium concentrations are fairly constant across States I and II. This is not true for State III as both [Al] and [Mg] go up, and hence, the speciation and related solubility may be different from those at higher pH.

Finally, an interesting source of data relevant for long-term stable alkaline geochemical conditions is provided by natural analogues. From natural analogue sites such as Maqarin (Jordan) with its hyperalkaline groundwater (pH 12.7–12.9), total dissolved nickel concentrations were found to be in the range 10^{-8}–10^{-7} M (Andra 2005). These values have the same order of magnitude as the experimental values discussed above.

5.2.2 Sorption Values from the Literature for the Benchmark Cement

Figure 5.7 shows the summarising plot of reviewed R_d values from the literature as a function of pH. Experimental conditions under which these R_d values were

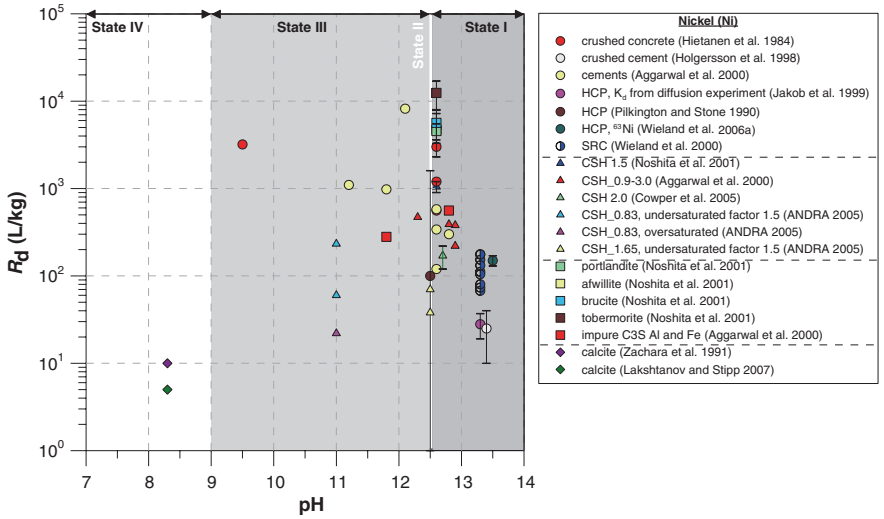

Fig. 5.7 Distribution ratio (R_d) of nickel in cementitious systems. *HCP* hardened cement paste; *OPC* ordinary Portland cement; *SRC* sulphate-resisting cement; *CSH* calcium silicate hydrate

measured are given in Table A.6 (see Annex). These values range over 6 orders of magnitudes, i.e. R_d is in the range of 0.01 to 10,000 L/kg.

Holgersson et al. (1998) performed batch sorption experiments on crushed cement at pH > 13 (data for pH were not available from the original publication, and we therefore assessed pH from the cement pore water composition) and found that the distribution ratio, defined as K_d, increases from 10 to 40 L/kg with increasing contact time from one day to 2 months. It was claimed that the initial Ni concentration was low enough not to cause precipitation.

Pilkington and Stone (1990) studied sorption of Ni on OPC cements and limestone at pH of about 12.5. Initial Ni concentrations were $<10^{-8}$ mol/L which are well below the experimental solubility of Ni hydroxides. A best estimate R_d of 100 L/kg was reported. A point of concern was the sorption of Ni on the container wall. About 80 and 30 % of the initially introduced Ni was found sorbed on the container wall in the absence and in the presence of cement, respectively. It is surprising that the sorption on the wall can be as high as 30 % even when cement sorbent was in the system. Wall sorption is generally considered as negligible in a batch sorption experiment as long as a finely suspended sorbent is present. This is because the specific surface area of the sorbent is normally much larger than the specific surface area of the container wall.

Nevertheless, Bradbury and Sarrot (1995) expressed their concern about wall sorption in the work of Pilkington and Stone (1990) and considered it as a major uncertainty. It is not clear whether the wall sorption is the reason for the observed large range in R_d, i.e. from 1 to 1600 L/kg. Although the sorption of Ni in terms of R_d was found larger than zero, the final concentrations of Ni in the control

experiment (without cement) were often found to be similar to those observed in a sorption experiment, making the calculation of an R_d value difficult. There seemed no influence of cement types on sorption of Ni. There was an indication that R_d increased slightly with increasing liquid to solid ratio. Within an order of magnitude variation in initial Ni concentration (7×10^{-9}–4×10^{-10} M), R_d decreased slightly but consistently. Filtration did not show any impact on the final R_d values, suggesting a solution free of Ni colloids or particulates.

R_d values on a large number of pure cement phases, including portlandite, CSH gels, crystalline phases, and calcium aluminates, were determined by Noshita et al. (2001). Experiments were performed with Ni concentrations of 10^{-8} M, hence well below the solubility of $Ni(OH)_2$ (s). R_d values ranged from around 100 to 20,000 L/kg (for real R_d values, see Table 5.3 reproduced from the original paper). The fact that only the initial pH was given (pH 12.6) and the experiment was performed in air makes it difficult to judge the quality of the data because the final pH might vary when no pH buffer was present in the system. The R_d for portlandite was 5500 and 3600 L/kg in NaOH and $Ca(OH)_2$ solutions, respectively, and is considered as good-quality data because the pH of 12.6 must have been well buffered. The authors argued that R_d is independent of the C/S ratio on CSH gels, which indicates sorption of neutral $Ni(OH)_2$ (aq) species through non-electrostatic sorption. From Table 5.3, it is clear that R_d varies when C/S ratio changes, but without a consistent trend. However, assuming $Ni(OH)_2$(aq) as the dominant Ni

Table 5.3 R_d values (L/kg) for Ni on different cement components

Cement components		C/S ratio	Ni [$Ni(OH)_2$(aq)]	
			In NaOH solution[a]	In $Ca(OH)_2$ solution
Calcium silicate compounds	CSH	1.5	900	1200
		1.2	440	1000
		1.0	2300	3600
		0.83	230	320
	Afwillite	1.5	2300	7200
	Tobermorite	0.8	17,000	7900
	Gyrolite	0.67	170	21,000
Hydroxides	Portlandite		5500	3600
	Brucite		8000	3300
	Gibbsite		9800	260
Calcium	AF_m		1100	290
Aluminate	AF_t		260	73
Compounds	Hydrogarnet		750	290
Others	Quartz		6	290
	Calcite		140	32

Source Noshita et al. (2001)

[a]The authors of the title study estimated a NaOH concentration of about 0.04 molal (without activity corrections) for the pH given in Noshita et al. (2001) assuming that NaOH regulates the pH

species, as Noshita et al. (2001) did, is inconsistent with the "best available" thermodynamic data from NEA (see discussion in Sect. 5.2.1). There is indication that well-crystalline CSH phases have larger R_d for Ni than CSH gels. Removal of Ni by hydroxides such as portlandite was thought to be related to co-precipitation of Ni in a $Ca(OH)_2$ structure when Ni replaces Ca. Finally, calcium aluminates had the lowest R_d compared to CSH and hydroxides. The sorption of Ni on calcium aluminates was thought to occur on surface hydroxyl groups. R_d for calcite is low compared to other minerals, suggesting that calcite is not an effective sorption sink. Since the experiments were performed at the assumed pH 12.6 for all the minerals including calcite, the R_d for calcite was not added in Fig. 5.7 since pH 12.6 is not relevant for State IV in the present evaluation.

Aggarwal et al. (2000) measured R_d of Ni on cements, CSH gels, minor minerals, and NRVB materials. Experiments were performed in the pH range of 11–13. In cement systems, pore waters were in contact with cements, while in the experiments using CSH as sorbents, saturated portlandite water was used. Initial Ni concentration was less than 10^{-8} M. R_d values are in the range of 200–8000 L/kg. In terms of Ni uptake, CSH was thought to be the dominant sorption phase because the extent of sorption depends predominantly on the quantity of CSH gel present in cement. Particularly, R_d increased as the C/S ratio decreased. The authors suggested that increasing sorption with decreasing C/S on CSH is probably due to the replacement of Ca by Ni. Nickel sorption is relatively high on all cements, with the highest sorption occurring on cements containing low-lime CSH with a high alumina content.

Hietanen et al. (1984) reported R_d values determined on crushed concrete (<4 and 2 mm particle size at pH 12.5 and 9.5). The R_d was found to be in the range of 560–5000 L/kg. Although the data are for concrete, they are included because the R_d values are not significantly higher than data from cement phases suggesting little or no influence of fresh aggregates on sorption. The data are also included because they provide the only data point at pH range 9–10. Equilibration times of 3–30 days were employed and had no impact on R_d values; hence, fast uptake kinetics should have been the case. Filtration increased R_d values up to two orders of magnitudes, suggesting that Ni particulates or colloids were removed from the system while measuring R_d. This is in contrast to the findings of Pilkington and Stone (1990). These different observations concerning the filtration effect on R_d occur probably because Hietanen et al. (1984) applied 10^{-6} mol/L initial Ni concentration, which is two orders of magnitudes higher than the one used by Pilkington and Stone (1990). The authors suspected that Ni may have been removed from the cement water by precipitation of Ni hydroxide. The initial concentration of 10^{-6} mol/L is close to the theoretical solubility of $Ni(OH)_2$(beta) at pH 12.6 (it was 2×10^{-6} at pH 12.5). It is not excluded that the observed effect of filtration on R_d was caused by precipitation of Ni-containing minerals [not necessarily pure $Ni(OH)_2$]. Also interesting is that the study revealed from radiographs that Ni was distributed equally between cement phases and sandy ballast. This suggests that cement phases are not the only sorption sinks for Ni.

In a subsequent study, Hietanen et al. (1985) measured R_d of Ni on mixtures of crushed concrete and rock and found much lower R_d, in the range of 2–15 L/kg. The decrease in R_d compared to values for individual components was explained by accounting for the relative mass of each component and their associated R_d, and by correcting for differences in experimental conditions (i.e. composition of concrete pore water, S/L ratios). Strong dependence of R_d on S/L ratio was also observed, suggesting that the measured R_d values are not equilibrium distribution ratios (Hietanen et al. 1985). A two orders of magnitude drop in R_d was noticed when S/L increased from 0.1 to 3.6 kg/L. A similar dependency on S/L ratio was reported by Wieland and Van Loon (2002) and was attributed to "non-sorption" behaviour.

R_d values for Ni on several cement components were extracted from Andra (2005) (see Fig. 5.8). Data that were practically indistinguishable from zero have not been retained in the summary graph: CSH_1.65, CSH_0.83, and hydrogarnet (all data). All other data points for CSH, ettringite, and hydrotalcite were retained and represented in the summary (Fig. 5.7). One data point for CSH_0.83 from Andra (2005) was retained because it is judged as reflecting a real sorption value, despite being determined from an oversaturation condition with respect to $Ni(OH)_2$ solubility. Ettringite is relevant because it was shown to accommodate Ni^{2+} at the divalent metal site in the crystal structure (Evans 2008). Hydrotalcite is also relevant as it is a magnesium- and aluminium-containing mineral, with aluminium being an important element in governing nickel solubility. To present these R_d values in Fig. 5.7, we assigned the following pH values to the following CSH phases: pH 11 and 12.5 for CSH_0.83 and CSH_1.65, respectively. From

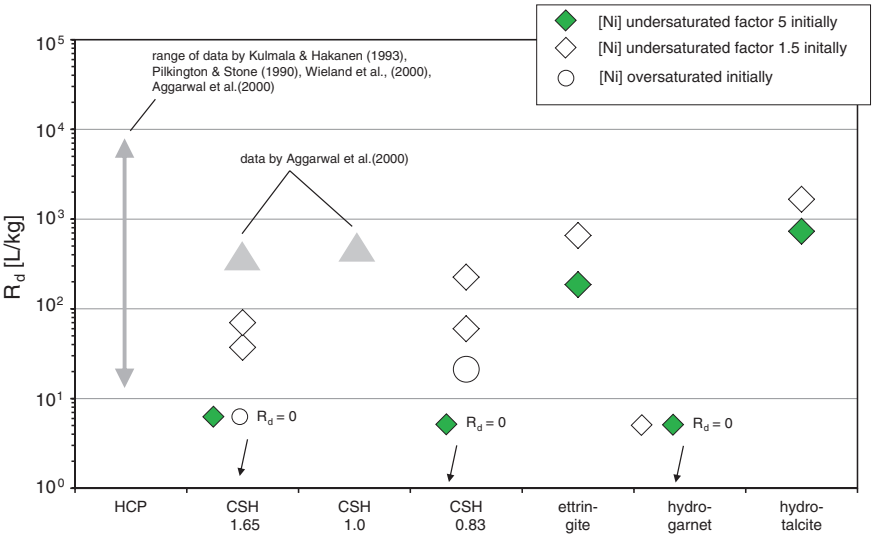

Fig. 5.8 Distribution ratio R_d of nickel on some cement components [modified from Andra (2005)]

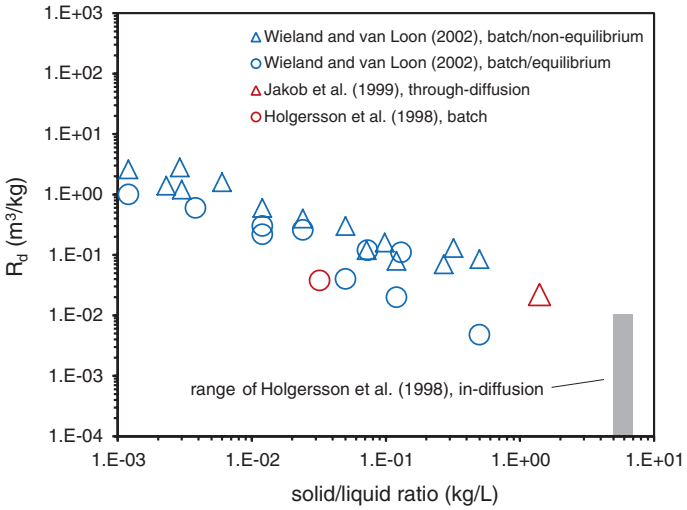

Fig. 5.9 Distribution ratio R_d of nickel on HCP as a function of S/L ratio used in the uptake experiments (modified from Wieland and Van Loon 2002). They estimated the solid/water ratio of the near field as 2 kg/L

Fig. 5.8, one can see that R_d varies over 3 orders of magnitudes depending on sorbent phases and the Ni saturation state.

Very detailed and relevant studies on uptake of Ni onto cement were carried out by Jakob et al. (1999), Wieland et al. (2006), Wieland et al. (2000), Vespa et al. (2006a, b), and Scheidegger et al. (2000). These authors performed wet chemistry solubility and sorption studies, diffusion experiments, and spectroscopic investigations on the surface speciation of Ni on cement. The uptake of Ni was demonstrated to depend on the S/L ratio; hence, the uptake is presumably not an adsorption process [see Fig. 5.9 for the data compilation from Wieland and Van Loon (2002)].

Different from other studies applying wet chemistry methods for sorption measurements, Wieland et al. (2006) determined stable Ni concentration in equilibrium with HCP to be in the range 10^{-8}–10^{-7} mol/L, regardless of the S/L ratios from 10^{-6} to 0.13 kg/L. This concentration range agrees fairly well with Ni solubility experimentally determined in cementitious systems (the solubility at pH 13.3 determined by Wieland and Van Loon (2002) was 2×10^{-7} M). The authors further demonstrated that calculated Ni concentrations based on the relationship between the Ni taken up by the solid and the concentration of dissolved Ni at equilibrium, using observed distribution ratios ($R_d = 150$ L/kg as lower bound[4] and $R_d = 1600$ L/kg as upper bound) at S/L ratios $>10^{-4}$ kg L^{-1}, are significantly higher than the experimental data. They therefore concluded that the partitioning

[4]Lower bound because R_d value obtained without adding stable Ni (inventory of dissolved stable Ni for HTS (Haute Teneur en Silice) Portland cement was 6.5×10^{-8} M).

of Ni between HCP and pore water cannot be interpreted in terms of a linear reversible sorption process but is more likely controlled by solubility of a Ni solid phase formed upon Ni cement interaction.

The uptake studies further revealed that an equilibrium was obtained less than 7 days after ^{63}Ni addition, suggesting fast kinetics of ^{63}Ni uptake (Wieland et al. 2006). The latter observation is in agreement with the fast kinetics uptake reported by Hietanen et al. (1984). When no stable Ni was added to the HCP, an R_d value of 150 L/kg was determined at pH 13.3. The latter R_d value is consistent with the best estimate reported by Pilkington and Stone (1990). When stable Ni-loaded HCP samples were used at a S/L ratio of 2.5×10^{-2} kg/L, the distribution ratio of ^{63}Ni increased from 200 (added stable [Ni] of 10^{-6} M) to 1200 L/kg (added stable [Ni] of 10^{-4} M). Isotopic exchange of ^{63}Ni with a small fraction of non-radioactive Ni in the cement matrix was considered to be responsible for the uptake of ^{63}Ni by HCP. Isotopic exchange was described by means of a partition coefficient $\alpha_p = R_{d,\,M^*}/R_{d,\,M}$, where $R_{d,\,M^*}$ and $R_{d,\,M}$ are the distribution ratios of, respectively, ^{63}Ni and stable Ni. The partition coefficient α_p ranged between 2.8×10^{-2} and 4.5×10^{-2} as a result of different experimental conditions (7 or 30 days of equilibration; $[Ni]_{stable}$ added, between zero and 10^{-4} M). The findings from this study indicate that isotopic exchange accounts for ^{63}Ni uptake by HCP. Isotopic exchange of ^{63}Ni, however, is determined by the total Ni concentration in pore water and the inventory of exchangeable Ni in HCP. Determination of uptake of nickel radioisotopes in cementitious materials therefore requires knowledge of the non-radioactive nickel inventory. Such analyses were carried out for selected cements to be used in the future ONDRAF/NIRAS repository in Dessel (see Sect. 5.2.3.2).

With the support of spectroscopic data, the same authors concluded that the distribution of Ni in a cement system can be best explained by a solubility-limited mechanism (Scheidegger et al. 2000). Mixed Ni–Al layered double hydroxides (LDHs) are probably present in cement and play the role of solubility-controlling phases. The solubility of such a phase in terms of Ni concentration is about 10^{-8}–10^{-7} mol/L at a pH around 13. Upon adding ^{63}Ni tracer into the cement water system, ^{63}Ni is exchanged with stable Ni present in Ni–Al LDHs through isotopic exchange. Because the latter process was defined in this review as a sorption mechanism, we propose to quantify the uptake of ^{63}Ni by means of an apparent distribution ratio, R_d, based on the following arguments:

- Although Ni distribution in general is controlled by a solubility mechanism (Wieland et al. 2006), the uptake of ^{63}Ni in particular is not and is regulated by isotopic exchange;
- ^{63}Ni uptake by cement is fast and reaches an equilibrium within 7 days (Wieland et al. 2006)
- The only unsatisfied condition for treating ^{63}Ni uptake by cement as a sorption process is that uptake linearity has not been demonstrated. However, since the uptake of ^{63}Ni is proportional to the Ni content on cement (isotopic exchange/dilution), an apparent R_d for ^{63}Ni can be estimated based on the total Ni content of the specific cement/concrete used.

A detailed procedure for calculating an apparent R_d for ^{63}Ni uptake is given in Sect. 5.2.3.2 based on an isotopic exchange mechanism, provided that the content of stable Ni in cement is known. Data on total nickel in cements are rarely determined; hence, relevant R_d values for ^{63}Ni uptake by cement are scarce in the literature. Wieland et al. (2006) determined R_d for ^{63}Ni as 150 L/kg on a commercial cement without adding extra stable Ni. The R_d was interpreted as being controlled by isotopic exchange between ^{63}Ni and stable Ni impurities present in cement.

Apparent R_d values are also affected by the S/L ratio, as is illustrated in Fig. 5.9. Higher S/L ratios more appropriate for disposal conditions result in lower R_d values. While the trend is clear between S/L 10^{-3} and 10^{-1} kg/L, it is less clear at higher S/L values. The R_d value obtained from diffusion tests (S/L ~ 1.5) is about five times smaller than the value at 10^{-1} kg/L, but based on the difficulties to model reliably the diffusion test data (Jakob et al. 1999), the importance of the diffusion test was downweighed. Re-evaluating the data from Fig. 5.9 then suggests that the downward trend flattens off between S/L 10^{-1} and 1 kg/L, with an R_d between 100 and 200 L/kg. Therefore, also for higher S/L ratios, an R_d of 150 L/kg still seems justified.

The apparent R_d determined by Wieland and Van Loon (2002) was obtained at pH 13.3; hence, it is valid for degradation State I. No information was provided as concerns extrapolation to other states. Previous investigations (Pilkington and Stone 1990; Ochs et al. 1998) and speciation modelling (Fig. 5.4) have demonstrated that β-$Ni(OH)_2$ may be the solubility-controlling phase. Recent spectroscopic data, however, revealed that mixed Ni–Al layered double hydroxides control immobilisation of Ni in HCP across States I to III. The β-$Ni(OH)_2$ solubility was shown to decrease from pH 13 to 10, with a minimum solubility at approximately pH 10 (Fig. 5.4) and then increases again with decreasing pH. The solubility of Ni controlled by the mixed Ni–Al layered double hydroxides likely decreases with pH in a similar way as does the beta-$Ni(OH)_2$ because (1) both Ni and Al hydroxides become less soluble as pH decreases towards a neutral value. When the stoichiometry and the solubility constant of the Ni–Al double hydroxides are not available for estimating accurately its solubility, the mixture of pure Ni and Al phases may be used as a proxy for a rough approximation; (2) the dominant aqueous species of Ni in the concerned pH range is $Ni(OH)_3^-$ which has a decreased concentration from State I to State III. Based on these analyses, a general decrease of Ni solubility with pH is expected and it is likely to be controlled by the slope of the solubility curve shown in Fig. 5.4 (the $Ni(OH)_3^-$ line in the bottom figure). In terms of sorption, an opposite trend is anticipated, i.e. Ni sorption will increase with decreasing pH because of an increasing stability of the dominant aqueous species $Ni(OH)_3^-$ when pH decreases from State I to States II and III. The summary R_d data seem to be in agreement with this hypothesis. Therefore, in principle, a higher R_d may be assigned to States II and III.

Based on the data from the NEA database (Gamsjager et al. 2005), the solubility decreasing factor from pH 13.3 to 12.5 is 1.3×10^{-5} M/2.1×10^{-6} M = 6.2, while from pH 13.3 to 10, it is 1.3×10^{-5} M/6.7×10^{-9} mol/L = 1940. Note that these solubility decreasing factors are based on calculated solubilities and thus depend on the database used. A solubility decrease by a factor of 10 seems acceptable from

pH 13.3 to 12.5 (the difference in speciation between States I and II is only one hydroxyl group), but a factor of ~2000 seems very large for a pH drop from 13.3 to 10 (there is considerable uncertainty about the change in aqueous speciation when going from State I to State III, and therefore, a more careful approach would be to limit the solubility reduction factor to 10 for States I to III). Also, solubility calculations using the NEA database did not consider other elements such as aluminium and magnesium, which are likely to influence Ni solubility.

At State IV, another solubility-controlling mineral phase was identified through geochemical modelling, i.e. $NiCO_3$ becomes apparent (Fig. 5.4). Because its solubility is considerably larger than that of β-$Ni(OH)_2$ in States I to III (Fig. 5.7), the Ni uptake will be much reduced when uptake is controlled by a solid-solution aqueous-solution equilibrium system similar to that for States I–III. Lower uptake values are indeed shown in Fig. 5.7 for State IV, i.e. from 5 to 10 L/kg. The two data points show R_d on calcite determined by Zachara et al. (1991) and Lakshtanov and Stipp (2007). The latter work attributed the uptake of Ni by calcite to co-precipitation rather than real adsorption (i.e. incorporation of Ni into freshly formed calcium carbonate); nevertheless, the uptake data were represented as K_d. The work of Zachara et al. (1991), however, suggested that the uptake was really adsorption through surface complexation.

The above review of literature data revealed a large variation in R_d values as is shown in Fig. 5.7. One hypothesis that could possibly explain this variation is based on the recent knowledge—mainly through the PSI investigations—that stable Ni concentration in cement waters plays an important role in Ni uptake. In other words, because stable Ni concentrations as high as 10^{-8}–10^{-7} mol/L have often been overlooked, uptake of radioactive Ni may have been misinterpreted. To the authors' understanding, the interpretation may still be correct, based on the following reasoning. Once ^{63}Ni is added as tracer to a cement system in which the Ni concentration is solubility-limited, the removal of ^{63}Ni will still occur through isotopic exchange. Hence, the measured apparent R_d in terms of ^{63}Ni should reflect a genuine adsorption process. The conclusion therefore is that although most of published experiments did not take into account the stable Ni in solution, the R_d measured with radiotracer should still be valid for evaluating uptake of Ni in the context of safety assessment. A possible explanation of the large scatter in Ni R_d values (Fig. 5.7) could be the natural variation of stable nickel in the various cements used in Ni uptake experiments.

5.2.3 Sorption Mechanisms and Selected Sorption Values

5.2.3.1 Sorption Mechanisms

Compared to most of the elements involved in this review, Ni uptake on cement has been studied more intensively by batch sorption/solubility experiments, column experiments, and spectroscopic investigations. Evans (2008) summarised

that possible uptake mechanisms on cement phases for Ni include the following: ettringite accommodating Ni^{2+} at the divalent metal site in the crystal structure; non-electrostatic sorption on CSH independently to C/S ratio; and co-precipitation or surface complexation via the hydroxyl group on cement phases or onto hydroxides. Furthermore, Ni may also be removed from cement waters by solubility-limiting processes. Mixed Ni–Al layered double hydroxides have been regarded as solid phases that potentially control nickel uptake in cementitious systems. Although uptake of Ni on cement seems to be controlled by a variety of complex processes, simplified approaches based on improved understandings (e.g. isotopic exchange process) are available to allow an appropriate use of the R_d concept under the relevant range of Ni concentrations.

The aqueous concentration of Ni in cement is likely controlled by the solubility of a Ni solid phase formed in cement or by the equilibrium with Ni solid solutions. The uptake of Ni by cement is therefore not controlled by adsorption. Because of the presence of stable Ni in commercial cement, the uptake of nickel radioisotopes may be controlled by isotopic exchange.

Factors that were shown to impact nickel sorption in HCP include pH, S/L ratio, and total (stable) nickel content. The batch tests performed by Hietanen et al. (1984) using saline and non-saline groundwater resulted in similar sorption values.

It was further noted that the difference between nickel and most other elements is that the nickel solubility limit is potentially reached by the stable nickel background concentration in typical cement. Any nickel tracer that is added may not "sorb" if the system is already at the solubility limit. This is potentially very different from most other elements where a solubility limit can be reached but not just by the background content of the cement. Isotope dilution, coupled with an "accessibility factor", thus becomes an important retardation process for nickel. Because of the complicated situation, (i) the procedure for deriving best estimates will be discussed first, and (ii) an application of the procedure will be presented using site-specific data from the ONDRAF/NIRAS cement characterisation programme. The best estimate sorption values thus obtained are not generic "scientific" best estimates, but site-specific values (i.e. specific to the assumed Ni background). These values may need to be recalculated for different cement compositions.

5.2.3.2 Approach to Derive Sorption Values Taking Account of Stable Nickel

Uptake of ^{63}Ni by HCP can be modelled as an isotopic exchange process where ^{63}Ni exchanges with a small fraction of non-radioactive nickel in cement. In such a case, partitioning of ^{63}Ni between HCP and the cementitious pore water can be described in terms of the partition coefficient α_p (Wieland et al. 2006):

$$\alpha_p = \frac{R_{d,M^*}}{R_{d,M}} \tag{5.3}$$

where $R_{d,\,M^*}$ and $R_{d,\,M}$ are, respectively, the distribution ratio for radioactive and non-radioactive nickel. Wieland et al. (2006) determined α_p for HCP suspensions and found values between 2.8×10^{-2} and 4.5×10^{-2}, i.e. 2.8–4.5 % of the total stable Ni is accessible for isotopic exchange with ^{63}Ni. At stable nickel concentrations of 19.9 ppm (3.39×10^{-4} mol/kg) in HCP, the distribution ratio $R_{d,\,M^*}$ was 150 L/kg. The distribution ratio of ^{63}Ni was found to increase with increasing concentration of stable nickel sorbed, i.e. from 200 ± 2 L/kg at 22.1 ppm to 1200 ± 100 L/kg at 255.3 ppm stable nickel sorbed.

Knowledge of the amount of stable nickel may thus be used to estimate the distribution coefficient for radioactive nickel $R_{d,\,M^*}$, based on Eq. (5.4) and considering known values for α_p and $R_{d,\,M}$. The assumption taken forward here is that the α_p-values determined by Wieland et al. (2006) on CEM I 52.2 N HTS (Haute Teneur en Silice) are applicable also to the cement-based materials that will be developed for the Dessel repository. In other words, the fraction of stable nickel available for isotopic exchange with radioactive nickel ranges between 2.8 and 4.5 %.

Values for $R_{d,\,M}$ were determined in this review on the basis of the assumption that the effective sorption of stable nickel, $R_{d,\,M}$, is equal to the ratio of stable nickel in cement, C_s^0, (mol/kg) to the solubility of nickel in the cementitious pore water, S (M), which is analogous to the general definition of R_d:

$$R_{d,M} = \frac{C_s^0}{S} \tag{5.4}$$

The same approach was used by Bradbury and Sarott (1995) in determining the effective distribution ratio for $^{14}CO_3^{2-}$ from the amount of stable carbonate in cement and the solubility of $CaCO_3$ in the pore water solution. Analogy between the isotopic exchange mechanism for $^{14}CO_3^{2-}$ and ^{63}Ni is thus invoked here to determine $R_{d,\,M^*}$. Note that determination of the $^{14}CO_3^{2-}$ effective distribution coefficient is independent of the $^{14}CO_3^{2-}$ inventory; it is determined by the system itself when oversaturated in calcite, i.e. by the amount of stable carbonate and the solubility of $CaCO_3$. The same reasoning is true for ^{63}Ni, because the stable nickel inventory (expressed in moles/kg HCP) is much larger than the radioactive nickel inventory (expressed in moles/kg HCP). Combination of Eq. (5.3) and (5.4) results in the following expression for $R_{d,\,M^*}$

$$R_{d,M^*} = \alpha_p \times R_{d,M} = \alpha_p \times \frac{C_s^0}{S} \tag{5.5}$$

Values for C_s^0 were determined by measuring the stable nickel content in three cement types proposed for use in the Dessel repository, CEM I, CEM III-B, and CEM III-C. Total nickel was measured using a high-performance energy-dispersive X-ray fluorescence apparatus (X-LAB2000, Spectro Analytical Systems, Kleve, Germany). For laboratory analysis, all samples were analysed as powders (dried and finely ground) and placed in XRF sampling cups (Bruker AXS, Karslruhe, Germany) provided with a 2.5-μm Mylar foil (Chemplex, Tuckahoe, NY, USA). Values for total nickel ranged between 11 and 47.6 ppm (Table 5.4).

Table 5.4 Elemental composition of cement powder determined by high-performance ED-XRF

Element	Cement type			Unit
	CEM I	CEM III-B	CEM III-C	
Al	0.57	2.03	2.50	wt%
Si	6.86	9.79	10.8	wt%
P	0.028	0.028	0.015	wt%
S	8190	23230	24990	µg/g
Cl	<55	300	261	µg/g
K	0.43	0.33	0.32	wt%
Ca	39.8	29.4	28.1	wt%
Ti	0.15	0.22	0.23	wt%
V	101	<20	<20	µg/g
Cr	46.4	42.3	32.8	µg/g
Mn	0.08	0.12	0.18	wt%
Fe	3.6	0.94	0.53	wt%
Ni	**47.6**	**17.0**	**11.0**	µg/g
Cu	61.0	21.9	14.9	µg/g
Zn	439	142	92.1	µg/g
Rb	21.9	14.7	11.9	µg/g
Sr	785	659	564	µg/g
Y	15.7	55.1	48.1	µg/g
Zr	81.7	167	156	µg/g
Nb	7.60	5.10	5.30	µg/g
Mo	3.40	3.60	3.20	µg/g
Ba	295	697	736	µg/g
Pb	15.4	32.0	7.90	µg/g

The consideration of $Ni(OH)_2$ as solubility-limiting phase is conservative, as other nickel phases will result in lower solubilities. The derived sorption values are therefore also conservative as concerns the uncertainty about Ni chemistry (i.e. the lower the solubility, the higher the sorption value (see Eq. 5.5)).

A third parameter required for the calculation of $R_{d,\,M^*}$ is the nickel solubility. Wieland and Van Loon (2002) demonstrated, based on wet chemistry data and spectroscopic evidence, that mixed Ni–Al layered double hydroxides (LDHs) was the nickel-controlling solid phase in fresh cement. The range of Ni concentration, considered as a solubility limit, was from 5×10^{-8} to 2×10^{-7} M at pH 13.3. In another experiment, Wieland et al. (2006) confirmed the upper-bound value by some oversaturation experiments (adding extra Ni to cement). Therefore, the minimum and maximum values from Wieland and Van Loon (2002) are taken for further calculations.

Values for $R_{d,\,M^*}$ were calculated by means of Eq. (5.5) accounting for uncertainties about all three parameters:

- α_p-values used were 2.8×10^{-2} and 4.5×10^{-2} (Wieland et al. 2006);
- S-values used were 5×10^{-8} and 2×10^{-7} M (Wieland and Van Loon 2002);

Table 5.5 Effective distribution ratio $R_{d,M}$* (L/kg) for ^{63}Ni for State I

Alpha	Ni solubility 2×10^{-7} M			Ni solubility 5×10^{-8} M		
	CEM I	CEM III-B	CEM III-C	CEM I	CEM III-B	CEM III-C
2.8×10^{-2}	1.14×10^{2}	4.05×10^{1}	2.62×10^{1}	4.54×10^{2}	1.62×10^{2}	1.05×10^{2}
4.5×10^{-2}	1.82×10^{2}	6.52×10^{1}	4.22×10^{1}	7.30×10^{2}	2.61×10^{2}	1.69×10^{2}

- C_s^0 values are taken from Table 5.4: 11, 17, and 47.6 ppm (1.87×10^{-4}, 2.90×10^{-4}, and 8.11×10^{-4} mol/kg).

Uncertainties in α_p- and S-values will be considered for determination of upper and lower bounds. Table 5.5 shows sorption ratios for all parameter combinations. The lowest values 26.2 and 42.2 L/kg are for CEM III-C using the highest nickel solubility, whereas the highest values are for CEM I using the lowest nickel solubility, i.e. 454 and 730 L/kg.

5.2.3.3 Sorption at State I

Values for $R_{d,\,M^*}$ discussed in Table 5.5 are representative of degradation State I, because α_p-values determined by Wieland et al. were obtained at pH 13.3. The solubility range 2×10^{-8}–5×10^{-7} mol/L was considered representative of State I (Sect. 5.2.1); hence, the selected S-values fall into this range. For cementitious barriers made from either CEM III-B or CEM III-C, an $R_{d,\,M^*}$ in the range 26.2–40.5 L/kg presents a lower limit (conservative in terms of solubility and α_p) for State I. For CEM I-based materials, a defensible and conservative $R_{d,\,M^*}$ value would be 1.14×10^2 L/kg for State I.

As lower and upper limits for State I, the maximum and minimum calculated value will be used, i.e. 26.2 (rounded to 30) and 730 L/kg. As best estimate 65.2 L/kg was selected, rounded to 65 L/kg. The $R_{d,\,M}$* values calculated on the basis of Eq. (5.5) are consistent with the experimental values of Wieland et al. (2006) for HCP suspensions with 19.9 ppm ($R_{d,\,M}$* = 150 L/kg) and 22.1 ppm ($R_{d,\,M}$* = 200 ± 2 L/kg) stable nickel.

5.2.3.4 Sorption at State II

For States II and III, the same value will be proposed based on a solubility reduction factor that is applied here as a sorption increasing factor. The solubility reduction factor is principally based on the slope of the aqueous Ni speciation across States I, II, and III, which is governed by hydrolysis. In this study, the slope was based on thermodynamic calculations considering β-$Ni(OH)_2$ as solubility-controlling phase (Sect. 5.2.2). The same slope is assumed when mixed Ni–Al layered double hydroxides seem to be more relevant solubility-limiting solid phase for fresh cement (Sect. 10.1.2). If the same uptake principles applied at State I can be applied at other states, then for States II and III, the apparent R_d would increase

Table 5.6 Calculated best estimate, upper and lower limit R_d values for Ni for States I, II, and III using site-specific data on stable nickel (values in bold face). Selected best estimate for Ni for State IV

pH state	Best estimate (L/kg)	Upper limit (L/kg)	Lower limit (L/kg)
State I	**6.5×10^1**	**7.3×10^2**	**3.0×10^1**
State II	**4.0×10^2**	**4.5×10^3**	**1.6×10^2**
State III	**4.0×10^2**	**4.5×10^3**	**1.6×10^2**
State IV	**5×10^0**	**i.d.**	**i.d.**

i.d.: insufficient data

in proportion to the decrease in solubility. The solubility decreases by a factor of 6.2 from pH 13.3 to 12.5, i.e. from 1.3×10^{-5} mol/L to 2.1×10^{-6} mol/L (based on NEA thermodynamic data; another approach would be to use actual measurements from State I and State II, but few reliable data are available). Combining data from Cowper et al. (2005) for State II and Wieland and data from Van Loon (2002) for State I suggests a solubility decrease by a factor of 20. We therefore estimated R_d for States II and III from the calculated best estimate for State I, i.e. $65 \times 6.2 \approx 400$ L/kg. Upper and lower limits were obtained in the same way, i.e. by multiplying (and rounding off) the upper and lower limits from State I by 6.2 (upper limit = 4500 L/kg, lower limit = 160 L/kg).

5.2.3.5 Sorption at State III

As stated above in Sect. 5.2.3.4, the same value of 400 L/kg is proposed for both States II and III. The same is true for upper and lower limits.

5.2.3.6 Sorption at State IV

For State IV, a different mechanism is assumed, which is most probably no longer isotopic exchange as the stable nickel has been removed from the cement phases due to cement degradation. Therefore, data from Zachara et al. (1991) and Lakshtanov and Stipp (2007) are taken as the basis (between 5 and 10 L/kg), with the minimum value conservatively taken as best estimate. No upper or lower limits were derived because of lack of data (Table 5.6).

5.3 Carbon

5.3.1 Chemical Form, Speciation, and Solubility

Eight isotopes of carbon exist with only two stable isotopes: ^{12}C and ^{13}C. Carbon-12 accounts for almost 98.9 % of the carbon on Earth. Carbon-13 accounts for most of the remaining 1.1 %, while other isotopes collectively make up less

than 0.1 % of the total amount of carbon on Earth. In nature, the radioactive ^{14}C (half-life 5700 years) is principally produced by cosmic rays.

In nuclear power plants, ^{14}C is produced in the fuel, from core structural materials, and in reactor coolant, due to the presence of the stable parent isotopes ^{14}N, ^{17}O, and ^{13}C. Production rates of ^{14}C in typical PWRs are about a factor of 4 higher for the nitrogen (^{14}N) impurities in the fuel (UO_2), compared to the oxygen (^{17}O) in the UO_2 matrix. Production rates of ^{14}C in core structural materials (from ^{14}N impurities in zircaloy cladding and fuel assemblies) are in between those of ^{14}N and ^{17}O from the fuel. Production rates of ^{14}C in reactor coolant as a result of reactions with ^{14}N (nitrogen dissolved in the water), ^{17}O (oxygen atoms in the water molecules), and ^{13}C (carbon dioxide and organic compounds dissolved in the water) are about the same as those from core structural materials (Yim and Caron 2006). Activated metal waste contains a substantial amount of ^{14}C. Additional ^{14}C produced in the coolant may add to the contamination of the other waste types. These waste types include ion exchange resins, concentrated liquids, filter sludge, cartridge filters, and trash. The predominant forms of ^{14}C available for transport at an LILW near-surface repository are carbon dioxide ($^{14}CO_2$), methane ($^{14}CH_4$), carbonate ion ($^{14}CO_3^{2-}$), bicarbonate ion ($H^{14}CO_3^{-}$), and elemental carbon in activated metals (USDOE 1996a, b).

Based on the ONDRAF/NIRAS 2003/2004 category A inventory, approximately one-third (34.56 %) of the ^{14}C inventory occurs in steel components from decommissioning of nuclear power plants. Some of this ^{14}C will be released in the organic form, the rest as inorganic carbon. The organic form will be partitioned between the gaseous (volatile hydrocarbons including CH_4 and CH_3–CH_3) and aqueous (low molecular weight carboxylic acids such as formic and acetic acids) phase. At present, the exact amount of both forms is not known, but it is certain that their release will be governed by the steel corrosion rate (e.g. Small 2004), which is a very slow process under alkaline conditions (fractions of μm per year). Two-thirds of the ^{14}C inventory is not associated with irradiated steel but with wastes from the operation of NPPs and other facilities. It is therefore probable that inorganic carbon will be the dominant chemical form (mainly as carbonate). Finally, microbial degradation of cellulose will produce carbon dioxide, including $^{14}CO_2$, but the amount will be relatively small given the very small amount of cellulose. The large amount of stable carbonate compared to 14-C carbonate will promote immobilisation processes such as isotopic exchange.

Speciation of inorganic carbon in natural water is well known, and the only species that exists at high pH relevant for a cement system is CO_3^{2-} (see Fig. 5.10). The expected aqueous species for inorganic carbon under near-surface repository conditions at pH > 10 is thus CO_3^{2-}. For pH < 10, the HCO_3^{-} species becomes predominant (degraded concrete).

Solubility of inorganic carbon in a cement system is generally considered as being controlled by calcite (Lothenbach and Winnefeld 2006). When portlandite is present, it controls the concentration of dissolved calcium, i.e. at pH above 12.5 at 25 °C, the concentration of dissolved carbon is controlled by the solubility of calcite which can be easily calculated by an activity–activity diagram as shown

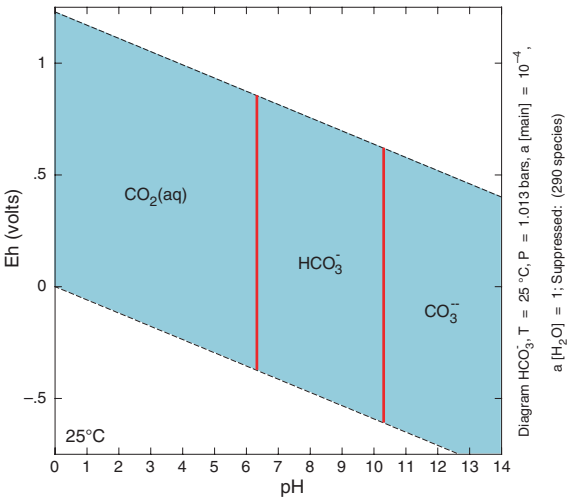

Fig. 5.10 Eh–pH diagram of inorganic carbon calculated with *The Geochemist's Workbench*®. Carbon activity 10^{-8}

in Fig. 5.11. The total dissolved carbon concentration is about 8 micromolal and 0.3 millimolal at pH 12.5 and 13.5, respectively. When portlandite dissolves away and the pH drops below 12.5, calcium concentration will be regulated by the solubility of CSH phases of decreasing C/S ratio. As the C/S ratio drops, calcium concentration in solution also drops and the dissolved carbon concentration will increase. Figure 5.12 shows the carbon solubility evolution simulated by a reaction modelling for a system containing free alkali metal ions, portlandite, and CSH phases. The system is "washed" by water until all cement phases are depleted and only calcite remains. Calculations were done with *The Geochemist's Workbench*® (Bethke 2006).

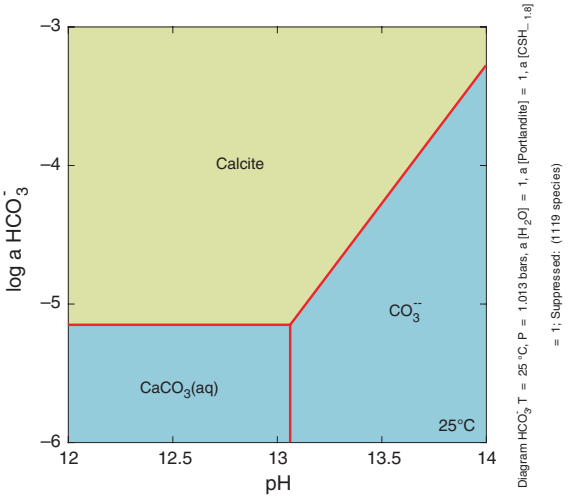

Fig. 5.11 Solubility of calcite as a function of pH in the presence of portlandite

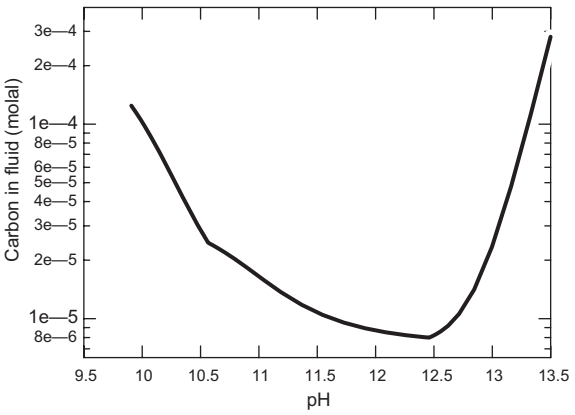

Fig. 5.12 Solubility of inorganic carbon in a cement system containing calcite, portlandite, dissolved alkali metal ions (K, Na), and CSH phases. The initial system (pH 13.5) is continuously "washed" by water until all cement phases dissolve away and only calcite remains

5.3.2 Sorption Values from the Literature for the Benchmark Cement

5.3.2.1 Introduction

Most cementitious systems contain certain amounts of calcite ($CaCO_3$), present as calcareous aggregates or generated during cement hardening and evolution. Hardened cement paste and concrete will have pore water that will be saturated with respect to $CaCO_3$. The CO_3^{2-} concentrations will depend on pH and the Ca^{2+} concentrations arising from other saturated phases, such as $Ca(OH)_2$. In the same pore water, $^{14}CO_3^{2-}$ originating from ion exchange resins will be present and will interact with solid phases. According to Bradbury and Sarott (1995), the main removal mechanism for $^{14}CO_3^{2-}$ is by isotopic exchange with the finely divided $CaCO_3$ phase. Under those conditions, an effective sorption parameter can be determined [for details, see Bradbury and Sarott (1995)]. From their analysis, Bradbury and Sarott (1995) concluded that the effective sorption parameter (or R_d) for ^{14}C as $^{14}CO_3^{2-}$ in any system after a long time is equal to the ratio of the quantity of stable CO_3^{2-} in the cement to the solubility limit of $CaCO_3$ in the pore solution:

$$R_d = \frac{\text{amount of } CO_3^{2-} \text{ in cement, in mol/kg}}{\text{dissolved } CO_3^{2-} \text{ concentration, in mol/l}} \tag{5.6}$$

In other words, the effective sorption parameter R_d for ^{14}C as $^{14}CO_3^{2}$ is independent of the $^{14}CO_3^{2}$ inventory. For application of the effective sorption parameter in safety assessment, Bradbury and Sarott (1995) suggest reducing the amount of stable CO_3^{2-} available for isotopic exchange by a factor α of ~0.1. This suggests that

Table 5.7 Distribution ratios R_d for $^{14}CO_3^{2-}$ as a function of pH (HTS cement in $NaHCO_3$ groundwater) [based on Table F-1 from Bradbury and Sarott (1995)]

pH	Cycle number	Carbonate concentration in solution	Carbonate concentration in solid phase	Distribution ratio for $^{14}CO_3^{2-}$ $\alpha = 1$	Distribution ratio for $^{14}CO_3^{2-}$ $\alpha = 0.1$
		(mol/L)	(mol/kg)	(m^3/kg)	(m^3/kg)
13.5	1	6.1×10^{-4}	4.2×10^{-2}	6.9×10^{-2}	6.9×10^{-3}
13.3	3	1.8×10^{-4}	4.6×10^{-2}	2.6×10^{-1}	2.6×10^{-2}
13.1	5	6.0×10^{-5}	5.1×10^{-2}	8.5×10^{-1}	8.5×10^{-2}
12.9	7	2.5×10^{-5}	5.4×10^{-2}	2.2	2.2×10^{-1}
12.8	9	1.4×10^{-5}	5.9×10^{-2}	4.2	4.2×10^{-1}
12.5	25	8.0×10^{-6}	9.2×10^{-2}	11	1.1
12.4	314	8.0×10^{-6}	0.75	93	9.3
11.7	1046	3.3×10^{-6}	2.6	79	7.9

In column 5, the total amount of calcite present is accessible, and in column 6, only 10 % of calcite is accessible

only 10 % of the total calcite surfaces are accessible for exchange. This assumption then results in an effective sorption parameter which is 10 times smaller:

$$R_d = \alpha \times \frac{\text{amount of } CO_3^{2-} \text{ in cement, in mol/kg}}{\text{dissolved } CO_3^{2-} \text{ concentration, in mol/l}} \tag{5.7}$$

An example is given in Table 5.7, where the effective sorption parameter R_d is calculated as function of pH.

Based on the above methodology for estimation of R_d, geochemical calculations were carried out to determine the carbonate concentration in solution and in the solid phase using the initial mineralogical composition of Table 5.8. These data represent the concrete composition to be used for the production of the concrete monoliths for the Dessel repository. Dissolution of the minerals occurs under steady infiltration of soil water as described by Jacques et al. (2008). The resulting evolution of carbonate concentration in solution and in the solid phase versus pH is shown in Fig. 5.13, together with the calculated R_d. Based on size fractions of calcareous aggregates (see further), the accessibility was calculated to be 0.23 % (i.e. 0.23 % of the carbonate in the solid phase is accessible). Under these conditions, R_d is in the range 400–1.9×10^4 L/kg.

In Andra's Dossier (2005), reference is made to additional experimental work to further elucidate on the fraction of carbonate available for isotopic exchange. Pointeau et al. (2002) re-evaluated the α factor for calcareous aggregates and experimentally obtained the following relationship:

$$\%\,\text{accessibility}, \alpha = (1 - \log \Phi) \tag{5.8}$$

Table 5.8 Amount of minerals used in the leaching model for concrete degradation at Dessel (Jacques and Mallants 2011)

Element	Concentration (molal)	Components	Amount (mol/dm^3 concrete)
Al	1.36×10^{-5}	Jennite	9.76×10^{-1}
C	8.09×10^{-5}	Tobermorite	1.26×10^{-1}
Ca	1.63×10^{-3}	Ettringite	4.37×10^{-2}
K	1.61×10^{-1}	Tricarboaluminate	1.33×10^{-2}
Mg	1.97×10^{-9}	Monocarboaluminate	6.38×10^{-2}
Na	6.83×10^{-2}	Hydrotalcite OH	3.04×10^{-2}
S	2.91×10^{-4}	Portlandite	1.50
Si	5.33×10^{-5}	Na_2O	3.66×10^{-3}
pH	13.8	K_2O	3.08×10^{-2}
Ionic strength	0.22	Calcite (cement)	7.00×10^{-2}
		Calcite (aggregate)	18.26

Calculated concrete porosity using PHREEQC and molar volumes of the relevant minerals is 12 %

where Φ is the grain diameter for aggregates (mm) such as calcite. The predictive capacity of the α factor was positively verified by Pointeau et al. (2002) for several cement systems. The accessibility factor for fines and calcite was found to be 0.5 % (average particle size ~0.01 mm). For coarser aggregates such as gravel (assumed average particle size of ~2.5 mm), the accessibility factor was 0.05 %. The accessibility relationship was obtained for sorption tests with a sufficiently long reaction time (~140 days) to reach equilibrium.

For the ONDRAF/NIRAS LILW backfill mortar (for the full composition, see "Table 1.2: proposed composition of backfilling mortar"), calcareous aggregates are used with size fractions ranging from 4 to 0.08 mm. For each size class, the accessibility coefficient α was calculated based on Eq. (5.8). The weighted mean value for α was 0.23 %.

5.3.2.2 Sorption Values

Individual data points from the reviewed R_d values are presented in Fig. 5.14, while Table A.7 (see Annex) summarises the experimental conditions adopted. Carbon is a difficult element, as cement itself contains much carbon which can complicate experiments. Therefore, relevance of literature data was mainly based on information about carbonate levels which should be well below the threshold point at which precipitation starts. This threshold is about 1–2 $\times$ 10^{-5} mol/L carbonate (Fig. 5.12).

At the occasion of their 2003 sorption database review, Wieland and Van Loon (2002) concluded for carbon sorption that there were "no compelling reasons to

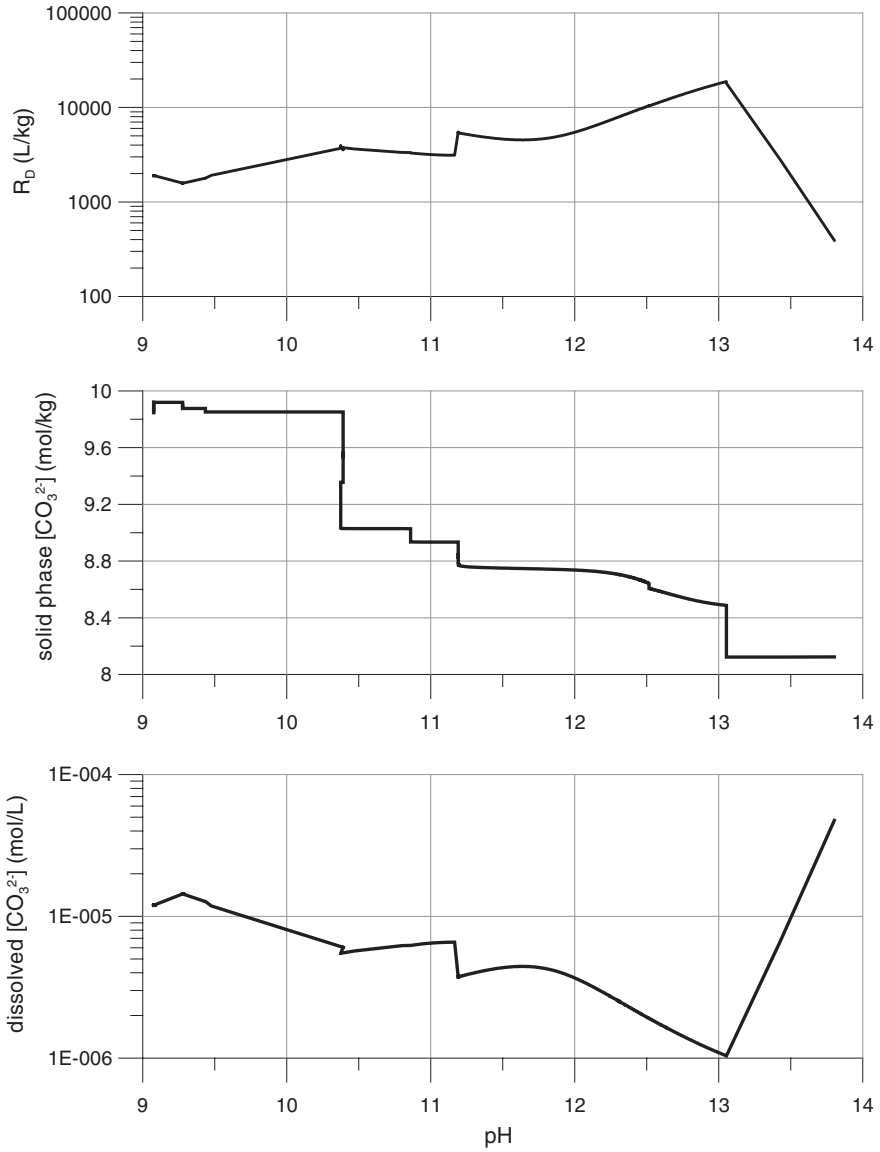

Fig. 5.13 Calculated distribution ratio as function of pH for the degradation of category A cement in contact with soil water at 10 °C (based on calculation case 7, Jacques et al. 2008). Approximately 0.23 % of the carbonate in the solid phase is accessible

revise the sorption values recommended in CEM-97 for C, …" For carbon, CEM-97 (Bradbury and Van Loon 1998) refers to the original work of Bradbury and Sarott (1995) for a discussion on carbon sorption. A summary of findings and recommendations based on the latter work is given below:

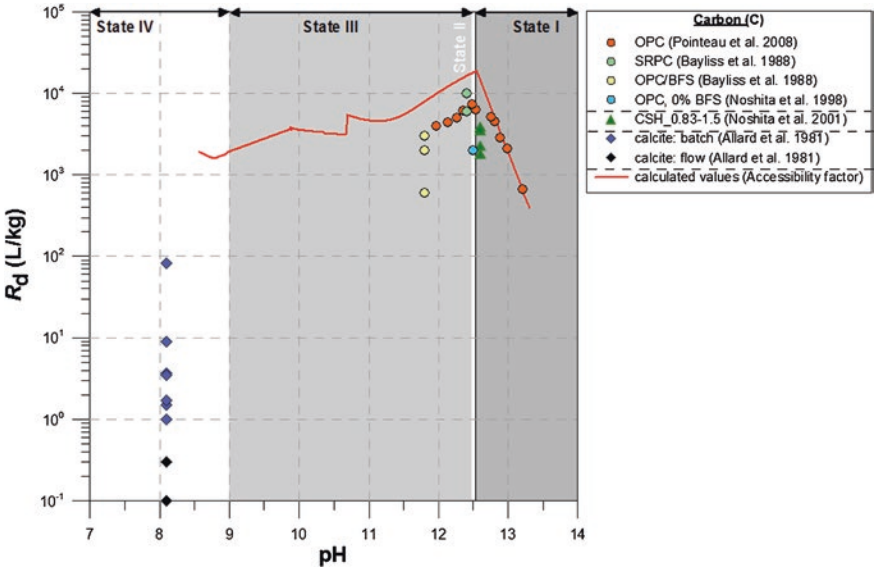

Fig. 5.14 Distribution ratio (R_d) of inorganic carbon in cementitious systems. *SRPC* sulphate-resistant Portland cement; *OPC/BFS* ordinary Portland cement/blast furnace slag; *CSH* calcium silicate hydrate. Calculated values from Bradbury and Sarott, who apply an accessibility factor (=0.23) to scale the data (see text)

- The earlier sorption studies report the following processes as likely mechanisms for carbon "sorption": (i) isotopic exchange with inactive CO_3^{2-} on $CaCO_3$ (Bayliss et al. 1988), (ii) mixture of precipitation and isotopic exchange (Allard et al. 1981), and (iii) precipitation (McKinley and Scholtis 1991).
- Most studies observed very high "sorption", with a distribution ratio R_d up to 10,000 L/kg and kinetic effects, i.e. time-dependent "sorption" processes.

Highlights from a number of other relevant sorption studies will also be discussed. Data from these studies served to produce the summary R_d graph shown in Fig. 5.14.

Concrete R_d Values

The batch sorption data from Allard et al. (1981) on 1–2-year-aged[5] concrete (based on slag cement) show a very strong dependency on equilibration time: R_d values of 1600 L/kg are obtained for 1-week equilibration, while for five weeks of equilibration, sorption values are nearly 10,000 L/kg (Fig. 5.14). Allard et al.

[5]Ageing of concretes and pastes occurred in the absence of air to avoid carbonatization.

(1981) proposed two sorption mechanisms: (i) precipitation of $^{14}CO_3^{2-}$ together with inactive carbonate (trace concentrations of $^{14}CO_3^{2-}$ were used, but the artificial groundwater was almost saturated with respect to $CaCO_3$) and (ii) an exchange mechanism with stable carbonate characterised by slow reaction kinetics (isotopic exchange). According to Allard et al., intra-particle diffusion does not seem to be the major process determining the reaction kinetics based on the slope of the R_d increase versus time. Because there was evidence that precipitation had occurred in the batch test, those R_d values will not be used in the summary R_d graph.

The uptake mechanism identified was precipitation; therefore, the sorption value reported was R_d because of the removal mechanism which involves precipitation of $^{14}CO_3^{2-}$ and formation of calcite, owing to the high dissolved Ca in the pore water and the high pH (12.5). Precipitation occurred on the aggregates. Because no other mechanism than precipitation has occurred, the R_d data will not be included in the summary graph.

Cement Paste R_d Values

The batch sorption data from Allard et al. (1981) on 1–2-year-aged cement pastes at an initial pH 8.1 (based on pure cement) also show a very strong dependency on equilibration time: K_d-values (R_d is more likely) of 1600 and 10,000 L/kg are obtained for, respectively, 1 and 5 weeks of equilibration. Sorption is considered to be due to two processes: $^{14}CO_3^{2-}$ precipitates together with stable carbonate and slow exchange between carbonates in solution and in the solid phase ($^{14}CO_3^{2-} \leftrightarrow CO_3^{2-}{}_{solid}$). Again, the data are not retained for the summary graph because precipitation cannot be ruled out. The data are also not retained because the final equilibrium pH is not known; the initial pH of 8.1 would make the data representative of State 4, but State 4 concerns calcite and not cement.

Figure 5.15 gives a summary of R_d values obtained by Bayliss et al. (1988) on SRPC and BFS/OPC. The initial aqueous phase concentration should have been below the threshold for precipitation. Batch tests were carried out using S/L ratios of 0.01 and 0.1 kg/L. The experts considered the former to be not representative. For BFS/OPC, the maximum R_d was 3000 L/kg, and for SRPC, it was 10,000 L/kg. The lower values for BFS/OPC suggest that the reaction had not gone very far even after 210 days, possibly due to the high slag content. The R_d ($^{14}CO_3^{2-}$) of ~10,000 L/kg measured on SRPC after 100 days by Bayliss et al. (1988) could be reasonably well predicted by the Bradbury and Sarott approach (see Eq. (5.6) for effective sorption parameter estimation. This suggests that isotopic exchange with stable CO_3^{2-} might have been the dominant sorption mechanism. This mechanism for carbon sorption was already identified by Bayliss et al. (1988), based on the observation that (i) increasing the ^{14}C inventory increases R_d and (ii) the ratios of $^{14}C/^{12}C$ in solution are 30 times higher than those in the solid for SRPC (300 times for OPC/BFS). The former observation, however, does not agree with the theory of Bradbury and Sarott (1995) that the effective sorption coefficient for

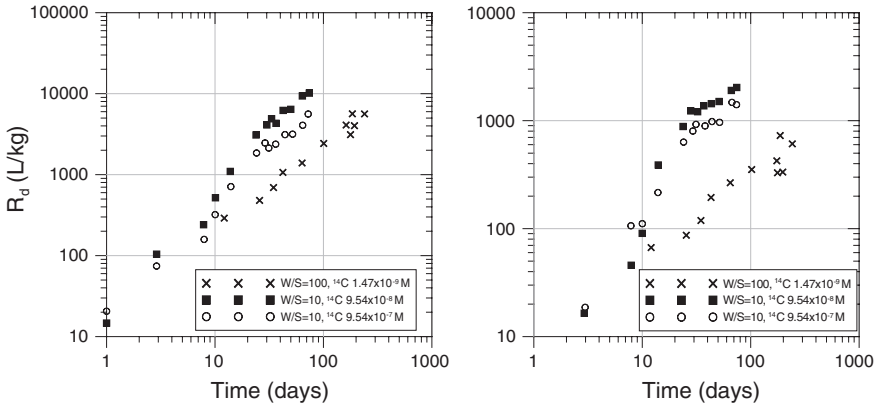

Fig. 5.15 Distribution ratio (R_d) for ^{14}C onto SRPC (*left*) and OPC/BFS (*right*) [data from Bayliss et al. (1988)]. R_d values increase with time, with S/L ratio, and with initial aqueous concentration of ^{14}C

^{14}C as $^{14}CO_3^{2-}$ is independent of the $^{14}CO_3^{2-}$ inventory (see Eq. 5.6). The latter observation leads Bayliss et al. (1988) to conclude that not all the carbon in cement is available for exchange with carbon (including ^{14}C) in the pore water. A diffusion-limited uptake mechanism is further proposed to explain the difference in carbon availability between OPC/BFS and SRPC: the higher the diffusion coefficient, the higher the carbon availability. Note that similar reaction kinetics were observed by Allard et al. (1981), but diffusion was not considered as a relevant mechanism. Finally, R_d values increase with increasing S/L ratio, a result of increasing the chance of contact between ^{14}C in solution and in the solids. The increasing S/L ratio may also have increased "sorption site" concentration, as the concentration of stable C on the solid will also have increased.

Batch sorption experiments on CEM I OPC were carried out by Pointeau et al. (2002) considering twelve degradation states between pH 11.5 and 13.3. The initial $^{14}CO_3^{2-}$ concentration (10^{-7} M) was lower than the calculated solubility of carbonate in saturated portlandite water. R_d values increased between pH 13.2 and 12.5 from 670 to 7400 L/kg. For degradation states under pH 12.6, R_d values decreased slightly. Sorption mechanisms were not identified.

CSH-Phase K_d-Values

Noshita et al. (2001) determined sorption behaviour on CSH with C/S = 0.83, 1, 1.2, and 1.5 (initial C = 10^{-6} mol/L). ^{14}C sorption in $Ca(OH)_2$ solution (pH = 12.6) decreases with decreasing C/S ratio: 3900 L/kg for C/S = 1.5, 3500 L/kg for C/S = 1.2, 2300 L/kg for C/S = 1.0, and 1800 L//kg for C/S = 0.83. In $Ca(OH)_2$ solution, the formation of $CaCO_3$ may have affected the R_d values, although the initial concentration of CO_3^{2-} was adjusted below its

maximum solubility to avoid precipitation. The adsorption mechanism for the oxy-anionic carbon (CO_3^{2-}) was suggested to be electrostatic adsorption onto cationic surfaces of CSH phases at high C/S ratio (-SiOCa$^+$).

Calcite-Phase $\boldsymbol{K}_d$-Values

Allard et al. (1981) determined distribution coefficients by means of batch tests imposing different equilibration times from 0.5 h to 6 months (at a pH of 8.2) using trace concentrations of $^{14}CO_3^{2-}$. The time dependency of the sorption process is clearly visible in Fig. 5.16: the range in R_d is 1–100 L/kg, and R_d increases with time. Allard et al. attributed the slow increase with time to slow exchange between carbonate in solution and carbonate in the solid (calcite). Intra-particle diffusion of carbonate probably is not the main uptake mechanism, because the K_d increase follows a (time$^{-0.7}$) behaviour, while for diffusion, a (time$^{-0.5}$) would be more appropriate.

Allard et al. (1981) also determined distribution coefficients by means of column tests. The applied water flow velocities were high (between 1.3×10^{-5} and 10^{-4} m/s) relative to the time required to obtain an equilibrium condition between carbonate in solution and carbonate in the solid phase. R_d values decreased with increasing flow rate: for the lowest flow rate (0.01 ml/min), R_d was 0.3 L/kg, while for the highest (0.08 ml/min), it was 0.1 L/kg. These flow conditions resulted in average residence times in the columns of a few hours (between 0.35 and 2.8 h). The shortest equilibration time for batch tests was similar (0.5 and 2 h), and the batch R_d values were small too ($R_d = 1$ L/kg, see Fig. 5.16). These similarities suggest consistency between batch R_d and flow column K_d, in that similar equilibration times provided similar sorption values. The low R_d value in the flow column is also consistent with the assumption that carbonate uptake is controlled by slow reaction kinetics (i.e. isotopic exchange between carbonate in solution and in solid). Nevertheless, the experts had little confidence in that range representing the real system.

5.3.2.3 ^{14}C Partitioning Between Organic and Inorganic Carbons

Main sources of ^{14}C in a LILW repository arise from activation products in steels (mainly reactor internal waste and decommissioning waste) and concrete, from $^{14}CO_3^{2-}$ on ion exchange resins and from organic waste streams. When ^{14}C is present in organic waste streams, it will be incorporated into organic compounds that can potentially dissolve into the cement pore water, immediately after conditioning or after degradation. The pathway for aqueous CO_2 is essentially independent of how it is generated, but an entirely separate pathway exists for carbon-containing gases such as methane or hydrocarbons, perhaps dissolved in pore fluid. The latter may not undergo sorption in the sense used in this report. For a detailed discussion on ^{14}C partitioning between organic and inorganic forms, the reader is referred to Ochs et al. (2011).

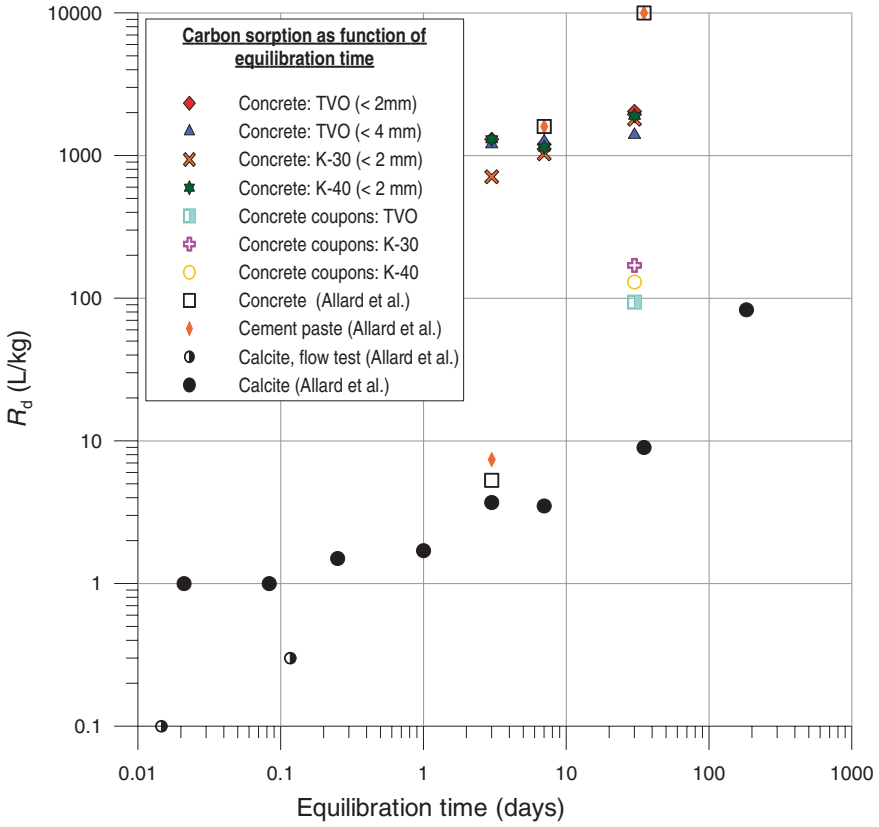

Fig. 5.16 Effect of equilibration time on carbon sorption [data from Allard et al. (1981), and Hietanen et al. (1984)]

5.3.3 Sorption Mechanisms and Selected Sorption Values

5.3.3.1 Factors Influencing R_d on the Benchmark Cement

The chemical form of ^{14}C is the most important factor influencing sorption. The organic form has been shown to be very weakly sorbed, whereas inorganic ^{14}C sorbs strongly (R_d between 2000 and 20,000 L/kg for State II). It is thus of utmost importance to have good estimates of the partitioning of ^{14}C between the organic and inorganic forms.

In the calculation of the effective sorption parameter R_d in case of isotopic exchange, both the concentration of carbonate in solution and that of carbonate in the solid phase are important parameters: increasing aqueous phase carbonate concentrations will decrease R_d, while the opposite is true for carbonate in the solid phase. For inorganic carbon, the S/L ratio was shown to be an important

parameter: R_d values increase with increasing S/L ratio, owing to increasing the chance of contact between ^{14}C in solution and in the solids. Reaction time is another parameter influencing R_d: as isotopic exchange is characterised by slow reaction kinetics, higher R_d values are obtained for longer reaction times.

5.3.3.2 Sorption Mechanisms

Evans (2008) considers two major uptake mechanisms for inorganic carbon: adsorption onto a positive site and precipitation. The adsorption mechanism for the oxyanionic carbon (CO_3^{2-}) was suggested to be electrostatic adsorption onto cationic surfaces of CSH phases at high C/S ratio (-SiOCa$^+$). Precipitation is not relevant in the context of this review. Real sorption mechanisms for inorganic carbon ($^{14}CO_3^{2-}$) occur only when carbonate levels are well below the threshold point at which precipitation starts. This threshold is about 1–2 $\times$ 10^{-5} mol/L carbonate. At higher carbonate concentrations, removal of $^{14}CO_3^{2-}$ is by precipitation and not by sorption.

Among the sorption mechanisms that have been further discussed in the literature, the following are the most probable:

- adsorption of the oxyanionic carbon ($^{14}CO_3^{2-}$) due to electrostatic adsorption onto cationic surfaces of CSH phases at high C/S ratio (SiOCa$^+$) (Noshita et al. 2001);
- isotopic exchange of $^{14}CO_3^{2-}$ with the finely divided $CaCO_3$ phase (Bayliss et al. 1988), characterised by slow reaction kinetics (Allard et al. 1981). Under those conditions, an effective sorption parameter can be determined (Bradbury and Sarott 1995; Pointeau et al. 2002);
- mixture of precipitation and isotopic exchange (Allard et al. 1981), although precipitation is ruled out here as true sorption mechanisms.

Carbon is a difficult element, as cement itself contains much carbon which can complicate experiments. We therefore only evaluated data obtained at carbon concentrations below the threshold of calcite precipitation (this would then refer to sorption rather than precipitation). The precipitation threshold can be taken to be about 1–2 $\times$ 10^{-5} mol/L for States II and III for example. From these data, values were assigned to most sorption parameters for the four states.

Organic carbon shows a much lower sorption, but is not entirely zero. Dissolved organic carbon has been shown to display much lower sorption values. For instance, Sasoh (2004) observed an R_d up to 6 L/kg for HPC. The R_d values determined by Kaneko et al. (2003) at pH 12.5 onto HPC ranged from 4 to 12 L/kg for carboxylic acids, methanol, ethanol, and formaldehyde. Reaction mechanisms were not discussed in these studies. Owing to the limited data on sorption of organic carbon in cementitious environment, and owing to the limited process information available, a conservative approach will be taken in this review by considering negligible sorption (i.e. $R_d = 0$). For volatile ^{14}C, also zero sorption is considered.

Table 5.9 Selected best estimate, upper and lower limit R_d values for (inorganic) C

pH state	Best estimate (L/kg)	Upper limit (L/kg)	Lower limit (L/kg)
State I	2×10^3	3×10^3	7×10^2
State II	5×10^3	2×10^4	2×10^3
State III	2×10^3	i.d.	i.d.
State IV	i.d.	1×10^2	1×10^{-1}

i.d.: insufficient data

5.3.3.3 Sorption at State I

There are few experimental data about inorganic carbon, but the spread is limited. From these few data, the upper bound was agreed to be 3000 L/kg and the lower bound 700 L/kg. The best estimate for State I was agreed to be 2000 L/kg (Table 5.9).

5.3.3.4 Sorption at State II

Most available data for carbon are for the State II—pH 12.5—region (portlandite-controlled stage). The spread is again quite limited. Crushed concrete gave R_d values of about 2000 L/kg, concrete coupons gave values of approximately 150 L/kg, and cement pastes gave values up to 10^4 L/kg. Low weighting was given where the nature of aggregates or other experimental parameters were not stated. Overall, for State II, it was agreed that appropriate data were in the range 2000 to 2×10^4 L/kg. Upper and lower bounds of 2×10^4 L/kg and 2000 L/kg (the spread of the data) were agreed, with a best estimate of 5000 L/kg (Table 5.9).

5.3.3.5 Sorption at State III

The only data for State III appeared to be for OPC (Bayliss et al. 1988). This study was considered acceptable however. The range shown was 600–3000 L/kg. It was noted that values of 1.9×10^3 and 1.6×10^3 L/kg were obtained for 10^{-6} and 10^{-7} mol/L carbonate concentrations, respectively. A value below 10^3 L/kg had come from an experiment with a 1/100 S/L ratio which was considered not representative of the system. It was agreed that the experts should base the best estimate on 2×10^3 L/kg (Table 5.9). On account of there being very few data, no upper or lower bounds were assigned.

5.3.3.6 Sorption at State IV

There was a range of data applicable for State IV with much variability. Despite the pH being appropriate, data on cement paste and concrete were ruled out as

they are not applicable to State IV (which is calcite). There appeared to be a trend of increasing R_d with increasing equilibration time. The experts found it difficult to select a best estimate and did not assign a value. However, they assigned 0.1 L/kg as the lower bound and an upper bound of 100 L/kg with the implication that the values may continue to increase. Data points on cement paste and concrete gave values higher than 100 L/kg (Table 5.9).

Calculated values using Eqs. (5.6) and (5.7) for the Dessel facility are available from Fig. 5.14. The resulting R_d values are as follows: 2800 L/kg at pH 13.5 (State I), 18,100 L/kg at pH 13 (State II because calculations at 10 °C, therefore pH 13 is State II), 10,200 L/kg at pH 12.5 (State III), 5460 L/kg at pH 12 (State III), and 1900 L/kg at pH 9 (State IV). Thus, the calculated values are always higher than the best estimates from Table 5.9. There is consistency in the R_d trends: both calculated and selected values show an increase in State I with decreasing pH, towards a maximum in State II, followed by a decrease in State III. The rate of decreasing R_d is somewhat larger in the data compared to the calculated one. Possibly, the higher initial amount of calcite in the ONDRAF/NIRAS LILW concrete is responsible for the higher R_d in States II and III.

References

S. Aggarwal, M.J. Angus, J. Ketchen, Sorption of radionuclides onto specific mineral phases present in repository cements. NSS/R312, AEA-DandR-0395 (2000)

B. Allard, B. Torstenfelt, K. Andersson, Sorption studies of H14CO3- on some geologic media and concrete. Mater. Res. Soc. Symp. Proc. **3**, 465–472 (1981)

Andra (2005), Référentiel de comportement des radionucléides et des toxiques chimiques d'un stockage dans le Callovo-Oxfordien jusqu'à l'homme, Site de Meuse/Haute-Marne, Tome 1/2: Chapitres 1 à 4, Dossier 2005 Argile (2005)

G. Audi, A.H. Wapstra, C. Thibault, J. Blachot, O. Bersillon, Isotope masses from Ame 2003 atomic mass evaluation. Nucl. Phys. **A729**, 129 (2003)

S. Bayliss, F.T. Ewart, R.M. Howse, J.L. Smith-Briggs, H.P. Thomason, H.A. Willmott, The solubility and sorption of lead-210 and carbon-14 in a nearfield environment. Mat. Res. Soc. Symp. Proc. **112**, 33–42 (1988)

S. Bayliss, A. Haworth, R. McCrohon, A.D. Moreton, P. Oliver, N.J. Pilkington, A.J. Smith, J.L. Smith-Briggs, Radioelement behaviour in a cementitious environment. Mat. Res. Soc. Symp. Proc. **257**, 641–648 (1992)

U. Berner, Project Opalinus Clay: Radionuclide concentration limits in the cementitious near-field of an ILW repository, PSI Bericht 02-26 (2002)

C.M. Bethke, The geochemist's workbench, release 6.0, GWB reference manual, hydrogeology program University of Illinois, May (2006)

M.H. Bradbury, F. Sarott, Sorption databases for the cementitious near-field of a L/ILW repository for performance assessment, PSI Bericht—95-06, (1995)

M.H. Bradbury, L.R. Van Loon, Cementitious near-field sorption data bases for performance assessment of a L/ILW disposal facility in a Palfris Marl Host Rock, CEM-94: update I, June 1997, PSI Bericht Nr. 98-01 (1998)

M. Cowper, A. Green, B.J. Myatt, S.W. Swanton, S.J. Williams, A laboratory study of the impact of picolinate and anion exchange resin degradation products on nickel, americium and plutonium behaviour in a repository, SA/ENV-0693 (2005)

J.E. Cross, A.D. Moreton, C.J. Tweed, Thermodynamic modelling of radioactive waste disposal: assessment of near-field solubility, NSS/R311 (1995)

W.A. Deer, R.A. Howie, W.S. Wise, J. Zussman, in *Rock-Forming Minerals. Volume 4B. Framework Silicates: Silica Minerals. Feldspathoids and the Zeolites*, 2nd edn. ed. (Geological Society of London, London, 2004), p. 982

N.D.M. Evans, Binding mechanisms of radionuclides to cement. Cem. Concr. Res. **38**, 543–553 (2008)

D. Fink, J. Klein, R. Middleton, 41Ca: past present and future. Nucl. Instr. Meth. B **52**, 572 (1990)

S.P.H.T. Freeman, J.C. King, N.E. Vieira, L.R. Woodhouse, A.L. Yergey, Human calcium metabolism including bone resorption measured with 41Ca tracer. Nucl. Instr. Meth. B **123**, 266–270 (1997)

H. Gamsjager, J. Bugajski, T. Gajda, R.J. Lemire, W. Preis, *Chemical Thermodynamics of Nickel* (Elsevier, OECD NEA, Issy-les-Moulineaux, France, 2005)

M. Hein, S. Arena, in *Foundations of College Chemistry*, 12th edn. (Wiley, 2006), 467 pages

W. Henning, W.A. Bell, P.J. Billquist, B.G. Glagola, W. Kutschera, Z. Liu, H.F. Lucas, M. Paul, K.E. Rehm, J.L. Yntema, Calcium-41 concentration in terrestrial materials: prospects for dating of pleistocene samples. Science **236**, 725 (1987)

R. Hietanen, E.-L. Kamarainen, M. Alaluusua, Sorption of strontium, caesium, nickel, iodine and carbon in concrete, Report YJT-84-04 (1984)

R. Hietanen, M. Alaluusua and T. Jaakkola, Sorption of caesium, strontium, iodine, nickel and carbon in mixtures of concrete, crushed rock and bitumen. Report YJT-85-38. Department of radiochemistry, University of Helsinki, September 1985

S. Holgersson, Y. Albinsson, B. Allard, H. Boren, I. Pavasars, I. Engkvist, Effects of Glucoisosaccharinate on Cs, Ni, Pm, and Th sorption onto, and diffusion into cement. Radiochim. Acta **82**, 393–398 (1998)

W. Hummel, E. Curti, Nickel aqueous speciation and solubility at ambient conditions: a thermodynamic elegy. Monatsh. fur Chemie **134**, 941–973 (2003)

C.S. Hurlbut, C. Klein, *Manual of Mineralogy*, 20th edn. (Wiley, New York, 1985)

M. Itoh, K. Watanabe, M. Hatakeyama, M. Tachibana, Determination of 41Ca in biological-shield concrete by low-energy X-ray spectrometry. Anal. Bioanal. Chem. **372**, 532–536 (2002)

D. Jacques, D. Mallants, Evolution of concrete pore water and solid phase composition during leaching with different types of water, project near surface disposal of category a waste at Dessel, NIROND-TR 2008-24 E V2 (2011)

D. Jacques, L. Wang, E. Martens, D. Mallants, Time dependency of the geochemical boundary conditions for the cementitious engineered barriers of the Belgian surface disposal facility, Project near surface disposal of category a waste at Dessel, NIRAS-MP5 DATA-LT(NF) Version 1, NIROND-TR 2008-24 E (2008)

A. Jakob, F. Sarott, P. Spieler, Diffusion and sorption on hardened cement pastes—experimental and modelling results. Nagra technical report 99-06, August (1999)

S. Kaneko, H. Tanabe, M. Sasoh, R. Takahashi, T. Shibano, S. Tateyma, A study on the chemical forms and migration behaviour of carbon-14 leached from the simulated hull waste in the underground conditions. Mat. Res. Soc. Symp. Proc. **757**, II.3.8.1–II.3.8.7 (2003)

S. Kulmala, M. Hakanen, The solubility of Zr, Nb and Ni in groundwater and concrete water, and sorption on crushed rock and cement. YJT Report N° YJT-93-21 (1993)

L.Z. Lakshtanov, S.L.S. Stipp, Experimental study of nickel (II) interaction with calcite: adsorption and coprecipitation. Geochim. Cosmochim. Acta **71**, 3686–3697 (2007)

B. Lothenbach, F. Winnefeld, Thermodynamic modelling of the hydration of Portland cement. Cem. Concr. Res. **36**, 209–226 (2006)

P. Mandaliev, E. Wieland, R. Dähn, J. Tits, S.V. Churakov, O. Zaharko, Mechanisms of Nd(III) uptake by 11 Å tobermorite and xonotlite. Appl. Geochem. **25**, 763–777 (2010)

S.V. Mattigod, D. Rai, A.R. Felmy, L. Rao, Solubility and solubility product of crystalline $Ni(OH)_2$. J. Solution Chem. **26**, 391–403 (1997)

I. McKinley, A. Scholtis, A comparison of radionuclide sorption databases used in recent performance assessments, in *Radionuclide Sorption from the Safety Evaluation Perspective, Proceedings of an NEA Workshop*, 16–18 Oct, Interlaken, Switzerland 1991

P. Muller, K. Blaum, B.A. Bushaw, S. Diel, Ch. Geppert, A. Nahler, W. Nortershauser, N. Trautmann, K. Wendt, Trace detection of 41Ca in nuclear reactor concrete by diode-laser-based resonance ionization mass spectrometry. Radiochim. Acta **88**, 487–493 (2000)

K. Noshita, T. Nishi, T. Yoshida, H. Fujihara, N. Saito, S. Tanaka, Categorization of cement hydrates by radionuclide sorption mechanism. Mat. Res. Soc. Symp. Proc. **663**, 115–121 (2001)

Nuclear Energy Agency (NEA-OECD), in *Proceedings of the Sorption Workshop: Conclusion of NEA Sorption Project Phase II and Status Analysis of Sorption Modelling for PA*, NEA/RWM/SORPTION(2005)3, OECD-NEA, Paris, France 2005

Nuclear Energy Agency (NEA-OECD), The jeff-3.1 nuclear data library, jeff report 21, oecd/nea, Paris, France 2006

M. Ochs, D. Hager, S. Helfer, B. Lothenbach, Solubility of radionuclides in fresh and leached cementitious systems at 22 °C and 50 °C. Mat. Res. Soc. Symp. Proc. **506**, 773–780 (1998)

M. Ochs, L. Vieille-Petit, L. Wang, D. Mallants, B. Leterme, Additional sorption parameters for the cementitious barriers of a near-surface repository, NIROND-TR 2010-06 E, March 2011

ONDRAF/NIRAS, Identification of critical radionuclides through a screening of the ondraf/niras 2003/2004 radiological inventory for category a waste, Nirond-tr 2007-05 e, April 2011

N.J. Pilkington, N.S. Stone, The solubility and sorption of nickel and niobium under high pH conditions, NSS/R 186 (1990)

I. Pointeau, N. Coreau, P. Reiller, Etude expérimentale et modélisation de la rétention de 14CO3 par les matériaux constituant le béton dans le cadre d'un entreposage de barres graphite UNGG. Note Technique CEA. NT DPC/SCPA 02-046 2002

M. Sasoh, The study for the chemical forms of C-14 released from activated metals, in *Proceedings of a Workshop on the Release and Transport of C-14 in a Repository Environment*. NAGRA Nagra Internal Report, Nagra, Wettingen, Switzerland, pp. 85–87 2004

A.M. Scheidegger, E. Wieland, A.C. Scheinost, R. Dahn, P. Spieler, Spectroscopic evidence for the formation of layered Ni–Al double hydroxides in cement. Environ. Sci. Technol. **34**, 4545–4548 (2000)

J. Small, Modelling the partitioning and transport of C-14 in a microbially active LLW site, in *Proceedings of a Workshop on the Release and Transport of C-14 in a Repository Environment*. NAGRA Nagra Internal Report, Nagra, Wettingen, Switzerland, pp. 109–120 2004

U.S. Department of Energy (USDOE), National low-level waste management program radionuclide report series, Selected radionuclides important to LLW management, DOE\LLW-238, November 1996a

U.S. Department of Energy (USDOE), Selected radionuclides important to low-level radioactive waste management, National low-level waste management program, DOE/LLW-138, November 1996b

M. Vespa, R. Dähn, D. Grolimund, M. Harfouche, E. Wieland, A.M. Scheidegger, Speciation of heavy metals in cement-stabilized waste forms: a micro-spectroscopic study. J. Geochem. Explor. **88**, 77–80 (2006a)

M. Vespa, R. Dahn, D. Grolimund, E. Wieland, A.M. Scheidegger, Spectroscopic investigation of Ni speciation in hardened cement. Environ. Sci. Technol. **40**, 2275–2282 (2006b)

L Wang, E. Martens, D. Jacques, P. De Canniere, J. Berry, D. Mallants, Review of sorption values for the cementitious near field of a near surface radioactive waste disposal facility, NIROND-TR 2008-23E, April 2009

E. Wieland, J. Tits, P. Spieler, J.P. Dobler, A.M. Scheidegger, Uptake of nickel and strontium by a sulphate-resisting Portland cement. Appl. Mineral. **2**, 705–708 (2000)

E. Wieland, L. Van Loon, Cementitious near-field sorption data base for performance assessment of an ILW repository in Opalinus Clay, PSI Bericht Nr. 03-06 (2002)

E. Wieland, J. Tits, A. Ulrich, M.H. Bradbury, Experimental evidence for solubility limitation of the aqueous Ni(II) concentration and isotopic exchange of 63Ni in cementitious systems. Radiochim. Acta **94**, 29–36 (2006)

M.E. Wieser, Atomic weights of the elements 2005 (IUPAC Technical Report). Pure Appl. Chem. **78**(11), 2051–2066 (2006)

M.-S. Yim, F. Caron, Life cycle and management of carbon-14 from nuclear power generation. Prog. Nucl. Energy **48**, 2–36 (2006)

J.M. Zachara, C.E. Cowan, C.T. Resch, Sorption of divalent metals on calcite. Geochim. Cosmochim. Acta **55**, 1549–1562 (1991)

Chapter 6
Sorption Values for Thorium, Uranium, Plutonium, Neptunium, and Protactinium

Abstract The actinide elements—thorium, uranium, plutonium, neptunium, and protactinium—are important constituents of radioactive waste from nuclear fuel. Uranium also occurs in a variety of wastes, e.g. from mining. These elements all hydrolyse extensively in aqueous solutions and correspondingly strong sorption onto concrete, hydrated cement paste and individual CSH phases is observed. Sorption is also more or less constant over all states of cement evolution. The sorption mechanisms are, however, not well understood to date. In case of Th, relatively fast kinetics of uptake and reversibility are observed, indicating that uptake occurs through surface processes and probably does not involve incorporation into the structures of hydrated cement phases. In contrast to Th, which exists only in the tetravalent oxidation state in aqueous environments, uranium, plutonium, neptunium, and protactinium can exist also in lower and/or higher oxidation states. In analogy to their aqueous chemistry, very similar sorption behaviour is expected for all tetravalent forms. Sorption of U(VI) on cementitious materials is similar to Th(IV)/U(IV) in magnitude, but appears to involve different mechanisms (probably solid-solution formation). In lack of specific information, the same is assumed for Pu(VI). Relatively little is known for the pentavalent forms. Strong sorption is observed for Pa(V), but the underlying mechanism is not known. For Np(V), relatively weak sorption is assumed in lack of specific data.

6.1 Thorium

6.1.1 Chemical Form, Speciation, and Solubility

Twenty-five (radioactive) thorium isotopes are known, of which six exist in nature, and are part of the following decay series:

- ^{238}U decay series: ^{234}Th (half-life = 24.1 days) and ^{230}Th (half-life = 8.0×10^4 years)
- ^{232}Th decay series: ^{232}Th (half-life = 1.41×10^{10} years) and ^{228}Th (half-life = 1.91 years)

© Springer International Publishing Switzerland 2016

M. Ochs et al., *Radionuclide and Metal Sorption on Cement and Concrete*,
Topics in Safety, Risk, Reliability and Quality 29,
DOI 10.1007/978-3-319-23651-3_6

- ^{235}U decay series: ^{231}Th (half-life = 25.5 h) and ^{227}Th (half-life = 18.5 days).

Natural thorium consists of essentially one isotope, ^{232}Th, with trace quantities of the other isotopes. Thorium occurs only in the +4 oxidation state in nature. The Th^{+4} ion is the largest tetravalent cation known with a radius of approximately 1 Å.

Thorium is not redox sensitive and the only aqueous species relevant in a cement environment is the hydrolysed species $Th(OH)_4(aq)$ as predicted by speciation calculation (Figs. 6.1 and 6.2). Equilibrium calculations using *The Geochemist's Workbench®* (Bethke 2006) predict that the solubility of amorphous $Th(OH)_4$ at pH > 7 is around 10^{-9} mol/L and independent of pH (Fig. 6.3). The predicted $Th(OH)_4$ solubility has been found to be in good agreement with literature data concerning solubility experiments in cement systems using thorium hydroxide precipitate as solubility controlling phase (Tits et al. 2008; Wierczinski et al. 1998; Serne et al. 1996; Pilkington et al. 1988; Ewart et al. 1992).

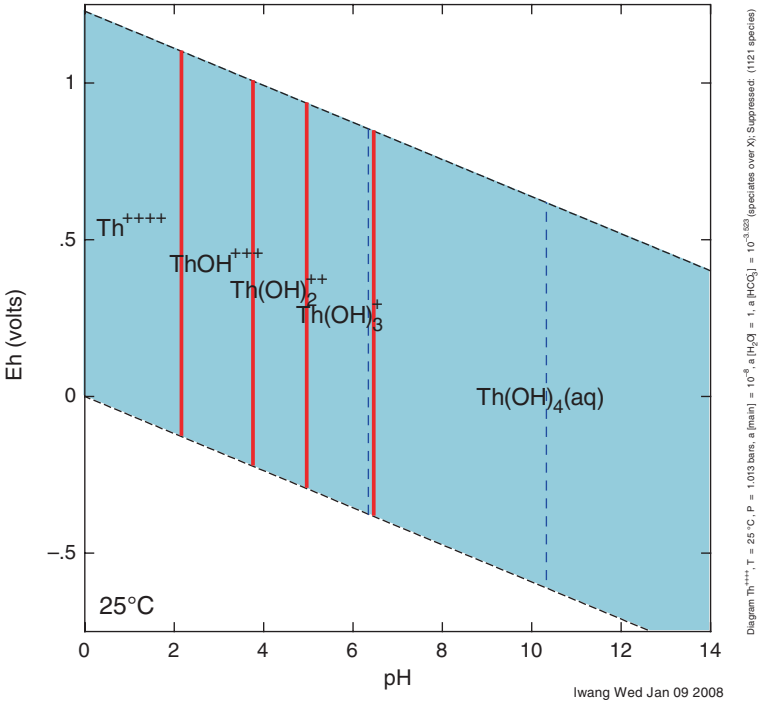

Fig. 6.1 Eh–pH diagram of thorium calculated with *The Geochemist's Workbench®*. Thorium activity equals 10^{-8}. Calculations based on solubility and speciation thermochemical data of Neck and Kim (2001)

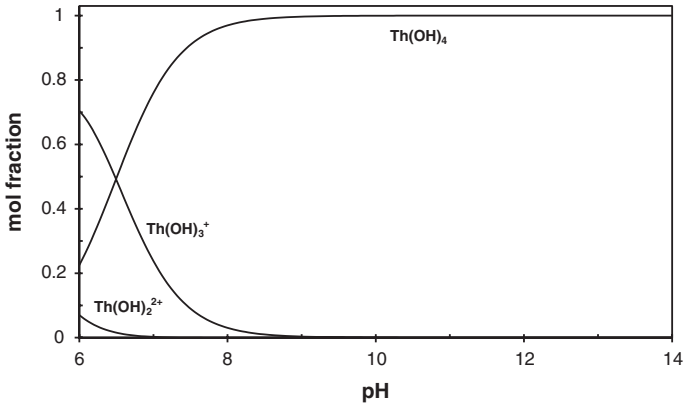

Fig. 6.2 Dissolved thorium speciation (total dissolved Th $= 1 \times 10^{-8}$ molal, no precipitation of solids) at 25 °C

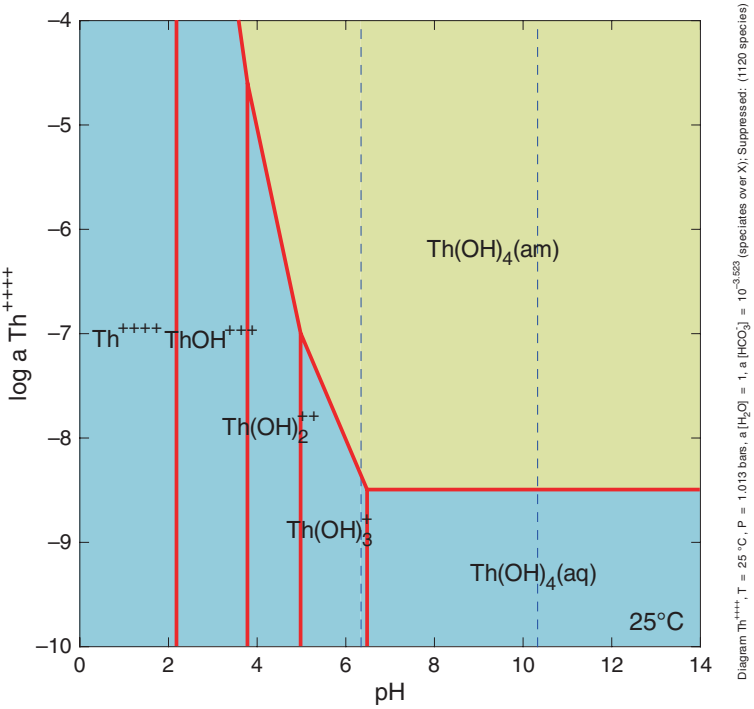

Fig. 6.3 Solubility of amorphous thorium hydroxide as a function of pH. Calculations with *The Geochemist's Workbench*® based on solubility and speciation data of Neck and Kim (2001)

6.1.2 Sorption Values from the Literature for the Benchmark Cement

Figure 6.4 shows the compilation of reviewed R_d data as a function of pH. The summary of the reviewed R_d values and the experimental conditions under which they were determined are given in Table A.8 (see Annex).

Allard et al. (1984) measured R_d of Th on 7 different concretes and found that the concrete type had only a minor impact on the R_d value. The initial ^{234}Th (^{232}Th as carrier) concentration used was 2×10^{-10} mol/L, while the final Th concentration was much lower (i.e. ~10^{-12} mol/L based on a *S*/*L* ratio of 0.02 kg/L and an assumed R_d of 6300 L/kg, also see Table 6.1); hence, both concentrations were below the solubility of $Th(OH)_4(am)$. Since the detection limit of the experimental approach was not given, a definite appraisal of the equilibrium concentration remains difficult. Reportedly, R_d values were generally larger than 1000 L/kg and increased with contact time (until 100 days) to a few thousands L/kg. In a similar study, Heath et al. (1996) found similar R_d values on standard Portland cement.

R_d for Th on CEM I and V determined in a French R&D programme (Andra 2005) is in the range of 10^4 to 10^5 L/kg. Because the Andra (2005) data contain both literature values and new measurements not reported previously in the open literature, only the new experimental data were retained (literature values were also retained if they were not yet included in the compilation). The data compiled

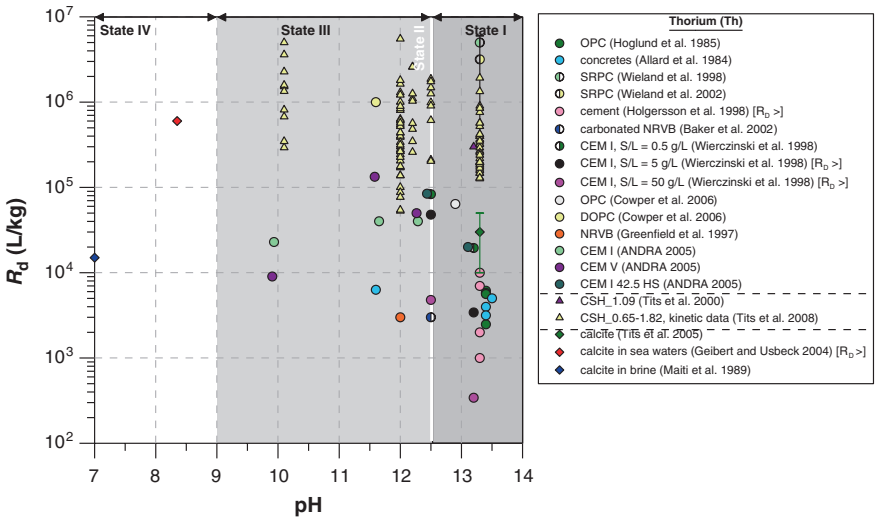

Fig. 6.4 Distribution ratio (R_d) of thorium in cementitious systems. Values are presented as a function of pH and belong to one of four different states of cement evolution. *SRPC* sulphate-resisting Portland cement; *DOPC* degraded ordinary Portland cement; *NRVB* Nirex reference vault backfill; *CSH* calcium silicate hydrate. R_d > means the minimum value of a set of reported R_d values is plotted here

Table 6.1 Experimental data for thorium sorption tests onto HCP (pH > 13)

Reference	Tracer	C_0 (M)	R_d (L/kg)	*S/L* (kg/L)	C_{eq} (M)	Detection limit	Experimental window	Data quality
Allard et al. (1984)	^{234}Th, ^{232}Th carrier	2E−10	6300	2E−2	1.58E−12	n.a.	$R_{d,max}$ = n.a. $R_{d,min}$ = 7.5	Low
Hoglund et al. (1985)	^{234}Th, ^{232}Th carrier	2E−10	6200	2E−2	1.62E−12	n.a.	$R_{d,max}$ = n.a. $R_{d,min}$ = 7.5	Low
Wierczinski et al. (1998)	^{232}Th	1.1E−11	83,000	5E−4	1.10E−12	4.3E−11	$R_{d,max}$ = 500 $R_{d,min}$ = 300	Medium
Holgersson et al. (1998)	^{234}Th	n.a.	10,000	5E−2	n.a.	n.a.	$R_{d,max}$ = n.a. $R_{d,min}$ = 3	Low (excluded)
Cowper et al. (2006)	^{228}Th	1.1E−11	63,000	0.01	1.58E−14	1.45E−16	$R_{d,max} = 7.5 \times 10^6$ $R_{d,min} = 1.5 \times 10^4$	High
Cowper et al. (2006)	^{228}Th	4E−11	63,000	0.01	6.35E−14	1.45E−16	$R_{d,max} = 2.7 \times 10^7$ $R_{d,min} = 5.4 \times 10^4$	High
Wieland et al. (1998)	^{234}Th	1E−10	5E+6	1E−5	2E−12	<3.8E−13	$R_{d,max} = 4 \times 10^8$ $R_{d,min} = 1.5 \times 10^4$	High
Wieland et al. (2002)	^{228}Th, ^{234}Th	1E−10	6E+6	1E−5	1.67E−12	n.a.	$R_{d,max} = 4 \times 10^8$ $R_{d,min} = 1.5 \times 10^4$	High
Wieland et al. (2002)	^{228}Th, ^{234}Th	1E−10	3.5E+5	1E−4	2.86E−12	n.a.	$R_{d,max} = 4 \times 10^7$ $R_{d,min} = 1.5 \times 10^3$	High

Experimental window calculated from Eq. (6.1), with $A_{l,min} = 2.45 \times 10^{-14}$ mol/L for Wieland et al. data, or $A_{l,min}$ = detection limit for all other data.
n.a. not available

by Andra (2005) indicate that thorium uptake is the strongest at a pH of around 11.6; from this value onwards either decreasing or increasing the pH leads to a decrease in R_d values. No apparent impact of cement type on R_d is shown as CEM I and CEM V both exhibit similar R_d values.

Part of the sorption data reported by Wierczinski et al. (1998) was also included in the Andra (2005) data (CEM I 42.5 sulphate resistant with $S/L = 0.5$). As is observed in Fig. 6.4, R_d determined by Wierczinski et al. indicated that R_d increases by an order of magnitude with decreasing pH from 13.2 to 12.5. Results further indicated that there was a tendency for R_d to decrease with increasing S/L ratio (within the reported range from 5×10^{-4} to 5×10^{-2} kg/L, see Sect. 6.1.3.1). However, there seemed a difficulty in measuring R_d accurately when the S/L ratio is higher than 5×10^{-4} kg/L.

Further studies on Th uptake by cement materials have been carried out at PSI (Tits et al. 2000, 2002, 2005; Wieland and Van Loon 2002; Wieland et al. 1998, 2002). A summary of their main results will be discussed here, while all relevant data are included in Fig. 6.4. R_d for Th on cement materials at State I (pH 13.3) is generally very large with values $>10^5$ L/kg. At the lowest S/L ratio employed (10^{-5} kg/L), R_d is larger than 10^6 L/kg. Note that the PSI investigations emphasise on the importance of using very low solid content in order to measure R_d accurately. This is because sorption of Th on cement materials is very strong so that the solid content should be small to allow an accurate determination of the dissolved Th concentration in solution (see further). It was found that R_d decreased an order of magnitude if the S/L ratio increased from 10^{-5} to 10^{-4} kg/L. Further increase in S/L ratio did not change R_d. Based on these findings, Wieland and Van Loon (2002) suggested that lower R_d values in literature (e.g. those of Allard et al. 1984; Hoglund et al. 1985) are probably due to the higher S/L ratio used (2×10^{-2} kg/L) than that applied in the PSI experiments.

Tits et al. (2008) recently performed detailed batch experiments to determine the uptake of Th on synthesised CSH phases with C/S ratio between 0.65 and 1.82. Major observations from this study are as follows:

- Uptake values are large (R_d 10^5 to 10^7 L/kg);
- The uptake of Th is fast and reversible demonstrated by a quick equilibrium reached within one day and the sorption and desorption R_d values were found to be similar within the expected uncertainty range. The authors then suggested to consider that the binding of Th to CSH phases is a reversible process;
- There is indication that R_d values determined in co-precipitation experiments are slightly higher than the ones determined in sorption experiments suggesting that Th might be incorporated into the CSH structure;
- R_d is not influenced by pH (10.1–13.3) or chemical composition of the pore waters used in experiments. In particular, R_d does not seem to vary as C/S ratio of CSH phases changes suggesting that degradation of cement materials has no observable effect on Th uptake at the States I–III.

Sorption of thorium on OPC and degraded OPC (DOPC) was investigated by Cowper et al. (2006). These authors found a significant increase of R_d with cement

degradation suggesting that degraded cement (essentially pure CSH, at pH 11.5) sorbs thorium stronger than freshly cured cement containing portlandite and alkalis (at pH 12.8). One possible explanation proposed by the authors is the formation of a Th co-precipitate with CSH or Th-bearing silicate. The observed increase in sorption may also be attributed, at least partly, to the increase in specific surface area when CSH content increased as OPC degraded. The specific surface was not measured however in the experiment. In the same study, R_d for americium showed the same behaviour, i.e., increasing with decreasing pH as cement degraded. The observed increase of R_d with cement degradation seems to contradict the findings of Tits et al. who measured relatively unvaried R_d on synthetic CSH phases at pH of 10–13.3. More discussion concerning the influence of cement degradation on R_d of Th is given in Sect. 6.1.3.2.

Tits et al. (2005) also determined R_d of thorium on calcite but in pH of 13.3 (State I). Considering that speciation of Th at State IV might be the mixed complex $Th(CO_3)(OH)_3^-$ (although this species is not shown in Fig. 6.2), which might reduce sorption, R_d for Th at State IV is expected to be lower than the one determined by Tits et al. at State I pH.

6.1.3 Sorption Mechanisms and Selected Sorption Values

From the reviewed R_d values presented in the previous section, the most important factors influencing R_d of thorium on cement materials appear to be *S*/*L* ratio and cement degradation state. For the latter, some studies showed a tendency of decreasing R_d from States I to III, while other studies illustrate relative constant R_d at States I–III.

6.1.3.1 Influence of *S*/*L* Ratio

Prior to the discussion of the potential influence of *S*/*L* ratio on thorium sorption, a discussion on the measurement window of thorium sorption under different *S*/*L* ratios is needed. Thorium is known to sorb very strongly on hydrated cements. Therefore, use of a high *S*/*L* ratio may easily result in thorium equilibrium concentrations that fall below the current analytical detection limits. In other words, the detection limit will imply an upper limit to the *S*/*L* ratio which will still result in reliable R_d values (i.e. allow reliable measurements of dissolved thorium concentrations).

A very useful discussion on the maximum and minimum measurable sorption value for thorium can be found in Tits et al. (2002). Although the measurements and subsequent uncertainty analysis were done for sorption onto calcite, much of the concept and results can be extrapolated to the sorption measurements performed onto HCP by the same laboratory (Wieland et al. 1998, 2002), as the same equipment and approach were used. According to Tits et al., the minimum

measurable activity $A_{l,min}$ for ^{228}Th is about 34.5–50 counts per min/mL (values vary for different experiments), or 2.2–2.45 × 10^{-14} mol/L ^{228}Th. The authors define the maximum distribution ratio, $R_{d,max}$, which is measurable with a sufficient precision (i.e. relative uncertainty of 10 %) as

$$R_{d,max} = \frac{\left(A_{susp} - A_{l,min}\right)}{A_{l,min}} \times \frac{L}{S} \tag{6.1}$$

where A_{susp} is total initial activity in the suspension, S is mass of solid (kg), and L is volume of the aqueous phase (L). For a constant A_{susp} and $A_{l,min}$, $R_{d,max}$ depends only on the S/L ratio. For a S/L ratio of 2 × 10^{-2} and 10^{-4} kg/L, Tits et al. determined $R_{d,max}$ (L/kg) as, respectively, 2.4 × 10^5 and 2.6 × 10^7.

Because $A_{l,min}$ depends on the background activity of the experiment, in principle each experimental condition will have its specific $A_{l,min}$ value (depending on matrix, equipment, among others). Thus, $R_{d,max}$ values are also specific to a specific experiment (J. Tits, personal communication), and extrapolation to other experimental conditions is not recommended. For measurements done within PSI, extrapolation of $R_{d,max}$ values obtained from calcite to HCP can be done as a first approximation (similar set-up, same analytical technique and instruments used).

In addition to $R_{d,max}$, Tits et al. (2002) also defined $R_{d,min}$, the corresponding minimum measurable distribution ratio, as $R_{d,min} = 0.15 \times L/S$ for a 10 % relative uncertainty. $R_{d,min}$ for sorption onto calcite was 7.5 and 1500 L/kg for a S/L ratio of 2 × 10^{-2} and 10^{-4} kg/L, respectively. By means of $R_{d,min}$ and $R_{d,max}$, a measurement window was thus defined by Tits et al. for thorium sorption measurements onto calcite as function of S/L ratio. We here assume that the magnitude of $A_{l,min}$ is also appropriate for the sorption measurements on HCP carried out by Wieland et al. (1998, 2002). Under those assumptions, the $R_{d,max}$ values as function of S/L ratio may be used as first indication of the upper branch of the measurement window. This has been implemented in Fig. 6.5, where literature data about thorium R_d versus S/L ratio have been combined (data for State I only). Prior to including the literature data in the graph, a screening was performed to evaluate the quality of the data in view of experimental difficulties, especially at high S/L ratios. As a result of the screening, not all data were included in the graph (see Fig. 6.5).

An attempt was made to define the measurement window for each data set listed in Table 6.1 using Eq. (6.1) for $R_{d,max}$ and $R_{d,min} = 0.15 \times L/S$. In using Eq. (6.1), $A_{l,min} = 2.45 \times 10^{-14}$ mol/L for the Wieland et al. data, or $A_{l,min}$ = detection limit for all other data. $R_{d,min}$ and $R_{d,max}$ values given in Table 6.1 should be seen as tools to assess the experimental window, i.e., whether the reported R_d values were measured within or outside the experimental window. Note, that for assessing data quality the experimental window is only one criterion.

Initially, seven sources of data were considered for the evaluation of the potential effect of S/L ratio on thorium R_d (Table 6.1). For each reported R_d value, the equilibrium concentration in solution (C_l) was calculated, and this value was evaluated versus detection limit (if the latter was available). The calculated experimental window is also included. Data were qualified as low, medium, or high

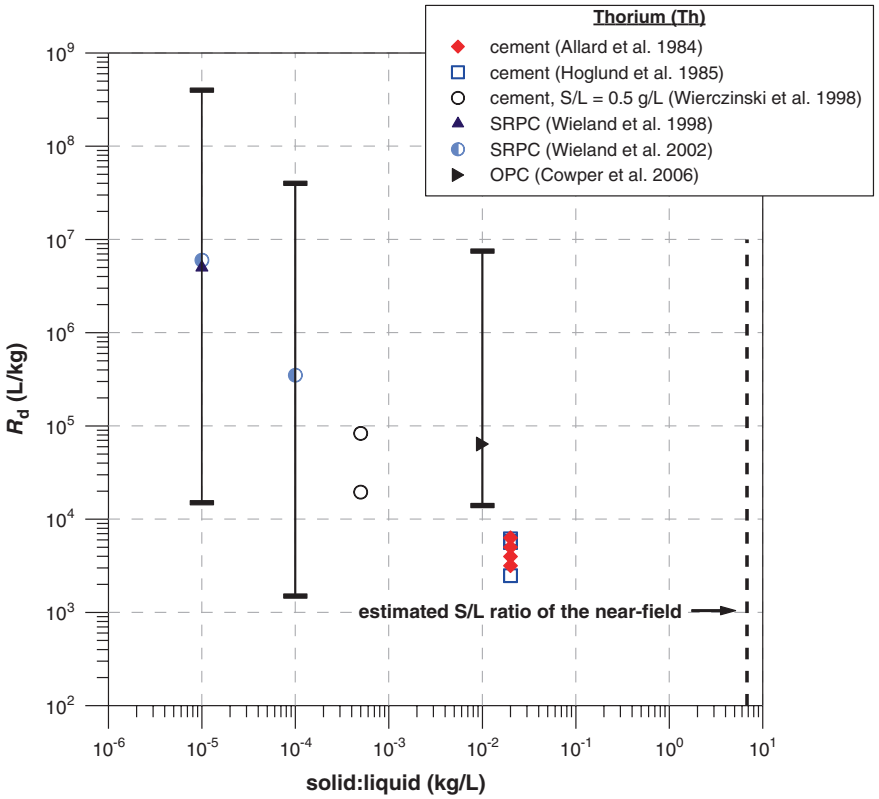

Fig. 6.5 Effect of *S/L* ratio on sorption of thorium on cementitious materials. Only data for pH > 13 (State I) are plotted. *Vertical bars* indicate measurement window, based on $R_{d,max}$ and $R_{d,min}$ taken from Table 6.1

quality depending on the availability of information about experimental conditions, including detection limit, the magnitude of the equilibrium concentration vis-à-vis the detection limit, and experimental window. Data were assigned a high-quality weighting if the detection limit was given, the equilibrium concentration was well above detection limit, and the R_d values were within the experimental window. Data were of low quality if insufficient data were available to determine the equilibrium concentration, or when the latter could not be evaluated because of missing detection limit, or when R_d was outside the experimental window.

Three data sets were found to be of low quality (Allard et al. 1984; Hoglund et al. 1985; Holgersson et al. 1998), of which one (Holgersson et al. 1998) was excluded from further analysis because of insufficient experimental information. The equilibrium concentrations for the two data sets screened in are about 1.6×10^{-12} M, but the detection limit is not given; hence, the quality of such low values cannot be reliably assessed. The upper limit to the measurement window could not be determined. The data are nevertheless included in Fig. 6.5, but a low weight is given to their values.

The Wierczinski et al. (1998) data are of a medium quality because the calculated equilibrium concentration is at or below the detection limit. The R_d value is outside the experimental window (based on a detection limit of 4.3×10^{-11} M). High-quality data sets are those from Cowper et al. (2006), and Wieland et al. (1998, 2002). Their calculated equilibrium concentrations are above the detection limit (note the very low detection limit given by Cowper et al.), or at least higher than the presumed detection limit (data of Wieland et al. (2002) did not provide detection limits, but the overall experimental conditions were well designed with proper knowledge of experimental windows).

Wieland and Van Loon (2002) found that R_d of thorium decreases by an order of magnitude if the *S/L* ratio used in batch sorption experiments increases from 10^{-5} to 10^{-4} kg/L. Further increase in *S/L* ratio to 5×10^{-4} did not seem to affect R_d. Wierczinski et al. (1998) also observed an effect of *S/L* ratio on R_d measurement (the *S/L* ratio ranged from 5×10^{-4} to 5×10^{-2} kg/L). Note that at the high *S/L* values Th concentration in the liquid phase (^{232}Th was used) was too low to determine the R_d accurately (at *S/L* of 5×10^{-3} and 5×10^{-2}, R_d was determined by the detection limit). Even at $S/L = 5 \times 10^{-4}$ the accuracy of R_d is questionable: assuming an initial concentration of 1.1×10^{-11} M, the equilibrium concentration was calculated to be 1.1×10^{-12} mol/L (see Table 6.1), while the reported detection limit was $<4.3 \times 10^{-11}$ M. The effect of *S/L* ratio is probably caused by the problem of detection in measuring Th concentration in solution and is not related to sorption mechanism.

The maximum acceptable *S/L* ratio for reliable R_d measurements can sometimes be very low, as was reported by Geibert and Usbeck (2004) for calcite; they illustrated that the *S/L* must be below 5×10^{-7} kg/L in order to measure any sorption of ^{234}Th on calcite.

Figure 6.5 plots R_d of thorium on cementitious materials as a function of *S/L*. In order to make a relevant comparison, only data at pH > 13 are plotted. The quality of the data points has been discussed on the basis of Table 6.1. We note that comparison for an effect of *S/L* ratio between different laboratories may not be relevant because of different experimental routines applied and different degrees of uncertainties involved. Nevertheless, Fig. 6.5 suggests that the effect of *S/L* ratio on R_d is pertinent, but only in the *S/L* range 10^{-5} to 10^{-3} (based on high-quality data): there is about one order of magnitude decrease in R_d for a one order of magnitude increase in *S/L*. Again based on the high-quality data, the trend in R_d seems to flatten off between 10^{-3} and 10^{-2} M. The low-quality data are included in the graph, but it is considered at present that they do not add much value to the discussion on the influence of *S/L* on R_d.

Based on the $R_{d,max}$ and $R_{d,min}$ values from Table 6.1, all experiments except one were carried out within their respective experimental window, using the approach of PSI. This is merely a confirmation for the appropriateness of the high-quality data; it does not add any value to the medium- or low-quality data. In conclusion, a real *S/L* effect was observed at least for part of the range of *S/L* values (10^{-3} to 10^{-5}) reported by the various experiments. How R_d behaves for *S/L* values higher than 10^{-3} needs further corroboration, especially in view of the much higher *S/L* ratios valid under repository conditions.

6.1.3.2 Influence of Cement Degradation

Studies from Cowper et al. (2006), Andra (2005) and Wierczinski et al. (1998) investigated in particular the influence of cement degradation on Th sorption and seem to suggest that R_d increases with degradation of cement from State I to States II and III. The observed R_d increase with cement degradation may be linked to mineralogy change in cement because thorium aqueous speciation does not change at pH above 7.

Similarly, Allard et al. (1984) found that R_d of Th on concrete was about 6000 L/kg at pH 11.6 and was slightly higher than R_d values measured at pH 13.5, which was about 3000–5000 L/kg. Hoglund et al. (1985) in a similar study concluded that the sorption of actinides was highest in the lower end of the observed pore water pH range (12–13.5).

On the other hand, Tits et al. (2008) found that R_d for Th is relatively invariant on synthetic CSH phases of different C/S ratios and pH. If Th is sorbed mainly by CSH phases in cementitious materials and if sorption of Th should increase as cement degrades (as suggested by other studies discussed in this section), one should expect an increase of R_d with decreasing C/S ratio and pH. Since this is not the case, the data of Tits et al. seem to suggest that uptake of Th by cement should be unaffected by cement degradation.

After reviewing all the data, it is concluded that there is no clear evidence to support a trend of increasing Th sorption with cement degradation at States I to III.

At State IV, Th speciation may change to $Th(CO_3)(OH)_3^-$ which might influence sorption. Also, calcite as the dominating sorbing mineral at State IV is expected to have much less sorbing potential than cement materials so R_d for Th at State IV is likely to be lower than the ones at States I to III.

6.1.3.3 Impacts of High Chlorine Concentration on Sorption

Bayliss et al. (1996) revealed that a hypersaline water (essentially a NaCl solution) has no effect on the sorption of tetravalent uranium and plutonium. Considering that a chemical analogy exists between Th(IV) and U(IV)–Pu(IV), one may also expect minor influence of NaCl on sorption of thorium. It is thus unlikely that an increase in NaCl concentration in cement pore water will affect adversely the sorption of thorium in the near field.

6.1.3.4 Sorption Mechanisms

Thorium hydrolyses strongly and is therefore expected to be adsorbed strongly by geologic materials with sorbing surfaces containing hydroxyl groups (Bradbury and Baeyens 2005). Not surprisingly, strong sorption ($R_d > 1000$ L/kg) is generally observed for thorium onto crushed cement, concrete, and synthetic CSH phases (see references cited in the next section). The sorption mechanisms are, however,

not well understood. Application of advanced spectroscopic techniques, such as EXAFS, is limited for the study of uptake mechanism of Th because of the very low concentration of Th that has to be used in sorption experiments to avoid processes other than adsorption such as precipitation and/or formation of Th colloids (Tits et al. 2010). Possible uptake mechanisms for Th on cementitious materials include surface adsorption, co-precipitation of Th with CSH phases, and formation of solid solution, e.g., to form a zircon-like $Th(IV)SiO_4$ phase.

Work by Tits et al. (2000) and Wieland et al. (1998) support the hypothesis that uptake of Th on sulphate-resisting Portland cement (SRPC) and CSH phases at State I (pH 13.3) is kinetically fast (completed within 2 days) so that the uptake mechanism is likely controlled by adsorption processes. This implies that uptake of thorium on cementitious materials occurs through surface processes and probably does not involve incorporation of thorium into structures of cementitious materials. A recent study on sorption of Th on synthetic CSH phases also supports this type of adsorption mechanism (Tits et al. 2010).

Studies of the interactions of CSH phases with cerium (IV), as a chemical analogue to tetravalent actinides, have found the zircon-like mineral $Ce(IV)SiO_4$ to be stable at high pH (11–12.5) (Adenot et al. 2001). This suggests that also thorium may form silicate phases with CSH in a cementitious environment.

To interpret their batch R_d data, Sugiyama et al. (2003) and Sugiyama and Fujita (1999) applied a sorption model and alternatively a co-precipitation model and found that the latter explains better the thorium sorption data on OPC than the former. From these observations, they suggest that uptake of actinides in the form of neutral species such as $Th(OH)_4$ can be better modelled by co-precipitation. The suggested uptake mechanism of thorium on cement is by formation of a co-precipitate between thorium and $Ca(OH)_2$ in CSH.

Having considered the data described above, the expert group agreed the following on the selected sorption values for different degradation states. It was agreed that sorption at States I, II, and III would be similar. Sorption in State IV would be weaker than for the other states, but relevant data were lacking for this state (there was also agreement on the model-predicted thorium speciation, which was the same for all four states of cement evolution, i.e. $Th(OH)_4$). Most published R_d values were greater than 1000 L/kg showing high sorption. There were few data at pH values below 12 (relevant to States III and IV). Data from Allard et al. (1984), however, indicated that R_d values were moderately independent of pH.

The expert group noted the wide range of solid–liquid ratios used in the thorium experiments and also the sensitivity of R_d values to solid–liquid ratios, which resulted from several reported values to be likely limiting values (i.e. corresponding to detection limit) (see Sect. 6.1.3.1). Some concern was expressed about the use of very low solid–liquid ratios in some experiments. There was wariness of sorption data on a phase that is not dominant at the quoted pH, e.g. sorption data for calcite at pH 13. It was felt that such data should not be disregarded, but that there should be an awareness of the weighting given to it.

6.1.3.5 Sorption at State I

On the basis of the Th speciation as well as Allard et al. (1984) and other data, it was felt that it was not possible to differentiate between States I to III, so the same values should be used in each state. Having noted that the two families of data had a spread on them that was then reflected in the lower bound and upper bound adopted in States I–III. The best estimate was placed in the centre.

The upper limit was assessed as 1×10^6 L/kg or possibly higher, but it was noted that values higher than ~10^6 L/kg are difficult to measure experimentally. The best estimate for States I, II, and III was put at 3×10^4 L/kg, following examination of oxides and sorption data for clays, and taking account of the decision that Th should not have a higher R_d than U(IV) (see Sect. 6.2.3).

6.1.3.6 Sorption at State II

The experts agreed that it was not possible to differentiate between States I to III, which is in line with the thermodynamic prediction that thorium speciation is the same in all states (Sect. 6.1.3.4). Therefore, the same values are used in each state (Table 6.2).

6.1.3.7 Sorption at State III

It was not possible to differentiate between States I and III, so the same values should be used in each state (see Sects. 6.1.3.5 and 6.1.3.6). However, it was recognised that State III is more complicated than the others and that there are few data for thorium sorption under State III conditions. CSH offers good sites for sorption, but the amount and nature of CSH is variable across State III and is difficult to predict, and the predominance of CSH will cease towards the end of State III. Overall, however, the experts decided that the R_d values for State III should be the same as those for States I and II, because (1) a constant R_d for Th across all degradation states is proposed based on constant speciation and (2) data for State III are for the centre of this state (~pH 11), and not for the low C/S extreme.

Table 6.2 Selected best estimate, upper and lower limit R_d values for Th(IV)

pH state	Best estimate (L/kg)	Upper limit (L/kg)	Lower limit (L/kg)
State I	3×10^4	1×10^6	1×10^3
State II	3×10^4	1×10^6	1×10^3
State III	3×10^4	1×10^6	1×10^3
State IV	3×10^4	1×10^6	3×10^3

6.1.3.8 Sorption at State IV

It was noted that there are few data for State IV. Calcite data from Tits et al. (2000, 2005) for State I show CSH to sorb more strongly than calcite at State I. The data for calcite from Tits et al. (2000) are at the top end of the range, but they build confidence that thorium sorption in State IV is similar to sorption in States I–III.

It was decided to keep the same best estimate (3.0×10^4 L/kg) as for States I–III to reflect the fact that the speciation is identical and that therefore the data from Tits et al. (2000, 2005) are applicable to State IV. A broader range of values is proposed for State IV, reflecting a wider band of uncertainty in the absence of good data.

It was noted that there are data for plutonium sorption onto calcite (Sect. 6.3): the Berry et al. (2000) data give R_d values for sorption of plutonium onto calcite (~300 L/kg). Equivalent data are not available for thorium. The analogy for the plutonium lower limit was applied to thorium, thus giving an upper bound of 1.0×10^6 L/kg, and a lower bound of 3.0×10^1 L/kg. Table 6.2 shows the selected best estimate as well as upper and lower bound R_d values for thorium.

6.2 Uranium

6.2.1 Chemical Form, Speciation, and Solubility

Uranium (U) has sixteen isotopes; all are radioactive. Several isotopes of uranium are naturally occurring radionuclides, including ^{238}U (half-life 4.47×10^9 years), ^{235}U (half-life 7.04×10^8 years), and ^{234}U (half-life 2.46×10^5 years). Naturally occurring uranium typically contains 99.274 % ^{238}U, 0.720 % ^{235}U, and 0.0057 % ^{234}U by weight (IAEA 2001). Uranium can exist in the +3, +4, +5, and +6 oxidation states, of which the +4 and +6 states are the most common states found in the environment.

Much of the uranium that is used in commercial applications is used to produce nuclear fuel. A typical ^{235}U enrichment for commercial reactors is approximately 3 % (i.e. 3 % of the uranium in a nuclear fuel rod is ^{235}U, the rest is ^{238}U). Since it is the fissile ^{235}U that is used up in the fission reaction, most of the ^{238}U remains in the fuel and is mixed with highly radioactive fission and activation products that result from the fission process. Corrosion of fuel elements will result in leakage of uranium isotopes (mainly ^{238}U and ^{235}U) into the primary cooling circuit. LILW waste streams that originate from treatment of the primary cooling circuit will contain low levels of those isotopes. Uranium may also end up in waste streams that originate from nuclear fuel production facilities, from operation and decommissioning of nuclear research facilities, etc. A large number of uranium isotopes may be present in LILW, including ^{233}U, ^{234}U, ^{235}U, ^{236}U, ^{237}U, and ^{238}U (NDA 2011; NIRAS 2008).

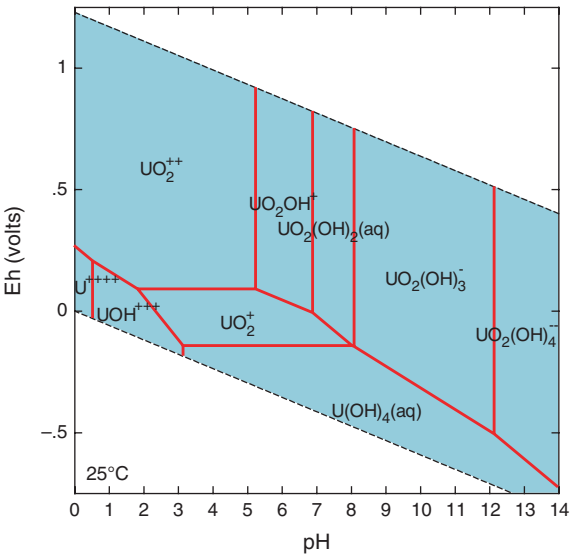

Fig. 6.6 Eh–pH diagram of uranium in the absence of cement components, calculated with *The Geochemist's Workbench®*

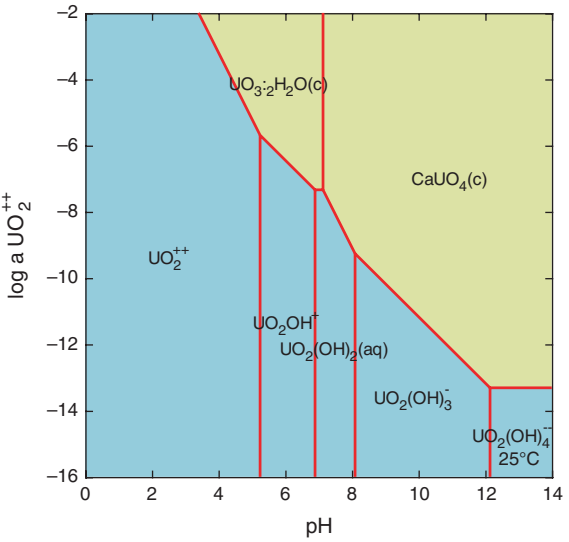

Fig. 6.7 Solubility diagrams of uranium in the presence of Ca and Si in a cementitious system. Stable phases $CaUO_4$ (*top*) and $CaU_6O_{19}{:}11H_2O$ (*bottom*). Log *a* [Ca] = −3.155. Calculations with *The Geochemist's Workbench®*, based on NEA thermodynamic database (Guillaumont et al. 2003)

The speciation and solubility diagrams are presented in Figs. 6.6 and 6.7. Uranium (VI) speciation in an oxidising cementitious environment is dominated by the hydrolysis species $UO_2(OH)_3^-$ and $UO_2(OH)_4^{2-}$ (Fig. 6.8). Solubility calculations using the NEA database (Guillaumont et al. 2003) indicate that calcium urinate $CaUO_4$(c) is the only stable U(VI) phase controlling the U solubility in a cement pore water containing calcium and sodium. The predicted solubility

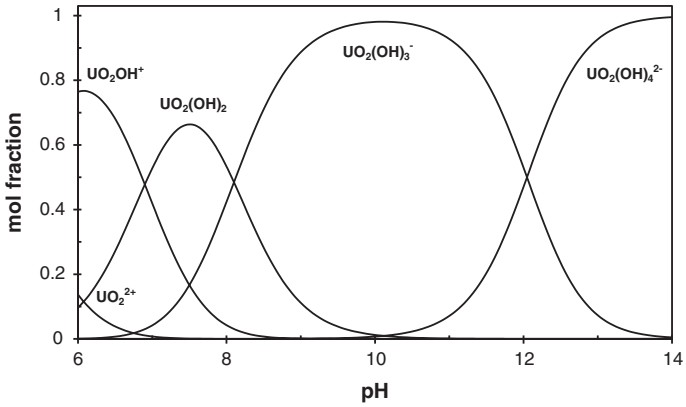

Fig. 6.8 Dissolved uranium speciation under oxidising conditions, $P_{O_2} = 0.2$ atm (total dissolved U $= 1 \times 10^{-8}$ molal, no precipitation of solids)

of U(VI) controlled by this well crystalline phase is extremely low at around 10^{-14} mol/L at pH > 12 (Fig. 6.6). Note that the [Ca] used in our calculation is 0.7 mM, which is relevant for State I. At a higher [Ca], e.g., 15 mM for the State II, the solubility of $CaUO_4$(c) is even lower. The predicted low U(VI) solubility is a consequence of the NEA uranium database in which the high stability of $CaUO_4$(c) dominates over other phases. Hummel et al. (2002) (PSI database) suggest that the data selected by the NEA are based on calorimetric experiments at high temperature and may not be relevant for a low-temperature aqueous system. Moroni and Glasser (1995) found that the U(VI) phase designated as $CaUO_4$ has a lower stability than the data selected by Guillaumont et al. (2003) and measured a U(VI) solubility of 10^{-8} to 10^{-7} mol/L at pH 9–13.5. However, their study was carried out at 85 °C and the derived thermochemical data were not selected for inclusion in Guillaumont et al. (2003). $CaUO_4$(c) is therefore accepted as the solubility-limiting solid. Another candidate solid, likely to be encountered in State I, is $Na_2U_2O_7$ (hydrate). At a sodium concentration of about 14 mM relevant for State I, U(VI) solubility is around 10^{-7} mol/L.

For the solubility of U at State II, a recent study (Altmaier et al. 2005) illustrated the stability of $CaU_2O_7{\cdot}3H_2O$ (cr) at pH 9–12 and the solubility constant of the solid was determined to be $\log K = 11.7$ at 25 °C for the following reaction:

$$0.5CaU_2O_7{\cdot}3H_2O(cr) + 3H^+ \Leftrightarrow 0.5Ca^{2+} + UO_2{}^{2+} + 3H_2O \qquad (6.2)$$

Using the above reaction and the associated solubility constant in combination with the uranium data reviewed by the NEA (Guillaumont et al. 2003), the solubility of U(VI) controlled by $CaU_2O_7{\cdot}3H_2O$(cr) at State II is calculated to be 10^{-5} mol/L.

Under a sufficiently reducing condition for U(IV) to prevail, the uranium speciation will be dominated by the aqueous species $U(OH)_4$(aq) and the solubility

will be controlled by the UO_2 solid as suggested by Berner (2002). It is generally believed that U(IV) solubility is lower than U(VI) and a concentration limit controlled by UO_2 solid is expected to be below 10^{-8} M at the cementitious pH range.

The majority of the U(VI) solubility measurements reviewed show a pH dependency and are fairly consistent in terms of solubility values which are in the range of 10^{-7} to 10^{-5} M. As concerns the sorption data to be reviewed in the next section, data qualifies as "sorption" if initial U concentrations are below the indicated solubility range.

6.2.2 Sorption Values from the Literature for the Benchmark Cement

Reviewed R_d values for uranium sorption on cementitious materials are presented in Fig. 6.10. These R_d values were measured under experimental conditions summarised in Table A.9 (see Annex). All data sets are for U(VI) except the work of Bayliss et al. (1996), in which one data set was intended for measuring U(IV) sorption. These R_d values were all measured in batch experiments that were carried out in the UK (Bayliss et al. 1996; Baker et al. 2002; Berry et al. 2000), France (Andra 2005; Harfouche et al. 2006), and Switzerland (Tits et al. 2008), with all the three groups of data being self-consistent (Fig. 6.10).

Sorption values reported by Baker et al. (2002) onto leached NRVB, hydrothermally treated leached NRVB and a 1:1 C/S CSH gel were in the range of 2000–10,000 L/kg. The main observation was that R_d values are similar between the degraded and freshly prepared NRVB samples suggesting that sorption of U(VI) is relatively unaffected by degradation of NRVB (loss of portlandite).

Bayliss et al. (1996) measured R_d for U(VI) at State II pH around 12.5 on NRVB samples under non-saline and hypersaline conditions at two different temperatures (room temperature and 77 °C). R_d values about 6000 L/kg were obtained and these were not affected to a large extent by either the change of salinity or temperature. The same study also tried to measure sorption of U(IV) on NRVB and a similar R_d value to the one for U(VI) was observed. The initial uranium solution was prepared by adding sodium dithionite as the reducer to the acidic uranium solution in a N_2 glove box. No reducing agent was used in the sorption experiment however. The authors therefore concluded that the oxidation state of U(IV) may not have been maintained and U(IV) might have been oxidised to U(VI) during the sorption experiments.

Sorption of U(VI) on OPC/PFA grout (pulverised fuel ash) was studied in grout leaching solutions (Sutton et al. 2003). Kinetic experiments showed that sorption occurred in two steps, fast and slow, and it was thought to be related to the increasing accessibility of sorbing sites on grout surfaces as function of time. At a pH of about 12, a R_d value was determined to be in a narrow range of 1500 and 3600 L/kg. A zeta potential measurement indicated that grout surfaces are negatively charged at

pH above 2. Sorption of negatively charged uranyl hydrolysing species $UO_2(OH)_3^-$ and $UO_2(OH)_4^{2-}$ on negatively charged grout surfaces was explained as due to inner-sphere surface complexation.

U(VI) sorption on calcite was measured by Berry et al. (2000) and a R_d value about 50 L/kg was obtained. Sorption of U(VI) on calcite was found to be insensitive to pH in the range of 8–12, and this seems reasonable considering that U(VI) speciation is not varying in that pH range and the only important species present is $UO_2(OH)_3^-$ (see Fig. 6.8).

According to the data of Pointeau et al. (2004a), uranium (VI) uptake for degraded (portlandite free) CEM I and CEM V cements [C/S at 1.3 (pH 12.2), 1.0 (pH 11.5), and 0.7 (pH 9.9)] and CSH [C/S at 1.3 (pH 12.1) and 0.7 (pH 10)] is controlled by adsorption supported by the observed linear and reversible uptake isotherms. Uptake values are indicated as R_d not K_d because of the short contact time (3–21 days) between solids and cement pore fluids; that is, the equilibrating time is too short to assume a thermodynamic equilibrium (Fig. 6.9). The sorption linearity was present for U(VI) concentrations from 10^{-13} to 10^{-7} M. Because of the similarity of the sorption behaviour between the degraded cement and CSH phases, the latter is considered as being the sorption sink for uranium in cement. Also, uranium sorption slightly increases from 3×10^4 to 1.5×10^5 L/kg when cement degrades from pH 12.2 to pH 10. Surface complexation on silanol sites (>SiOH) with variable charge, depending on C/S ratio, were indicated as possible mechanisms for uptake. The observed increase in R_d with decreasing pH was explained due to the competition effect of calcium for the sorbing sites. Calcium

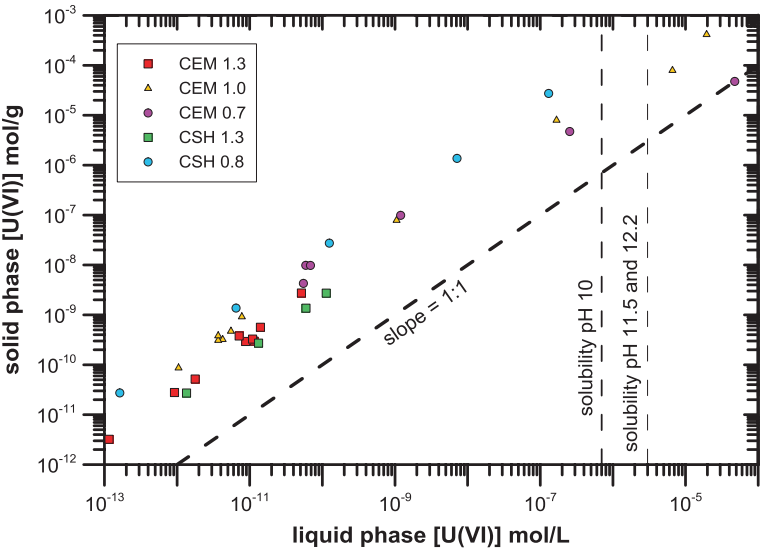

Fig. 6.9 Sorption isotherms on degraded (i.e. portlandite free) CEM I and CEM V cement pastes (replotted from Pointeau et al. 2004a)

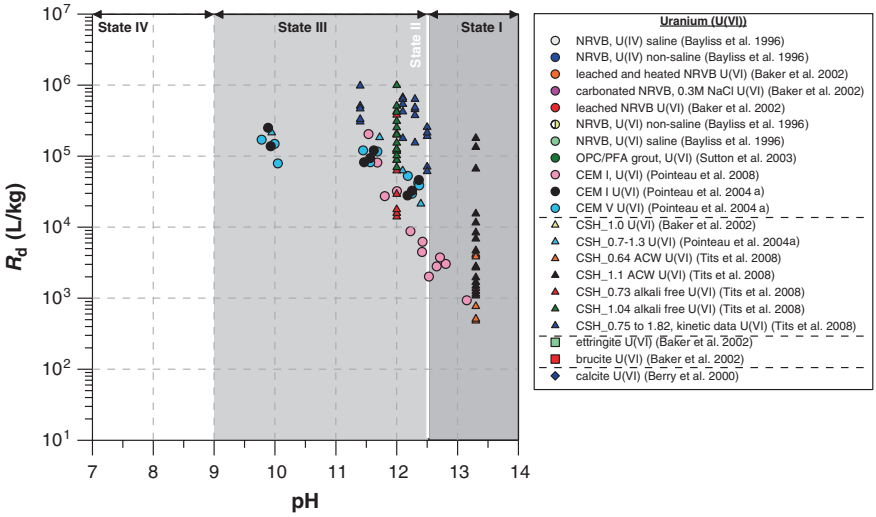

Fig. 6.10 Reviewed R_d values for uranium (VI) as a function of pH. Two data points for U(IV) are also included. *OPC/PFA* ordinary Portland cement/pulverised fuel ash; *NRVB* Nirex reference vault backfill; *CSH* calcium silicate hydrate. Data series for Tits et al. are for different U(VI) concentrations. Error bars for Berry et al. data based on experiments done in triplicate. Tits et al. data (CSH/ACW; CSH/alkali free) shows range of values as function of initial U(VI) concentration. *ACW* artificial cement water

concentration is at the highest at pH 12.5 (State II), so the sorbing sites are occupied largely by calcium following the surface reaction:

$$\mathrm{SiOH} + \mathrm{Ca}^{2+} \Leftrightarrow \mathrm{SiOCa}^{+} + \mathrm{H}^{+} \tag{6.3}$$

Therefore, based on this concept, the sorption of U is at the lowest at State II. When pH decreases as cement degrades, calcium concentration in solution decreases leading to higher density of sorbing sites for U and thus higher R_d values. U(VI) uptake did not seem to be affected by cement types, which is supported by the fact that R_d values are similar on CEM I and V. The latter is a slag type of cement (slag content from 18 to 50 wt%) with reducing capacity. These results may suggest that U(VI) may not have been reduced to a significant extent.

In a more recent study, Pointeau et al. (2008) measured R_d for U(VI) on CEM I paste in the pH range of 11.5–13.3 and observed similar R_d values as in the earlier work (Pointeau et al. 2004a). At pH 13.3, R_d for U(VI) was about a few thousands L/kg and increased to 200,000 L/kg after portlandite was depleted and the solution composition was controlled by CSH phases. During the first stage of degradation (States I and II), the R_d values are nearly constant (1000–4000 L/kg), and it is only when the CSH phases control the solubility of Ca in the second part of the degradation (State III) that the R_d values increase significantly. The trend suggests at least a one order of magnitude increase in R_d when degradation progresses from State I/II to State III. The observed increase in R_d with degradation of cement towards lower

pH and lower Ca concentration range seems to be consistent with the theory that Ca is competing with sorbing sites on cement for uranium. The authors explained that a formation of inner-sphere surface complexes is likely to be the dominating sorption mechanism. A formation of uranium solid solutions with Ca and Si is also possible following an initial step of sorption by surface complexation.

The R_d data by Tits et al. (2008) for U(VI) on synthetic CSH phases are in a range of 10^3 to 10^6 L/kg. U(VI) sorption has a general tendency to increase with decreasing pH (roughly one order of magnitude from States I to III) and this is in agreement with the studies of Pointeau et al. (2004a, 2008), although different solid materials were used (CSH by Tits et al. 2008 vs. HCP by Pointeau et al. 2004a, 2008). Also, sorption of U(VI) is enhanced if aqueous Ca concentration increases and that was explained as being due to a formation of solid solution involving U and Ca. These authors further found that uptake of uranium onto CSH is nonlinear suggesting solid-solution formation. Higher uranium concentrations resulted in a solubility controlled behaviour, i.e., uranium was removed from the aqueous phase by forming either precipitates or solid solutions involving U and Ca. In a separate study with a similar CSH system, wet chemistry data pointed to formation of a calcium urinate solid (Harfouche et al. 2006). Tits et al. (2008) interpreted the latter data assuming that a $CaUO_4$ phase is regulating the dissolved uranium concentration. The solubility of $CaUO_4$ was found to be in agreement with the results reported by Moroni and Glasser (1995). As discussed above, the solubility of $CaUO_4$ determined by Moroni and Glasser (1995) is several orders of magnitudes higher than the solubility value selected by the NEA data review. This may suggest that a metastable $CaUO_4$ phase might be present in the systems investigated by Moroni and Glasser (1995) and Tits et al. (2008).

6.2.3 Sorption Mechanisms and Selected Sorption Values

6.2.3.1 Sorption Mechanisms

One of the most important parameters influencing U(VI) sorption was shown to be calcium concentration. Some studies found that Ca was in competition with U for sorption sites on cement so R_d in general decreases with increasing Ca concentration in the pore fluid. Other studies observed that uptake increases with increasing Ca concentration because of formation of solid solutions of U–Ca endmembers. The measured R_d data are, however, too scattered to confirm or reject the trends that have been proposed. Also, in the above mentioned studies, the variation of Ca concentration in solution is related to pH change. So it is difficult to assess independently the influence of the two system variables Ca and pH on R_d. The effect of oxidation state on uranium sorption could not be investigated because nearly all available experimental data refer to U(VI). The only exception is the study of Bayliss et al. (1996), in which both U(IV) and U(VI) sorptions were measured in otherwise identical conditions. No major difference in R_d was reported.

Since it cannot be ruled out that U(IV) may exist at least in the initial period in the lifetime of a near-surface repository when anoxic conditions may exist (see the discussion related to plutonium, Sect. 6.3.2), sorption values for reduced species also need to be assessed. Because most measurements have been made under oxidising (aerobic) conditions, one has to rely on measured sorption data available from other elements (chemical analogy). The best analogue for U(IV) would be Th(IV). Comparison between Th(IV) best estimates (Sect. 6.1.3) and those for U(VI) (see Sect. 6.2.3) reveals that thorium exhibits the same sorption as U(VI) for States II and III, except for State I [30,000 L/kg for Th vs. 1000 L/kg for U(VI)] and State IV [30,000 L/kg for Th vs. 5 L/kg for U(VI)]. This is consistent with the observation of Bayliss et al. (1996).

To date, the following uptake mechanisms are reported: (1) linear sorption up to ~10^{-7} mol/L onto HCP and CSH (Evans 2008; Pointeau et al. 2004a, b, c), possibly followed by the formation of a calcium uranate precipitate at higher concentrations (Evans 2008), (2) linear sorption onto CSH in the concentration range 10^{-6} to 10^{-4} mol/L without formation of pure U(VI) precipitates (Harfouche et al. 2006), and (3) nonlinear sorption onto CSH phases with increasing calcium concentrations resulting in increasing U(VI) uptake (Tits et al. 2008).

Further information on uranium sorption mechanisms was obtained from spectroscopic studies. Harfouche et al. (2006) performed an EXAFS study in order to reveal uptake mechanisms of U(VI) by synthetic CSH phases (C/S ratios 0.65–1.1). CSH samples for EXAFS were prepared in solutions containing initial U(VI) concentration of 0.25 and 2.5 mM. These U(VI) concentrations are higher than the anticipated solubility of uranium in a cement pore water (see Sect. 6.2.1). Linear sorption was observed for all CSH phases, with a sorption-type process in which uranyl polyhedra are considered to act as bridging units between neighbouring Si chains of the CSH structure. EXAFS data further suggest that U(VI) uptake in co-precipitation samples occurs in a chemical environment similar to uranophane ($Ca(UO_2)_2(SiO_3OH)_2{\cdot}5H_2O$), i.e., U(VI) may possibly form solid solutions with calcium and silica.

Recent uptake tests by Tits et al. (2008) onto CSH reveal sorption isotherms to be nonlinear, which was explained as a solid-solution formation mechanism ("precipitation-type") where Ca and U(VI) are simultaneously bound to the sorbent. It was further shown that higher R_d values were obtained with increasing Ca concentration in solution (R_d increased with increasing C/S ratio of CSH phases).

Uranium (VI) removal from cementitious pore waters is probably solubility controlled if total dissolved uranium is higher than 10^{-6} to 10^{-5} M. Under these conditions, uranium tends to form solid phases: $CaUO_4$ has been proposed as a potential solubility controlling phase (Tits et al. 2008). Others have proposed CaU_2O_7[1] to be the solid phase (Valsami-Jones and Vala Ragnarsdottir 1997). The evolution of the solubility is expected to be influenced by the change in Ca concentration, but the exact mechanism is not clear. Since the solid contains calcium, it is likely that the solubility of uranium is at the lowest level when Ca concentration is highest.

[1]Very poorly crystallised hydrous calcium uranate.

At a lower U(VI) concentration, i.e. below 10^{-6} to 10^{-5} M, different sorption behaviour has been reported. Pointeau et al. (2004a, 2008) illustrated a linear and reversible sorption of U(VI) on cement pastes and proposed that sorption is likely controlled by inner-sphere surface complexation. Tits et al. (2008), however, found that U(VI) sorption on some synthetic CSH phases is highly nonlinear suggesting a mechanism of solid-solution formation of U(VI) with Ca.

As a near-surface disposal system is expected to evolve from a mixed oxic/anoxic condition to a mainly oxic condition, the emphasis is on deriving sorption values for uranium (VI). It was firstly observed from Fig. 6.8 that the speciation of uranium (VI) changes somewhat over the pH range considered. As can be seen from Fig. 6.10, there appears to be a general trend of an increase in R_d from State I to States II and III and then a decrease in State IV. The experts agreed that mechanistic interpretations differ for apparently the same experimental conditions (increase in uptake due to co-precipitation with Ca or increase due to decreased competition with Ca at lower pH), but the available data do not allow to clearly distinguish which explanation is correct. Due to the number and quality of available experimental data, this uncertainty regarding mechanism does not impact significantly on data selection.

For U(IV) sorption values, analogy with Th(IV) was invoked for all states; their speciation is simple and similar, with only one relevant dissolved species for the whole pH range of interest ($U(OH)_4$ and $Th(OH)_4$, respectively). Application of such values for U(IV) should be done with great care until more reliable data becomes available.

6.2.3.2 Sorption at State I

The data indicate that sorption would be weaker in State I than in States II and III. For both States II and III, a value of 3.0×10^4 L/kg is proposed as the best estimate and anchor point (see below). Roughly a decrease of one order of magnitude into State I results in a best estimate for U(VI) of 2.0×10^3 L/kg for State I, based on the summary graph. The upper bound is proposed as 1.0×10^4 L/kg and the lower bound as 4.0×10^2 L/kg. On the basis of the chemical analogy between Th(IV) and U(IV), the best estimate (30,000 L/kg) from Th(IV) is also assigned to U(IV). No upper and lower limits are presently defined for U(IV).

6.2.3.3 Sorption at State II

The largest amount of relevant U(VI) data exists for State II, and they indicate that sorption in State II may be slightly lower than in State III. In State II, the R_d values seem to lie between a few thousand up to a few hundred thousand L/kg, reflecting different experimental conditions. After reviewing the data the experts agreed on a best estimate for U(VI) of 3.0×10^4 L/kg, with an upper limit of 3.0×10^5 L/kg, and a lower limit of 3.0×10^3 L/kg, although no good explanation in terms of

sorption mechanisms is available. On the basis of the chemical analogy between Th(IV) and U(IV), the best estimate (30,000 L/kg) from Th(IV) is used also for U(IV). No upper and lower limits are presently defined for U(IV).

6.2.3.4 Sorption at State III

It can be noted from the data that sorption appears to be quite constant across State III at varying pH values. While this somewhat contradicts the trend in R_d observed in individual studies (Pointeau et al. and Tits et al.), this observation is based on several data sources and is considered robust. Calcite data and brucite data are not considered for this state as they are not believed to be relevant. Because there is no good explanation of the behaviour in State III compared to State II, it was agreed based on Fig. 6.10 that values would be very similar to State II with the best estimate for U(VI) for State III being 3.0×10^4 L/kg, with an upper limit again of 3.0×10^5 L/kg but with an increased lower limit of 1.0×10^4 L/kg. On the basis of the chemical analogy between Th(IV) and U(IV), the best estimate (30,000 L/kg) from Th(IV) is used also for U(IV). No upper and lower limits are presently defined for U(IV).

6.2.3.5 Sorption at State IV

There are a number of calcite measurements from Berry et al. (2000) with an R_d of approximately 50–80 L/kg spreading over a substantial pH range. The experts had expected weaker sorption than for CSH and the experimental data were consistent with this. It was agreed that the best estimate for U(VI) for State IV would be 50 L/kg. This represents a substantial decrease in R_d in comparison with States I–III, but is in line with the expected complexation of uranium under the relevant conditions and the loss of CSH as the dominant sorbing phase. The upper bound was agreed to be 500 L/kg and the lower bound 5 L/kg. It is noted that there is a large degree of uncertainty regarding the effect of calcium and carbonate in solution on uranium (VI) chemistry in State IV and that the surface properties of calcite are also uncertain. On the basis of the chemical analogy between Th(IV) and U(IV), the best estimate (30,000 L/kg) from Th(IV) is assigned to U(IV). No upper and lower limits are presently defined for U(IV) (Table 6.3).

Table 6.3 Selected best estimate, upper and lower limit R_d values for U(IV) and U(VI)

pH state	Best estimate (L/kg)		Upper limit (L/kg)		Lower limit (L/kg)	
	U(VI)	U(IV)	U(VI)	U(IV)	U(VI)	U(IV)
State I	2×10^3	3×10^4	1×10^4	i.d.	4×10^2	i.d.
State II	3×10^4	3×10^4	3×10^5	i.d.	3×10^3	i.d.
State III	3×10^4	3×10^4	3×10^5	i.d.	1×10^4	i.d.
State IV	5×10^1	3×10^4	5×10^2	i.d.	5×10^0	i.d.

i.d. insufficient data

6.3 Plutonium

6.3.1 Chemical Form, Speciation, and Solubility

LILW typically contains ^{238}Pu (half-life 87.7 year), ^{239}Pu (half-life 24,100 year), ^{240}Pu (half-life 6560 year), and ^{241}Pu (half-life 14.3 year) (NDA 2011; NIRAS 2008). Except for trace quantities of plutonium in pitchblende, and small amounts produced in natural reactors (e.g. the Oklo natural rector in Gabon), none of these plutonium isotopes is a naturally occurring radionuclide. ^{241}Pu is produced within nuclear reactors via the neutron absorption in ^{240}Pu (^{240}Pu + neutron → ^{241}Pu + gamma rays) or through multiple absorptions and decays of other isotopes (^{239}Pu or ^{238}U). The majority of the plutonium that is produced in nuclear reactors is contained within the spent fuel elements. Generally, plutonium waste (^{241}Pu together with other isotopes of plutonium) ends up as transuranic or high-level waste; however, small amounts of plutonium can exist in LILW, mostly in reactor operational waste such as decontamination resins and cartridge filters. At fuel fabrication facilities, liquid LILW is generated from washing, etching, and solvent extraction operations. Some plutonium waste sources also appear from decommissioning activities (USDOE 1996a, b).

The Eh–pH (Fig. 6.11) and solubility diagrams (Fig. 6.12) for plutonium are produced with the thermodynamic data given in Table 6.4. It is important to keep in mind that this is a simplified representation for the likely plutonium geochemistry. How different aqueous plutonium species vary with pH is shown in Fig. 6.13.

Plutonium is a redox-sensitive element and its speciation in alkaline environments is dominated by oxidation states +IV and +VI as shown in Fig. 6.11. Pu(IV) dominates in a large Eh range and the dominant speciation under a cementitious condition is $Pu(OH)_4(aq)$. Berner (2002) concluded that Pu(IV) will be dominant at Eh below 350 mV based on the PSI-NAGRA thermodynamic database (Hummel et al. 2002). With the data given in Table 6.4, one may calculate the Eh at which the line separating $Pu(OH)_4(aq)$ and $PuO_2(OH)_2(aq)$ occurs, using the following relationship:

$$37.98 = -\log\{PuO_2(OH)_2(aq)\} + \log\{Pu(OH)_4(aq)\} + 2\,pH + 33.8\,Eh \quad (6.4)$$

If the activity ratio of the two Pu species becomes unity, the above relationship reduces to the following:

$$37.98 = 2\,pH + 33.8\,Eh \quad (6.5)$$

At pH 12.5, this condition occurs at Eh +380 mV. This means that Pu(VI) will start to dominate aqueous speciation of Pu at redox potentials higher than +380 mV. Theoretically, redox potential in an air-saturated ($fO_2 = 0.2$) cement water at pH 12.5 may reach +480 mV as calculated by the following:

$$83.1 = -\log f\left[O_2(g)\right] + 67.61\,Eh + 4\,pH \quad (6.6)$$

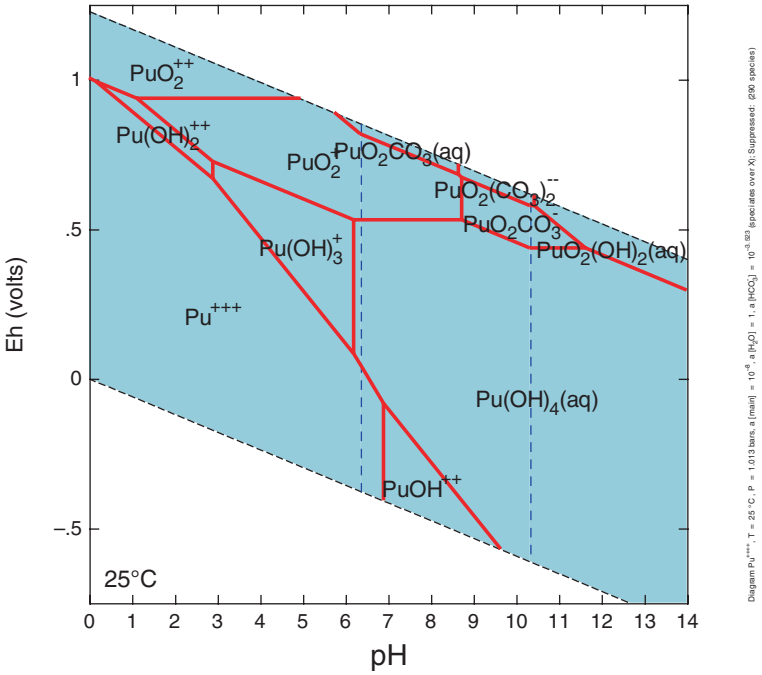

Fig. 6.11 Eh–pH diagram of plutonium calculated with *The Geochemist's Workbench*®. Plutonium activity is fixed at 10^{-8}, activity of $HCO_3^- = 10^{-3.523}$

Therefore, Pu may theoretically appear as Pu(VI), i.e. $PuO_2(OH)_2(aq)$ in an oxidising cement system. Formation of Pu carbonate complexes is not relevant because of the low dissolved carbonate concentration present in cement pore water.

According to solubility calculations (Fig. 6.12) using *The Geochemist's Workbench*® (Bethke 2006), the solubility of Pu(IV) controlled by amorphous $PuO_2(am)$ is very low: 1.5×10^{-10} M. Pu(VI) solubility is regulated by dissolution of crystalline $PuO_2(OH)_2{:}H_2O(c)$ at 2×10^{-8} M. At pH around 11 to 12, solubility of Pu may be controlled by oxidising dissolution of an amorphous Pu(IV) phase [i.e. $PuO_2(am)$] to the Pu(VI) hydrolysis species $PuO_2(OH)_2(aq)$. Hence, the solubility is redox dependent:

$$\log\{PuO_2(OH)_2(aq)\} = 2\,pH + 33.8\,Eh - 48.8 \tag{6.7}$$

Part of the bottom diagram in Fig. 6.12 is calculated by means of the above relationship at Eh = 500 mV. In conclusion, using the recent NEA thermodynamic database (Guillaumont et al. 2003), the calculated solubility of Pu in a cement system is in the range of 10^{-10} to 10^{-8} M.

Most abundant aqueous plutonium (VI) species at high pH and oxidising conditions relevant to cement systems is $PuO_2(OH)_2(aq)$ as predicted by the speciation diagram produced with the recent NEA thermodynamic data (Guillaumont et al.

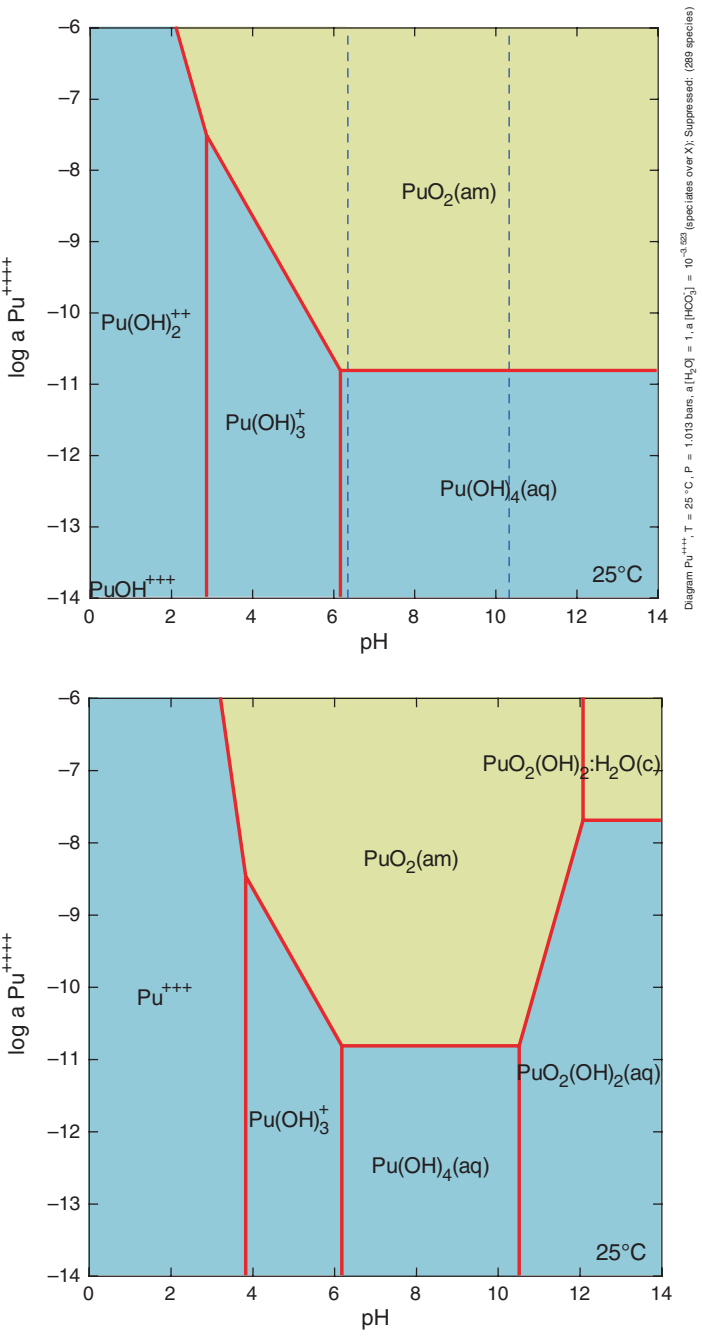

Fig. 6.12 Solubility of PuO_2 under reducing (*top*) and oxidising (*bottom*) condition. For oxidising conditions, Eh = +500 mV. Vertical axis displays total Pu concentration (Pu^{4+} is master species)

Table 6.4 Thermodynamic data of plutonium

Reaction	log$K$ (25 °C)
$Pu(OH)_4(aq) + 0.5O_2(aq) = PuO_2(OH)_2(aq) + H_2O$	5.0241
$Pu(OH)_4(aq) + H^+ = Pu(OH)_3^+ + H_2O$	6.2001
$PuO_2(am) + 2H_2O = Pu(OH)_4(aq)$	−10.8237
$PuO_2(am) + H_2O + 0.5O_2(aq) = PuO_2(OH)_2(aq)$	−5.7996
$PuO_2(OH)_2{:}H_2O(c) = PuO_2(OH)_2(aq) + H_2O$	−7.6998
$PuO_2(am) + H^+ + 0.25O_2(aq) + CO_3^{2-} = PuO_2CO_3^- + 0.5H_2O$	6.8410

Source NEA Database (Guillaumont et al. 2003)

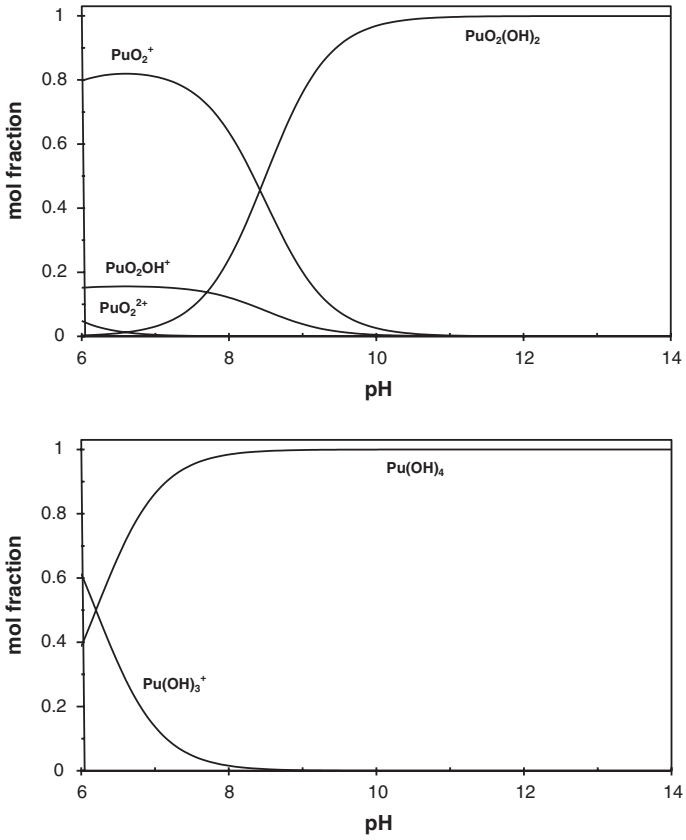

Fig. 6.13 Dissolved plutonium speciation (total dissolved Pu $= 1 \times 10^{-8}$ molal, no precipitation of solids). *Top* oxidising condition—$P_{O_2} = 0.2$ atm. *Bottom* reducing condition. (Pu^{4+} is master species)

2003) (Fig. 6.12, bottom). For reducing conditions, the dominant Pu(IV) species is $Pu(OH)_4(aq)$ (Fig. 6.12, top). Carbonate species were found unimportant under both oxidising and reducing conditions and of the carbonate activities obtained in intimate contact with fresh cement, as dominate Stages I and II and extend into Stage III.

6.3.2 *Sorption Values from the Literature for the Benchmark Cement*

Figure 6.14 and Table A.10 (see Annex) show the reviewed R_d values for Pu and the experimental conditions. The main sorption sink for Pu in concrete seems to be cement phases rather than aggregates illustrated by α-radiographs of four types of concrete after sorption experiments (Jakubick et al. 1987).

Aggarwal et al. (2000) studied sorption of ^{238}Pu on different OPC blends, CSH, C_3S, and minor phases (hydrotalcite, C_3A). Domination of tetravalent plutonium species was considered to be likely in the pH range 9–13. Sorption was high in all cases ($R_d > 10^4$ L/kg). Pu starting concentration was 2×10^{-10} M, which is slightly above the solubility of Pu(IV). This was reportedly done for analytical reasons, given the very high sorption. Blank experiments revealed that precipitation was negligible despite the high initial concentrations. There was a tendency towards higher sorption in the blends containing the larger amount of OPC,

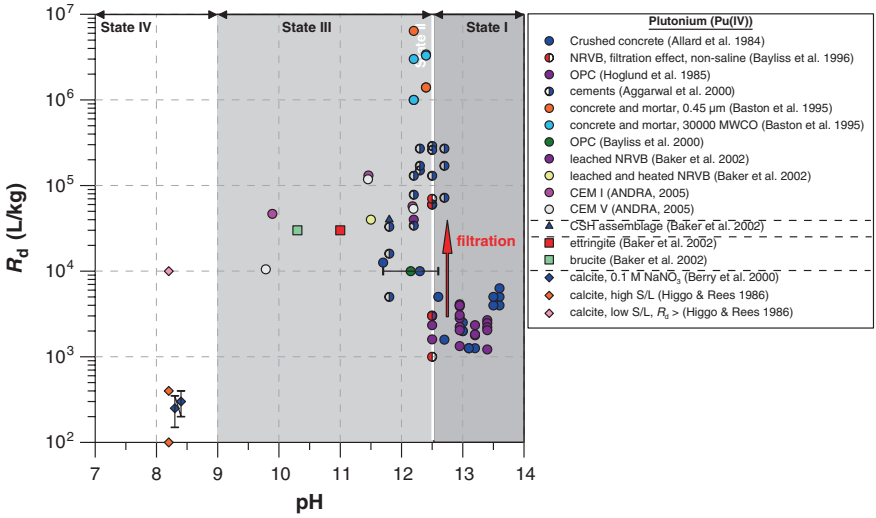

Fig. 6.14 Distribution ratio (R_d) of plutonium (IV) in cementitious systems. *NRVB* Nirex reference vault backfill; *HCP* hardened cement paste; *OPC* ordinary Portland cement; *CSH* calcium silica hydrates. Large variation in Bayliss et al. (1996) data due to filtration effect. Horizontal error bar for Bayliss et al. (2000) data due to pH variation (11.7–12.6)

suggesting that sorption took place mainly on hydration products. There was no clear dependency of R_d on C/S ratio although there were some indications of a downward trend in R_d with decreasing C/S ratio for the C_3S hydrates. Apart from C/S ratio, crystallinity of the CSH phases was also different among the CSH phases used in the experiments, however. That might be the reason why the effect of C/S ratio could not be seen. Comparison of the sorption on cements and on the CSH suggests that the sorption properties of cement for Pu are mainly due to sorption on CSH.

Hoglund et al. (1985) and Allard et al. (1984) reported R_d for Pu on concretes and standard Portland cements. Sorption tests were carried out in a glove box under a CO_2-free N_2 atmosphere. The redox potential in the concrete pore waters was measured to be in the range of −380 to +140 mV (five out of seven waters had positive redox values). According to Fig. 6.11, Pu is expected to exist mainly as tetravalent Pu(IV) under these redox conditions. Initial ^{239}Pu concentration was 1.2×10^{-9} M, which is relatively high compared to the previously determined solubility. These authors found that cement/concrete composition had little influence on R_d values. Equilibration time did not affect the R_d values within several months.

There was no Pu oxidation state determination performed in the sorption experiments. Bayliss et al. (1996, 2000) studied sorption of Pu on cement of different compositions and NRVB materials. No reductants were added to keep reducing conditions. There was no mention of the oxidation state for Pu. In analogy with all the other studies reviewed here, it was assumed that it was Pu(IV). No significant difference in R_d was observed on 3:1 PFA/OPC and 3:1 BFS/OPC. R_d on crushed cement samples were an order of magnitude higher than on cement coupons. This was seen as due to the slow penetration of Pu into coupons. According to the authors, when the volume of cement available for sorption over the experimental timescale (a few months) was taken into account, the R_d on the coupons did not differ significantly from those on the crushed cement systems. R_d increased with increasing amount of Pu in the system. R_d increased also with the intensity of the phase separation techniques applied, i.e., from allowing the solids to settle down under gravity, centrifugation, to filtration. The difference in R_d after centrifugation and filtration was minor. There was no significant effect of *S*/*L* ratio on R_d evidenced by experiments using only two *S*/*L* ratios (1/40 and 1/400). A typical R_d value for Pu on OPC cements was 10^4 L/kg. The effect of filtration on R_d for Pu was also investigated by sorption experiments on NRVB. The R_d value increased from 1000 to 7×10^4 L/kg as the pore size of the filter was decreased from 5 μm to 30,000 MWCO.

Data concerning R_d for State IV (i.e. on calcite) are limited. Berry et al. (2000) determined R_d for Pu on calcite in 0.1 N $NaNO_3$ solutions in pH 8–12.4 (only R_d at pH ~ 8 is shown in Fig. 6.14). Experimental conditions were fairly oxic (Eh +150 mV), and plutonium was believed to be present as Pu(IV). An R_d value around 300 L/kg was obtained and appeared to be independent of pH and the phase separation techniques used. This R_d value is about three orders of magnitude lower than the R_d (>10^5 L/kg) determined by Tits et al. (2002) for Th on calcite in an artificial cement water at pH 13.3. Although water compositions and pH values

are different between the two studies, a relevant question to be asked is: what are the uptake mechanisms giving rise to the range of R_d values for Pu, compared with those for Th? Precipitation can be ruled out since both studies used very low initial Pu/Th concentrations (7×10^{-11} mol/L for Berry et al. and 10^{-11} mol/L for Tits et al. 2002). Furthermore, Tits et al. (2002) observed linear sorption of Th on calcite. Difference in specific surface areas of calcite materials used in these two studies seemed not to be the cause of the difference in R_d because the higher R_d of Tits et al. (2002) was measured on calcite of lower surface area (0.3 m^2/g) as compared to 1.5 m^2/g which was associated with a much lower R_d (Berry et al. 2000).

Additional data sets are available from the literature review by Stout and Carroll (1993) and results from a coordinated research programme organised by the IAEA (1986). From these reviews, one particularly well conducted and characteristic study on actinide sorption on marine sediments is presented, including carbonates (Higgo and Rees 1986; Higgo et al. 1986). Higgo and Rees studied plutonium sorption from sea water at pH 8.2 by natural carbonate sediments (calcite ranged from 45 to 80 %). Initial plutonium concentration of 2.3×10^{-10} mol/L was reacted with a wide range of *S*/*L* ratios (0.002–0.2 kg/L). At *S*/*L* ratios larger than 0.04 kg/L, R_d values ranged from 100 to 400 L/kg (Pu in oxidised state). Lower *S*/*L* ratios (0.003 kg/L) yielded R_d values larger than 10,000 L/kg (Pu in reduced state). The lower R_d values obtained at high *S*/*L* ratios were explained by the formation of Pu–carbonate complexes that sorb less effectively. The latter were termed "low-R_d" species which could be in the form of complexes with organic matter or anions such as carbonates or it could be microparticulates which remained with the liquid phase during phase separation.

Differences in R_d between Pu and Th may be explained by the aqueous speciation of the two actinides. Wieland and Van Loon (2002) suggested to assign the R_d value of Th (~10^5 L/kg) to tetravalent actinides including Pu(IV) for the States I and II of cement degradation based on chemical analogy. Considering that the speciation of Pu(IV) does not change with pH across States I to III (Fig. 6.13), a similar R_d should also be applicable for State III if sorption mechanisms remain the same within States I to III. There is little information about sorption processes in general for plutonium, and there is even less information about the sorption mechanisms relevant for degradation states. One of the few relevant studies is that of Baston et al. (1995), in which sorption on cement was successfully described by means of surface complexation modelling. The final pH measured was 12.4 and 12.2 for concrete and mortar, respectively. The higher pH of 12.4 is characteristic for State II (confirmed by the solution composition), while the lower pH of 12.2 is more typical for State III (mortar-equilibrated solution composition showed markedly higher Al, Si, and S (SO_4^{2-}) concentrations and lower Ca concentrations compared to the concrete-equilibrated water). Because the surface complexation modelling was found appropriate for both geochemical conditions, this tends to support the hypothesis that sorption mechanisms are similar for States II and III. Because for State I the major ions except Na and K (Al, Si, Ca, S) are within the range of values observed for States II and III (see Fig. 2.2), the

surface complexation model should also be valid also for State I. Therefore, sorption mechanisms are likely similar for State I through State III.

In most aqueous systems, plutonium may exist in oxidation states IV, V, and VI while Th only in the oxidation state IV. It cannot be completely excluded that the aqueous speciation of Pu in the experiments reported by Berry et al. (2000) might have been Pu(V) or Pu(VI) rather than the presumed Pu(IV). If this is the case, one may ask if the majority of R_d values measured for Pu(IV) are still relevant if applied to an oxic near-surface disposal facility. In terms of Pu speciation, relevant issues include the following:

- What is the initial speciation of Pu in the waste?
- If Pu is present initially in oxidation state (IV), what are the kinetics to oxidise Pu(IV) to (VI) under the disposal conditions?
- If Pu is present initially in oxidation state (VI), do we have appropriate R_d data to perform a safety assessment?

Sorption of Pu(V) and Pu(VI) may also be of concern since oxidising redox conditions are likely to exist in a near-surface disposal facility in the long term, even if it is only locally, for example, in areas with higher permeability allowing oxygen-rich water to access the engineered barriers. To account for oxidising conditions in disposal environments, Wieland and Van Loon (2002) proposed to use the R_d (100 L/kg) of Sr(II) and Pb(II) for Pu(V) because PuO_2^+ and Sr^{2+}/Pb^{2+} have a similar effective charge thus show alike complexation behaviour. There is no information known to us on R_d data for cementitious materials in which Pu(V) or Pu(VI) was unequivocally identified. Wieland and Van Loon (2002) assume Pu(V) and the aqueous species PuO_2^+ to be present under oxidising conditions. Note, however, that the recent NEA thermodynamic database (Guillaumont et al. 2003) does no longer consider Pu(V) as a relevant oxidation state (only States IV and VI exist) thus R_d for Pu(V) is not considered as relevant presently.

A final issue is the oxidation state at which plutonium will be initially present in the conditioned waste. Pu(IV) is considered to be the predominant oxidation state for all degradation states (I through IV). The lines of evidence in support of this assertion are as follows:

- In high-pH environments, Pu(IV) will be the predominant species, while Pu(VI) will not normally exist under these circumstances (Nelson et al. 1989);
- Pu(VI) is not stable except in extremely oxidised and acidic environments, typically not found in natural environments (Kim 1986);
- The change in plutonium chemistry identified by Haschke et al. (2000), i.e. oxidation of PuO_2 to form plutonium in the hexavalent form (PuO_{2+x}, where x can range up to 0.27, i.e. 27 % of the Pu can be oxidised to the +6 oxidation state), seems to have a very slow reaction rate (determined using plutonium oxide with a higher surface area than normally encountered in LIWL waste) and will therefore not produce large quantities of Pu(VI), which would not be stable anyhow (see higher);

- The presence of reductants such as BFS in certain cements (in slag-rich cement blends the redox condition is dominated and buffered by reduced S species, mainly S^{2-}) provides a reducing environment. This results in strongly reducing conditions. Reducing conditions will probably develop within a year in slag-rich cement owing to release of sulphides from the hydrating slag (Atkins and Glasser 1992). Even in slag-free Portland cement, reducing conditions may develop at and near corroding surfaces after approximately 100 years owing to corrosion of steel (Sharland et al. 1986; Atkins and Glasser 1992).
- Any Pu(VI) generated in the disposal facility, e.g. according to the principles of Haschke et al., will most likely be reduced again to the more stable Pu(IV) provided reducing components are present in the cement.

6.3.3 Sorption Mechanisms and Selected Sorption Values

6.3.3.1 Sorption Mechanisms

Plutonium sorption will be influenced by the degradation state as well as by the oxidation state of Pu. Pu can take on the oxidation States III–VI. For the present cement systems, oxidation states IV and VI are seen as most relevant.

Based on the constant speciation of Pu(IV) (Fig. 6.13), similar sorption can be expected across States I–III, in analogy to the behaviour to Th. This is illustrated in Fig. 6.15. Th(IV) has indeed been proposed as chemical analogue to Pu(IV) (Bradbury and Sarott 1995). However, this is not entirely supported by the summary data (Fig. 6.14), which indicate lower R_d for State I compared to States II and III.

In terms of sorption mechanisms for cements and concretes, literature specific to plutonium is scarce. Baston et al. (1995) successfully modelled plutonium sorption for concentrations below 10^{-10} to 10^{-8} mol/L Pu on a wide range of materials by means of surface complexation. In addition, the actinides Pu, Np, Am, Th, and U are chemically analogous, and all are known to sorb strongly onto cementitious materials. Sorption mechanisms in a broad sense may be similar too. Therefore, sorption mechanisms potentially relevant for plutonium may include surface complexation (americium, see also above), sorption of oxidised forms onto OPC followed by reduction and formation of actinide (IV) precipitates (neptunium), linear reversible sorption onto degraded cement pastes (uranium), linear sorption followed by a concentration-dependent precipitation of calcium urinate (uranium), and incorporation into CSH structures following sorption (curium).

For selecting R_d values for Pu, it was agreed that more weight should be given to experimental data for Pu than to the analogy with Th. The experimental data indicate a lower R_d at State I than States II and III. Note, however, that the lower R_d observed for State I was obtained from two data sets (Allard et al. 1984; Hoglund et al. 1985) produced with similar experimental procedures and on similar cementitious materials. These studies applied centrifugation as phase

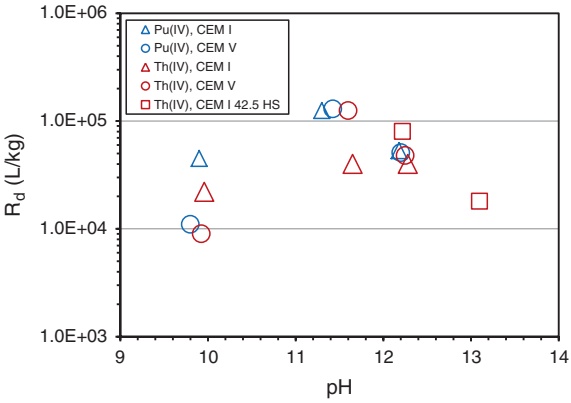

Fig. 6.15 Distribution ratio (R_d) of plutonium (IV) and of thorium in cementitious systems. Data for CEM I and CEM V are from Pointeau et al. (2004a) data for CEM I 42.5 HS are form Wierczinski et al. (1998), replotted from Andra (2005)

separation technique, but it is not excluded that some colloids were present and were not removed by centrifugation, so R_d might have been underestimated. Considering these factors, lower R_d values for State I are therefore conservative.

Analysis of the summary R_d graph (Fig. 6.14) shows a distinction between State I values (range 10^3 to 10^4 L/kg) and States II and III values (range 10^4 to 10^5 L/kg and more). There are more data for State III than for State II. It was decided that it would be appropriate to use the same values for States II and III because R_d values in Fig. 6.14 are believed to be valid for the anticipated Pu(IV).

The selection of sorption values for Pu(IV) is based on the following arguments: most of the reliable data are for State III and State II, which would be the starting point for data selection. Because the speciation of Pu(IV) does not change from States II to III, it was decided that it would be appropriate to use the same values for both States (i.e. a difference in pH would make no difference regarding speciation and sorption). The absence of any trend between States II and III is consistent with the assumptions for other tetravalent actinides, especially Th(IV). The consistency in sorption values for States II and III between Pu(IV) and Th(IV) was also shown in Fig. 6.15. Selection of values is continued from here for States I and IV (Sects. 6.3.3.2 and 6.3.3.5).

In the absence of reliable data for Pu(VI), it was recommended to use values from U(VI) in the meantime (for all states), even though from an hydrolysis point of view, one would expect Pu(VI) to sorb more strongly than U(VI). For State II and State III, best estimate sorption values from U(VI) were found to be identical to those from Pu(IV). Until reliable measurements of Pu(VI) sorption become available, the invoked similarity between U(VI) and Pu(VI) will be implemented, as this was agreed to be the best option possible at the moment. No upper or lower limits for Pu(VI) have been defined.

Table 6.5 Selected best estimate, upper and lower limit R_d values for Pu(IV) and Pu(VI)

pH state	Best estimate (L/kg)		Upper limit (L/kg)		Lower limit (L/kg)	
	Pu(IV)	Pu(VI)	Pu(IV)	Pu(VI)	Pu(IV)	Pu(VI)
State I	5×10^3	2×10^3	1×10^6	i.d.	1×10^3	i.d.
State II	3×10^4	3×10^4	1×10^6	i.d.	1×10^3	i.d.
State III	3×10^4	3×10^4	1×10^6	i.d.	1×10^3	i.d.
State IV	3×10^2	5×10^1	1×10^4	i.d.	3×10^1	i.d.

i.d. insufficient data

6.3.3.2 Sorption in State I

It was found that there were very few Pu(IV) data for State I. The Andra (2005) point was discounted due to State I conditions in their analysis being different from the State I conditions considered for the current study. The brucite and ettringite data were discounted for not being directly relevant. Despite (1) the similarity in anticipated sorption mechanism between States I, II, and III (possibly surface complexation) and (2) an invariant speciation across the different degradation states, a different best estimate sorption value was assigned to State I. This selection was based on giving more weight to the (few) available data, rather than assuming similarity between degradation states. For the same reason, no analogy with Th(IV) was invoked. Therefore, for State I a best estimate of 5×10^3 L/kg was selected based on Fig. 6.14, with upper and lower limits of 10^3 and 10^6 L/kg, respectively (Table 6.5).

6.3.3.3 Sorption in State II

The experts believed it was appropriate, given the paucity of data for State II and the apparent independence of R_d on pH, to assign the same Pu(IV) R_d values for States II and III. The best estimate was 3×10^4 L/kg, which is consistent with (tetravalent) thorium, uranium, and neptunium best estimates. The lower bound was chosen to be 10^3 L/kg. The upper bound was agreed to be 1×10^6 L/kg and the best estimate to be 3×10^4 L/kg. Both bounds are 1.5 orders of magnitude from the best estimate to reflect the uncertainty.

6.3.3.4 Sorption in State III

Based on the above arguments (i.e. same speciation for States II and III suggesting similar sorption behaviour which is shown not to be in contradiction with the summary graph, and consistency between Pu(IV) and Th(IV) further supported by data from Fig. 6.15), the same best estimate as for State II was selected, i.e. 3×10^4 L/kg.

As stated above for State II, the lower bound for States II and III was chosen to be 10^3 L/kg. The upper bound was agreed to be 1×10^6 L/kg. Again, both bounds are 1.5 orders of magnitude from the best estimate to reflect the uncertainty.

6.3.3.5 Sorption in State IV

Based on the same Pu(IV) speciation, similar sorption behaviour could be expected for State IV and State III/II. Using the same values for States II, III, and IV would also not have been inconsistent with Th(IV). However, as was decided for State I, more weight was given to the available data [two independent data sets (see Fig. 6.14)]. Therefore, for State IV, the best estimate for Pu(IV) was 300 L/kg. The upper limit of 10^4 L/kg accounts for the minimum data observed by Higgo and Rees (1986); the lower bound is 30 L/kg (Table 6.5).

6.4 Neptunium

6.4.1 Chemical Form, Speciation, and Solubility

Fifteen isotopes of neptunium are known; all are radioactive, with half-lives ranging from ~1 min (^{227}Np) to millions of years (^{237}Np, half-life 2.14×10^6 years). ^{237}Np is principally produced in nuclear reactor fuel rods from ^{238}U neutron activation. Some naturally occurring ^{237}Np (trace amounts) is produced when natural uranium ore is activated with neutrons generated as a result of spontaneous fission. A more obvious source of this radionuclide is in the spent fuel of nuclear power plants, as some contamination of the reactor coolant system is possible. After irradiation, neptunium isotopes can be transported with the coolant to other parts of the reactor, filters, concentrates, resins, etc. Typical neptunium isotopes of LILW are ^{237}Np, ^{238}Np, ^{239}Np, ^{240}Np, and ^{240m}Np (NDA 2011; NIRAS 2008).

The Eh–pH diagram for neptunium is shown in Fig. 6.16 which is produced with the thermodynamic data given in Table 6.6. Neptunium can exist in several oxidation states, +III, +IV, +V, and +VI. Its most stable form is +V. Speciation of Np is thus redox dependent. Under oxidising conditions, Np(V) species $NpO_2(OH)_2^-$ and NpO_2OH(aq) are important; carbonate complexes are not significant because of the low concentration of carbonate in cement pore water. Under reducing conditions, the Np(IV) hydrolysis species $Np(OH)_4$ (aq) is the only stable species.

Based on state-of-the-art thermodynamic data (Gamsjäger et al. 2005; Neck and Kim 2001), the dissolved neptunium concentration is limited under reducing conditions by the solubility of amorphous $Np(OH)_4$(am) phase. Figure 6.17 shows that the solubility of $Np(OH)_4$(am) at pH above neutral is 10^{-9} M. Under

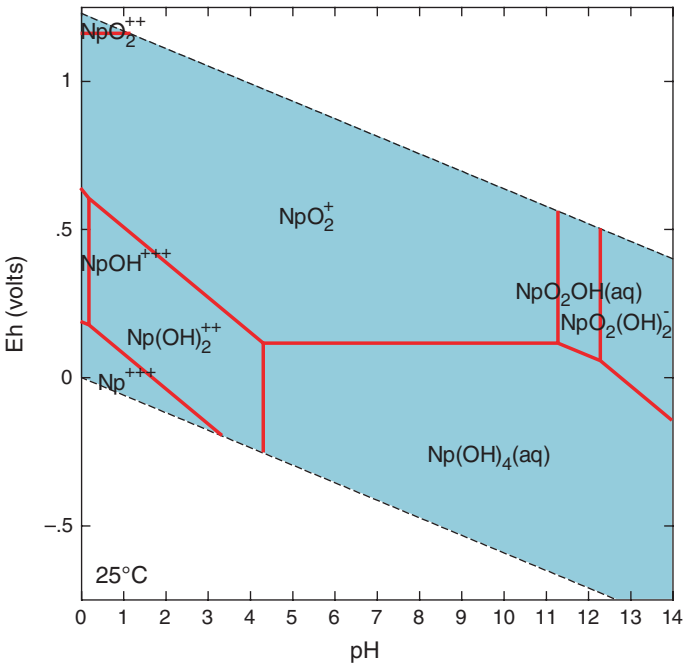

Fig. 6.16 Eh–pH diagram of neptunium calculated with *The Geochemist's Workbench*®. Neptunium activity 10^{-8}

Table 6.6 Thermodynamic data of neptunium

Reaction	log*K* (25 °C)
$NpO_2(OH)_2^- + H^+ + 0.5H_2O = Np(OH)_4(aq) + 0.25O_2(aq)$	4.0087
$NpO_2CO_3^- + 2.5H_2O = Np(OH)_4(aq) + 0.25O_2(aq) + HCO_3^-$	−14.2265
$Np(OH)_4(am) = Np(OH)_4(aq)$	−9.0000
$NpO_2OH(am, aged) + H_2O = H^+ + NpO_2(OH)_2^-$	−18.8997
$NpO_2OH(am, fresh) + H_2O = H^+ + NpO_2(OH)_2^-$	−18.2997

Database Gamsjager et al. (2005), Neck and Kim (2001)

oxidising conditions, Np solubility is predicted to be controlled by Np(V) solid-phase $NpO_2OH(am)$. Two phases with different stabilities limit the Np concentration at about 10^{-7} to 10^{-5} M at pH 12.5–13.5 (Fig. 6.18).

The solubility of Np(IV) in cement waters has been experimentally determined in a pH range of 10–13 (Ewart et al. 1992). Using sodium hydrosulphite as reducing agent, neptunium (IV) solubility was found to be independent of pH at about

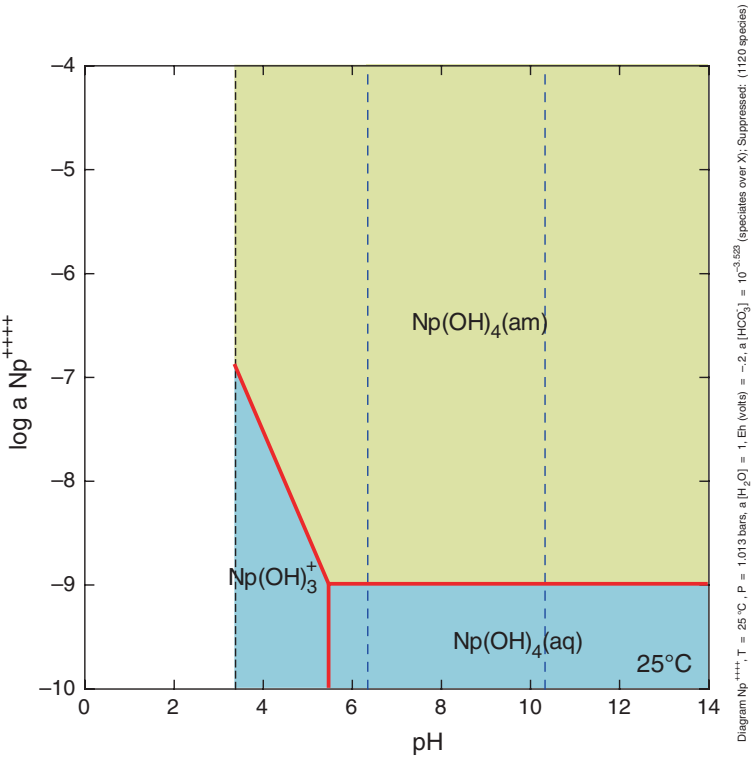

Fig. 6.17 Solubility of $Np(OH)_4(am)$ at Eh = −200 mV

10^{-8} mol/L which is about an order of magnitude higher than the theoretical solubility of $Np(OH)_4(am)$ at alkaline pH (Fig. 6.17).

Most abundant aqueous Np(V) species at high pH relevant to cement systems are $NpO_2(OH)_2^-$ (pH > 13), $NpO_2(OH)(aq)$ (11.5 < pH < 12), and NpO_2^+ as predicted by the speciation diagram (Fig. 6.19) produced with the NEA thermodynamic data (Gamsjager et al. 2005).

It is shown that speciation and solubility of Np depend highly on oxidation state of the element. Neptunium (IV) is prone to be oxidised to Np(V) if traces of oxygen are present. In a sorption or solubility experiment, uncertainties are often related to the fact that the oxidation state of Np is not known. Reducing agents are often used to keep Np in the reduced oxidation state of IV but cannot guarantee a complete removal of Np(V). Since Np(V) is more soluble and less sorbed, presence of Np(V), even at low concentration, will result in an increase in solubility and a decrease in sorption.

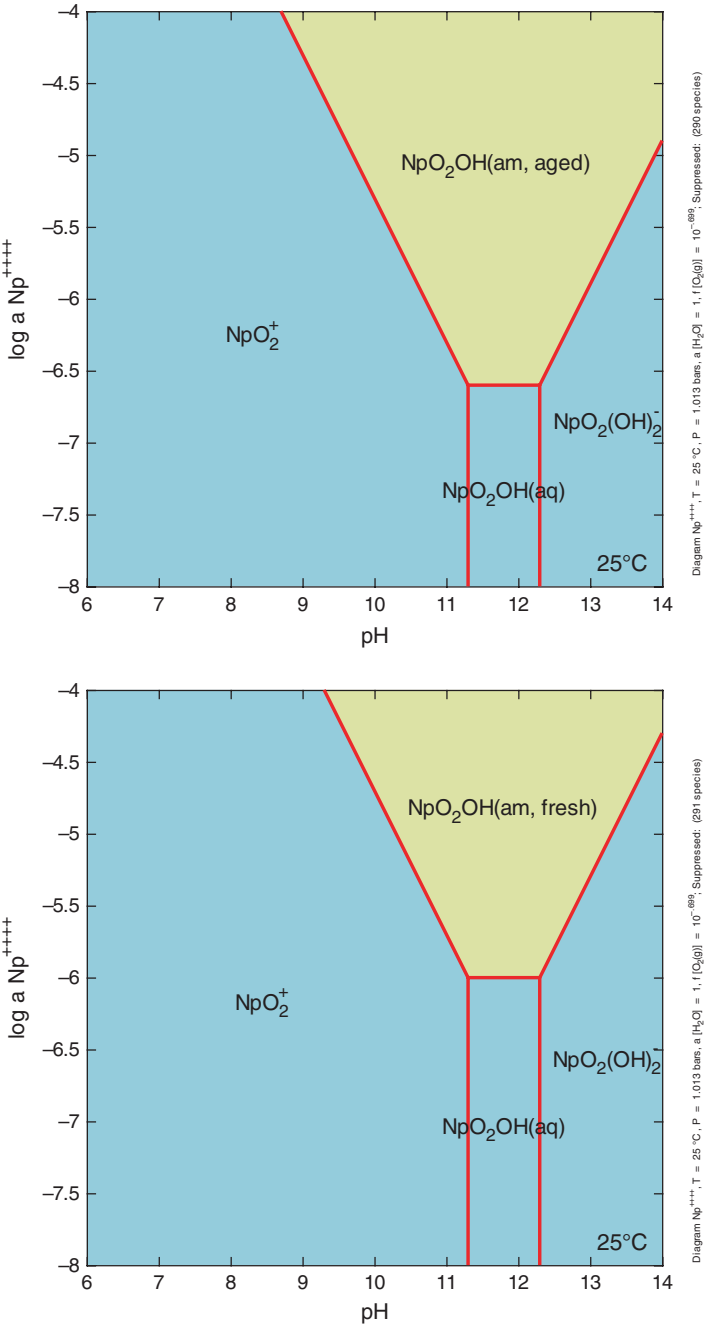

Fig. 6.18 Solubility of NpO_2OH for aged (*top*) and fresh (*bottom*) cement under oxidising conditions, $P_{O_2} = 0.2$ atm

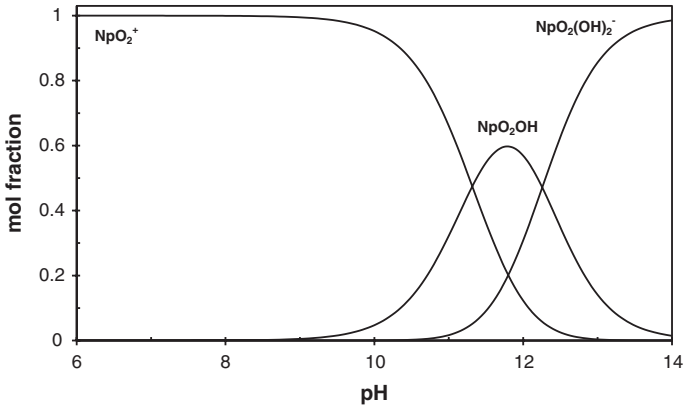

Fig. 6.19 Dissolved neptunium (V) speciation under oxidising condition, $P_{O_2} = 0.2$ atm (total dissolved Np 1×10^{-8} molal, no precipitation of solids)

6.4.2 Sorption Values from the Literature for the Benchmark Cement

There are not many experimentally determined R_d values for neptunium on cement systems in the literature. Figure 6.20 and Table A.11 (see Annex) present the reviewed data obtained from two independent laboratories. All data seem to indicate that uptake of neptunium on cement materials increases with contact time and is relatively independent of the redox conditions of the experiments.

Hoglund et al. (1985) and Allard et al. (1984) performed R_d measurement on 7 different concretes and cements. In these experiments, Np was reported to be introduced as Np(V) although no direct speciation determination was carried out (for fresh concrete samples, only one cement type exhibited reducing conditions). Uptake of Np by some cement materials was decreasing with increasing time (especially when $t > 100$ days). As possible explanation was given a change in speciation or cement phase. For the concrete with blast furnace slag (MB), no decrease was observed after a few tens of days. Bayliss et al. (2000) also measured a fast increase in uptake during the first days of equilibration time and then reaching a more or less constant value at longer contact times (Fig. 6.20).

Bayliss et al. (1996, 2000) studied the effect of phase separation techniques, the system redox condition, and salinity on R_d of Np on cement materials of different composition. In the former study, Np(IV) was added, but no holding reductant was used. Oxidation to Np(V) could not be excluded, due to uncertainty about oxidation state, but the opinion was that Np(V) would not sorb more strongly than Np(IV). Results further demonstrated that for non-saline conditions filter size had no significant effect on R_d. In other words, colloids and particulate species were not important. When a saline solution was used (NaCl concentration

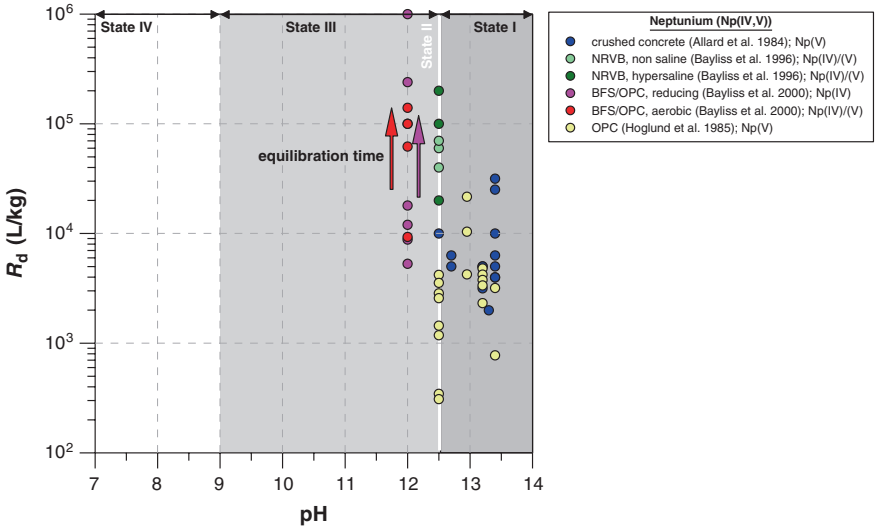

Fig. 6.20 Distribution ratio (R_d) of neptunium (Np(IV, V)) in cementitious systems. *OPC* ordinary Portland cement; *NRVB* Nirex reference vault backfill; *BFS* blast furnace slag

was 1.5 mol/L), R_d values were 3.3 times higher. Results for the latter study were somewhat different from the former; Np(V) was introduced, and tests were done under both reducing and oxidising conditions. Neptunium-containing colloids were present, resulting in an order of magnitude higher R_d values with 30,000 MWCO filtration compared to 0.45-μm filtration. Np(IV) and Np(V) uptake was similar for similar equilibration times. It was not excluded that Np(V) was reduced to Np(IV) even in the so-called oxidising condition. The latter hypothesis is in line with the XAFS study of Sylwester et al. (2000), suggesting that Np(V) is first sorbed on cement followed by reduction to Np(IV).

It is generally accepted that tetravalent actinides sorb very strongly on cement materials (Wieland and Van Loon 2002). The high R_d for Np determined from sorption experiments might be attributed to the fact that Np is taken up by cement as Np(IV), rather than Np(V). However, thermodynamic data (Fig. 6.16) suggest that Np in an oxidising condition exists as Np(V).

Wieland and Van Loon (2002) suggested if no experimental measurements are available, sorption values for bivalent cations, e.g., Sr(II) and Pb(II) can be used for NpO_2^+ because of the similar effective charge of these ions (Berner 2002). In our opinion, such approximation should be used with caution since Np(V) has a very different speciation to that of Sr(II) or Pb(II) at pH > 12. At pH less than or equal to 11, however, NpO_2^+ becomes the dominant Np(V) species (Fig. 6.19). Thus, at least for degradation States III and IV, the similarity with Sr(II) and Pb(II) could be invoked.

6.4.3 Sorption Mechanisms and Selected Sorption Values

Neptunium sorption was found sensitive to salinity (higher R_d under saline conditions compared to non-saline). Although the sensitivity with respect to redox potential was evaluated experimentally, in the pH range considered (> ~12) no significant differences were observed between Np(IV) and Np(V). At lower pH, redox state may have a more significant impact, but such was not demonstrated experimentally.

6.4.3.1 Sorption Mechanisms

Neptunium, as all other actinides, shows strong sorption onto cementitious materials, including HCP and concrete. Experimental studies have been focussing on effects of cement type, oxidation state, and filtration, while uptake mechanisms have been studied to a much lesser extent (Evans 2008).

The only study available on sorption mechanisms is that of Sylwester et al. (2000). In this study, spectroscopic analysis provided evidence that Np(V) is first sorbed on cement (crushed concrete made from Portland cement) followed by reduction to Np(IV). The mechanism responsible for reduction of neptunium was unclear (no reducing agents were added in the experiments and the reducing capacity of the cement is not known). Given this uncertainty, it is not recommended, based on this single study, to assign the same R_d for both Np(IV) and Np(V).

In the absence of further data for Np, chemical analogy is used to infer general sorption mechanisms. Under oxidising conditions, and at pH > 11, aqueous Np(V) is present as hydrolysed species and is expected to behave similarly to Pa(V). Under oxidising conditions but at pH < 11, Np(V) is present as NpO_2^+, with a sorption behaviour possibly similar to bivalent metal cations (Wieland and Van Loon 2002). Although different tetravalent actinides have identical speciation at high pH ($Np(OH)_4$, $Pu(OH)_4$, and $Th(OH)_4$), Pu(IV) is more similar to Np(IV) in terms of hydrolysis constant, etc. (Guillaumont et al. 2003). Sorption by surface complexation proposed for Pu(IV) might be a relevant uptake mechanism for Np(IV) as well. However, it is well known that Pu(IV) is easily oxidisable to Pu(VI) in sorption experiments. It is often difficult to validate an experimental data set in which Pu(IV) is the only oxidation state. In such case, Th(IV) could be used as chemical analogue to Np(IV) (same speciation across a wide pH range) although in terms of chemistry Np(IV) resembles Pu(IV) more closely.

In summary, under reducing conditions Np(IV) is expected to be present, while under oxic conditions Np(V) would be anticipated. The experts agreed that all published data were of some use, but they were concerned that they could not be certain of the oxidation state of neptunium in any of the experiments. They would expect mostly Np(IV) to be present, but it was possible that Np(V) was also present in some cases. It was decided that Np(IV) should have similar sorption R_d values as Th(IV) and the experts chose to compare these with the agreed thorium

values [analogy with Th was also invoked by Bradbury and Sarott (1995)], as thorium (IV) data are not in disagreement with data that appears to be for Np(IV). Also note that Th(IV) data are not in disagreement with Pu(IV) data for States II and III, suggesting that all three IV-valent actinides behave similarly. There was uncertainty regarding the applicability of the measured data to Np(V) which may, for example, be sensitive to the presence of carbonate.

One data set (Bayliss et al. 2000) attempts to generate reducing conditions. However, within the range of R_d values it was difficult to tell if the results for oxidised and reduced conditions were different, as values were in a similar range. Earlier data from the same workers (Bayliss et al. 1996) began with Np(IV) in the experiments, but there was the potential for Np(V) to be present. Both sets of values (saline and hypersaline) could represent Np(IV) or Np(V), and both give similar high R_d values. Overall, R_d values are high but with variation which may be due to uncertainty regarding Np speciation.

The following sections assume that in the experiments discussed here, Np was present as Np(IV) and the experts agreed that these R_d values would probably require downward adjustment to take account of Np(V) if that were necessary. The selection of sorption values is done first for Np(IV) for which data are available. Then, analogy will be invoked to estimate sorption values for Np(V).

6.4.3.2 Sorption at State I

After comparing the available neptunium (IV) data with the thorium (IV) data, the experts assigned the same values as for thorium; a best estimate value of 3×10^4 L/kg, with upper and lower bounds of 1×10^6 L/kg and 1×10^3 L/kg, respectively. This selection is based primarily on the Np(IV) data and supported by Th(IV) data, given the agreed assumption that Np(IV) and Th(IV) should behave similarly by considering that their speciation is identical.

6.4.3.3 Sorption at State II

The experts decided to use Th(IV) data for State II, noting that the existing neptunium data are not inconsistent with these values (whichever oxidation state they may be). As for State I, speciation for Np(IV) and Th(IV) is identical. The experts noted they were uncertain about the applicability of the measured data to Np(V) (see above). Values selected were the same as for State I.

6.4.3.4 Sorption at State III

The experts again decided to use thorium data, neptunium data being not inconsistent with Th, and values selected were the same as for State I. Again, as for States I and II, speciation for Np(IV) and Th(IV) is predicted to be identical.

Table 6.7 Selected best estimate, upper and lower limit R_d values for Np(IV) and Np(V)

pH state	Best estimate (L/kg)		Upper limit (L/kg)		Lower limit (L/kg)	
	Np(IV)	Np(V)	Np(IV)	Np(V)	Np(IV)	Np(V)
State I	3×10^4	i.d.	1×10^6	i.d.	1×10^3	1×10^2
State II	3×10^4	i.d.	1×10^6	i.d.	1×10^3	1×10^2
State III	3×10^4	i.d.	1×10^6	i.d.	1×10^3	1×10^2
State IV	3×10^2	i.d.	1×10^4	i.d.	1×10^1	1×10^2

i.d. insufficient data

6.4.3.5 Sorption at State IV

There were no data for State IV. It was noted that for thorium, the experts reduced sorption by two orders of magnitude for State IV. In the absence of data for State IV, the experts again agreed to use the values for Th(IV), except that the lower bound was reduced to 10 L/kg to take account of additional uncertainty. Thorium was selected as an analogue also for State IV to be consistent with the assumptions on analogy in previous States.

6.4.3.6 Sorption Values for Np(V)

For Np(V), a conservative approach is used as below:

- For States I and II: it was previously discussed that Wieland and Van Loon (2002) conservatively used values from Sr(II)/Pb(II) for NpO_2^+ (100 L/kg) for States I and II. Although the speciation diagram (Fig. 6.19) predicted $NpO_2(OH)_2^-$ and $NpO_2OH(aq)$ to be the dominant species at, respectively, pH ~13 and pH ~12, small quantities of NpO_2^+ are likely to be present for which the sorption analogy with divalent cations still applies. A conservative approach is to use 100 L/kg as lower limit (Table 6.7) for States I and II.
- No best estimates are defined for States III and IV because of lack of data. Values from Sr(II)/Pb(II) for NpO_2^+ in States III and IV may be used as lower limit, which means a value of 100 L/kg based on Wieland and Van Loon (2002) (Table 6.7). Based on the speciation diagram (Fig. 6.19), NpO_2^+ is the dominant species which supports the proposed analogy with divalent cations.

6.5 Protactinium

6.5.1 Chemical Form, Speciation, and Solubility

Currently, 20 protactinium isotopes are known; the naturally occurring ^{234}Pa is a short-lived (6.7 h) member of the naturally occurring ^{238}U decay series. The most common naturally occurring protactinium isotope is ^{231}Pa (half-life 32,800 years).

Protactinium in radioactive waste mainly originates from decay of ^{238}U. Following protactinium isotopes in LILW have been reported: ^{231}Pa, ^{233}Pa, ^{234}Pa, and ^{234m}Pa (NDA 2011; NIRAS 2008).

No thermodynamic data are available to our knowledge for plotting speciation and solubility diagrams for Pa under the considered near-field conditions. However, a recent JAEA report (Berry et al. 2007; Baston et al. 1999) has speciation modelling for Pa in pure water, i.e. at the lower boundary of the water stability domain in the Eh–pH diagram and in granodiorite-equilibrated water, and solubility predictions for Pa_2O_5 in pure water and in granodiorite-equilibrated water. The most stable oxidation states are considered to be Pa(IV) and Pa(V) (Berner 1999). In general, very few thermodynamic data exist for protactinium. Baes and Mesmer (1986) discussed the hydrolysis behaviour of protactinium, and it is evident that Pa(IV) exhibits hydrolysis properties similar to other actinides. Berner (1999) also assumed that Pa(IV) should behave like Th(IV) and U(IV), with similar hydrolysis properties, based on the position of Pa in the periodic table of the elements (in between Th and U). However, it is well known that Pa(IV) is only stable in very acidic solutions or very low Eh and is easily oxidised to Pa(V) (Berner 2002). It is much more likely that Pa(V) is the stable oxidation state in a cement system. It is not clear what the aqueous speciation is of Pa because of the lack of reliable thermodynamic data. Chemical analogy between other pentavalent actinides does not help much here as pointed out by Berner (2002), in that Pa(V) is considerably different from Np(V) with much stronger hydrolysis tendency for Pa(V).

There exist series of experimental and modelling analyses concerning determination of Pa(V) speciation and solubility. The results of these analyses became recently available and have not yet been included in the current review. Based on these studies (E. Giffaut, personal communication), Pa(V) seems to be the relevant oxidation state under the considered cementitious near-field conditions, with $PaO_2(OH)_2^-$ being the main species present, while Pa(IV) is not relevant.

Also because of lack of thermodynamic data, the solubility of Pa is not accurately known. It is, however, believed that the solubility of Pa should be extremely low since the element hydrolyses strongly in an aqueous solution. Berner (2002) cited the thermodynamic data used in Japanese programs and determined a solubility of 10^{-8} mol/L for Pa assuming Pa_2O_5(s) is the solid phase in equilibrium with $PaO(OH)_3$(aq) in solution. The latter value, 10^{-8} mol/L, was used by the Swiss program as the solubility of Pa under a cementitious near-field condition for geological disposal.

6.5.2 Sorption Values from the Literature for the Benchmark Cement

Wieland and Van Loon (2002) discussed the selection of R_d for Pa in a cement near field and suggested to take the R_d of tetravalent actinides for Pa(IV). For oxidising conditions, sorption values for Pa(V) were based on those for Sr(II) and

Pb(II) because of similarities in complexation property between PaO_2^+ and Sr^{2+} and Pb^{2+}. If Pa(V) speciation is considered similar to that of pentavalent neptunium (see Wieland and Van Loon 2002), Pa(V) would exist as PaO_2^+ species which would have similar complexation properties as divalent cations so that R_d should be similar in value as well. Wieland and Van Loon (2002) therefore assigned a R_d value as being 100 L/kg for Pa(V) for their States I and II based on data for Sr and Pb. The 100 L/kg value is exactly the same as the lower end of the experimental R_d range determined by Berry et al. (1988), but is much lower than the R_d values obtained after 30,000 MWCO ultrafiltration (lowest value being $>3 \times 10^3$ L/kg) and, on that account, may be pessimistic.

Because of the lack of literature data concerning sorption of Pa on cementitious materials (only two studies were retained in the analysis, see Table A.12 in Annex), and since Pa does not have a true analogue, one may look at the sorption behaviour of Pa on geological materials in order to have some information about the general sorption behaviour and its analogy to other actinides. Bradbury and Baeyens (2006) measured R_d for Pa(V) on montmorillonite clay and observed strong sorption (R_d around 10^5 L/kg). The pH dependency for Pa(V) sorption was different from that of Np(V) suggesting further that there is no analogy in terms of sorption behaviour between the two actinides for the pentavalent oxidation state.

In their study, Berry et al. (1988) measured R_d values for Pa on geological materials including granite and clays, as well as on cements. Values were typically high, in the range of 1×10^4 to $>10^6$ L/kg (after 0.45-μm filtration). Similar to the case of cement systems, R_d on geological materials was also found to be sensitive to the phase separation techniques. Although these experiments were carried out under a nitrogen atmosphere, no holding reductant was present and conditions were most probably mildly oxidising.

In a separate study, Berry et al. (2007) also looked at sorption of Pa onto bentonite, tuff, and granodiorite under strongly reducing conditions (Baston et al. 1999; Berry et al. 2007). Eh values for these experiments were −330, −180, and −480 mV, respectively, versus the standard hydrogen electrode (SHE), and pH values were between 9.4 and 10.4 (thus comparable to State III). R_d values were very high, being $>10^5$ L/kg after either 0.45-μm filtration or 10,000 MWCO ultrafiltration in all cases. Parallel modelling studies predicted that the speciation was exclusively PaO_2OH, except with granodiorite (−480 mV) where the prediction was 98 % PaO_2OH and 2 % $Pa(OH)_4$.

The distribution coefficient K_d for Pa on calcite was found to be larger than 10^5 L/kg in sea waters (Geibert and Usbeck 2004). The same study indicated that Pa sorption on calcite in sea waters is slightly less strong ($0.03–0.34 \times 10^6$ L/kg) than for Th (range $0.5–7.9 \times 10^6$ L/kg). This was true for other geological minerals studied as sorbent; that is, smectite, MnO_2, and opal, although again R_d values were very high in all cases. However, this study was undertaken using very finely divided solids (thus very high surface areas) and an exceptionally high liquid-to-solid ratio of 2000:1. These facts would both tend to lead to higher R_d values than from more conventional experiments.

With only one well-documented data set on Pa sorption onto cementitious materials (States I, II, and III) (Berry et al. 1988), the experts would not normally assign too much weight on one study. However, these data are backed-up by three separate studies on geological materials (Baston et al. 1999; Berry et al. 1988, 2007). The experts therefore propose to assign R_d values for Pa based on these data rather than use chemical analogy. For sorption onto calcite (State IV), results from Geibert and Usbeck (2004) were obtained using very high surface area solids and extremely low *S*/*L* ratios which led to correspondingly high R_d values.

6.5.3 Sorption Mechanisms and Selected Sorption Values

In the only experimental study available, Berry et al. (1988) investigated effects of initial protactinium concentration and filter size. R_d increased with increasing initial concentration and also increased with decreasing filter size. Cement with or without BFS did not significantly influence R_d. Sorption onto geological materials also appeared to be independent of redox conditions (Baston et al. 1999; Berry et al. 2007).

6.5.3.1 Sorption Mechanisms

The working hypothesis was adopted that under reducing conditions, Pa will be present as Pa (IV). From the chemical analogy between Pa(IV) and Th(IV), similar speciation as $Pa(OH)_4$ and high sorption values could be assumed in States I, II, and possibly III. The behaviour under oxidising conditions is more uncertain, as speciation of pentavalent Pa is more uncertain.

6.5.3.2 Sorption at States I, II, III, and IV

Very few sorption data are available for Pa(V) (Berry et al. 1988), and there are insufficient thermodynamic data available for producing reliable speciation and solubility diagrams. Strong sorption was found and calculated R_d values are very

Table 6.8 Selected best estimate, upper and lower limit R_d values for Pa(V) and Pa(IV)

pH state	Best estimate (L/kg)		Upper limit (L/kg)		Lower limit (L/kg)	
	Pa(V)	Pa(IV)	Pa(V)	Pa(IV)	Pa(V)	Pa(IV)
State I	1×10^4	3×10^4	1×10^7	i.d.	5×10^2	i.d.
State II	1×10^4	3×10^4	1×10^7	i.d.	5×10^2	i.d.
State III	1×10^4	3×10^4	1×10^7	i.d.	5×10^2	i.d.
State IV	3×10^2	3×10^4	1×10^4	i.d.	1×10^1	i.d.

i.d. insufficient data

dependent upon phase separation method. The experts agreed to assign the same values to States I–III (Table 6.8). Selection of the values was based on one study (Berry et al. 1988) backed-up by several studies on geological materials showing similarly high sorption. R_d values used are those obtained after ultrafiltration since R_d values are extremely sensitive to phase separation method. For sorption onto calcite (State IV), results from Geibert and Usbeck (2004) were obtained using very high surface area solids and extremely low *S*/*L* ratio which led to correspondingly high R_d values. It is suggested that these R_d values are scaled down by two to three orders of magnitude to make them more comparable with measurements made under more conventional experimental conditions. For Pa(IV) chemical analogy with Th(IV) is assumed (similar speciation and similar hydrolysis behaviour), with the same values for all states (Table 6.8).

References

F. Adenot, C. Maxoin, C. Tognazzi, P. Bredy, X. Bourbon, P.J.C. Bloem, J. Fachinger, L. Abdou, A., Sneyers, S. Labat, P. Van Iseghem, G. Marx, C. Altenhein-Haese, H. Bischoff, K., Brodersen, M. Cowper, F. P. Glasser, M. Paul, C. L. Dickson, D. Reed, M. Tyrer, Barrier performance of cements and concretes in nuclear waste repositories. Final report, ed. by F.P. Glasser, EUR 19780 EN, 2001

S. Aggarwal, M.J. Angus, J. Ketchen, Sorption of radionuclides onto specific mineral phases present in repository cements, NSS/R312, AEA-DandR-0395, 2000

B. Allard, L. Eliasson, S. Hoglund, K. Andersson, Sorption of Cs, I and actinides in concrete systems. SKB technical report 84-15, 1984

M. Altmaier, V. Neck, R. Muller, Th. Fanghanel, Solubility of U(VI) and formation of CaU_2O_7 $3H_2O$ (cr) in alkaline $CaCl_2$ solutions, in *Abstracts, 10th Migration Conference, Avignon*, France, 18–23 Sept 2005

Andra 2005, Référentiel de comportement des radionucléides et des toxiques chimiques d'un stockage dans le Callovo-Oxfordien jusqu'à l'homme, Site de Meuse/Haute-Marne, Tome 1/2: Chapitres 1 à 4, Dossier 2005 Argile, 2005

M. Atkins, F.P. Glasser, Application of portland cement-based materials to radioactive waste immobilization. Waste Manag. **12**, 105–131 (1992)

C.F. Baes, R.E. Mesmer, *The Hydrolysis of Cations,* 2nd edn. (Robert E. Krieger, New York, 1986)

S. Baker, P. Oliver, R. McCrohon, Near-field batch sorption studies—1992 to 1998, AEAT/ERRA-0345, 2002

G.M.N. Baston, J.A. Berry, M. Brownsword, T.G. Heath, D.J. Ilett, R. McCrohon, C.J. Tweed, M. Yui, The sorption of Polonium, Actinium and Protactinium onto geological materials, in *Materials Research Society Symposium Proceedings*, vol. 556 (1999), p. 1107

G.M.N. Baston, J.A. Berry, M. Brownsword, T.G. Heath, C.J. Tweed, S.J. Williams, Sorption of plutonium and americium on repository, backfill and geological materials relevant to the JNFL low-level radioactive waste repository at Rokkasho-Mura, in *Materials Research Society Symposium Proceedings*, vol. 353 (1995), pp. 957–964

S. Bayliss, R. McCrohon, P. Oliver, N.J. Pilkington, H.P. Thomason, Near-field sorption studies: January 1989 to June 1991, NSS/R277, AEA-ESD-0353, 1996

S. Bayliss, R.M. Howse, R. McCrohon, P. Oliver, Near-field sorption studies, AEAT/ERRA-0073, 2000

U. Berner, Concentration limits in the cement based Swiss repository for long-lived, intermediate-level radioactive wastes (LMA), PSI Bericht Nr. 99-10, Dec 1999

U. Berner, Project Opalinus Clay: Radionuclide concentration limits in the cementitious near-field of an ILW repository, PSI Bericht 02-26, 2002

J.A. Berry, J. Hobley, S.A. Lane, A.K. Littleboy, M.J. Nash, P. Oliver, J.L. Smith-Briggs, S.J. Williams, The solubility and sorption of protactinium in the near-field and far-field environments of a radioactive waste repository, NSS/R122, 1988

J.A. Berry, K.A. Bond, A. Green, C.M. Linklater, A.J. Smith, An experimental study of actinide sorption onto calcite, aluminium oxide and hematite. A report produced for United Kingdom Nirex Limited, AEAT/R/ENV/0205, 2000

J.A. Berry, M. Yu, A. Kitamura, Sorption studies of radioelements on geological materials. JAEA research report 2007-074, 2007

C.M. Bethke, The Geochemist's Workbench, Release 6.0. GWB reference manual, Hydrogeology Program University of Illinois, May 2006

M.H. Bradbury, B. Baeyens, Modelling the sorption of Mn(II), Co(II), Ni(II), Zn(II), Cd(II), Eu(III), Am(III), Sn(IV), Th(IV), Np(V) and U(VI) on montmorillonite: Linear free energy relationships and estimates of surface binding constants for some selected heavy metals and actinides. Geochim. Cosmochim. Acta **69**, 857–892 (2005)

M.H. Bradbury, B. Baeyens, Modelling sorption data for the actinides Am(III), Np(V) and Pa(V) on montmorillonite. Radiochim. Acta **94**, 619–625 (2006)

M.H. Bradbury, F. Sarott, Sorption databases for the cementitious near-field of a L/ILW repository for performance assessment, PSI Bericht—95-06, 1995

M. Cowper, S. Baker, A.V. Chambers, T.G. Heath, M. Mihara, S.J. Williams, The sorption of thorium and americium onto fresh and degraded ordinary Portland cement and onto green tuff, in *Materials Research Society Symposium Proceedings*, vol. 932 (2006), pp. 925–932

N.D.M. Evans, Binding mechanisms of radionuclides to cement. Cem. Concr. Res. **38**, 543–553 (2008)

F.T. Ewart, J.L. Smith-Briggs, H.P. Thomason, S.J. Williams, The solubility of actinides in a cementitious near-field environment. Waste Manag. **12**, 241–252 (1992)

H. Gamsjager, J. Bugajski, T. Gajda, R.J. Lemire, W. Preis, *Chemical Thermodynamics of Nickel* (Elsevier, OECD NEA, Issy-les-Moulineaux, 2005)

A. Geibert, R. Usbeck, Adsorption of thorium and protactinium onto different particle types: experimental findings. Geochim. Cosmochim. Acta **68**, 1489–1501 (2004)

B.F. Greenfield, M.H. Hurdus, M.W. Spindler, H.P. Thomason, The effects of the products from the anaerobic degradation of cellulose on the solubility and sorption of radioelements in the near field, NSS/R376, 1997

R. Guillaumont, T. Fanghanel, V. Neck, J. Fuger, D. Palmer, I. Grenthe, M.H. Rand, *Update on the chemical thermodynamics of uranium, neptunium, plutonium, americium and technetium* (Elsevier, OECD, Issy-lès-Moulineaux, 2003)

M. Harfouche, E. Wieland, R. Dahn, T. Fujita, J. Tits, D. Kunz, M. Tsukamoto, EXAFS study of U(VI) uptake by calcium silicate hydrates. J. Colloid Interface Sci. **303**, 195–204 (2006)

J.M. Haschke, T.H. Allen, L.A. Morales, Reaction of plutonium dioxide with water: formation and properties of PuO_{2+x}. Science **287**, 285–287 (2000)

T. G. Heath, D. J. Ilett and C. J. Tweed, Thermodynamic modelling of the sorption of radioelements onto cementitious materials, in *Materials Research Society Symposium Proceedings*, vol. 412 (1996), pp. 443–449

J.W. Higgo, L.C. Rees, Adsorption of actinides by marine sediments: effect of the sediment/seawater ratio on the measured distribution ratio. Environ. Sci. Technol. **20**, 483–490 (1986)

J.W. Higgo, L.C. Rees and D.S. Chonan, Actinide sorption on marine sediments, in *Behaviour of Long-Lived Actinides Associated with Deep-Sea Disposal of Radioactive Wastes*, IAEA-TECDOC-368 (1986), pp. 7–25

S. Hoglund, L. Eliasson, B. Allard, K. Andersson, B. Torstenfelt, Sorption of some fission products and actinides in concrete systems, in *Materials Research Society Symposium Proceedings*, vol. 50 (1985), pp. 683–690

S. Holgersson, Y. Albinsson, B. Allard, H. Boren, I. Pavasars, I. Engkvist, Effects of Gluco-isosaccharinate on Cs, Ni, Pm, and Th sorption onto, and diffusion into cement. Radiochim. Acta **82**, 393–398 (1998)

W. Hummel, U. Berner, E. Curti, F.J. Pearson, T. Thoenen, *Nagra/PSI Chemical Thermodynamic Data Base 01/01* (Universal Publishers, Parkland, 2002)

International Atomic Energy Agency (IAEA), Behaviour of long-lived actinides associated with deep-sea disposal of radioactive wastes, IAEA-TECDOC-368, 1986

International Atomic Energy Agency (IAEA), *Environmental Isotopes in the Hydrological Cycle: Principles and Applications*, vol. 1 (IAEA and UNESCO, Vienna, 2001)

T. Jakubick, R.W. Gillham, I. Kahl, M. Robin, Attenuation of Pu, Am, Cs, and Sr mobility in concrete, in *Materials Research Society Symposium Proceedings*, vol. 84 (1987), pp. 355–368

J.I. Kim, Chemical behaviour of transuranic elements in natural aquatic systems, in. *Handbook of the Physics and Chemistry of the Actinides,* vol. 4, ed. by A.J. Freeman, C. Keller (North-Holland Press, Amsterdam, 1986), pp. 413–455

T.C. Maiti, M.R. Smith, J.C. Laul, Sorption of uranium, thorium, and radium on matrices under oxic environments. Radioactive Waste Manage. Nucl. Fuel Cycle **11**(3), 269–278 (1989)

L.P. Moroni, F.P. Glasser, Reactions between cement components and U(VI) oxide. Waste Manag. **15**, 243–254 (1995)

V. Neck, J.I. Kim, Solubility and hydrolysis of tetravalent actinides. Radiochim. Acta **89**, 1–16 (2001)

D.M. Nelson, K.A. Orlandini, W.R. Penrose, Oxidation states of plutonium in carbonate-rich natural waters. J. Environ. Radioact. **9**, 189–198 (1989)

Nuclear Decommissioning Authority (NDA), The 2010 UK radioactive waste inventory: main report. Report prepared for the Department of Energy and Climate Change (DECC) and the Nuclear Decommissioning Authority (NDA) by Pöyry Energy Limited, February 2011

ONDRAF/NIRAS, Identification of critical radionuclides through a screening of the ONDRAF/NIRAS 2003/2004 radiological inventory for category A waste, Brussels, April 2008

N.J. Pilkington, P.J. Shadbolt, J.D. Wilkins, Experimental measurements of the solubilities of selected long-lived fission products, activation products and actinide daughters under high pH conditions, NSS/R116, ILWRP/87/P7, 1988

I. Pointeau, C. Landesmann, E. Giffaut, P. Reiller, Reproducibility of the uptake of U(VI) onto degraded cement pastes and calcium silicate hydrate phases. Radiochim. Acta **92**, 645–650 (2004)

Pointeau, C. Landesman, N. Coreau, C. Moisan, P. Reiller, Etude de la rétention chimique des radionucléides Cs(I), Am(III), Zr(IV), Pu(IV), Nb(V), U(VI) et Tc(IV) par les matériaux cimentaires dégradés. CEA report 2004, RT DPC/SECR 03-037 indice A, 2004b

Pointeau, C. Landesman, N. Coreau, C. Moisan, P. Reiller, Etude de la rétention des radionucléides Cs(I), Am(III), Zr(IV), Pu(IV), Nb(V), U(VI) et Tc(IV) par les matériaux cimentaires dégradés, Andra 2005 report C RP PSTR 04-0012, 2004c

I. Pointeau, N. Coreau, P.E. Reiller, Uptake of anionic radionuclides onto degraded cement pastes and competing effect of organic ligands. Radiochim. Acta **96**, 367–374 (2008)

R. J. Serne, D. Rai, P. F. Martin, A.R. Felmy, L. Rao, S. Ueta, Leachability of Nd, U, Th, and Sr from cements in a CO_2 free atmosphere, in *Materials Research Society Symposium Proceedings*, vol. 412 (1996), pp. 459–467

S.M. Sharland, P.W. Tasker, C.J. Tweed, The evolution of Eh in the pore water of a model nuclear waste repository. Report AERE/R/12442, UK AEA, Harwell, 1986

D.L. Stout, S.A. Carroll, A literature review of actinide-carbonate mineral interactions, SAND92-7328, 1993

D. Sugiyama, T. Fujita, Sorption of radionuclides onto cement materials altered by hydrothermal reaction, in *Materials Research Society Symposium Proceedings*, vol. 556 (1999), pp. 1123–1130

D. Sugiyama, T. Fujita, M.N. Baston, J.A. Berry, M. Brownsword, A. Green, D.J. Ilett, W.M., Tearle, C.J. Tweed, Experimental measurements and integrated modelling studies of actinide sorption onto cement. in *Abstract, Science link Japan*, Accession number: 04A0047963, Denryoku Chuo Kenkyujo Hokoku, 2003

M. Sutton, P. Warwick, A. Hall, Uranium (VI) interactions with OPC/PFA grout. J. Environ. Monit. **5**, 922–925 (2003)

E.R. Sylwester, P.G. Allen, P. Zhao, B.E. Viani, Interactions of uranium and neptunium with cementitious materials studied by XAFS, in *Materials Research Society Symposium Proceedings*, vol. 608 (2000), pp. 307–312

J. Tits, E. Wieland, M.H. Bradbury, J.-P. Dobler, The uptake of Eu(III) and Th(IV) by cement-type minerals in the alkaline disturbed zone of a nuclear waste repository, in *Applied Mineralogy in Research, Economy, Technology, Ecology and Culture*, ed. by D. Rammlmair, J. Mederer, T. Oberthür, R.B. Heimann, H. Pentinghaus (Balkema, Rotterdam, 2000)

J. Tits, E. Wieland, M.H. Bradbury, P. Ecker, A. Schaible, The uptake of Eu(III) and Th(IV) by Calcite under hyperalkaline conditions, PSI Bericht 02-03, 2002

J. Tits, E. Wieland, M.H. Bradbury, The effect of isosaccharinic acid and gluconic acid on the retention of Eu(III), Am(III) and Th(IV) by calcite. Appl. Geochem. **20**, 2082–2096 (2005)

J. Tits, T. Fujita, M. Tsukamoto, E. Wieland, Uranium(VI) uptake by synthetic calcium silicate hydrates, in *Materials Research Society Symposium Proceedings*, vol. 1107 (2008), pp. 467–474

J. Tits, T. Fujita, M. Harfouche, R. Dähn, M. Tsukamoto, E. Wieland, Radionuclide uptake by calcium silicate hydrates: case studies with Th(IV) and U(VI), PSI Bericht, 2010 (in press)

U.S. Department of Energy (USDOE), National low-level waste management program radionuclide report series. Selected radionuclides important to LLW management, DOE\LLW-238, Nov 1996

U.S. Department of Energy (USDOE), Selected radionuclides important to low-level radioactive waste management. National low-level waste management program, DOE/LLW-138, Nov 1996

E. Valsami-Jones, K. Vala Ragnarsdottir, Solubility of uranium oxide and calcium urinate in water, and $Ca(OH)_2$-bearing solutions. Radiochim. Acta **79**, 249–257 (1997)

E. Wieland, J. Tits, P. Spieler, J.-P. Dobler, Interaction of Eu(III) and Th(IV) with sulphate-resisting Portland cement, in *Materials Research Society Symposium Proceedings*, vol. 506 (1998), pp. 573–578

E. Wieland, L. Van Loon, Cementitious near-field sorption data base for performance assessment of an ILW repository in Opalinus Clay, PSI Bericht Nr. 03-06, 2002

E. Wieland, J. Tits, J.-P. Doble, P. Spieler, The effect of a-isosaccharinic acid on the stability of and Th(IV) uptake by hardend cement paste. Radiochim. Acta **90**, 683–688 (2002)

B. Wierczinski, S. Helfer, M. Ochs, G. Skarnemark, Solubility measurements and sorption studies of thorium in cement pore water. J. Alloy Compd. **271–273**, 272–276 (1998)

Chapter 7
Sorption Values for Americium

Abstract Like other actinides, americium (Am) is an important constituent of radioactive waste from nuclear power production. In any typical aqueous environmental setting, americium exists exclusively in the trivalent oxidation state. Similar to tetravalent actinides, americium hydrolyses extensively in aqueous solutions and sorbs strongly onto concrete, hydrated cement paste and individual CSH phases. Due to the chemical similarity of trivalent actinides and lanthanides, information for americium can be supplemented with additional data for other well-researched elements, such as curium and europium. The combined evidence clearly demonstrates strong sorption under all conditions, with no clear trend across the different states of cement degradation. Spectroscopic information suggests that sorption occurs through surface adsorption as well as through incorporation into the CSH structure, replacing Ca. Similarly, incorporation into the calcite lattice is supported by spectroscopic evidence.

7.1 Chemical Form, Speciation, and Solubility

Americium is a radioactive element which can only be synthesised by neutron activation of plutonium. For example, ^{241}Pu, produced by neutron absorption of ^{238}U and ^{239}Pu, decays to ^{241}Am. ^{241}Am generation is related to nuclear reactor operations and decommissioning. Commonly observed americium isotopes in LILW include ^{241}Am (half-life $= 4.33 \times 10^2$ years), ^{242}Am, ^{242m}Am, and ^{234}Am (NDA 2011; NIRAS 2008).

Americium may exist in more than one oxidation state but only Am(III) is stable in natural aquatic systems (Berner 2002; Kim 1986). Similar to other transuranic elements, americium is known to have a strong tendency of hydrolysis and thus at a pH above neutral, americium is expected to be very insoluble (Kim 1986) and to sorb strongly on geological materials (Bradbury and Bayens 2005).

Figures 7.1 and 7.2 present the aquatic speciation and solubility of americium predicted by equilibrium calculations using the recent OECD–NEA thermodynamic data (Guillaumont et al. 2003). The influence of complexation with Am carbonate

© Springer International Publishing Switzerland 2016

M. Ochs et al., *Radionuclide and Metal Sorption on Cement and Concrete*,
Topics in Safety, Risk, Reliability and Quality 29,
DOI 10.1007/978-3-319-23651-3_7

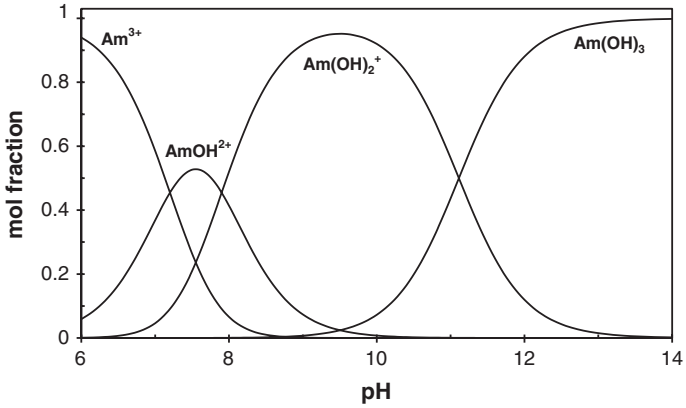

Fig. 7.1 Dissolved americium speciation (total dissolved Am $= 1 \times 10^{-8}$ molal)

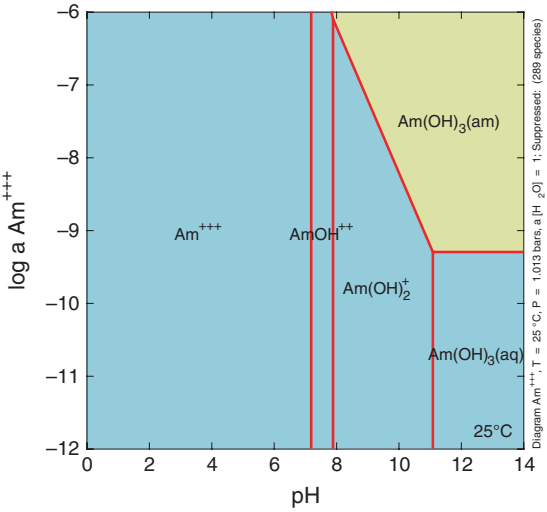

Fig. 7.2 Solubility of amorphous americium hydroxide as a function of pH calculated with *The Geochemist's Workbench*® based on solubility and speciation data of Guillaumont et al. (2003)

is not important because the concentration of dissolved carbonate is very low in cement systems. It is seen that americium speciation is dominated by the neutrally charged hydrolysis species $Am(OH)_3$ (aq) at pH above 11 and the solubility is about 5×10^{-10} mol/L limited by the equilibrium of amorphous $Am(OH)_3$ (am).

7.2 Sorption Values from the Literature for the Benchmark Cement

In the following chapter, Eu is in some cases used as an analogue for Am. Information pertinent to that analogy is discussed in Sect. 7.2.2.

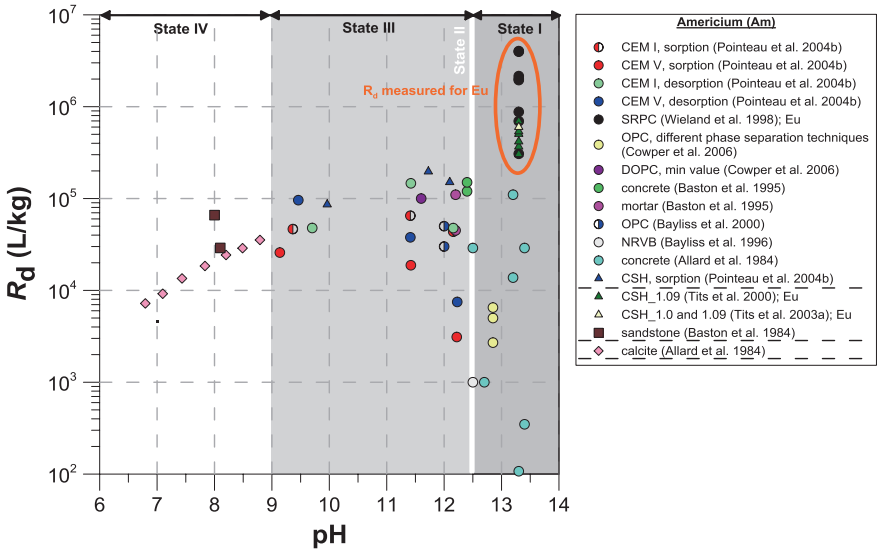

Fig. 7.3 Distribution ratio (R_d) of americium in cementititous systems. *SRPC* sulphate resisting Portland cement; *CSH* calcium silicate hydrate; *NRVB* nirex reference vault backfill; *DOPC* degraded ordinary Portland cement. R_d values for europium are included for State I

7.2.1 Reviewed Sorption Values for Am and Eu

Reviewed sorption values for Am and Eu (as the chemical analogue) are presented in Fig. 7.3 as a function of pH. The summary of experimental conditions under which these sorption values were determined is given in Table A.13 (see Annex).

Pointeau et al. (2004) studied sorption of Am on degraded CEM I, CEM V, and synthetic CSH phases in a pH range 9–12. In these measurements, cement pastes were leached to the point that all portlandite had dissolved, and therefore, the sorption values are representative for State III of cement degradation. The sorbing solids including cement and CSH phases with C/S ratios 1.3, 1.0, and 0.7 were prepared. This allows studying particularly the effect of the C/S ratio, i.e., the cement degradation, on the evolution of the sorption values. The main observations from this study are summarised below:

- The initial Am concentration used in experiments was below the predetermined "operational" solubility of Am in the cement pore fluids. Therefore, the R_d values measured should represent genuine sorption values and are not caused by precipitation;
- Sorption is generally high and is not considerably influenced by the C/S ratio in CSH phases and by pH;
- Sorption seemed not reversible as R_d values were in general higher in desorption experiment than in sorption experiments (see Fig. 7.4). In other words,

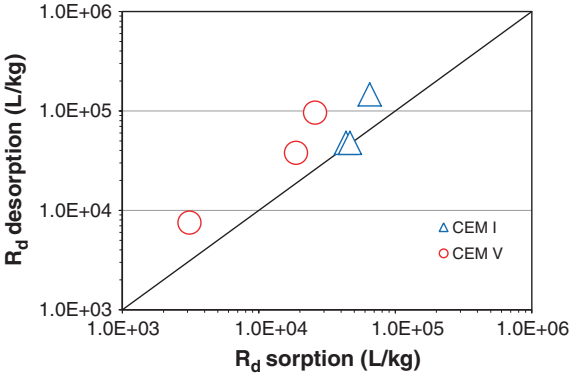

Fig. 7.4 Sorption and desorption of Am on cement paste (data from Pointeau et al. 2004). Note that the data points for CEM I are not different from the 1:1 line when considering the reported error margins

sorbed americium species are partly fixed on cement materials and are not in equilibrium with the solution concentration. In the selection of best estimates, R_d from sorption experiments should be considered as having more weight than those from desorption experiments; the latter provide upper-bound values;

- Am is sorbed more strongly by pure CSH than by cement pastes. The EXAFS study on CSH samples prepared in the same way but using europium as the chemical analogue suggested that Eu uptake was likely to be due to co-precipitation with Ca and Si in CSH (Schlegel et al. 2004). These authors concluded that uptake of Am occurred mainly on CSH and that uptake is due to both sorption and co-precipitation. The higher R_d values for CSH compared to cement pastes are thought to be due to a combination of sorption and co-precipitation mechanisms for the former and sorption only for the latter;
- CEM I seemed a better sorbing material for Am than CEM V, but the underlying mechanism is not clear; and
- Based on the above information, and if only sorption data for cement pastes (exclude desorption data) are considered, then R_d values for Am are in the range of 3000–65,000 L/kg.

Wieland et al. (1998) determined R_d of europium on sulphate-resistant Portland cement in a State I cement pore fluid at pH 13.3. The R_d value was $\geq 10^6$ and $\geq 10^5$ L/kg at S/L ratios of, respectively, 10^{-5} and 10^{-4} kg/L. Note that because of the very strong sorption, special attention was given to use very low solid (i.e. cement) concentration in the experiments in order to accurately measure the Eu solution concentration remaining in the liquid phase after sorption. The need to use small amounts of sorbing material in sorption experiments for strongly sorbing elements was also demonstrated for thorium (see Sect. 6.1.3).

Tits et al. (2000) found similarly high R_ds (10^5 to 10^6 L/kg) for Eu on a CSH phase with a C/S ratio of 1.09 at pH 13.3. This supports other observations that CSHs are important sorption sinks in cement paste. Wieland et al. (1998) concluded that the sorption values for Eu are expected to be similar in value on hardened cement paste and CSH phases.

A combined batch and spectroscopic study was performed by Tits et al. (2003) for sorption of Eu and Cm on CSH phases. In this case, both Eu and Cm were used as chemical analogues for Am; the advantage of Cm over Am was its higher sensitivity for spectroscopic measurements. The R_d for Eu on CSH phases with two different C/S ratios, 1.0 and 1.09, prepared by different procedures, was as high as 6×10^5 L/kg. The uptake is fast (within 1 day) and linear in a solution concentration range of 10^{-12} to 10^{-8} mol/L of Eu.

Batch sorption experiments for Am on fresh OPC and degraded OPC were reported by Cowper et al. (2006). The degraded OPC was prepared by leaching the intact OPC with distilled water until portlandite was dissolved away. The pore fluid was made by equilibrating distilled water with fresh and degraded OPC. Sorption values for OPC at pH around 13 were significantly lower than other R_d values discussed so far and were in the range of 3000–6000 L/kg. The R_d for degraded OPC was, however, larger than the fresh OPC and the value is generally larger than 10^5 L/kg at pH 11.6 if the pore fluid was filtered with filters of 10 kD (kilodalton) MWCO. The increase in R_d for the degraded OPC was explained by the relative higher content of CSH as compared to the fresh OPC after leaching. The mineralogical analysis did indicate that the degraded OPC is about 100 % CSH, while the intact OPC has about 70 % CSH and 30 % portlandite. It is remarkable that the relative content of CSH has such a profound impact on Am sorption. If this is the real mechanism governing the observed difference in R_d, then sorption in State III should in principle be much higher than in States I and II. Another factor that may have influenced the R_d is the aqueous speciation of americium. Based on Fig. 7.2, Am speciation is quite different at pH 13 compared to 11.6, which is the pH of intact and degraded OPC, respectively.

Sorption values of Am on different concretes were measured by Allard et al. (1984). R_d was in a range of 100 to 10^5 L/kg. Among many radionuclides studied by these authors, americium and thorium had similar sorption behaviour and were sorbed most strongly for all concrete materials tested. Although preference is given to sorption values from cement pastes and CSH phases for determining best estimates, the values for concrete were included in the summary graph for reasons of comparison. However, lower weight will be given to the concrete values in determining the best estimates.

Sorption of Eu on calcite at State I cement pore water was studied by Tits et al. (2002). In general, sorption values were as high as 10^4 to 10^5 L/kg suggesting that calcite is also an important sorption sink for a trivalent actinide such as Am. The data, however, showed a strong dependency on S/L ratio and on the crystallinity of the calcite, suggesting uptake processes other than surface sorption are at work. Formation of a solid solution with neo-formed calcite was proposed as the uptake mechanism. It is also noted that although the R_d was for calcite, values cannot be used for the State IV of cement degradation because measurements were carried out at high pH (13.3).

Baston et al. (1995) investigated sorption of Am on sandstone containing feldspars and calcite as major components. This work is relevant to be included for evaluating State IV R_d. The sorption experiments were performed at pH around

8 and the R_d values found were between 30,000 and 66,000 L/kg. Care must be taken when using these numbers since the sandstone used as sorbing material has some clays and iron oxides in it.

Another study relevant for State IV R_d assessment is that of Allard et al. (1984). Americium sorption on calcite was investigated by batch experiments in an artificial $NaHCO_3$-type groundwater. The R_d was found to increase with pH, and the value was in the range of 10,000–25,000 L/kg in the range pH 7–9. In the same study, sorption of Am on many other geologic materials including silicates, oxides/hydroxides, and sulphides was reported. It was found that the sorption behaviour was similar for all minerals. From such an observation, it was concluded that the increase in R_d with pH was probably governed by the change of solution speciation, and not by the type of sorbing minerals.

Based on the two data sources mentioned above, Am sorption on calcite seems strong. The reported R_d values are in agreement with other general reviews given by Bradbury and Baeyens (1997), Stout and Carroll (1993). The sorption mechanism is, however, not well understood. Probable processes include surface adsorption, co-precipitation, formation of solid solution, and precipitation of americium carbonate. A recent time-resolved laser fluorescence investigation revealed that adsorption is only one of several mechanisms responsible for Eu uptake on calcite. The high affinity is due to incorporation of Eu into the calcite lattice on Ca^{2+} sites (Fernandes et al. 2008). These authors also discovered that Eu incorporation is stronger in the presence of sodium than potassium, although no explanation was given.

7.2.2 Europium as a Chemical Analogue for Americium in Sorption Experiments

It is well known that chemical compounds and aqueous species of the trivalent actinides and lanthanides have similar chemical properties (Choppin and Rizkalla 1994). Europium is thus often used as a chemical analogue for americium in studies of solution chemistry and sorption. Inspecting R_d values presented in Fig. 7.3 shows, however, that R_d for Eu is much larger than R_d for Am. All R_d for Eu were determined in the PSI laboratories (Wieland et al. 1998; Tits et al. 2000) and the values scatter around 10^6 L/kg (3×10^5 to 4×10^6). The remaining R_d values in Fig. 7.3 are all measured using Am as the sorbing element, and these are generally below 10^5 L/kg. This observation seems to suggest that there is difference in the sorption of Am and Eu onto cement materials where Eu appears to sorb much more strongly than Am. It must be noted that although the chemical analogy between Eu and Am has been built on a solid basis, differences are observed between these elements in solution chemistry and the related thermodynamic properties (Guillaumont et al. 2003; Hummel et al. 2002; Silva et al. 1995).

Hummel et al. (2002) show that Eu hydrolyses stronger than Am with the following stability constants for the tri-hydroxo complex:

$$\mathrm{Am(OH)_3(aq) + 3H^+ = 3H_2O + Am^{3+}} \quad \log K\left(25\,^{\circ}\mathrm{C}\right) = 25.7 \tag{7.1}$$

$$\mathrm{Eu(OH)_3(aq) + 3H^+ = 3H_2O + Eu^{3+}} \quad \log K\left(25\,^{\circ}\mathrm{C}\right) = 23.7 \tag{7.2}$$

It is seen that the stability of $Eu(OH)_3$ (aq) is two orders of magnitudes higher as compared to that of $Am(OH)_3$ (aq). Considering the more recent americium review by Guillaumont et al. (2003), the log K for $Am(OH)_3$ (am) is 26.2 suggesting that Eu hydrolyses is even larger.

Tits et al. (2003) have also noticed the discrepancy between the conceptual view, i.e., the anticipated chemically analogous behaviour of Eu(III) and Am(III), and the hydrolysis constants presently available from the open literature. In addition, two other points from the work of Tits et al. (2005) are particularly relevant and provide interesting and important information about using Eu and Am in sorption experiments:

- R_d for Eu and Am on calcite is similar in value if corrected for the observed effect of solid-to-liquid ratio. This suggests that Am and Eu are very similar in terms of sorption on calcite;
- Use of cement water containing high concentrations of potassium may introduce natural radioactive ^{40}K which may interfere with the counting of ^{241}Am in sorption experiments. To avoid interference with potassium, Tits et al. (2005) used only sodium to prepare the State I cement water. We checked the experimental procedures applied for obtaining R_d values in Fig. 7.3 and it turns out that the only study in which an elevated concentration of potassium was added is that of Allard et al. (1984). Other studies may have some potassium leached from cement, but the concentrations are supposed to be low and therefore will not affect the R_d determination to a large extent merely due to the interference of ^{40}K.

7.3 Sorption Mechanisms and Selected Sorption Values

7.3.1 Sorption Mechanisms

There is a general consensus that trivalent actinides (Am, Cm) and lanthanides (Eu) sorb strongly on cementitious materials (Wieland and Van Loon 2002). Analogy with Cm and Eu is often invoked to infer sorption values and mechanisms. Sorption R_d values determined by batch-type experiment are commonly in the range of 1000 to 10^6 L/kg. Evans (2008) proposed that sorption of americium on cement may be due mainly to surface complexation or surface adsorption and co-precipitation with Ca and Si.

Stumpf et al. (2004) suggested several uptake mechanisms of Cm(III) on cement paste based on their time-resolved laser fluorescence spectroscopy studies: trivalent actinides may be sorbed on cement through surface sorption on portlandite, formation of colloidal hydroxides, and incorporation into CSH structures. Sorption of Cm(III) on CSH involved determination of species responsible for uptake on CSH surfaces (Tits et al. 2003). The analysis demonstrated that Cm is incorporated into CSH structures by replacing Ca.

Spectroscopic studies carried out by Schlegel et al. (2004), Pointeau et al. (2001) revealed that the uptake of Eu on CSH is through incorporation into the structure of CSH and possibly surface precipitation or co-precipitation of Eu with Ca and Si. The relative strong uptake of Am and Eu on calcite is supported by spectroscopic evidences showing strong incorporation (Eu) into the calcite lattice (Tits et al. 2002).

Having considered R_d data in Fig. 7.3, there is no doubt that Am sorbs strongly on cementitious materials. For State I, data produced in PSI for Eu sorption are of high quality, but there were concerns[1] over its use and that best estimates should be based mainly on Am data (e.g. Allard et al. 1984). There does not appear to be a significant trend across the states, although there is more scatter for State I data at the lower range of values. This was most probably due to the use of centrifugation rather than filtration.

7.3.1.1 Solid-to-Liquid Ratio

Only in the work of PSI (Wieland et al. 1998; Tits et al. 2003) was the influence of S/L ratio on R_d values for Eu investigated. For all other R_d data presented in Fig. 7.3, usually only one S/L ratio was used.

Wieland and Van Loon (2002) demonstrated that R_d for Eu decreased for about an order of magnitude if S/L increased from 10^{-5} to 10^{-4} kg/L. Other literature R_d values (e.g. those from Allard et al. 1984) had lower R_ds than those from PSI. This was considered to be due to the higher S/L ratio used by Allard et al. (1984). Tits et al. (2005) found a similar influence of S/L ratio on calcite, i.e. R_d generally decreases if a higher amount of calcite was used as sorbing material.

To summarise, the effect of S/L ratio on R_d of Am seems genuine and was demonstrated for both cement and calcite systems and for both elements Eu and Am. Although the real mechanism behind the effect of S/L ratio on R_d is not understood, a conservative approach should be to use R_d determined with a higher S/L ratio if these data are determined with a sufficient accuracy within the appropriate experimental window.

[1]The experts had a divided opinion on this; therefore, for conservative reasons, the Eu data were not used for selecting best estimates.

7.3.1.2 Cement Degradation

If considering all R_d values presented in Fig. 7.3, i.e. making no difference between R_d for Eu and Am, R_d values in State I cover almost 5 orders of magnitudes from 100 to 10^7 L/kg. This would also imply that Fig. 7.3 shows a decreasing tendency in R_d with decreasing pH. It is questionable to draw such conclusion though because (1) there is no argument supporting a stronger sorption of Am or Eu in State I than in States II and III; (2) the question remains if R_d for Eu is fully representative for Am in this case; and (3) it is not clear if other factors lead to the observed difference between the R_d values from PSI's work and others.

Pointeau et al. (2001) demonstrated that R_d for Am does not vary in State III when cement and CSH phases had different C/S ratios. Cowper et al. (2006), however, found that R_d for Am increased significantly in State III as compared to State II. It was suggested that this might be due to the increase of the relative content of CSH after the leaching of portlandite. The change of americium speciation from State II to III may also contribute to a possible R_d variation although the issue has not been particularly discussed in the studies reviewed so far. An exception is from the study of Allard et al. (1984) where decrease of R_d on calcite with decreasing pH was observed.

7.3.1.3 Sorption Reversibility

Evidence exists that uptake of trivalent actinides (Am, Cm) and lanthanides (Eu) on cement is likely irreversible (see Fig. 7.4). Sorption of Eu(III) and Cm(III) on cementitious materials were demonstrated to be kinetically fast and linear. Desorption was, however, slow and that was attributed to surface precipitation and incorporation into CSH structures by substituting Ca (Wieland et al. 1998; Tits et al. 2003). Other studies showed a similar behaviour for Am. Sorption of Am was followed by fixation into CSH structures and thus becomes irreversible (Pointeau et al. 2004; Schlegel et al. 2004). Note that irreversible sorption is in principle not accounted for by the K_d concept used in safety assessment.

7.3.2 Sorption at State I

High-quality data have been produced by PSI for Eu as an analogue of americium and these results show higher R_d values than Am itself. It was felt best to use mainly Am data for selecting the best estimate but to note that proposed R_d values would be higher if Eu data were included. The best estimate R_d for State I was selected as 10^4 L/kg, being a mean value in the Am data. To reflect the large scattering in R_d values observed by different laboratories, the upper and the lower limits were chosen as 5×10^6 and 100 L/kg, respectively. The upper limit is extended to 5×10^6 L/kg to account for the Eu data. Many of the data came from a study

that used centrifugation rather than filtration and this could have resulted in greater experimental scatter (Allard et al. 1984).

The lower limit for State I is lower in comparison with the lower limit for other States, although the sample size for the other states is smaller than that for State I. Therefore, the opposite would have been more logic from a statistical point of view. The error ranges indicated (i.e. upper and lower bound) should therefore be cautiously used, as their derivation is more driven by visual analysis of summary data plots rather than a statistical one. This is especially true in view of the new evidence that the Allard et al. (1984) study was problematic due to (1) use of centrifugation rather than filtration and (2) potential analytical problems encountered when using elevated levels of ^{40}K.

7.3.3 Sorption at State II

Based on the speciation, the experts would expect similar R_d values for States I, II, and much of III. Overall, the experts were comfortable with the same R_d values for best estimates and upper limits for States I–III. The lower limits were varied to reflect the experimental scatter. The best estimate R_d for State II is again 10^4 L/kg and the upper and the lower limits are 5×10^6 and 10^3 L/kg, respectively. There were no known Eu data for State II.

7.3.4 Sorption at State III

The experts expected the speciation of Am to change across State III, but the R_d values did not show any effect, there being comparatively little scatter. It was, however, decided to keep the same values for best estimate (10^4 L/kg) and upper bound (5×10^6 L/kg) but to raise the lower bound slightly to 3×10^3 L/kg. This slight rise could be justified by considering that Am should be a cationic species for much of State III. The Eu sorption data were taken into account by keeping the upper bound at 5×10^6 L/kg for all four states.

7.3.5 Sorption at State IV

It was felt that, based on the data available, there was a logic in maintaining the same values for State IV as State III, there being no obvious reason why this was not appropriate. The best estimate is therefore 10^4 L/kg, upper bound 5×10^6 L/kg and lower bound 3×10^3 L/kg (Table 7.1).

Table 7.1 Selected best estimate, upper and lower limit R_d values for Am

pH state	Best estimate (L/kg)	Upper limit (L/kg)	Lower limit (L/kg)
State I	1×10^4	5×10^6	1×10^2
State II	1×10^4	5×10^6	1×10^3
State III	1×10^4	5×10^6	3×10^3
State IV	1×10^4	5×10^6	3×10^3

References

B. Allard, L. Eliasson, S. Hoglund, K. Andersson, Sorption of Cs, I and actinides in concrete systems, SKB Technical Report (1984), pp. 84–15

G.M.N. Baston, J.A. Berry, M. Brownsword, T.G. Heath, C.J. Tweed, S.J. Williams, Sorption of plutonium and americium on repository, backfill and geological materials relevant to the JNFL low-level radioactive waste repository at Rokkasho-Mura, in *Proceedings of the Material Research Society Symposium*, vol. 353 (1995), pp. 957–964

S. Bayliss, R. McCrohon, P. Oliver, N.J. Pilkington, H.P. Thomason, Near-field sorption studies: January 1989–June 1991. NSS/R277, AEA-ESD-0353 (1996)

S. Bayliss, R.M. Howse, R. McCrohon, P. Oliver, Near-Field sorption studies. AEAT/ERRA-0073 (2000)

U. Berner, *Project Opalinus Clay: Radionuclide Concentration Limits in the Cementitious Near-Field of an ILW Repository* (PSI Bericht, Villigen, 2002), pp. 02–26

M.H. Bradbury, B. Baeyens, *Far-field Sorption Data Bases for Performance Assessment of a L/ILW Repository in an Undisturbed Palfris Marl Host Rock* (PSI Bericht, Villigen, 1997), pp. 97–15

M.H. Bradbury, B. Baeyens, Modelling the sorption of Mn(II), Co(II), Ni(II), Zn(II), Cd(II), Eu(III), Am(III), Sn(IV), Th(IV), Np(V) and U(VI) on montmorillonite: linear free energy relationships and estimates of surface binding constants for some selected heavy metals and actinides. Geochim. Cosmochim. Acta **69**, 857–892 (2005)

G.R. Choppin, E.N. Rizkalla, Solution chemistry of actinides and lanthanides, in *Handbook on the Physics and Chemistry of Rare Earths*, ed. by K.A. Gschneidner Jr., L. Eyring, G.R. Choppin, G.H. Lander (Elsevier, Amsterdam, 1994)

M. Cowper, S. Baker, A.V. Chambers, T.G. Heath, M. Mihara, S.J. Williams, The sorption of thorium and americium onto fresh and degraded ordinary Portland cement and onto green tuff, in *Proceedings of the Material Research Society Symposium*, vol. 932 (2006), pp. 925–932

N.D.M. Evans, Binding mechanisms of radionuclides to cement. Cem. Concr. Res. **38**, 543–553 (2008)

M.M. Fernandes, M. Schmidt, T. Stumpf, C. Walther, D. Bosbach, R. Klenze, T. Fanghanel, Site-selective time-resolved laser fluorescence spectroscopy of Eu3+ in calcite. J. Colloid Interface Sci. **321**, 323–331 (2008)

R. Guillaumont, T. Fanghanel, V. Neck, J. Fuger, D. Palmer, I. Grenthe, M.H. Rand, *Update on the Chemical Thermodynamics of Uranium, Neptunium, Plutonium, Americium and Technetium* (Elsevier, OECD, Issy-lès-Moulineaux, 2003)

W. Hummel, U. Berner, E. Curti, F.J. Pearson, T. Thoenen, *Nagra/PSI Chemical Thermodynamic Data Base 01/01* (Universal Publishers, Parkland, 2002)

J.I. Kim, Chemical behaviour of transuranic elements in natural aquatic systems, in *Handbook of the Physics and Chemistry of the Actinides*, vol. 4, ed. by A.J. Freeman, C. Keller (North-Holland Press, Amsterdam, 1986), pp. 413–455

Nuclear Decommissioning Authority (NDA), The 2010 UK radioactive waste inventory: main report, Report prepared for the Department of Energy and Climate Change (DECC) and the Nuclear Decommissioning Authority (NDA) by Pöyry Energy Limited, Feb 2011

ONDRAF/NIRAS, Identification of critical radionuclides through a screening of the ONDRAF/NIRAS 2003/2004 radiological inventory for category: a waste, Brussels, Apr 2008

I. Pointeau, B. Piriou, M. Fedoroff, M.-G. Barthes, N. Marmier, F. Fromage, Sorption mechanisms of Eu3+ on CSH phases of hydrated cements. J. Colloid Interface Sci. **236**, 252–259 (2001)

I. Pointeau, C. Landesman, N. Coreau, C. Moisan, P. Reiller, Etude de la rétention chimique des radionucléides Cs(I), Am(III), Zr(IV), Pu(IV), Nb(V), U(VI) et Tc(IV) par les matériaux cimentaires dégradés, CEA report 2004, RT DPC/SECR 03-037 indice A (2004)

M.L. Schlegel, I. Pointeau, N. Coreau, P. Reiller, Mechanism of Europium retention by calcium silicate hydrates: an EXAFS study. Environ. Sci. Technol. **38**, 4423–4431 (2004)

R.J. Silva, G. Bidoglio, M.H. Rand, P.B. Robouch, H. Wanner, I. Puigdomenech, *Chemical Thermodynamics of Americium*. (OECD/NEA, Paris, 1995), p. 374

D.L. Stout, S.A. Carroll, A literature review of actinide-carbonate mineral interactions. SAND92-7328 (1993)

T. Stumpf, J. Tits, C. Walther, E. Wieland, T. Fanghanel, Uptake of trivalent actinides (curium(III)) by hardened cement paste: a time-resolved laser fluorescence spectroscopy study. J. Colloid Interface Sci. **276**, 118–124 (2004)

J. Tits, E. Wieland, M.H. Bradbury, J.-P. Dobler, The uptake of Eu(III) and Th(IV) by cement-type minerals in the alkaline disturbed zone of a nuclear waste repository, in *Applied Mineralogy in Research, Economy, Technology, Ecology and Culture*, ed. by D. Rammlmair, J. Mederer, T. Oberthür, R.B. Heimann, H. Pentinghaus (Balkema, Rotterdam, 2000)

J. Tits, E. Wieland, M.H. Bradbury, P. Ecker, A. Schaible, *The Uptake of Eu(III) and Th(IV) by Calcite under Hyperalkaline Conditions* (PSI Bericht, Villigen, 2002), pp. 02–03

J. Tits, T. Stumpf, T. Rabung, E. Wieland, T. Fanghanel, Uptake of Cm(III) and Eu(III) by calcium silicate hydrates: a solution chemistry and time-resolved laser fluorescence spectroscopy study. Environ. Sci. Technol. **37**, 3568–3573 (2003)

J. Tits, E. Wieland, M.H. Bradbury, The effect of isosaccharinic acid and gluconic acid on the retention of Eu(III), Am(III) and Th(IV) by calcite. Appl. Geochem. **20**, 2082–2096 (2005)

E. Wieland, L. Van Loon, *Cementitious Near-Field Sorption Data Base for Performance Assessment of an ILW Repository in Opalinus Clay* (PSI Bericht Nr., Villigen, 2002), pp. 03–06

E. Wieland, J. Tits, P. Spieler, J.-P. Dobler, Interaction of Eu(III) and Th(IV) with sulphate-resisting Portland cement, in *Proceedings of the Material Research Society Symposium*, vol. 506 (1998), pp. 573–578

Chapter 8
Sorption Values for Selenium, Molybdenum, and Technetium

Abstract Selenium, molybdenum, and technetium belong to groups VIB, VIA, and VIIA, of the periodic table, respectively, and form highly soluble and mobile oxo-anions in aqueous solutions under oxidising and moderately reducing conditions (molybdenum only exists as the hexavalent MoO_4^{2-} oxo-anion under all conditions). As uranium fission products, isotopes of these elements are common in radioactive wastes. Based on good evidence for selenate, Se(VI), and on supplemental information and chemical analogies for molybdate, Mo(VI), and pertechnetate, Tc(VII), these elements are preferentially taken up by the sulphate–aluminate minerals (ettringite, monosulphate) in their highest oxidation states, where the oxo-anions can substitute for sulphate ions. Thus, sorption of these ions would be favoured by a high content of sulphate–aluminate minerals and a low aqueous concentration of competing sulphate ions. This is also relevant for selenite oxo-anions, Se(IV), but selenite sorbs additionally on all other mineral phases of importance in HCP. Under strongly reducing conditions, Se(−II) and Tc(IV) become relevant. No reliable information is available for Se(−II), and zero sorption must be assumed. On the other hand, technetium (IV) sorbs strongly onto hydrated cement paste and CSH phases, which is consistent with its hydrolysis behaviour.

8.1 Selenium

8.1.1 Chemical Form, Speciation, and Solubility

Selenium is a non-metal, chemically related to sulphur and tellurium. Elemental selenium is occasionally found. There are around 40 known selenium-containing minerals, some of which can have as much as 30 % selenium. All of them are rare and occur generally together with sulphides of metals such as copper, zinc, and lead. The average concentration of stable selenium in the earth's crust is approximately 0.05 ppm. The concentration of stable selenium in surface water varies

© Springer International Publishing Switzerland 2016

M. Ochs et al., *Radionuclide and Metal Sorption on Cement and Concrete*,
Topics in Safety, Risk, Reliability and Quality 29,
DOI 10.1007/978-3-319-23651-3_8

from 0.1 to 100 ppb, with an average concentration of 0.2 ppb. ^{79}Se is generally not detected in the environment (IRSN 2005).

Six stable isotopes occur in the natural environment, from which most abundant isotopes are ^{80}Se(50 %) and ^{78}Se(24 %) (Lide 1998). Five oxidation states occur: selenide Se^{2-}, an anion with oxidation number of −2(−II), elemental selenium Se^0(0), thioselenate $Se_2O_3^{2-}$(+II), selenite SeO_3^{2-}(+IV), and SeO_4^{2-} selenate(+VI) (Sors et al. 2005; Simonoff and Simonoff 1991).

Some selenium isotopes are radioactive. ^{79}Se is a fission product of ^{235}U. It is present in spent nuclear fuel, in the radioactive waste coming from the reprocessing plants and in the discharges from nuclear plants and fuel reprocessing plants. Its half-life has been variously reported as 6.5×10^5 years, 6.5×10^4 years, 1.13×10^6 years, 4.8×10^5 years (IRSN 2005), 2.95×10^5 years (Song-Sheng et al. 2001), and 2.8×10^5 years (He et al. 2002). In our calculations, we use the value proposed in the JEFF database, which is 3.56×10^5 years (NEA 2006). ^{79}Se decays by emitting a beta particle with no attendant gamma radiation. Another important radioactive isotope of selenium is ^{75}Se. This artificial isotope is commonly used as a tracer (Haygarth 1994) and has a half-life of 120 days (NEA 2006). ^{79}Se is typically present in LILW.

Data on the probable speciation of selenium in cement are scarce. To facilitate understanding, calculations have been undertaken of the speciation state in respect of water and on the impact of changing redox conditions.

Selenium is redox sensitive, with oxidation states −2, 0, +2, +4, and +6. Eh–pH diagrams in a pure water system are presented in Fig. 8.1. It is seen that the most important aqueous species of Se in a pure water system are SeO_4^{2-} (selenate) and SeO_3^{2-} (selenite) under oxidising and relatively reducing conditions. Note that in producing the aqueous speciation diagram (top graph) the solid phases were ignored. When solid phases are included, selenium can be readily reduced to relatively insoluble Se^0 (bottom graph). The aqueous Se(−II) species are only stable under strongly reducing conditions.

In a cement system, Se speciation may also be influenced by forming complexes with Ca (see Fig. 8.2). It seems, however, that the Ca–Se complexes are only relevant at State II because both $CaSeO_4$ and $CaSeO_3$ species are stable only when the Ca concentration is relatively high (i.e. higher than mmol level).

In a reducing environment, Se^0 can be insoluble and its potential as a solubility controlling phase is discussed in the following paragraphs. Other precipitated Se(−II) phases associated with Fe (present in cement as corrosion product) and Ni (present as impurity in cement) also have low solubilities. Scoping calculations[1] (results not shown) indicated that these phases are not formed under the expected conditions in the proposed Dessel facility. Therefore, Se^0 and Se–Ca phases are believed to be the only relevant phases for this discussion.

[1]The following conditions were used: redox −230 mV, Se inventory concentration ~10^{-6} mol/L, and Ni and Fe concentration of 10^{-7} mol/L.

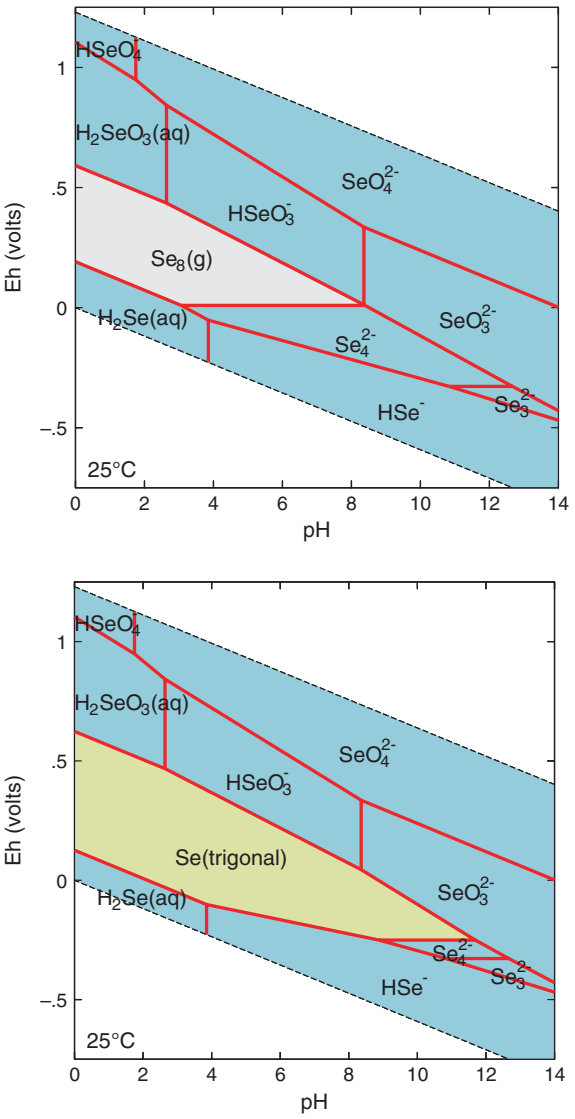

Fig. 8.1 Eh–pH diagram for a Se–H_2O system without (*top*) and with (*bottom*) precipitation of oversaturated solids. Se activity is 10^{-8}. Thermodynamic database: ThermoChimie 7b with addition of gaseous species of Se based on the NEA review

Under reducing conditions, the solubility of Se^0 in the presence of Ca can be expressed by the following:

$$\mathrm{Se(s) + 3\ H_2O + Ca^{2+} = 4e^- + 6H^+ + CaSeO_3} \tag{8.1}$$

At 25 °C, the solubility equation can be written as follows:

$$-58.16 = -67.61 \times \mathrm{Eh} - 6\mathrm{pH} + \log \mathrm{a[CaSeO_3]} - \log \mathrm{a}\left[\mathrm{Ca^{2+}}\right] \tag{8.2}$$

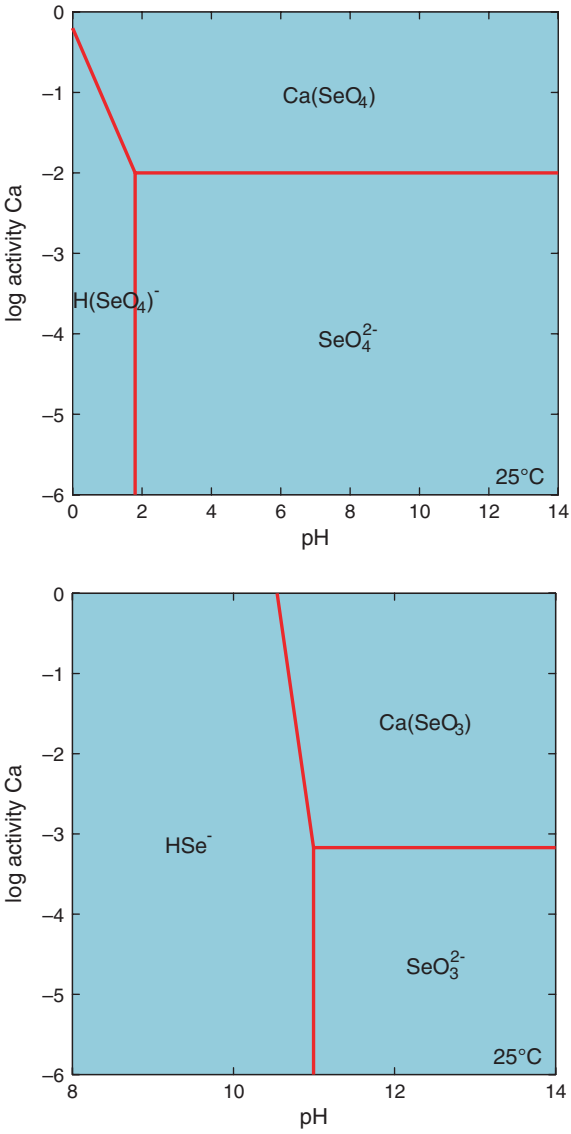

Fig. 8.2 Selenium speciation as a function of pH and calcium activity under oxidising (oxygen fugacity $f(O_2) = 0.2$ (dimensionless), *top*) and reducing (Eh = −230 mV, *bottom*) conditions. Se activity 10^{-8}, no precipitation of solids over the range of activities depicted. Thermodynamic database: ThermoChimie 7b

At Eh of −230 mV, pH 12.5, and Ca activity about 0.02, the solubility of Se^0 with dominant aqueous species as $CaSeO_3$ is about 0.4 mol/kg. With such a high solubility, we may expect that at the State II of cement degradation, Se concentration is unlikely to be solubility limited by Se^0.

In States I, III, and IV where Ca concentration is relatively low, the solubility of Se^0 is probably controlled by the following reaction with SeO_3^{2-} as the main aqueous species:

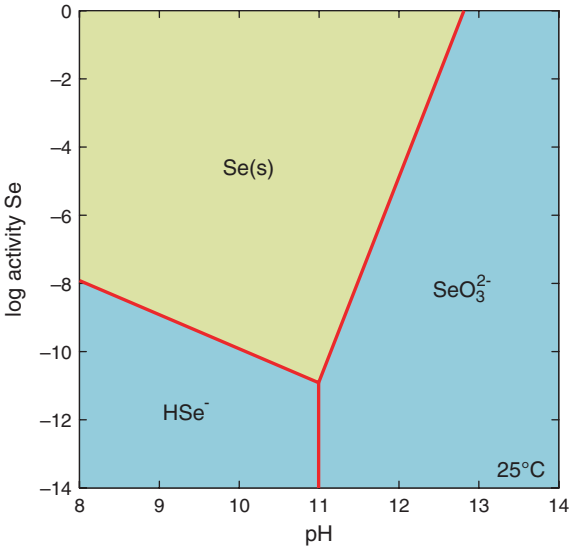

Fig. 8.3 Solubility of Se^0 at Eh −230 mV in a Se–H_2O system. Thermodynamic database: ThermoChimie 7b

$$Se(s) + 3H_2O = 4e^- + 6H^+ + {SeO_3}^{2-} \log K = -61.32(25\ ^\circ C) \quad (8.3)$$

Under reducing conditions, e.g. at Eh −230 mV (see discussion in Sect. 2.4), the above reaction can be expressed as solubility of Se^0 as shown in Fig. 8.3. It can be seen that the solubility of Se^0 is very high at States I and II pH values but decreases sharply with pH, e.g. if pH decreases one unit from 12 to 11 (State III), Se^0 solubility drops from 10^{-5} to 10^{-11} mol/kg.

Relevant Se solid phases for controlling solubility might be Se^0, and calcium–selenium phases $CaSeO_4{\cdot}2H_2O$ and $CaSeO_3{\cdot}H_2O$.

Solubility diagrams representative for States I and II for $CaSeO_4{\cdot}2H_2O$(s) and $CaSeO_3{\cdot}H_2O$(s) are given in Figs. 8.4 and 8.5, assuming that the system is in equilibrium with portlandite.

Figure 8.4 shows that under oxidising conditions, $CaSeO_4{\cdot}2H_2O$(s) is very soluble so it is not likely to form. Under relatively reducing conditions (Eh −230 mV), the solubility of $CaSeO_3{\cdot}H_2O$(s) is around 10^{-5} mol/kg in States I and II as shown in Fig. 8.5 following the dissolution reaction used in the "ThermoChimie v7b" database:

$$CaSeO_3 :\ H_2O(s) \leftrightarrow Ca^{2+} + {SeO_3}^{2-} + H_2O\ \log K_{SO} = -6.4 \quad (8.4)$$

As a conclusion, the dissolved selenium concentration in a cement system is likely to be unlimited by solubility. Only under reducing conditions at a pH above 12 where Ca concentrations are high, Se concentration could be controlled by the solubility of $CaSeO_3{\cdot}H_2O$ at around 10^{-5} mol/kg. However, in the near-surface disposal facility of Dessel, reducing conditions may only develop very locally. It is therefore relevant to consider that aqueous Se is likely to exist only in the +VI

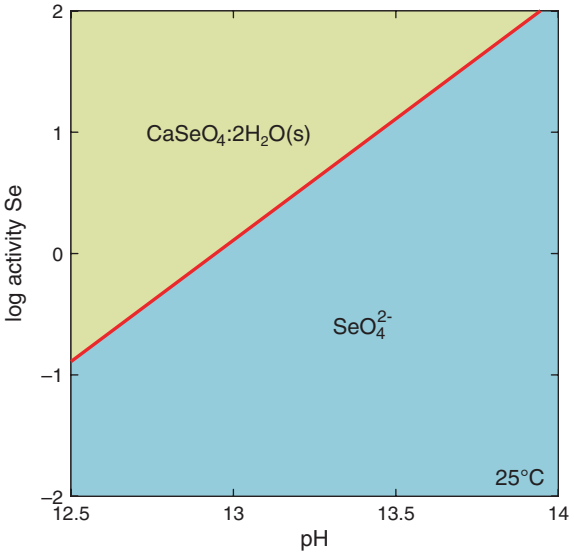

Fig. 8.4 Solubility of $CaSeO_4 \cdot 2H_2O$ under oxidising conditions (O_2 fugacity 0.2) in the presence of portlandite. Thermodynamic database: ThermoChimie 7b

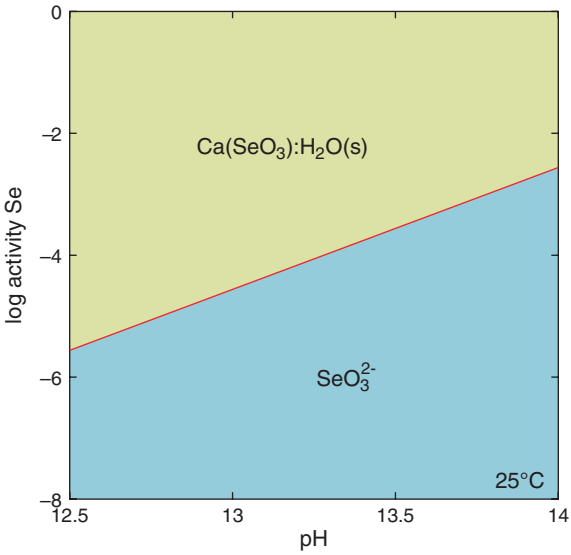

Fig. 8.5 Solubility of $CaSeO_3 \cdot H_2O$ at Eh −230 mV in the presence of portlandite. Thermodynamic database: ThermoChimie 7b

oxidation state whose concentration will not be limited by solubility. This view is consistent with solubility assessments done by Berner (2002) and Pickett et al. (2009).

Note that the applicability of the speciation diagram (Fig. 4.10) is limited, as several phenomena are not anticipated. Indeed, if data in Fig. 4.10 are extrapolated to

lower pH, they do not agree well with the data by Baur (Table 4.5), and the experimental solubility seems to be about an order of magnitude higher. The position is undoubtedly complicated by solid-solution formation (Lothenbach et al. 1999).

8.1.2 *Sorption Values from the Literature for the Benchmark Cement*

Based on the previous section, sorption of selenate and selenite, and possibly also of selenide, needs to be considered. No data were found for selenide. Reviewed R_d values for selenium(IV) and selenium(VI) in a cementitious system are presented in Figs. 8.6 and 8.7, respectively. A summary of experimental conditions of the above studies is given in Table A.14; further relevant information is summarised below. These data are from Ochs and Talerico (2006), Sugiyama and Fujita (1999), Baur and Johnson (2003), Kato et al. (2002), Lothenbach et al. (1999), Ochs et al. (2002), Johnson et al. (2000), Pointeau et al. (2006, 2008), Mace et al. (2007), Cowan et al. (1990), Ticknor et al. (1988), and Staudt et al. (1994).

Ochs and co-workers: *Se(IV) and Se(VI)*

- Se(VI) sorption was studied in detail on ettringite as a function of selenate as well as sulphate concentrations for a range of equilibration times (up to about 700 days). Additional experiments were carried out with fresh (~State I) and

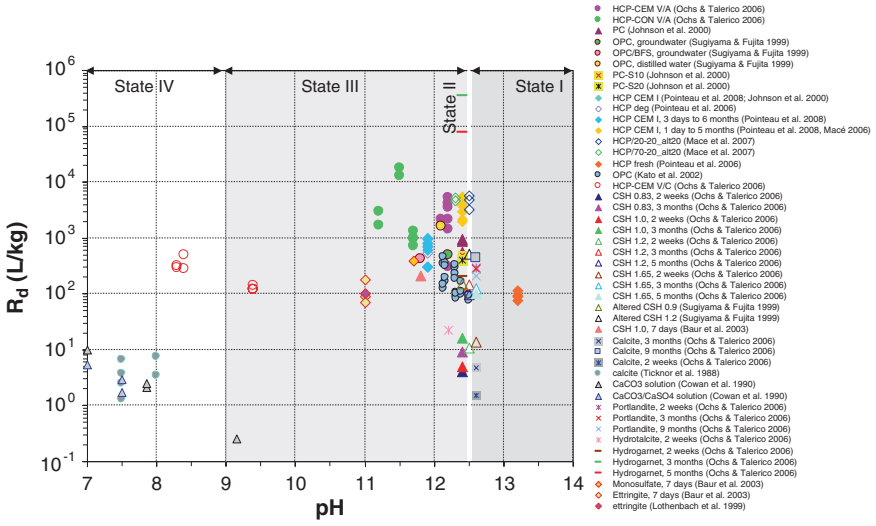

Fig. 8.6 Distribution ratio (R_d) of selenium(IV) in cementitious systems as a function of pH. *HCP* hardened cement paste; *OPC* ordinary Portland cement paste; HCP CEM V samples: */A* leached, */C* carbonated, *CON* mortar; *CSH* Ca-Si hydrate, *BFS* blast furnace slag

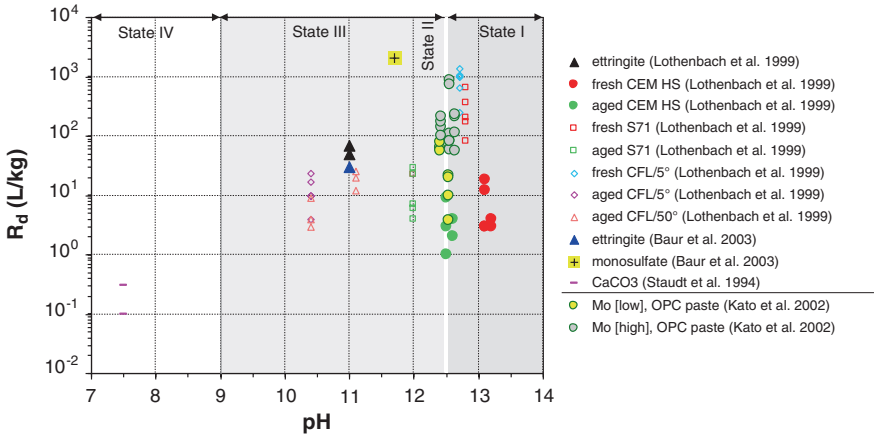

Fig. 8.7 Distribution ratio (R_d) of selenium(VI) and molybdenum(VI) in cementitious systems as a function of pH. *OPC* ordinary Portland cement; *CEM HS* sulphate resisting Portland cement. The values for calcite are a range estimated by Ochs et al. (2001). Mo [low] refers to an initial Mo concentration in the range of ca. 5–7.5 $\times$ 10^{-7} mol/L, Mo [high] to a range of ca. 4 $\times$ 10^{-6} to 6 $\times$ 10^{-5} mol/L

leached (~State II) HCP made from SRPC (as well as samples of Ca-aluminate cements). The experiments were also performed with Cr(VI). An empirical solid-solution model was developed that allowed reproduction of sorption of several oxo-anions (Se(VI), Cr(VI), Re(VII)) on cementitious materials for a wide range of solid and solution composition (Ochs et al. 2002).

- For selenate, relatively weak sorption was observed on HCP, but strong sorption was observed on ettringite. A series of experiments with different selenate/sulphate ratios suggests strongly that selenate replaces sulphate in the ettringite structure and allowed development of an empirical solid-solution model relating the sorption of selenate to the sulphate concentration in the solid and solution. This is consistent with the findings of Baur and Johnson (2003).
- For selenite, sorption on ettringite was weaker than in case of Se(VI). On the other hand, selenite sorbed appreciably on nearly all HCP minerals investigated as well as on HCP. This suggests a more generic sorption mechanism (such as surface sorption/ligand exchange, incorporation in CSH) in addition to possible replacement of sulphate in Al-sulphates.

Pointeau and co-workers Se(IV)

- Mace et al. (2007) investigated the influence of temperature by performing curing/alteration and sorption experiments at 20 and 70 °C. At the higher temperature, sorption of Se(IV) was reduced to about 30 % of the value observed at 20 °C, which was presumably due to the destabilisation of ettringite and an increase of the crystallinity of CSH (concomitant with a decrease in specific surface area). *For the present version of the report, only those data corresponding to 20 °C are considered.*

Baur and Johnson: Se(IV) and Se(VI)

- Baur and Johnson (2003) measured the sorption of selenite and selenate to ettringite, monosulphate, and CSH phases. They observed fast sorption kinetics, and equilibrium was reached within 1 day.
- For selenate, they observed only weak sorption on ettringite, but strong sorption on monosulphate. XRD analyses indicating changes of monosulphate layer spacing as a function of selenate concentration are consistent with selenate replacing sulphate. Only insignificant sorption of selenate was observed on CSH minerals.
- For selenite, they propose sorption via some type of surface reactions, based on roughly equally strong sorption on ettringite, monosulphate, and CSH.

Cowan et al.: *Se(IV) and Se(VI)*

- Selenite sorption was observed to decrease in the presence of phosphate and sulphate. Sorption was interpreted and modelled in terms of a carbonate/selenite ligand exchange reaction, with < 5 % of the surface sites being available for this process (Cowan et al. 1990).

8.1.3 Sorption Mechanisms and Selected Sorption Values

8.1.3.1 Sorption Mechanisms

Based on the literature reviewed, it appears relatively well established that Se(VI) is preferentially taken up by the sulphate–aluminate minerals (ettringite, monosulphate) and that the oxyanions—selenite and selenate—can substitute for sulphate ions. Potentially, this could result in either or both Se species appearing in the AFt and AFm phases of cement by lattice substitution as well as their sorption on CSH. Thus, sorption of selenate would be favoured by a high content of sulphate–aluminate minerals and a low aqueous concentration of competing sulphate ions.

Selenite appears to sorb on all mineral phases of importance in HCP, with no pronounced influence of relevant conditions (pH, degradation state). The sorption mechanism is not known.

To account for uncertainties in the oxidation state of selenium, sorption values are proposed separately for selenide(−II) (Table 8.1), selenite(IV) (Table 8.2) and selenate(VI) (Table 8.3). An overview for each oxidation state is given below, and further details regarding data for the individual degradation states are given in the following sections.

- Se(−II): no relevant sorption data could be found for selenide; “insufficient data” was assigned to all States. A supplemental value of zero sorption is proposed throughout, although it is expected that Se(−II) may be immobilised by HCP. This is consistent with the absence of sorption onto clay. Selenide formation is a slow process as reduction is kinetically very slow.

Table 8.1 Selected best estimate, upper and lower limit R_d values for selenide, Se(−II)

pH state	Best estimate (L/kg)	Upper limit (L/kg)	Lower limit (L/kg)
State I	i.d.[a]	i.d.	i.d.
State II	i.d.	i.d.	i.d.
State III	i.d.	i.d.	i.d.
State IV	i.d.	i.d.	i.d.

[a]*i.d.* insufficient data

Table 8.2 Selected best estimate, upper and lower limit R_d values for selenite, Se(IV)

pH state	Best estimate (L/kg)	Upper limit (L/kg)	Lower limit (L/kg)
State I	2×10^2	6×10^3	10
State II	2×10^2	6×10^3	10
State III	2×10^2	6×10^3	10
State IV	3	10	1

Table 8.3 Selected best estimate, upper and lower limit R_d values for selenate, Se(VI)

pH state	Best estimate (L/kg)	Upper limit (L/kg)	Lower limit (L/kg)
State I	3	20	1
State II	3	10	1
State III[a]—ettringite present	3	10	1
State III[b]—ettringite absent	0.1	0.3	0.01
State IV	0.1	0.3	0.01

[a]R_d may also be obtained by considering a functional relationship with the amount of ettringite and its evolution (R_d would not be a fixed number but variable). A value corresponding to pure ettringite present would be 50 L/kg

[b]Assumed no ettringite present. Values taken to be those for State IV

- Se(IV): in case of selenite, sorption mechanisms are not known, but sorption appears to be fairly uniform throughout States I–III of cement degradation. Most data for Se(IV) are available for State II. Sorption in State IV on calcite is lower than on the various HCP minerals. Based on these observations, it is proposed that recommended values for selenite are the same for States I–III. Data for State II will be the basis for deriving sorption values, as most available data are for State II and these are further supported by very similar data corresponding to the beginning of State III. Sorption on calcite is evaluated separately.
- In case of Se(VI), many fewer data are available. Sorption appears to take place mainly on sulpho-aluminates. Measurements on HCP are preferred for evaluating sorption, to avoid scaling from a R_d for a single mineral to whole HCP. Such values are available for conditions corresponding closely to State II.

8.1.3.2 Sorption at State I

The values proposed for Se(IV) for State II are also proposed for State I, i.e. 2×10^2 L/kg. This is not inconsistent with the values of Pointeau et al. (2006), i.e. nearly 120 L/kg for their maximum equilibration time of 170 days. Because only the data set of Pointeau et al. (2006) is available for State I, and because these data are within the range observed for State II (see below), no basis is seen for proposing a different value for State I than for State II.

In case of Se(VI), the best estimate and lower limit for State II are accepted for State I, which may be somewhat conservative. The upper limit is directly taken from the data for fresh HCP as 20 L/kg.

8.1.3.3 Sorption at State II

Based on the available experimental data for various HCP samples shown in Fig. 8.8, a best estimate R_d of 2×10^2 L/kg is proposed for selenite(Se(IV)). As lower limit, a value of 10 L/kg is proposed, taking into account the lowest values for CSH 1.2 and CSH 1.65. A value of 6×10^3 L/kg is proposed as upper limit.

For selenate, a best estimate R_d of 3 L/kg is proposed based on the data by Lothenbach et al. (1999), with upper and lower limits of 10 and 1 L/kg, respectively.

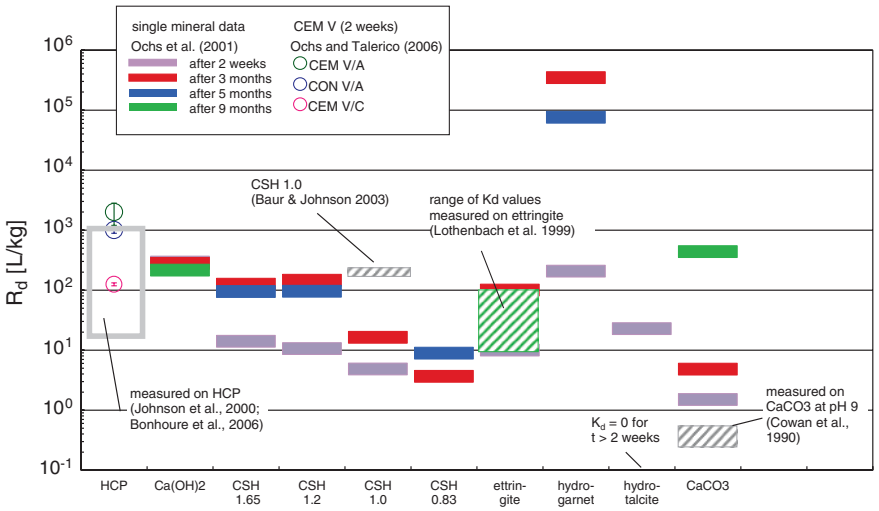

Fig. 8.8 Overview of measured R_d values for Se(IV) on various HCP and single mineral samples: CEM V samples (CEM samples: */A* leached, */C* carbonated, *CON* mortar) represent mean values ± their standard error; the values for the single mineral phases are single measurements recorded as a function of time. Modified from Andra (2005)

8.1.3.4 Sorption at State III

In case of Se(IV), the values proposed for State II are also accepted for State III. The data for leached calcareous CEM V mortar with calcareous aggregate (HCP-CON V/A) could be taken to indicate a slightly higher upper limit, but preference is given to data on HCP for the present purpose.

For the sorption of selenate, two options may be followed, based on the affinity of Se(VI) to ettringite and monosulphate, and the predicted disappearance of ettringite during State III (Fig. 2.2):

- In the absence of reliable data on the evolution of the concentration of ettringite, a more conventional approach can be followed: for the part of State III where the presence of ettringite can be assumed with certainty, the values proposed for State II are accepted (best estimate, upper and lower limit). For the remainder of State III, a cautious choice is made by proposing the values selected for State IV (see below). This approach is used to generate values in Table 8.3.
- If reliable data on the evolution of the concentration of ettringite in HCP are available, the following approach may be adopted. Rather than assigning discrete values for State III (note that State III is a heterogeneous system with different minerals disappearing one after the other potentially resulting in heterogeneous uptake mechanisms and sorption values), R_d is evaluated as a function of the amount of ettringite present. As ettringite disappears, R_d is believed to decrease proportionally. Estimates of ettringite evolution are available from calculations such as that shown in Figs. 2.2 and 8.12. The only parameter that is required then is an appropriate estimate for R_d on pure ettringite. Based on the data shown in Fig. 8.7, a best estimate R_d for pure ettringite (at pH values relevant for State III) of 50 L/kg is proposed, with 30 and 70 L/kg as lower and upper limit, respectively. Note that the higher value observed for monosulphate is conservatively neglected.

8.1.3.5 Sorption at State IV

All values measured for Se(IV) on calcite are in the range of 1–10 L/kg, except for the values by Cowan et al. (1990) and one value by Ochs and Talerico (2006) obtained after 9 months equilibration time. Contrary to the other data, the values by Cowan et al. (1990) indicate a decrease of sorption with increasing pH. However, their data were measured after only 24-h equilibration time and may reflect short-term surface sorption processes which may not be the relevant sorption mechanism for calcite over longer time frames. If long-term measurements in cement are considered, many elements will probably experience some kind of 3D uptake processes, which usually results in higher sorption values. Note that the latter consideration is true for sorption in all degradation states.

On the basis of these considerations, a best estimate R_d of 3 L/kg is proposed, with an upper limit of 10 L/kg [ignoring the higher value at high pH by Ochs and Talerico (2006)] and a lower limit of 1 L/kg.

Table 8.4 Supplemental R_d values for selenide, Se(−II)

pH state	Best estimate (L/kg)	Upper limit (L/kg)	Lower limit (L/kg)
State I	0	0	0
State II	0	0	0
State III	0	0	0
State IV	0	0	0

In case of Se(VI), only the estimates by Ochs et al. (2001) are available. To account for uncertainties that may not have been considered and because the sorption of Se(VI) had been observed during coprecipitation, a best estimate of 0.1 L/kg is proposed [corresponding to the lowest value estimated by Ochs et al. (2001)]. The upper limit of 0.3 L/kg is accepted on the basis of their estimates. As lower limit, a value of 0.01 L/kg is proposed, which is an order of magnitude lower than the lowest value estimated by Ochs et al. (2001). A value of zero is judged as overly conservative, because

- Staudt et al. (1994) observed small but nonzero uptake of both selenate and sulphate;
- Curti (1997) also calculated a small but nonzero partitioning coefficient for selenate on the basis of the data by Staudt et al. (1994); and
- on the basis of a weak analogy with Se(IV).

8.1.4 Supplemental Values for Assessment Calculations

In the cases where there are insufficient data are available to derive best estimate values and their upper and lower limits, so-called supplemental values are derived for the purpose of assessment calculations. Supplemental values are usually not supported by a vast amount of solid literature data, but may be based on chemical analogy and expert opinion. As the data are of a lesser quality, this approach necessarily leads to selection of conservative values. All supplemental values for assessment purposes for Se(−II) are zero (Table 8.4) (see Sect. 8.1.3.1).

8.2 Molybdenum

8.2.1 Chemical Form, Speciation, and Solubility

Molybdenum is a metallic element which belongs to the same group as tungsten and chromium. In natural waters, stable Mo concentrations vary between 0.01 (salt water) and 0.001 mg/L (fresh water) (Calmon et al. 2003). The most

stable oxidation state in water is +VI. The latter oxidation state is common in molybdenum(VI) oxide MoO_3, while the normal sulphur compound is molybdenum disulphide MoS_2.

Natural molybdenum is a mixture of several stable isotopes and consists of 14.84 % ^{92}Mo, 9.25 % ^{94}Mo, 15.92 % ^{95}Mo, 16.68 % ^{96}Mo, 9.55 % ^{97}Mo, 24.13 % ^{98}Mo, and 9.63 % ^{100}Mo (Tuli 1995). The isotopes ^{90}Mo, ^{91m}Mo, ^{91}Mo, ^{93m}Mo, ^{93}Mo, ^{99}Mo, ^{101}Mo, ^{102}Mo, and ^{105}Mo are radioactive. ^{99}Mo is a beta transmitter with a half-life of 65.9 h (NEA 2006) and is frequently used as a radioactive tracer (Yu et al. 2003). Typical molybdenum radionuclides in LILW are ^{93}Mo (half-life 4.00×10^3 year) and ^{99}Mo (half-life 4.52×10^{-3} year).

Data on the probable speciation of molybdenum in cement are scarce. To facilitate understanding, calculations have been undertaken of the speciation state in respect of water and on the impact of changing redox conditions.

Figure 8.9 gives a Eh–pH diagram for Mo, and it is obvious that the only aqueous species relevant to a cement system is the MoO_4^{2-} anion. In slag cements, however, sufficient sulphide could be present to form MoS_2.

With regard to solubility, calculations with the v7b Andra (2005) database demonstrated that the only solid phase relevant to control the dissolved Mo concentration should be $CaMoO_4$(s). Figure 8.10 shows the solubility diagram of the latter mineral phase assuming the system is in equilibrium with portlandite (constant dissolved calcium concentration). It shows that the activity of MoO_4^2, i.e. the solubility, decreases with decreasing pH and is controlled by the reaction:

$$CaMoO_4(s) + 2H_2O = Ca(OH)_2(s) + MoO_4^{2-} + 2H^+ \log K = -30.7 \quad (5)$$

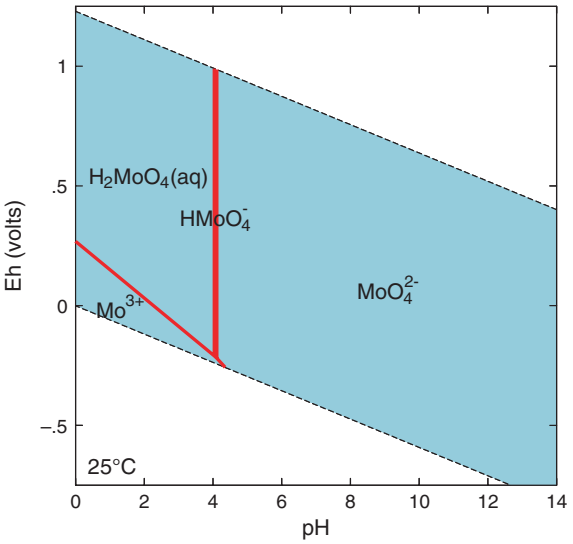

Fig. 8.9 Eh–pH diagram for molybdenum in a Mo-H_2O system. Mo activity 10^{-8}, no precipitation of solids. Thermodynamic database: ThermoChimie 7b

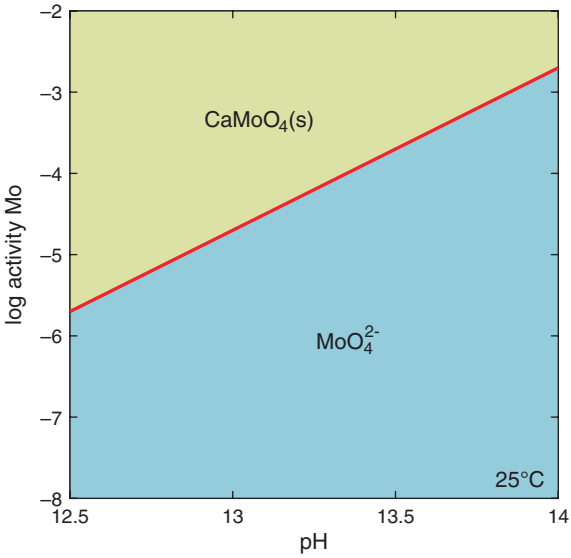

Fig. 8.10 Solubility of $CaMoO_4$(s) in the presence of portlandite (pH range is characteristic for degradation State I and II where portlandite is stable). Thermodynamic database: ThermoChimie 7b

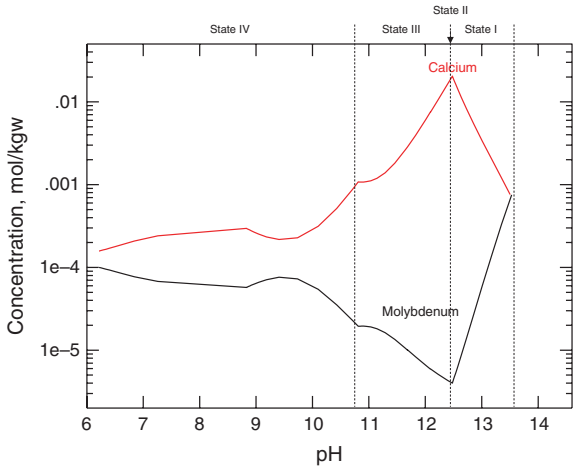

Fig. 8.11 Solubility of $CaMoO_4$(s) in a system where the concentration of calcium is controlled by the solubility of portlandite at State I–II (pH 13.5–12.5), at State III CSH_1.6 to pH ~ 12.1, CSH_1.2 to pH ~ 11.7, and CSH_0.8 to pH 10.8. Thermodynamic database: ThermoChimie 7b

At pH 13.5 and 12.5, the dissolved Mo concentration is 2×10^{-4} and 2×10^{-6} mol/kg, respectively. In States III and IV, the aqueous Ca concentration varies as function of pH, as the Ca concentration is regulated by the solubility of CSH phases, so that the solubility of $CaMoO_4$(s) will be affected.

Reaction path modelling was performed to simulate the solubility of $CaMoO_4$(s) with changing Ca concentration (Fig. 8.11). Dissolved calcium concentration is also shown.

In summary, the solubility of $CaMoO_4$(s) is at its lowest value around 10^{-6} mol/kg in State II (pH 12.5 and the dissolved Ca is 20 mmol/kg). In States I and IV, the $CaMoO_4$(s) solubility is at its highest value at about 10^{-4} mol/kg. In State III, the $CaMoO_4$(s) solubility increases from 10^{-6} to 10^{-4} with decreasing pH.

8.2.2 Sorption Values from the Literature for the Benchmark Cement

Only one study was found regarding sorption data of Mo on HCP. Kato et al. (2002) measured the sorption of molybdate on hydrated OPC paste that had been pre-equilibrated with water to reach about pH 12.1–12.5. They varied Mo(VI) concentration and solid/liquid ratio, but no other conditions (Table A.15). The data are plotted together with the data for selenate in Fig. 8.7. The values obtained at low initial Mo concentrations, where formation of $CaMoO_4$(s) is very unlikely, are in good agreement with values for selenate (see further in Sect. 8.2.3).

8.2.3 Sorption Mechanisms and Selected Sorption Values

With the exception of the data by Kato et al. (2002), no independent information is available for Mo(VI). However, selenate is a very good analogue for molybdate because these anions are isostructural and the anions (double negative) as well as the central atoms (+VI) have the same charge. In terms of sorption to HCP, it is of particular relevance that both molybdate and selenate have similar behaviour in terms of being able to replace sulphate in the key solid phases. In other words, in terms of critical sorption processes, both are almost identical. The few data available are in close agreement with those for Se(VI) (see this chapter).

In the absence of good data for Mo, and noting that fragmentary data for Mo show apparent agreement with those for Se, we use selenate as a chemical analogue. However, we note that Kindness et al. (1994) found much stronger bonding of Mo onto AFm relative to AFt, whereas the bonding of Se into AFt appears to be stronger. Clearly, more work is needed, but in the absence of conclusive data, the Se/AFt data probably represent a conservative data set as applied to Mo. Table 8.5 provides best estimates and associated upper and lower limits.

As for selenium(VI), no best estimate was derived for State III. The approach proposed for selenium(VI) will also be adopted for molybdenum, with R_d being related to the presence (and the amount) of ettringite in the system (Fig. 8.12). At 10 °C, ettringite is exhausted at about pH 11.3. Further details are proved in Sect. 8.1.3.4.

Table 8.5 Selected best estimate, upper and lower limit R_d values for molybdenum

pH state	Best estimate (L/kg)	Upper limit (L/kg)	Lower limit (L/kg)
State I	3	33	0.3
State II	3	33	0.3
State III[a]—ettringite present State III—ettringite absent	3 0.1	33 0.3	0.3 0.01
State IV	0.1	0.3	0.01

The condition "ettringite present" is valid up to ~pH 11.3; below this value, ettringite is exhausted ("ettringite absent")

[a]R_d may also be obtained by considering a functional relationship with the amount of ettringite and its evolution (R_d would not be a fixed number but variable). A value corresponding to pure ettringite present would be 50 L/kg

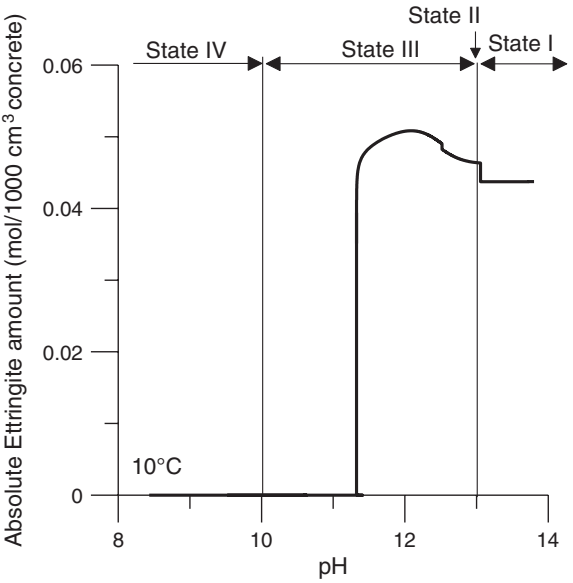

Fig. 8.12 Evolution of ettringite as function of pH

8.3 Technetium

8.3.1 Chemical Form, Speciation, and Solubility

Twenty-two isotopes of technetium exist, all radioactive. ^{99}Tc (half-life 2.14×10^5 years) is produced by the fission of uranium and plutonium in nuclear reactors (the majority of ^{99}Tc produced in a reactor is a result of ^{99}Zr decay, a primary fission product) and is not a naturally occurring radionuclide. It is typically present in reactor waste such as ion-exchange resins, evaporator bottoms or concentrated liquids, filters and sludges, and decommissioning waste (contaminated concrete and

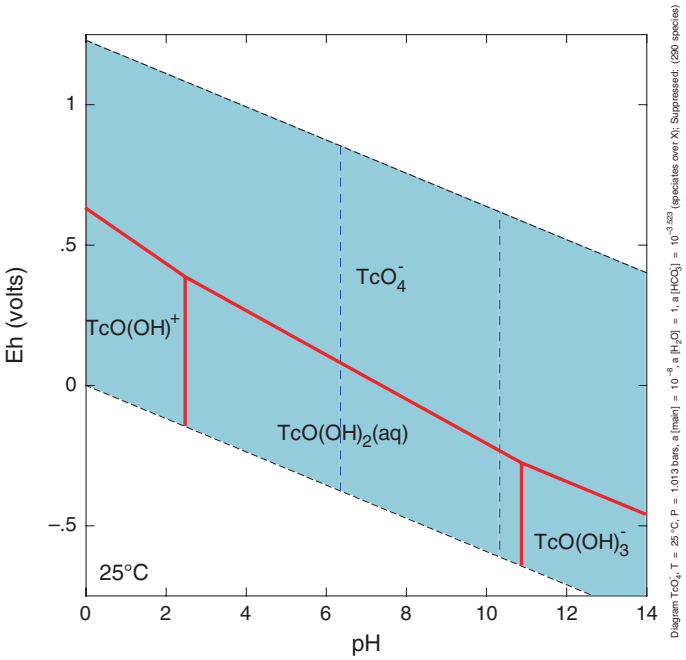

Fig. 8.13 Eh–pH diagram of technetium. Technetium activity 10^{-8}

metal vessels and piping). Small amounts of ^{99}Tc can also be present in LILW-SL generated at medical laboratories and research centres. Although ^{99}Tc is a fission product, it is also an activation product of stainless steel and Inconel (especially in 300-series stainless steel, as an activation product of stable ^{98}Mo). The predominant form of ^{99}Tc at a LILW-SL disposal facility is most probably the pertechnetate ion (TcO_4^-), because pertechnetate is the predominant chemical form of ^{99}Tc found in reactor wastes (USDOE 1996a, b).

^{99}Tc is redox sensitive: its electron structure makes it possible for technetium to exist in eight oxidation states ranging in charges from +7 to −1. The two most common oxidation states are +7 (pertechnetate) and +4 (technetium dioxide, TcO_2). The reduction of pertechnetate to the insoluble technetium dioxide species is not easily achieved and often requires strong reducing conditions before it can proceed. It is therefore assumed that Tc(VII) is always present to a certain extent.

The Eh–pH diagram for technetium is shown in Fig. 8.13, where speciation is produced with the thermodynamic data given in Table 8.6.

Technetium is redox sensitive, and the commonly occurring oxidation states in natural waters are Tc(+IV) and Tc(+VII). As predicted by the Eh–pH diagram in Fig. 8.13, under oxidising conditions technetium (+VII) exists as TcO_4^- (pertechnetate) across the whole pH range. In a reducing environment, technetium (+IV) may be present as $TcO(OH)_3^-$ at pH above 11 and the neutral species $TcO(OH)_2$ (aq) at other pHs of interest.

Table 8.6 Thermodynamic data of technetium species

Reaction	log K (25 °C)
$TcO(OH)_2(aq) + 0.75O_2(aq) = TcO_4^- + H + + 0.5H_2O$	35.0644
$TcO(OH)_3^- + 0.75O_2(aq) = TcO_4^- + 1.5H_2O$	45.9646
$TcO_2{:}1.6H_2O(s) + 0.75O_2(aq) = TcO_4^- + H + + 1.1H_2O$	26.6642
$TcO_2{:}1.6H_2O(s) + 0.4H_2O = TcO(OH)_3^- + H^+$	−19.3004
$TcO_2{:}1.6H_2O(s) = TcO(OH)_2(aq) + 0.6H_2O$	−8.4002

Database NEA 03 update (Guillaumont et al. 2003)

Technetium is not solubility limited under oxidising conditions since Tc(+VII) is very soluble. Under reducing conditions, Tc(+IV) may precipitate and form hydroxides. Because of its high hydrolysis tendency, technetium may form hydrated technetium dioxides in a cementitious environment as suggested by studies of Berner (2002) and Pilkington and Wilkins (1988). Figure 8.14 presents the calculated solubility of tetravalent $TcO_2{\cdot}1.6H_2O(s)$, the hydroxide likely to precipitate in a cementitious environment, at redox potential of −0.2 and −0.4 V.

The solubility of $TcO_2{\cdot}1.6H_2O(s)$ is constant at neutral and slightly alkaline pH but varies with Eh and pH in the alkaline pH range. At pH < 11 where $TcO(OH)_2(aq)$ species dominates the aqueous speciation of Tc, the solubility is about 4×10^{-9} mol/L as can be estimated by the reaction given:

$$TcO_2{\cdot}1.6H_2O(s) = TcO(OH)_2(aq) + 0.6H_2O \log K = -8.4\left(25\ ^\circ C\right) \quad (6)$$

At a higher pH where the aqueous speciation is $TcO(OH)_3^-$, the solubility can be calculated by:

$$\log\left\{TcO(OH)_3^-\right\} = pH - 19.3 \quad (7)$$

which is derived from the second last reaction given in Table 8.6. For example, at pH 12.5, the solubility of $TcO_2{\cdot}1.6H_2O(s)$ is around 1.6×10^{-7} M.

When the solution speciation of Tc(+VII) is controlled by TcO_4^-, the solubility of $TcO_2{\cdot}1.6H_2O(s)$ is a function of both pH and Eh following:

$$\log\left\{TcO_4^-\right\} = 4pH + 50.7Eh + 37.84 \quad (8)$$

which is obtained from the third reaction listed in Table 8.6 after replacing $O_2(aq)$ by Eh and proton activity by pH.

The solubility of freshly prepared technetium dioxide has been measured in cement waters of different compositions at pH 8–13 (Pilkington and Wilkins 1988). In the presence of sodium dithionite as reducing agent, the solubility of Tc(+IV) was determined as being around 10^{-7} mol/L which is in good agreement with the prediction made in Fig. 8.14, assuming $TcO(OH)_3^-$ as the dominant aqueous species. The same study revealed that in the absence of sodium dithionite, the solubility of Tc increased significantly, suggesting oxidation of Tc(IV) to Tc(VII) might have occurred. The latter finding is in line with the prediction of Fig. 8.14 where TcO_4^- dominates the Tc(VII) aqueous speciation. Also, the study showed that Tc solubility is independent of the type of cement leachate used, and the aqueous phase is free of Tc-containing colloids.

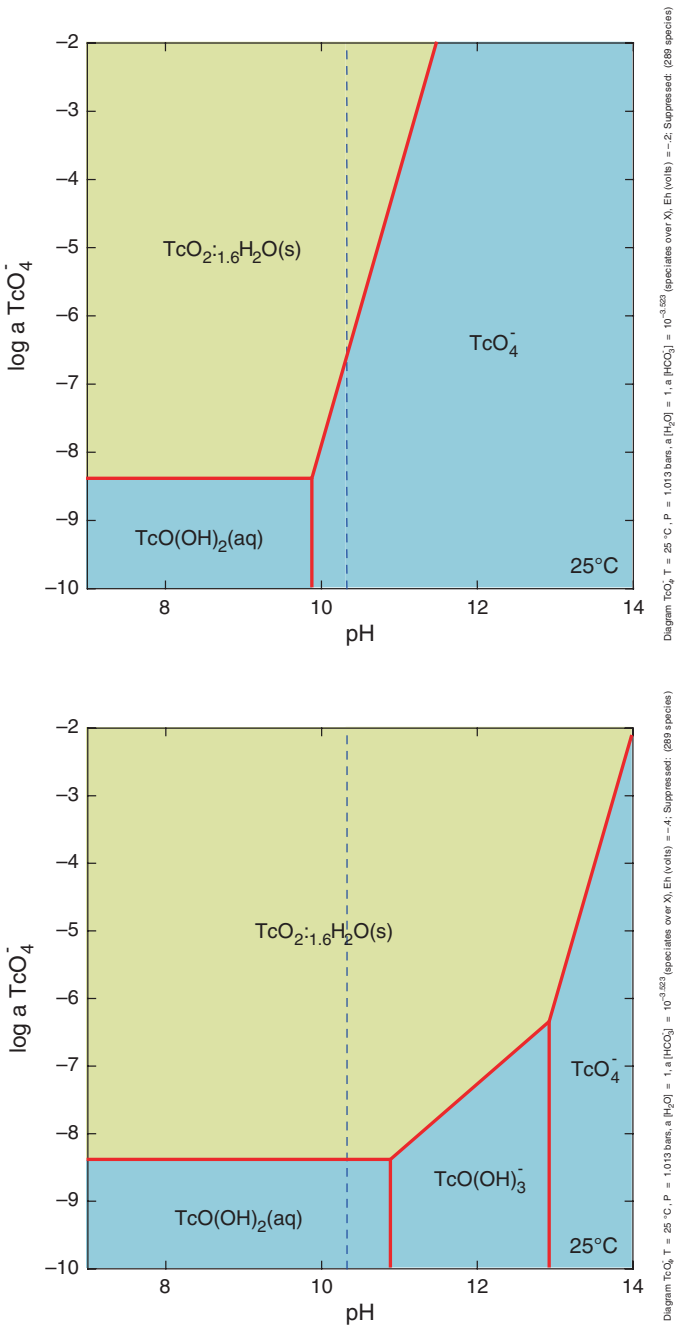

Fig. 8.14 Solubility of technetium as a function of pH at Eh = −0.2 V (*above*) and −0.4 V (*below*)

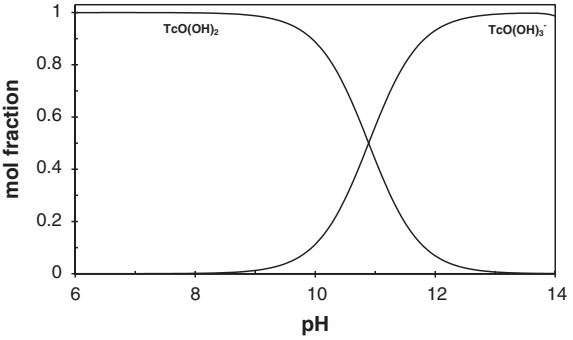

Fig. 8.15 Dissolved technetium (IV) speciation under reducing condition Eh = −500 mV (total Tc 1×10^{-8} molal, no precipitation of *solids*)

The most abundant aqueous Tc(IV) species at high pH relevant to cement systems are $TcO(OH)_3^-$ (pH > 11) and $TcO(OH)_2$(aq) (pH < 11), as predicted by the speciation diagram (Fig. 8.15) produced with the thermodynamic data from NEA (Guillaumont et al. 2003). For oxidising conditions, there is only one dominant species (TcO_4^-) across the entire pH range.

8.3.2 Sorption Values from the Literature for the Benchmark Cement

Reviewed literature R_d values and the experimental conditions under which these values are determined are summarised in Fig. 8.16 and Table A.16. It seems clear from the limited sets of data that R_d values are consistent in terms of the extent of uptake of Tc as a function of oxidation state: Tc(IV) sorbs strongly on cement materials, while Tc(VII) sorbs very weakly. Note that there should always be a reservation with Tc(IV) experiments as some data points may be influenced by trace oxidation to Tc(VII) which would decrease R_d. Because this cannot be quantified, one should be cautious with Tc(IV) data.

Besides the fact that precipitation of Tc(IV) could be an important retention mechanism in a high pH cement environment, mechanisms responsible for uptake of Tc(IV) by cements below the solubility limit are not known. For Tc(VII), Berner (1999) discussed the analogy of TcO_4^- to other oxo-anions, notably SO_4^{2-}, MoO_4^{2-}, and SeO_3^{2-} and presumed that a binding to/incorporation of TcO_4^- to AFm/AFt phases of the cements would be expected. There are no suitable analogies with any other element for Tc(IV).

Tc(VII) removal by NRVB, pulverised fuel ash/OPC, and blast furnace slag (BFS)/OPC was investigated by Baker et al. (2004). Starting with Tc(VII) in the system, R_d of Tc on NRVB was found to be small (R_d < 1) suggesting insignificant removal of Tc. In PFA and BFS containing OPC systems, Tc(VII) was found to be quantitatively removed. This latter finding was explained as being due to the reduction of Tc(VII) to Tc(IV) by sulphide present in the BFS system

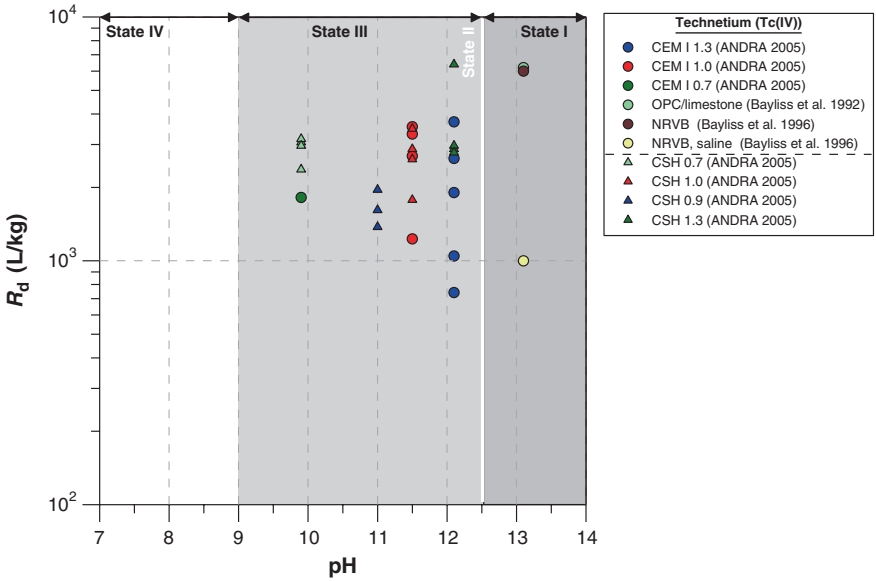

Fig. 8.16 Distribution ratio (R_d) of Tc(IV) in cementitious systems. Values are presented as a function of pH in terms of different states of cement evolution. *CSH* calcium silica hydrate; *NRVB* Nirex reference vault backfill

and subsequent precipitation of Tc(IV) sulphide (TcS_2 has been identified from EXAFS studies), but the mechanism in the PFA system was not clear (although reduction on the PFA/OPC surface was also assumed).

In a related study, Cowper et al. (2004) concluded that the removal of Tc from a PFA/OPC system was probably caused by the reaction between PFA and OPC (e.g. by sorption onto the product of the reaction between these materials). In a BFS/OPC equilibrated water, Tc was removed by the formation of Tc-sulphide solids, i.e. a solubility controlling process.

Uptake of Tc(IV) on cement CEM I and CSH phases was studied, and R_d values are reported by Andra (2005). The R_d values for cement materials and CSH phases were found to be quite similar so it was considered that the main uptake sinks for Tc(IV) in cements are CSH phases. Tc(IV) was prepared by electrochemical reduction. Hydrazine was employed as a holding reductant, solid/liquid separation was by 0.22 micron filtration, and equilibration times were 4–7 days. Measured redox potentials reported for CEM I and CSH were generally in the range of −220 to −360 mV. The results for Tc sorption onto CSH are very consistent and suggest that oxidation was not significant during the experiments. Therefore, the experiments provide good data for the sorption of Tc(IV).

A data point from the Andra (2005) data set with a value of just below 20,000 L/kg for CEM V was not included on the plot as the composition was considered irrelevant to the scenario under consideration. However, the experts felt

that the justification for excluding it was quite weak (CEM V is a little lower in aluminium content and a little higher in iron content, but this is a small difference). It was decided to take this value as the upper bound instead of 7000 L/kg.

8.3.3 Sorption Mechanisms and Selected Sorption Values

Technetium sorption onto cement is most of all influenced by the prevailing redox conditions in the cementitious environment. Data reveal that under oxidising conditions, Tc(VII) is considerably less strongly sorbed than Tc(IV) under reducing conditions: on average, a three orders of magnitude difference in R_d is observed (Fig. 8.16). In this respect, cements containing reducing components such as BFS (sulphides) will probably bring Tc into the tetravalent state which then results in high uptake values by formation of Tc-sulphide solids.

On the other hand, the experts noted that there is always a reservation with Tc(IV) R_d values as some data points may be influenced by trace oxidation to Tc(VII) which would decrease the value. This cannot be quantified but should be kept in mind.

The lower sorption of pertechnetate (TcO_4^-) may be explained on the basis of sorption studies using perrhenate (ReO_4^-) as an analogue (Ochs et al. 2002). The weak sorption of perrhenate in the system studied was due to competition with sulphate; perrhenate uptake was through solid-solution formation with ettringite. High pore water concentrations of sulphate give low R_d values, a result of ions such as perrhenate, selenate (SeO_4^{2-}), and chlorate (ClO_3^-) being replaced by sulphate in ettringite-like phases. Sulphate ions have a -2 charge, whereas pertechnetate is only -1: the former is therefore favoured for sorption onto positive sites compared to the latter.

Based on the speciation, there could be a trend depending on the pH: Tc(IV) could change from a -1 hydrolysis species at high pH to a neutral species as the pH decreases, but it is not possible to judge the effect of this from the available data. In other words, the observations of a constant R_d are in contradiction with the theories saying that speciation (and solubility) changes with pH (Fig. 8.14 and 8.15). The solubility increases with pH between pH 11 and 13, which would mean that the sorption would decrease. However, there is still some uncertainty on the formation constant of the species $TcO(OH)_3^-$. The current number is from the NEA database (Guillaumont et al. 2003), but there has been work since then (Warwick et al. 2007) which gives a lower estimate of the formation constant which would move the Tc(IV) neutral/anionic species boundary to higher pH (to the right). The latter would bring the theory into line with the current observations. In particular at low Eh, e.g. -550 mV, there may not be much speciation change.

8.3.3.1 Sorption Mechanisms

Technetium (IV) is known to sorb strongly onto HCP and CSH phases (Fig. 8.16), whereas sorption of technetium (VII) is considerably less strong.

There is little information available, however, about technetium sorption mechanisms onto such cementitious phases. Based on chemical analogy with other oxo-anions such as MoO_4^{2-} and $SnO(OH)_3^-$, sorption onto cement may be governed by binding to/incorporation of the AFm/AFt phases (Berner 1999). Quantitative information confirming such hypothesis is lacking at present.

Ochs et al. (2002) showed that solid-solution formation with ettringite explained in part the uptake of oxo-anions such as SeO_4^{2-} and ReO_4^- (an analogue[2] for TcO_4^-), with sulphate (in the hydrated cement and in the corresponding solution) being an important chemical parameter controlling the magnitude of sorption values. Here, the role of sulphate is to compete with oxo-anions so high sulphate concentration tends to hinder the uptake of oxo-anion radionuclides.

In one study, quantitative removal of Tc onto BFS/OPC was suggested as being due to the reduction of Tc(VII) to Tc(IV) by sulphides present in the BFS system and subsequent precipitation of Tc(IV) sulphide (TcS_2 has been identified from EXAFS studies elsewhere) (Baker et al. 2004).

Tc(VII)

Values for Tc(VII) are relevant for a near-surface repository that will experience both oxic and anoxic conditions throughout its lifetime. The experts agreed that they could attribute very low sorption to Tc(VII). Very few data are available, but all show very weak sorption. There was no evidence for differentiation between the states—there are no data for States II and III. On the basis of the very limited data, a best estimate of 1 L/kg was assigned for the four states. All known data fall within an order of magnitude of this value. No upper or lower limits were assigned.

Tc(IV)

For Tc(IV), the range of measured data was taken to provide the upper and lower bounds of R_d for States I–III (see Sect. 8.3.3.2).

It was noted that the R_d values from experiments with Tc(VII) are little affected by the presence of a small amount of Tc(IV), but the converse is not true. R_d values from experiments with Tc(IV) may be sharply influenced if some Tc(VII) is present.

8.3.3.2 Sorption at State I

Using the range of values in the data from Andra (2005) (which encompass and are in accord with other data), the experts agreed that there was no discernible

[2]Rhenium is often used as chemical analogue for technetium because the elements have similar radii and major oxidation states (+4 and +7).

Table 8.7 Selected best estimate, upper and lower limit R_d values for Tc(IV)

pH state	Best estimate (L/kg)		Upper limit (L/kg)		Lower limit (L/kg)	
	Tc(IV)	Tc(VII)	Tc(IV)	Tc(VII)	Tc(IV)	Tc(VII)
State I	3×10^3	1	2×10^4	i.d.	7×10^2	i.d.
State II	3×10^3	1	2×10^4	i.d.	7×10^2	i.d.
State III	3×10^3	1	2×10^4	i.d.	7×10^2	i.d.
State IV	i.d.	1	i.d.	i.d.	i.d.	i.d.

I.d. insufficient data

difference in R_d values between States I and III. It was noted that speciation is predicted to move from a (−1) species to a neutral species for Tc(IV) as the pH decreases, but this could not be seen to be having any effect from the current data. The experts agreed on a best estimate of 3000 L/kg with upper and lower bounds of 2×10^4 L/kg and 700 L/kg, respectively, the bounds being the limits of experimental data.

8.3.3.3 Sorption at State II

The experts agreed that there was no discernible difference in R_d values between States I and III (see above).

8.3.3.4 Sorption at State III

The experts agreed that there was no discernible difference in R_d values between States I and III (see above).

8.3.3.5 Sorption at State IV

No R_d values were proposed for State IV as no data were available that were relevant to this state. Additionally, there were felt to be no suitable analogous elements for Tc(IV) (Table 8.7).

References

Andra, in *Référentiel de comportement des radionucléides et des toxiques chimiques d'un stockage dans le Callovo-Oxfordien jusqu'à l'homme, Site de Meuse/Haute-Marne*. Tome 1/2: Chapitres 1 à 4, Dossier 2005 Argile (2005)

S. Baker, A. Green, S.J. Williams, The removal of technetium(VII) from alkaline solution by NRVB, PFA/OPC and BFS/OPC. A report produced for United Kingdom Nirex Limited, SA/ENV0606, AEAT/R/NS/0685 (2004)

I. Baur, C.A. Johnson, Sorption of selenite and selenate to cement materials. Environ. Sci. Technol. **37**, 3442–3447 (2003)
S. Bayliss, A. Haworth, R. McCrohon, A.D. Moreton, P. Oliver, N.J. Pilkington, A.J. Smith, J.L. Smith-Briggs, Radioelement behaviour in a cementitious environment. Mat. Res. Soc. Symp. Proc. **257**, 641–648 (1992)
S. Bayliss, R. McCrohon, P. Oliver, N.J. Pilkington, H.P. Thomason, Near-field sorption studies: January 1989 to June 1991, NSS/R277, AEA-ESD-0353 (1996)
U. Berner, *Concentration Limits in the Cement Based Swiss Repository for Long-Lived, Intermediate-Level Radioactive Wastes (LMA)* (PSI Bericht Nr. 99-10, Villigen, 1999)
U. Berner, *Project Opalinus Clay: Radionuclide Concentration Limits in the Cementitious Near-Field of an ILW Repository* (PSI Bericht 02-26, Villigen, 2002)
I. Bonhoure, I. Baur, E. Wieland, C.A. Johnson, A.M. Scheidegger, Se(IV/VI) immobilization by cementitious systems: An X-ray absorption study. Cem. Concr. Res. **36**, 91–98 (2006)
P. Calmon, J.M. Métivier, O. Simon, *Fiche radionucléide: Molybdène 99 et environnement (rév. 03/06/2003)* (Institut de Radioprotection et de Sûreté Nucléaire, Châtillon, 2003)
C.E. Cowan, J.M. Zachara, C.T. Resch, Solution ion effects on the surface exchange of selenite on calcite. Geochim. Cosmochim. Acta **54**, 2223–2234 (1990)
M. Cowper, A. Green, S.W. Swanton, The removal of technetium(VII) from alkaline solution by pulverised fuel ash, SA/ENV-0651 (2004)
E. Curti, *Coprecipitation of Radionuclides: Basic Concepts, Literature Review and First Applications* (PSI Bericht 97-10, Villigen, 1997)
R. Guillaumont, T. Fanghanel, V. Neck, J. Fuger, D. Palmer, I. Grenthe, M.H. Rand, *Update on the Chemical Thermodynamics of Uranium, Neptunium, Plutonium, Americium and Technetium* (Elsevier, Amsterdam, 2003). (OECD, Issy-lès-Moulineaux, France)
P.M. Haygarth, Global importance and global cycling of selenium, in *Selenium in the Environment*, ed. by W.T. Frankenberger Jr, S. Benson (Marcel Dekker, New York, 1994), pp. 1–27
M. He, S. Jiang, S. Jiang, L. Diao, S. Wu, C. Li, Measurement of the half-life of ^{79}Se with PX-AMS. Nucl Instr. Meth. B **194**(4), 393–398 (2002)
IRSN, Fiche Radionucléide, Sélénium et environnement (2005)
E.A. Johnson, M.J. Rudin, S.M. Steinberg, W.H. Johnson, The sorption of selenite on various cement formulations. Waste Manage. **20**, 509 (2000)
H. Kato, T. Mine, M. Mihara, T. Ohi, A. Honda, The sorption database of radionuclides for cementitious materials. JNC TN8400 2001-029, Japan Atomic Eneregy Agency (2002)
A. Kindness, E.E. Lachowski, A.K. Minocha, F.P. Glasser, Immobilization and fixation of molybdenum(VI) by portland cement. Waste Manage. **14**, 97–102 (1994)
D.R. Lide, *CRC Handbook of Chemistry and Physics*, 79th edn. (CRC Press, Boca Raton, 1998)
B. Lothenbach, M. Ochs, D. Hager, Confinement of radioactive waste in cementitious barriers for surface and deep geological disposal. Andra 2005 report 1999, C. RP.0BMG.99-001 (1999)
N. Mace, C. Landesman, I. Pointeau, B. Grambow, E. Giffault, Characterisation of thermally altered cement pastes. Influence on selenite sorption. Adv. Cem. Res. **19**, 157–167 (2007)
Nuclear Energy Agency (NEA-OECD), The jeff-3.1 nuclear data library. jeff report 21, oecd/nea, Paris, France (2006)
M. Ochs, C. Talerico, Development of models and datasets for radionuclide retention by cementitious materials. Andra 2005 report 2006, C.RP.0BMG.06.0001A (2006)
M. Ochs, B. Lothenbach, C. Talerico, Support of Kd models and datasets for the retention of radionuclides in cementitious repositories. Andra 2005 report C.RP.0BMG.01-001, Andra 2005, France (2001)
M. Ochs, B. Lothenbach, E. Giffaut, Uptake of oxo-anions by cements through solid-solution formation: experimental evidence and modelling. Radiochim. Acta **90**, 639–646 (2002)
D.A. Pickett, K.E. Pinkston, L. Myers, Assessing radionuclide solubility limits for cement-based, near-surface disposal. Mat. Res. Soc. Symp. Proc. **1124**, 1124–Q07-19 (2009)
N.J. Pilkington, J.D. Wilkins, Experimental measurements of the solubility of technetium under near-field conditions, NSS/R120 (1988)

I. Pointeau, D. Hainos, N. Coreau, P. Reiller, Effect of organics on selenite uptake by cementitious materials. Waste Manage. **26**, 733 (2006)
I. Pointeau, N. Coreau, P.E. Reiller, Uptake of anionic radionuclides onto degraded cement pastes and competing effect of organic ligands. Radiochim. Acta **96**, 367–374 (2008)
M. Simonoff, G. Simonoff, *Le Selenium et la Vie* (Masson, Paris, 1991)
J. Song-Sheng, H. Ming, D. Li-Jun, G. Jing-Ru, W. Shao-Yong, Remeasurement of the half-life of ^{79}Se with the projectile X-ray detection method. Chin. Phys. Lett. **18**(6), 746–749 (2001)
T.G. Sors, D.R. Ellis, D.E. Salt, Selenium uptake, translocation, assimilation and metabolic fate in plants. Photosynth. Res. **86**, 373–389 (2005)
W.J. Staudt, R.J. Reeder, M.A.A. Schoonen, Surface structural controls on compositional zoning of SO_4^{2-} and SeO_4^{2-} in synthetic calcite single crystals. Geochim. Cosmochim. Acta **58**, 2087–2098 (1994)
D. Sugiyama, T. Fujita, Sorption of radionuclides onto cement materials altered by hydrothermal reaction. Mat. Res. Soc. Symp. Proc. **556**, 1123–1130 (1999)
K.V. Ticknor, D.R. Harris, T.T. Vandergraaf, Sorption/desorption studies of selenium on fracture-filling minerals under aerobic and anaerobic conditions. TR-453, AECL, Pinawa (1988)
J.K. Tuli, *Nuclear Wallet Cards* (National Nuclear Data Center, Brookhaven National Laboratory, New York, 1995)
U.S. Department of Energy (USDOE), National low-level waste management program radionuclide report series. Selected radionuclides important to LLW management, DOE\LLW-238, November 1996 (1996a)
U.S. Departement of Energy (USDOE), Selected radionuclides important to low-level radioactive waste management. National low-level waste management program, DOE/LLW-138, November 1996 (1996b)
P. Warwick, S. Aldridge, N. Evans, S. Vines, The solubility of technetium(IV) at high pH. Radiochim. Acta **95**, 709–716 (2007)
D. Yu, D. Chuvilin, J.D. Meister, S.S. Abalin, R.M. Ball, G. Grigoriev, V.E. Khvostionov, D.V. Markovskij, H.W. Nordyke, V.A. Pavshook, An interleaved approach to production of ^{99}Mo and ^{89}Sr medical radioisotopes. J. Radioanal. Nucl. Chem. **257**(1), 59–63 (2003)

Chapter 9
Sorption Values for Palladium and Lead

Abstract The most prevailing oxidation state of palladium (Pd) in water is +II. It hydrolyses strongly, but forms also important complexes with soft ligands, such as chloride. Palladium is one of the most important transition metals among the fission products in waste from nuclear fuel. No data on the sorption of Pd (or other platinum groups elements) on cementitious materials are available to date. A reasonable estimate of Pd behaviour can be obtained by considering appropriate chemical analogies. Based on valency, hydrolysis behaviour, and availability of sorption data, lead (Pb) is selected as best choice. The main factors influencing Pb sorption on cementitious materials are the initial Pb concentration (an increase leads to a decrease of sorption) and especially pH or C/S ratio, where a decrease leads to an increase of lead sorption. Kinetic data for Pb sorption indicate a fast initial (chemical) sorption step, followed by a much slower process, possibly involving diffusion into the solid matrix.

9.1 Palladium

9.1.1 Chemical Form, Speciation, and Solubility

Palladium belongs in the periodic table of the chemical elements to the group of platinoids, which also include platinum, ruthenium, rhodium, iridium, and osmium. The most prevailing oxidation state of palladium in water is the +II state (Cotton and Wilkinson 1988). It is a very rare metal which is only present in trace amounts in the earth's crust (Wedepohl 1995). In sea water, the palladium concentration is about 0.02 ng/L (Schafer and Puchelt 1998).

Palladium has 42 isotopes of which 6 are stable (^{102}Pd, ^{104}Pd, ^{105}Pd, ^{106}Pd, ^{108}Pd, and ^{110}Pd). Among the remaining radioactive isotopes, only ^{107}Pd is likely to be detected in the environment because of its important physical period (e.g. 6.50×10^6 years (NEA 2006).

© Springer International Publishing Switzerland 2016

M. Ochs et al., *Radionuclide and Metal Sorption on Cement and Concrete*,
Topics in Safety, Risk, Reliability and Quality 29,
DOI 10.1007/978-3-319-23651-3_9

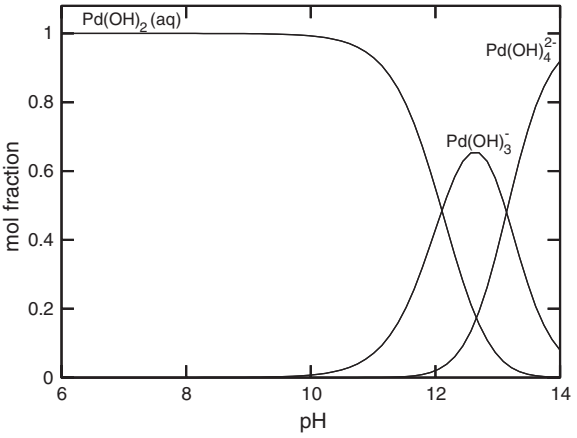

Fig. 9.1 Dissolved palladium speciation as mol fraction versus pH. Pd concentration is 10^{-8} mol/L. Thermodynamic database: ThermoChimie 7b

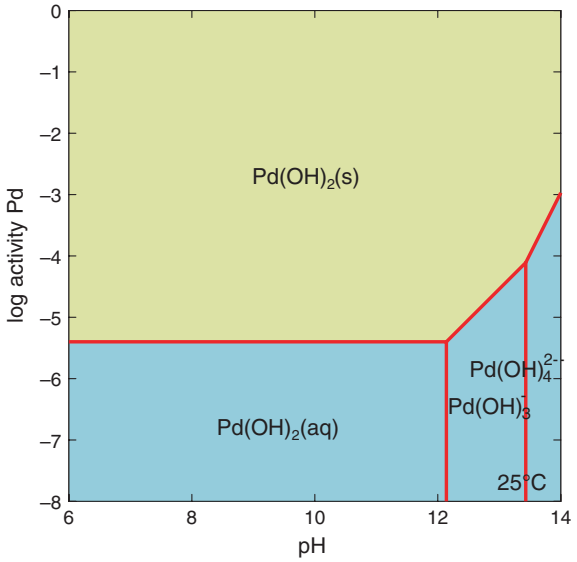

Fig. 9.2 Solubility of $Pd(OH)_2(s)$ in a Pd–H_2O system. Thermodynamic database: ThermoChimie 7b

The isotope ^{107}Pd does not exist in a natural state and is generated within the nuclear reactors. It is produced during the fission reaction with an efficiency of 0.14 %. It is one of the most important transition metals among the fission products in nuclear fuel (Gariel et al. 2002). In LILW, the radionuclide ^{107}Pd (half-life 6.50×10^6 year) is most often found.

Data on the probable speciation of palladium in cement are scarce. To facilitate understanding, calculations have been undertaken of the speciation state in respect of water. The only oxidation state of aqueous palladium is Pd(II) as shown in Fig. 9.1. The solubility of palladium hydroxide $Pd(OH)_2(s)$ is plotted in Fig. 9.2.

Another solid phase, PdO(s), gives much lower solubility (about 4 orders of magnitudes) than that of $Pd(OH)_2(s)$.

Solubility equilibria controlled by $Pd(OH)_2(s)$ at different states of cement degradation are as follows:

$$\text{State I: } Pd(OH)_2(s) + 2H_2O = 2H^+ + Pd(OH)_4{}^{2-} \log K = -30.97$$

At pH 13.5, the solubility of Pd is around 10^{-4} mol/kg.

$$\text{State II: } Pd(OH)_2(s) + H_2O = H^+ + Pd(OH)_3{}^- \log K = -17.54$$

At pH 12.5, the solubility of Pd is about 10^{-5} mol/kg.

$$\text{States III and IV: } Pd(OH)_2(s) = Pd(OH)_2(aq) \log K = -5.4$$

At pH < 10, the solubility of Pd is 4×10^{-6} mol/kg independent of pH.

9.1.2 Literature Information, Mechanisms, and Selected Sorption Values

No sorption data for Pd on cementitious materials have been found. Similarly, no data have been found for any of the obvious chemical analogues (platinum group metals). Of the elements where relevant experimental sorption data are available, possible analogue candidates include Ni and Pb. This is mainly based on the hydrolysis behaviour of Pd(II), which appears to be intermediate between Ni(II) and Pb(II), based on the assumption that the first sorption step is some surface complexation-type reaction. While Pd(II) has also a pronounced soft character and forms strong complexes with chloride, this is not very relevant as the strong hydrolysis dominates Pd behaviour except at fairly low pH. In that sense, Pd^{2+} is very different from other soft ions such as Ag^+ (Baes and Mesmer 1986).

- Under consideration of the actual uptake mechanisms on HCP, however, Ni cannot be viewed as a relevant analogue for other elements, due to the high background of (stable) Ni in cement leading to isotopic exchange and the low solubility of Ni-substituted layered double hydroxide (LDH) phases (see Wang et al. 2009). It is highly unlikely that Pd would interact with cement by an isotope exchange mechanism. Instead of Ni, Co may also be an option, but in contrast to Ni, Co appears to be bound in both the +II- and +III oxidation state in HCP (Vespa et al. 2006).
- Pd shows similarities to Pb in terms of hydrolysis as well as soft/hard character (Pd(II) is soft, Pb(II) is of intermediate character but bordering the soft region, see, e.g. Stumm and Morgan (1996). Pd has a higher affinity to dissolved chloride, but this is not very relevant at elevated pH and typical chloride concentrations. Pd(II) is also less soluble under alkaline conditions. The sorption of Pb on HCP, concrete, and cement mineral phases has been studied by Pointeau (2000), Ochs et al. (2003), and Ochs and Talerico (2006). The available information (see the following sections) indicates that Pb is taken up by sorption, rather than solubility limitation or isotope exchange.

Table 9.1 Selected best estimate, upper and lower limit R_d values for palladium

pH state	Best estimate (L/kg)	Upper limit (L/kg)	Lower limit (L/kg)
State I	i.d.[a]	i.d.	i.d.
State II	i.d.	i.d.	i.d.
State III	i.d.	i.d.	i.d.
State IV	i.d.	i.d.	i.d.

[a] *i.d.* insufficient data

Based on the above arguments, it is proposed that the analogy with Pb is used for assessing sorption of Pd. At the same time, it is pointed out above that Pb is a possible but not an ideal analogue, and it is obvious that additional uncertainties are being introduced by the use of this analogy. Therefore, the data for Pb are used to propose supplemental values for Pd in the context of PA applications, but no recommended distribution ratios are derived for Pd. As pointed out above, there are no relevant experimental data for Pd. Because Pb is viewed as a possible but not ideal analogue element, no recommended distribution ratios are selected for Pd (Table 9.1).

9.1.3 Supplemental Values for Assessment Calculations

Supplemental values for assessment purposes are proposed as follows (these data are of a lesser quality because not supported by a vast amount of solid data):

- The best estimate and upper limit selected for Pb are directly accepted. This is viewed as sufficiently conservative, considering that data selection for Pb focuses on data for HCP and does not take into account the higher sorption values observed on CSH phases.
- For supplemental lower limits, the values selected for Pb are reduced by an order of magnitude. For State II, this is also consistent with the lower end of the data by Bayliss et al. (1988) obtained for Pb sorption on calcareous mortar (Table 9.2).

Table 9.2 Supplemental R_d values for palladium

pH state	Best estimate (L/kg)	Upper limit (L/kg)	Lower limit (L/kg)
State I	3×10^2	1×10^3	1×10^1
State II	3×10^3	1×10^4	1×10^2
State III	3×10^4	1×10^5	1×10^2
State IV	8×10^2	2×10^3	2×10^1

9.2 Lead

9.2.1 Chemical Form, Speciation, and Solubility

Lead may exist in oxidation states Pb(II) and Pb(IV), but Pb(IV), as in the mineral plattnerite (PbO_2), seems only stable under very oxidising condition near the upper limit of the water stability region of a pH–Eh diagram (Fig. 9.3).

Aqueous speciation of Pb at trace concentration in high pH range relevant to cement and concrete is dominated by hydrolysis species $HPbO_2^-$ (equivalent to $Pb(OH)_3^-$) and $Pb(OH)_4^{2-}$ (Fig. 9.4).

In terms of solubility, lead oxides and hydroxides are all relatively soluble in a high pH range. The most stable oxide litharge (PbO_2) has solubility about 0.05 molal at pH 12.5 and even higher at state I pH following the equilibrium.

$$\text{Litharge} + 3H_2O = 2H^+ + Pb(OH)_4^{2-} \quad \log K = -26.2720\,(25\ ^\circ\text{C}) \qquad (9.1)$$

9.2.2 Sorption Values from the Literature for the Benchmark Cement

An overview of Pb sorption on various cement mineral phases is given in Ochs et al. (2003). Following a detailed analysis of the various data sets (HCP, CSH,

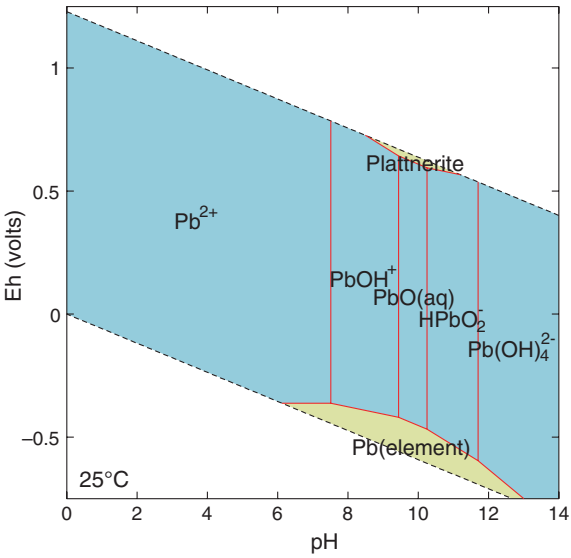

Fig. 9.3 Eh–pH diagram for a Pb–H_2O system with a lead activity 10^{-8}. Thermodynamic database: ThermoChimie 7b

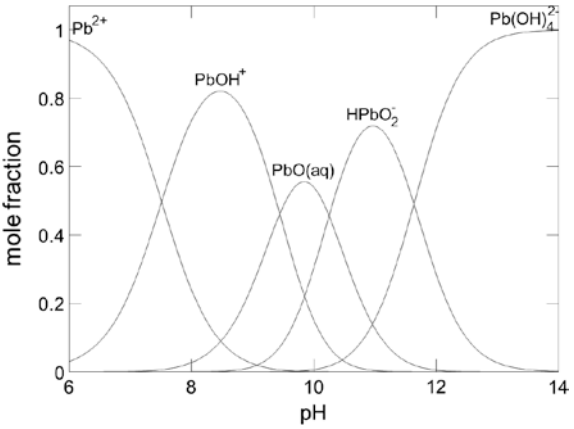

Fig. 9.4 Dissolved lead speciation as mol fraction versus pH in a Pb–H_2O system. Pb concentration is 10^{-8} mol/L. Thermodynamic database: ThermoChimie 7b

Ca-aluminate cements), Ochs et al. (2003) found that for HCP, the main factors influencing Pb sorption are pH and initial Pb concentration:

- increasing initial Pb concentrations lead to a decrease of sorption;
- decreasing equilibrium pH (corresponding to a decreasing C/S ratio) leads to an increase in Pb sorption.

Figure 9.5 gives an overview of R_d values for Pb on different HCP samples and individual mineral phases. The figure is modified from Andra (2005); for some of the data, the entire range of measured values is indicated. The data by Ochs et al. (2003) were determined in the form of isotherms using different CSH phases; in each case, pH corresponded to the respective C/S ratio. The single mineral data were determined at pH values near 12.4, except for the data on calcite. The various HCP samples also correspond approximately to this pH.

An additional data point obtained for the Nirex vault reference backfill (NRVB) with a mean R_d of 110 ± 40 L/kg at pH 12.7/12.8 (Brownsword et al. 2002) was consistent with the other data.

9.2.3 Sorption Mechanisms and Selected Sorption Values

While a comparatively rich database exists for the sorption of Pb on cementitious materials, which allows the identification of relevant factors influencing sorption and determination of trends, no detailed information on the actual sorption mechanisms is available. The kinetic data by (Ochs et al. 2003) indicate a fast initial (chemical) sorption step, followed by a much slower process, possibly involving diffusion into the solid matrix.

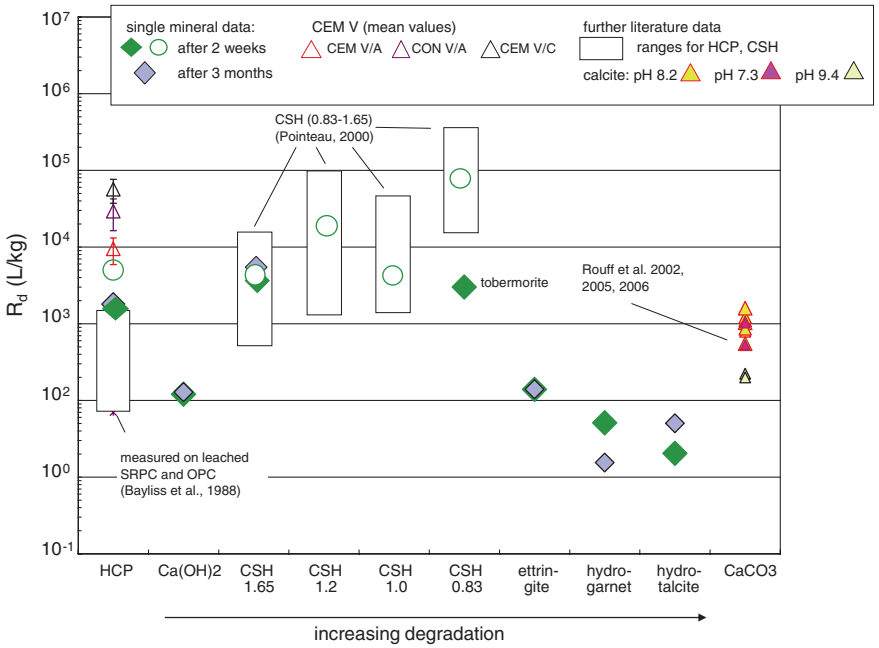

Fig. 9.5 Overview of R_d values for Pb on different HCPs and minerals. The single mineral data (Ochs et al. 2003) represent single values measured after equilibration times of 2 weeks and 3 months, the data represented by diamonds correspond to Pb concentrations in the range of 1×10^{-4} to 1×10^{-6} mol/L, and the data represented by circles correspond to Pb concentrations in the range of 1×10^{-7} to 1×10^{-8} mol/L. Data for the CEM V samples (Ochs and Talerico 2006), */A* leached, */C* carbonated, *CON* mortar) are mean values determined after equilibration times of 11 days and 9 months ± their standard error. For the Bayliss et al. (1988) data, solutions were pre-equilibrated, pH = 12.5 (except for one OPC sample that contained fuel ash, pH ca. 11.8–12, K_d within the range given by other samples), equilibration time (after pre-equil.) was 12–60 days, and sorption was higher after 60 days. Ranges of further data taken from the indicated literature are given in the figure; the data ranges of Pointeau (2000) correspond to sorption isotherms. Modified from Andra (2005)

9.2.3.1 Lead Sorption at State I

No data for Pb sorption on HCP are available that are directly applicable to State I. Based on the trend of Pb sorption on CSH phases, the hydrolysis of Pb, and the observations of Ochs et al. (2003) regarding Pb sorption as a function of pH, it is estimated that R_d for State I should be roughly an order of magnitude lower than for State II. Accordingly, a best estimate of 300 L/kg is proposed together with upper and lower limits of 10^3 and 100 L/kg, respectively.

9.2.3.2 Lead Sorption at State II

All available data for HCP correspond to State II. Not considering the values for the mortar samples (data by Bayliss et al. 1988), CON V/A) and the largely carbonated sample (CEM V/C), the data from the various experiments span a range from about 10^3 L/kg to about 10^4 L/kg. This range is accepted for representing upper and lower limits. As best estimate, a value of 3×10^3 L/kg is selected.

9.2.3.3 Lead Sorption at State III

As for State I, no directly applicable data are available. Based on the same circumstantial evidence already considered for State I, it is estimated that R_d for State III should be roughly an order of magnitude higher than for State II. This leads to a best estimate of 3×10^4 L/kg, an upper limit of 10^5 L/kg, and a lower limit of 10^3 L/kg.

9.2.3.4 Lead Sorption at State IV

Sorption data for Pb on calcite are available from Rouff et al. (2002, 2005a, b, 2006). These studies cover a range of pH values (7.3–9.4) and were performed in different background solutions (0.15–0.5 mol/L NaCl and $NaNO_3$ solutions). The effect of pH can be seen in Fig. 9.5, whereas the changes of the ionic strength of the solution influenced R_d by less than a factor of two.

Notable sorption of Pb on calcite is further indicated by the data for mortar: Ochs et al. (2006) measured higher sorption of Pb for the mortar sample than for the HCP sample (data points for CON V/A and CEM V/A in Fig. 9.5). This is further consistent with the finding of Curti (1997), who indicates high partitioning of Pb into calcite under environmental conditions.

Based on the data between pH 7–9 by Rouff and co-workers (Rouff et al. 2002), which are directly applicable to State IV, a best estimate of 8×10^2 L/kg and an upper limit of 2×10^3 L/kg were selected. As lower limit, a value of 2×10^2 L/kg is proposed, which also takes into account the values measured at pH 9.4 (i.e. just outside the range ascribed to State IV) (Table 9.3).

Table 9.3 Selected best estimate, upper and lower limit R_d values for lead

pH state	Best estimate (L/kg)	Upper limit (L/kg)	Lower limit (L/kg)
State I	3×10^2	1×10^3	1×10^2
State II	3×10^3	1×10^4	1×10^3
State III	3×10^4	1×10^5	1×10^3
State IV	8×10^2	2×10^3	2×10^2

References

Andra 2005, Référentiel de comportement des radionucléides et des toxiques chimiques d'un stockage dans le Callovo-Oxfordien jusqu'à l'homme, Site de Meuse/Haute-Marne, Tome 1/2: Chapitres 1 à 4, Dossier 2005 Argile, 2005

C.F. Baes, R.E. Mesmer, *The Hydrolysis of Cations*, 2nd edn. (Robert E. Krieger, Malabar, 1986)

S. Bayliss, F.T. Ewart, R.M. Howse, J.L. Smith-Briggs, H.P. Thomason, H.A. Willmott, The solubility and sorption of lead-210 and carbon-14 in a nearfield environment. Mat. Res. Soc. Symp. Proc. **112**, 33–42 (1988)

M. Brownsword, M.C. Manning, N.J. Pilkington, S.J. Williams, The effect of cellulose degradation products on the solubility and sorption of zirconium and the sorption of lead under cementitious repository conditions. Report AEAT/ENV/0549, January 2002

F.A. Cotton, G. Wilkinson, *Advanced Inorganic Chemistry*, 5th edn. (Wiley, New York, 1988)

E. Curti, Coprecipitation of radionuclides: basic concepts, literature review and first applications, PSI Bericht Nr. 97–10 (1997)

J.C. Gariel, K. Beaugelin-Seiller, Fiche radionucléide: Palladium 107 et environnement (rév. 02/12/2002), Institut de Radioprotection et de Sûreté Nucléaire (2002)

Nuclear Energy Agency (NEA-OECD), The jeff-3.1 nuclear data library. jeff report 21, oecd/nea, Paris, France, 2006

M. Ochs, C. Talerico, Development of models and datasets for radionuclide retention by cementitious materials. Andra 2005 report 2006, C.RP.0BMG.06.0001A, 2006

M. Ochs, C. Talerico, B. Lothenbach, E. Giffaut, Systematic trends and empirical modelling of lead uptake by cements and cement minerals. Mat. Res. Soc. Symp. Proc. **757**, 693–698 (2003)

M. Ochs, I. Pointeau, E. Giffaut, Caesium sorption by hydrated cement as a function of degradation state: experiments and modelling. Waste Manage. **26**, 725–732 (2006)

I. Pointeau, Etude mécanistique et modélisation de la retention de radionucléides par les phases de silicate de calcium des ciments hydrates. Thèse de l'Université de Reims-Champagne-Ardennes, France, 2000

A.A. Rouff, R.J. Reeder, N.S. Fisher, Pb(II) sorption with calcite: a radiotracer study. Aquat. Geochem. **8**, 203–227 (2002)

A.A. Rouff, R.J. Reeder, N.S. Fisher, Electrolyte and pH effects on Pb(II)—calcite sorption processes: the role of the $PbCO_3$(aq) complex. J. Coll. Inter. Sci. **286**, 61–67 (2005a)

A.A. Rouff, E.J. Elzinga, R.J. Reeder, N.S. Fisher, The influence of pH on the kinetics, reversibility and mechanics of Pb(II) sorption at the calcite-water interface. Geochim. Cosmochim. Acta **69**, 5173–5186 (2005b)

A.A. Rouff, E.J. Elzinga, R.J. Reeder, The effect of aging and pH on Pb(II) sorption processes at the calcite—water interface. Environ. Sci. Technol. **40**, 1792–1798 (2006)

J. Schafer, H. Puchelt, Platinum-group-metals (PGM) emitted from automobile catalytic converters and their distribution in roadside soils. J. Geochem. Explor. **64**, 307–314 (1998)

W. Stumm, J.J. Morgan, *Aquatic Chemistry: Chemical Equilibria and Rates in Natural Waters*, 3rd edn. (Wiley, New York, 1996), 1022 pp. ISBN 0-471-511854-6

M. Vespa, R. Dahn, D. Grolimund, E. Wieland, A.M. Scheidegger, Spectroscopic investigation of Ni speciation in hardened cement. Environ. Sci. Technol. **40**, 2275–2282 (2006)

L. Wang, E. Martens, D. Jacques, P. De Canniere, J. Berry, D. Mallants, Review of sorption values for the cementitious near field of a near surface radioactive waste disposal facility. NIROND-TR 2008-23E, April 2009

K.H. Wedepohl, The composition of the continental crust. Geochim. Cosmochim. Acta **59**(7), 1217–1232 (1995)

Chapter 10
Sorption Values for Niobium and Tin

Abstract Niobium and tin exist in the penta- and tetravalent state, respectively, over the entire redox span of aqueous solutions (>pH 3). Both Sn(IV) and Nb(V) hydrolyse extensively and exist under cementitious conditions as negatively charged hydroxo-complexes. Tin and niobium are contained in various wastes from nuclear power production. Both elements sorb strongly on cementitious materials under all conditions, in accordance with their hydrolysis behaviour and with the affinity of the hydrolytic species to calcium ions. While the significant extent of sorption is well established, the mechanisms of sorption on cement phases are not well understood. Spectroscopic information indicates that the structural environment of Sn sorbed to CSH and hydrated cement paste differs between the two solids, but corresponds to the formation of inner-sphere complexes in both cases. However, it has to be admitted that the available information is not conclusive with regard to (i) identifying the sorption-dominating mineral phase and (ii) the distinction between surface sorption or/and incorporation.

10.1 Niobium

10.1.1 Chemical Form, Speciation and Solubility

^{94}Nb (half-life 20,000 years) is not a naturally occurring radionuclide. It is produced from the neutron activation of ^{93}Nb, the only stable isotope of niobium, that is present in the structural components of nuclear reactor vessels, especially those constructed from important alloys such as Inconel (and, to a lesser extent, in those reactor vessels with stainless steels containing niobium). Hence, ^{94}Nb is found in metallic reactor components. This radionuclide will be present in dismantling material from nuclear power plants, but it will also be present in waste streams that originate from treatment of the primary cooling circuit. The latter will become contaminated with ^{94}Nb owing to corrosion of stainless steel and Inconel surfaces in the nuclear power plants. The ^{94}Nb inventory increases linearly

© Springer International Publishing Switzerland 2016

M. Ochs et al., *Radionuclide and Metal Sorption on Cement and Concrete*,
Topics in Safety, Risk, Reliability and Quality 29,
DOI 10.1007/978-3-319-23651-3_10

with reactor operation and does not significantly decrease with time (or burnup) (USDOE 1995). LILW also contains ^{94}Nb.

At the present time, reliable thermochemical data for niobium are not available to the authors of this report for predicting speciation and solubility of the element. A recent update (Version 7.a) of the Andra (2005) database *ThermoChimie* (developed since 2000, E. Giffaut, personal communication) suggests that $Nb(OH)_7^{2-}$, i.e. a species with Nb(V), is the dominating aqueous species at cementitious pH, which is consistent with solubility measurements under high pH conditions (E. Giffaut, personal communication). In terms of solubility controlling phases, Na-niobates and Ca-niobates are considered to be relevant; the latter phase is much less soluble and likely to be the phase controlling the solubility of Nb in cement systems. Solubility values of these phases based on thermochemical calculations under cementitious conditions of interest to ONDRAF/NIRAS are not available at the present time.

Solubility of a freshly precipitated Nb phase (reported as Nb_2O_5 but probably a hydrous oxide) was measured in cement leachates of different compositions (Pilkington et al. 1988). In BFS/OPC leachates, the solubility of the solid was below the detection limit of 2×10^{-7} M. In PFA (Pulverised Fuel Ash)/OPC leachates, however, the solubility after four months equilibration was considerably higher, i.e. 6×10^{-3} M. No explanation was found for the observed increase in the Nb solubility; it was considered unlikely to be due to differences in the composition of the leachates, since these were nearly identical. A subsequent sampling (after 18 months) of the same experiments did not reveal new information. Therefore, the solubility of Nb was considered to be around 10^{-3} mol/L (Pilkington and Stone 1990). In view of much lower solubilities determined by others in normal cements with calcium present, this value is considerably higher than the solubility limit. Unless the process responsible for the higher solubility can be identified, this value will not be considered appropriate in the current analysis.

Talerico et al. (2004) performed Nb solubility tests in solutions of different Ca concentrations (~0.1 – 20 millimolal) and pH (~9.5 – 13.2). $NbCl_5$ was added to the solutions leading to a dissolved Nb concentration of 3×10^{-9}–2×10^{-5} M. These are oversaturation experiments, i.e. without adding Nb solubility controlling phases in solution. X-ray diffraction measurements confirmed, however, the presence of a poorly crystalline Ca–Nb–oxide phase with $CaNb_4O_{11}{:}8H_2O$ (calcium niobate or hochelagaite) being the most likely composition. In all experiments, Nb solubility varies between 10^{-9} and 10^{-5} mol/L depending on both Ca concentration and pH. In general, Nb concentration decreased with increasing Ca concentration in solution. For a fixed calcium concentration (1 millimolal), Nb solubility increased with decreasing pH. At Ca concentrations >1 millimolal, the solubility also decreases with increasing pH. Based on these observations, an empirical relation was put forward for [Ca] >1 millimolal (Talerico et al. 2004):

$$[\mathrm{Nb}]_{\mathrm{dissolved}} = 1.4643\ \mathrm{e}^{-1.3402} \times \left([\mathrm{Ca}]^{-0.8922} / 10^{2.6766} \right) \qquad (10.1)$$

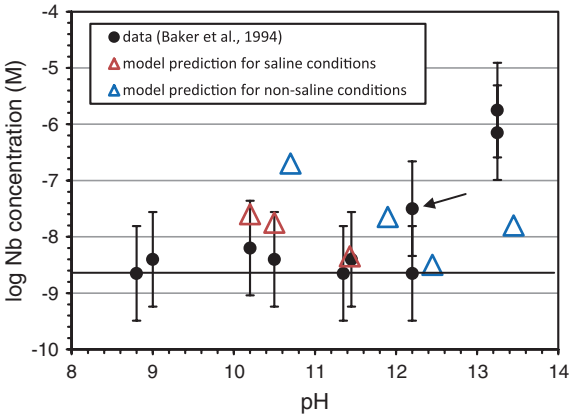

Fig. 10.1 Solubility of Nb as a function of pH determined under saline conditions. Model predictions are based on Talerico et al. (2004) using {pH, Ca/Mg} data from Baker et al. (1994). The uncertainties estimated for the data by Baker et al. (1994) are 10 % of the measured values; the *arrow* denotes a value obtained from solubility experiments with ^{95}Nb; the *horizontal line* denotes the detection limit in the study of Baker et al. (1994)

where [] denotes concentration (M). At a [Ca] of about 20 millimolal and a pH of 12.5, typical for State II of cement degradation, the above relation results in a Nb solubility of 5×10^{-9} M.

When pH and calcium concentration values appropriate for different states of cement degradation are used (see Fig. 2.2), a U-shaped solubility profile occurs (Fig. 10.1). The lower predicted solubility at pH 13.5 using Eq. (10.1) is related to the presence of the Ca–Nb oxide phase. In comparison with the solubility data from Baker et al. (1994), model predictions in the pH range 10–11.5 are higher. This is probably related to the saline groundwater used by Baker et al., with high sodium concentrations but also with elevated Ca (6.7×10^{-2} M) and Mg (1.5×10^{-2} M) concentrations. When the sum of Ca and Mg concentration is used in Eq. (10.1), predicted niobium solubility is in better agreement with experimental values (Fig. 10.1). This illustrates the potential usefulness of Eq. (10.1) to predict niobium solubility, also under rather extreme pore water compositions. Therefore, the reliability of this relationship to predict Nb solubility for conditions relevant to near-surface disposal merits further corroboration.

The potential relevance of calcium-oxo anion salts in determining niobium solubility at high pH was also advocated by Berner (2002), based on chemical analogy with Se and Sn (Sn (IV) easily hydrolyses at high pH to the negatively charged oxocomplex stannate—$Sn(OH)_6^{2-}$—as does niobium). Identified solubility controlling phases for Se and Sn include $CaSeO_3.H_2O$(s) and $Ca(Sn(OH)_6)$ (s) (calcium stannate).

The above literature indicates that at high pH, niobium solubility is likely to be determined by a set of calcium-oxo anion salts such as calcium niobate, and not just by the single species Nb_2O_5. This would be in agreement with other elements

that have a similar speciation with calcium-oxo anions controlling the solubility. Measurements showed that the solubility of these niobium salts is probably lower than that of Nb_2O_5, i.e. in the range of 5×10^{-9}–5×10^{-8} M, and depending both on pH and Ca concentration. This solubility range will be considered when evaluating appropriateness of niobium uptake data for R_d determination.

10.1.2 Sorption Values from the Literature for the Benchmark Cement

Sorption data for Nb are rare in the literature. Three data sets of R_d on cementitious materials are presented in Fig. 10.2 and Table A.17.

10.1.3 Sorption Mechanisms and Selected Sorption Values

Within the pH range 11–12.5, R_d values remain relatively constant. Only at pH values lower than 10 one does notice a significant decrease. In addition to pH,

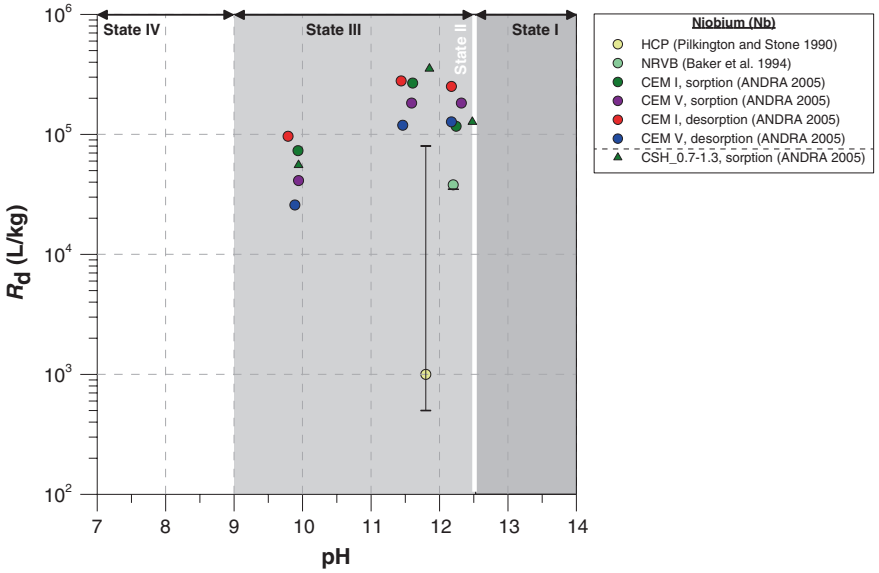

Fig. 10.2 Distribution ratio (R_d) of niobium in cementitious systems as a function of pH. *NRVB* Nirex reference vault backfill; *HCP* hardened cement paste; *CEM I* Portland cement type I; *CEM V* Portland cement type V; *CSH* Calcium Silica Hydrate. For the Pilkington and Stone data, 1000 is the best estimate proposed by the authors based on a range of 500–80,000 obtained from different experimental conditions (filtered versus unfiltered, S/L from 0.04 to 0.005, contact time from 1 to 2 months)

calcium was shown to have a clear influence on Nb solubility. Therefore, the calcium concentration will determine whether the uptake is really reversible sorption or whether precipitation is taking place. The latter process is much less reversible (for tin, the dissolution kinetics were shown to depend on OH^- concentrations, Lothenbach et al. 2000) and thus provides a better containment of radioactive niobium species.

Sorption of Nb under saline conditions was shown to be also high (R_d 40,000 L/kg, Baker et al. 1994). This is about a factor 5–10 lower than the other data shown in Fig. 10.2 at approximately the same pH. Although the high calcium and magnesium concentrations likely decreased niobium solubility (see Sect. 10.1.1), the lower sorption compared to non-saline conditions cannot be explained at present. One possible explanation may be competition with other ions such as sulphate (again based on chemical analogy with tin, Sn(IV) immobilization in ettringite was found and a possible mechanism was via binding of Sn(IV) in ettringite structures (Bonhoure et al. 2003)).

10.1.3.1 Sorption Mechanisms

Sorption mechanisms for niobium were not reported in the literature. Also Evans (2008) in his recent review did not discuss the uptake mechanisms for niobium. As was done for solubility, chemical analogy with tin (Sn) will be invoked to propose the uptake mechanisms for niobium. According to the earlier literature, Nb in solution exists primarily as $Nb(OH)_6^-$ across the whole pH/Eh range of interest (Baes and Mesmer 1986). More recent data suggest that $Nb(OH)_7^{2-}$ is the dominating species at cementitious pH (Sect. 10.1.1). Because the latter data became available only very recently to the authors of this report, they were not yet integrated in the analysis.

Several solid phases controlling Sn uptake were identified, including ettringite, HCP in combination with CSH (Bonhoure et al. 2003), and pure HCP (Séby et al. 2001). For uptake onto ettringite, the proposed (but still preliminary) process was sorption by means of corner sharing between Sn(IV) octahedral and Ca polyhedra (Bonhoure et al. 2003). When Sn(IV) concentrations were well below the solubility limit of calcium stannate ($CaSnO_3$), strong uptake onto HCP was characterised as linear sorption Bonhoure et al. 2003). Above the solubility limit (~1.1×10^{-6} mol/L at pH 13.3) precipitation of $CaSn(OH)_6$ occurred. In terms of uptake values, Wieland and Van Loon (2002) proposed a best estimate R_d of 10,000 L/kg for States I and II of cement degradation.

Proposed best estimate R_d (L/kg) values are provided in Table 10.1. These values are supported by the experimental data from Table 3.4 and Fig. 10.2 and are in line with those from the chemically similar tin (see discussion in Sect. 10.1.2). The experts disliked the idea of using thorium as an analogue as it does not hydrolyse at high pH in the manner that niobium does. Some data for niobium (Pilkington and Stone 1990) were discussed but then given low weighting as the starting concentration appeared well above the solubility limit, thus potentially leading to precipitation.

10.1.3.2 Sorption at State I

For State I, the review did not reveal any data. However, for tin, Wieland and Van Loon (2002) defined a best estimate R_d of 10,000 L/kg for States I and II of cement degradation. On the basis of chemical analogy between tin and niobium, it was decided also to use the same R_d for States I and II, hence extend the measured niobium R_d for State II to that of State I. A best estimate of 5×10^4 L/kg was selected with upper and lower limits of 1×10^6 and 1×10^3 L/kg, respectively. These best estimates for States I and II are considerably higher than the 1000 L/kg proposed by Bradbury and Van Loon (1998). However, in view of the experimental data, and the assurance that real sorption was measured and not precipitation, it is believed that the higher values in Table 10.1 are justified.

10.1.3.3 Sorption at State II

As stated in Sect. 10.1.3.2, it was decided to use the same R_d for States I and II. A best estimate of 5×10^4 L/kg was selected with upper and lower limits of 1×10^6 and 1×10^3 L/kg, respectively.

Sorption at State III

It was further agreed to use the same R_d values for State III as for State II; hence, a best estimate of 5×10^4 L/kg was selected with upper and lower limits of 1×10^6 and 1×10^3 L/kg, respectively.

10.1.3.4 Sorption at State IV

There were no data for State IV, but lower sorption onto calcite would be expected. R_d values generally two orders of magnitude lower were chosen: a best estimate of 500 L/kg, with upper and lower bounds of 5×10^3 L/kg and 50 L/kg.

Table 10.1 Selected best estimate, upper and lower limit R_d values for niobium (Nb(V))

pH state	Best estimate (L/kg)	Upper limit (L/kg)	Lower limit (L/kg)
State I	5×10^4	1×10^6	1×10^3
State II	5×10^4	1×10^6	1×10^3
State III	5×10^4	1×10^6	1×10^3
State IV	5×10^2	5×10^3	5×10^1

10.2 Tin

10.2.1 Chemical Form, Speciation, and Solubility

Tin is a highly crystalline metal. Tin combines directly with chlorine forming tin(IV) chloride, while reacting tin with hydrochloric acid in water gives tin(II) chloride and hydrogen. Several other compounds of tin exist in the +2 and +4 oxidation states, such as tin(II) sulphide and tin(IV) sulphide (Mosaic gold). There is only one stable hydride, stannane (SnH_4), where tin is in the +4 oxidation state.

Tin is the element with the greatest number of stable isotopes, ten. Of these, the most abundant ones are ^{120}Sn (at almost a third of all tin), ^{118}Sn, and ^{116}Sn. There are 28 additional unstable isotopes that are known. Aside from ^{126}Sn which has a half-life of 2.3×10^5 years, all the radioactive isotopes have a half-life of less than a year. The following radionuclides are typical of LILW: ^{119m}Sn (half-life 0.802 year), ^{121m}Sn (half-life 55 year), ^{125}Sn (half-life 0.0264 year), and ^{126}Sn (half-life 1.1×10^6 year).

Data on the probable speciation of tin in cement are scarce. To facilitate understanding, calculations have been undertaken of the speciation state in respect of water and on the impact of changing redox conditions.

Tin is redox sensitive and may exist in two oxidation states: Sn(II) and Sn(IV). When pH > 2 and for almost the entire redox domain of water stability, only Sn(IV) is important (Fig. 10.3). At pH > 8, which encompasses the relevant pH domain for an aqueous cement system, the speciation of Sn is dominated by hydrolysis species $Sn(OH)_5^-$ and $Sn(OH)_6^{2-}$ (see Figs. 10.3 and 10.4).

As concerns solubility, relevant solid phases that might control the solubility of Sn in aqueous and cement systems include SnO_2 (am) and Ca-stannate, $CaSn(OH)_6$ (s). In States I, II, and III of cement degradation where the aqueous

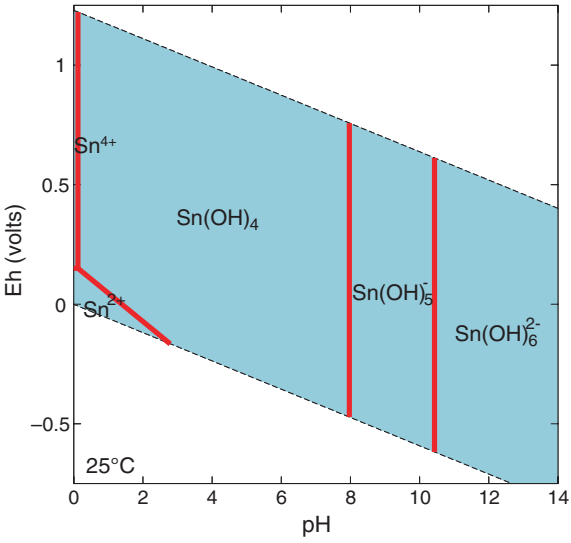

Fig. 10.3 Eh–pH diagram of tin for a Sn–H_2O system. Sn activity is 10^{-8}, no precipitation of solids. Thermodynamic database: ThermoChimie 7b

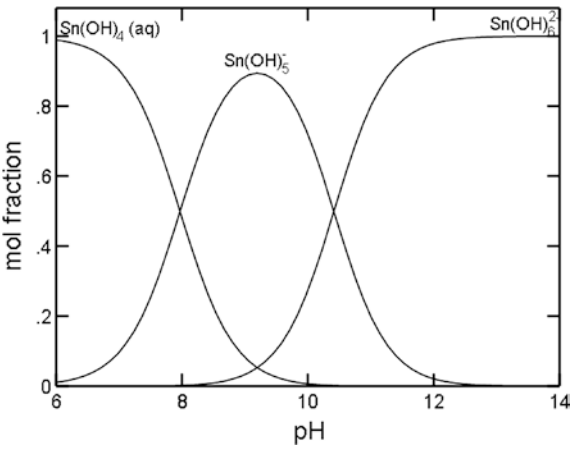

Fig. 10.4 Dissolved tin speciation as mol fraction versus pH. Sn concentration is 10^{-8} mol/L. Thermodynamic database: ThermoChimie 7b

Ca concentration is above millimol/L level, $CaSn(OH)_6$ (s) is the likely solubility controlling phase for Sn. In State IV, depleted in cement components and low in Ca concentration, SnO_2 (am) may replace $CaSn(OH)_6$ (s) as the solid controlling the dissolved Sn concentration.

Figure 10.5 shows the solubility of $CaSn(OH)_6$ (s) in the presence of portlandite and the solubility of SnO_2 (am). Note that $CaSn(OH)_6$ (s) is relevant only for States I, II, and part of State III when calcium concentration is still high. SnO_2 (am) becomes important only for State IV where calcium concentration and pH are low. For State III, where the dissolved Ca concentration varies, the solubility of Sn will be governed by both pH and Ca concentration.

Figure 10.6 shows the results of reaction path modelling simulating the leaching of a cement system by soil water which has a composition similar to that used by Jacques et al. (2008). The soil water contains 2.7×10^{-4} M dissolved carbon, 5.7×10^{-5} M calcium, 1.2×10^{-4} M sulphur, and a pH around 4. This soil water composition has been used to simulate cement degradation as shown in Fig. 2.2. The model cement system contains[1] Na/K hydroxides, portlandite, CSH phases (CSH_0.8, CSH_1.2, and CSH_1.6), and 0.1 millimol/L of Sn. The calculated Ca concentration varies from about 1 mmol/kg (State I) to about 20 mmol/kg (State II) and drops to millimol/L level after the depletion of CSH phases (from end of State III onwards). These Ca concentrations are comparable to the results obtained using the detailed solid-solution models for describing CSH phases (Jacques et al. (2008). At pH > 10, where cement phases are still present and the Ca concentration is still higher than the one in the soil water, the solubility of Sn is controlled by the solubility of $CaSn(OH)_6$ (s) and varies with pH and Ca concentration. At pH < 10, when the Ca concentration diminishes due to the depletion of cement phases, Sn solubility is governed by the solubility of SnO_2 (am) and decreases from 10^{-5} to 10^{-7} mol/kg.

[1]The mass of cement phases is chosen as arbitrary to facilitate the calculation.

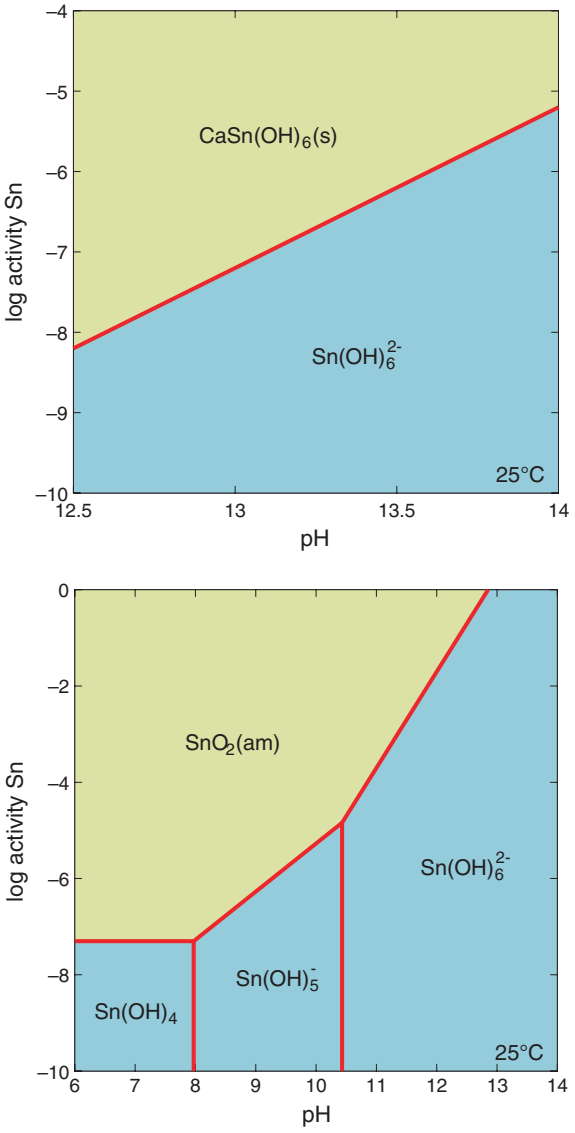

Fig. 10.5 Solubility of $CaSn(OH)_6$ (s) in the presence of portlandite (*top*) and SnO_2 (am) (*bottom*). Thermodynamic database: ThermoChimie 7b

A relevant experiment concerning Sn solubility in cement is one reported by Lothenbach et al. (2000). These authors determined Sn solubility from over- and undersaturation of Sn phases as a function of pH and dissolved Ca concentration. They concluded that in a cement system where Ca is present, the solubility controlling phase for Sn is $CaSn(OH)_6$ (s)—identified by XRD analysis—and the tin(IV) solubility is therefore strongly correlated with the calcium content dissolved in the cementitious solutions. The measured solubility of Sn has a maximum value of 10^{-6} mol/kg in State I and decreases to 10^{-8} mol/kg in State II.

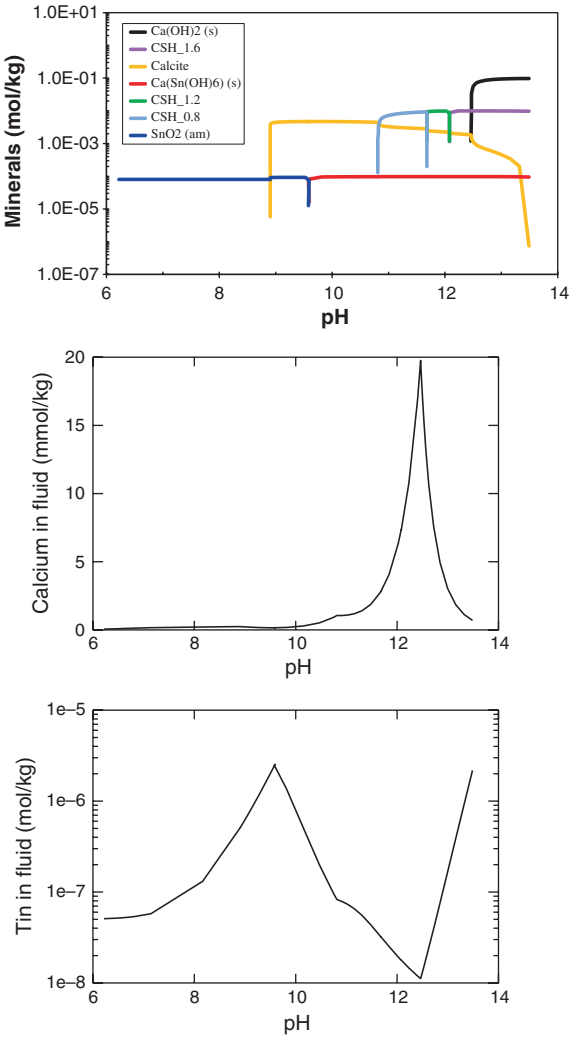

Fig. 10.6 Dissolution of some cement phases (*top*), aqueous concentration of calcium (*middle*), and solubility of $CaSn(OH)_6$ (s) and SnO_2 (am) (*bottom*). Thermodynamic database: ThermoChimie 7b. The calcite in the top graph is from precipitation, not from calcite aggregates

This range seems in good agreement with other experiments performed under similar conditions (Ochs et al. 1998; Bayliss et al. 1992; Bayliss et al. 1988).

Figure 10.6 indicates that the maximum solubility of Sn in State I is about 2×10^{-6} mol/kg. The dissolved Sn concentration decreases from its maximum to about 10^{-8} mol/kg, which is the solubility of Sn in State II when the pH reaches a value of 12.5 controlled by the dissolution of portlandite. In State III, the dissolved Sn concentration increases from 10^{-8} to about 2×10^{-6} (at pH 9.5) in accordance with the decrease of Ca concentration. After the CSH phases have dissolved completely, the solubility of Sn is controlled by SnO_2 (am) and decreases from 2×10^{-6} to about 5×10^{-8} mol/kg (at pH 6–7).

The solubility calculation presented in Fig. 10.6 is generally comparable to the estimates made by Berner (2002). Despite both estimations being based on computer modelling, they are not in disagreement and provide useful order of magnitude values. Berner (2002) concluded that the solubility of Sn in States I and II of cement degradation might be in the range of 10^{-7}–10^{-5} mol/kg.

In summary, our solubility calculation and some experimental literature data suggest that Sn solubility in a cement system is in the range of 10^{-8}–10^{-6} mol/kg. In States I and III, where the Ca concentration is relatively low compared to the State II, the Sn solubility is approximately 2×10^{-6} mol/kg. Sn solubility is the lowest in State II where it reaches about 10^{-8} mol/kg. In State IV, Sn solubility decreases from 10^{-6} to about 5×10^{-7} mol/kg with decreasing pH (boundary of State IV in our assessment is pH 9).

10.2.2 Sorption Values from the Literature for the Benchmark Cement

Reviewed R_d values for tin in a cementitious system are presented in Fig. 10.7 and Table A.18 based on the literature from Bonhoure et al. (2003), Baker et al. (1994), Heath et al. (1996), Ochs and Talerico (2006), Bayliss et al. (1989), and Ochs et al. (1997). Table A.18 gives also a summary of the pertaining experimental conditions. A summary of the above studies is given.

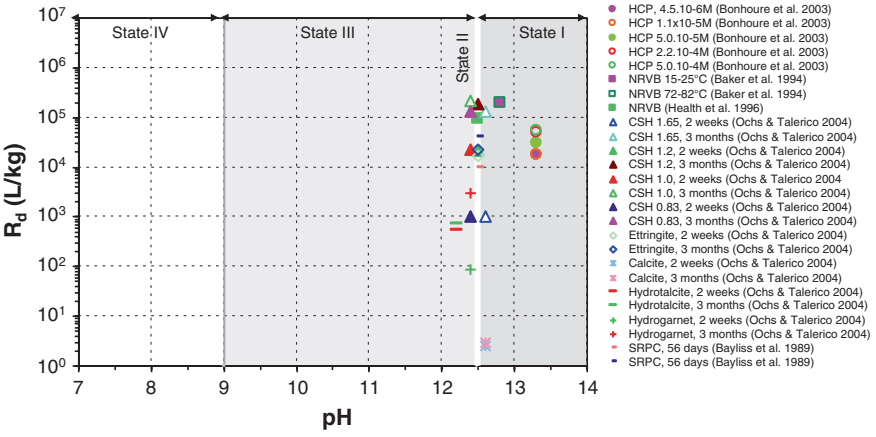

Fig. 10.7 Distribution ratio (R_d) of tin in cementitious systems as a function of pH. *NRVB* Nirex reference vault backfill; *HCP* hardened cement paste; *SRPC* sulphate resisting Portland cement

10.2.3 Sorption Mechanisms and Selected Sorption Values

Based on the literature reviewed, the sorption of Sn(IV) on HCP is strong under all conditions. This is consistent with the pronounced hydrolysis of Sn(IV) at intermediate to high pH on one hand and the affinity of the hydrolytic Sn species to Ca (and presumably other divalent cations) on the other hand. In their sorption study of Sn on individual HCP phases, Ochs and Talerico (2006) observed lower sorption only for calcite, hydrogarnet, and hydrotalcite. Wieland and van Loon (2002) also show that the sorption of Sn(IV) and Th is similar under identical conditions. This suggests that the influence of very high pH (i.e. the formation of negatively charged Sn species) on the sorption of Sn(IV) on HCP is only weak.

Based on available information, solid/liquid ratio has no influence on Sn sorption. Due to the low solubility of Sn(IV) in cement-equilibrated solutions, reliable sorption data are available for relatively low concentrations only. The isotherm data by Bonhoure et al. (2003) on HCP and by Ochs and Talerico (2006) on CSH minerals show that Sn sorption on cementitious materials is linear and sorption on both HCP and CSH can be interpreted by a single R_d (Fig. 10.9).

As long as CSH phases are present, the state of cement degradation (C/S ratio) appears to have no significant influence on Sn sorption.

10.2.3.1 Sorption Mechanisms

The mechanisms of Sn(IV) sorption on HCP are not well understood. To date, only the study of Bonhoure et al. (2003) provides information on the structural environment of Sn, using EXAFS spectroscopy. They observed the formation of inner-sphere complexes in case of Sn interaction with CSH phases, but a different type of inner-sphere complex in case of Sn interaction with HCP. In HCP, an alternative to CSH as sorption-dominating phase may be ettringite. Ultimately, it has to be admitted that the available information is not conclusive with regard to:

- the sorption-dominating mineral phase; and
- the question whether surface sorption of Sn or/and incorporation is taking place.

10.2.3.2 Sorption at State I

Based on the similarity of the Sn(IV) aqueous speciation between pH 12.5 and 13.3 (see Fig. 10.4), the values selected for State II are accepted (Table 10.2). This is also consistent with the data shown in Fig. 10.7.

Table 10.2 Selected best estimate, upper and lower limit R_d values for tin

pH state	Best estimate (L/kg)	Upper limit (L/kg)	Lower limit (L/kg)
State I	2×10^4	2×10^5	1×10^4
State II	2×10^4	2×10^5	1×10^4
State III	i.d.[a]	i.d.	i.d.
State IV	i.d.	i.d.	i.d.

[a]i.d. = insufficient data

10.2.3.3 Sorption at State II

In the absence of more recent information, the argumentation in Andra (2005) and Ochs and Talerico (2006) is followed, and the best estimate R_d is selected on the basis of the isotherm shown in Fig. 10.9 as 20,000 L/kg (Table 10.2). Based on the upper limit isotherm in Fig. 10.9, on the data for CSH phases in Figs. 10.8 and 10.7, and on the data for NRVB in Fig. 10.7, an upper limit of 200,000 L/kg is selected. This reflects the top end of the experimental data for HCP (Fig. 10.7). Based on the lower limit isotherm in Fig. 10.9 and on the minimum values for CSH in Fig. 10.8, a lower limit of 10,000 L/kg is selected. Note that the data selection for State II is based on a slightly enlarged pH-range-centred around pH 12.5 (rather than strictly on data for 12.5 only). This is based on the nearly constant speciation of Sn(IV) above pH 12, and on the similarity of corresponding data in the pH range of about 12.3–12.8.

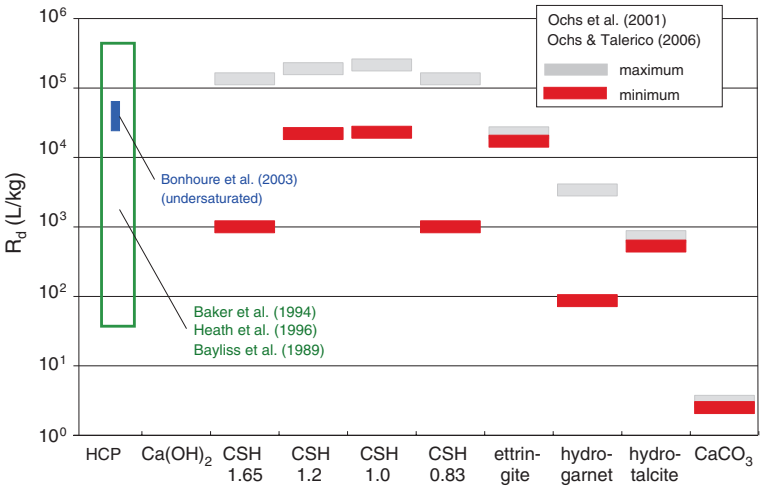

Fig. 10.8 Overview of R_d values for Sn(IV) on HCP and several cement minerals. In all cases, the entire range of observed R_d values is indicated. HAC is hydrated high-alumina cement paste. Literature data sources are indicated in the graph. Data for CSH phases represent minimum and maximum values of isotherms. Modified from Andra (2005)

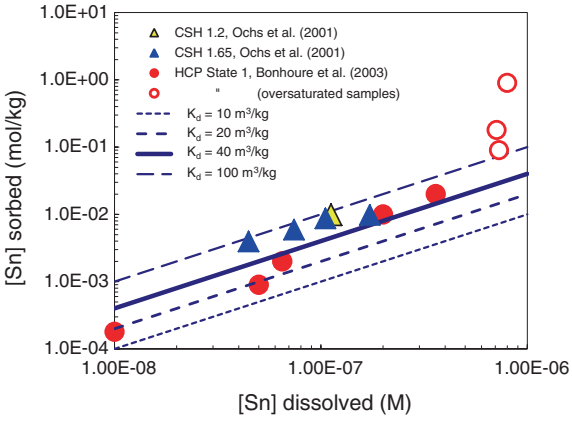

Fig. 10.9 Isotherm plot for the sorption of Sn by fresh HCP and CSH with C/S >1.2. The calculated *solid line* corresponds to a R_d of 40 m3/kg, the upper and lower *dashed lines* correspond to R_d values of 100, 10, and 20 m^3/kg, respectively. The *open circles* represent experiments where the precipitation of $SnCa(OH)_6^{2-}$ occurred, for experiments represented by *closed circles*, the absence of a solid Sn phase had been confirmed by EXAFS (Bonhoure et al. 2003). All symbols correspond to individual measurements. Modified from Andra (2005)

10.2.3.4 Sorption at State III

None of the available experimental data are directly applicable to State III. While some data obtained by Ochs and Talerico (2006) on CSH phases correspond to the relevant C/S ratio, they were obtained at pH values near 12.5. Therefore, no sorption values are selected.

10.2.3.5 Sorption at State IV

For the sorption of Sn(IV) at State IV, only the values by Ochs and Talerico (2006) on calcite at pH 12.6 were found. Because these data do not correspond directly to the conditions relevant for State IV, no recommended values are selected.

10.2.4 Supplemental Values for Assessment Calculations

For States III and IV, the following supplemental values can be provided

10.2.4.1 Supplemental Values for State III

- Best estimate as well as lower limit is taken from State IV. A very conservative best estimate of three is proposed based on the selected best estimate for

Table 10.3 Supplemental values for tin for States III and IV

pH state	Best estimate (L/kg)	Upper limit (L/kg)	Lower limit (L/kg)
State III	3	2×10^5	0.3
State IV	3	30	0.3

State IV, while the lower bound of 0.3 corresponds to the lower limit supplemental value for State IV. This is a conservative approach for State III, since only sorption by calcite is considered, whereas any contribution to sorption by HCP phases is not taken into account. Indeed, under the assumption that hydrolysis of Sn from $Sn(OH)_5^-$ to $Sn(OH)_6^{2-}$ has no influence on sorption values for State II (e.g. those for C/S of 1.2 and 1.65, see Fig. 10.7) would be close to those for State III.

- The upper bound is based on the assumption that HCP phases such as CSH and/or ettringite are still present (in addition to calcite). For this case, a value of 200,000 L/kg is selected for State II in Table 10.2. The hydrolysis behaviour of Sn(IV) suggests that sorption should increase when pH is lowered from pH 12.5 towards pH 9, as the negatively charged and highly hydrolysed species become less important. Therefore, the value of 200,000 L/kg selected for State II is proposed as upper limit supplemental value for State III.

10.2.4.2 Supplemental Values for State IV

The best estimate supplemental value of 3 L/kg is recommended, based on the values by Ochs and Talerico (2006) on calcite. The hydrolysis behaviour of Sn(IV) is again interpreted to imply that Sn sorption would not decrease between pH 12.5 and pH 9.

Supplemental values for upper and lower limits are set arbitrarily to 30 and 0.3 L/kg, respectively. This is a pure operational procedure, i.e. the best estimate an order of magnitude up and down (Table 10.3).

References

Andra, Référentiel de comportement des radionucléides et des toxiques chimiques d'un stockage dans le Callovo-Oxfordien jusqu'à l'homme, Site de Meuse/Haute-Marne, Tome 1/2: Chapitres 1 à 4, Dossier 2005 Argile (2005)

C.F. Baes, R.E. Mesmer, The hydrolysis of cations, 2nd edn. ed by R.E. Krieger (1986)

S. Baker, R. McCrohon, P. Oliver, N.J. Pilkington, The sorption of niobium, tin, iodine and chlorine onto NIREX reference vault backfill. Mat. Res. Soc. Symp. Proc. **333**, 719–724 (1994)

S. Bayliss, F.T. Ewart, R.M. Howse, J.L. Smith-Briggs, H.P. Thomason, H.A. Willmott, The solubility and sorption of lead-210 and carbon-14 in a nearfield environment. Mat. Res. Soc. Symp. Proc. **112**, 33–42 (1988)

S. Bayliss, F.T. Ewart, R.M. Howse, S.A. Lane, N.J. Pilkington, J.L. Smith-Briggs, S.J. Williams, The solubility and sorption of radium and tin in a cementious near-field environment. Mat. Res. Soc. Symp. Proc. **127**, 879–885 (1989)

S. Bayliss, A. Haworth, R. McCrohon, A.D. Moreton, P. Oliver, N.J. Pilkington, A.J. Smith, J.L. Smith-Briggs, Radioelement behaviour in a cementitious environment. Mat. Res. Soc. Symp. Proc. **257**, 641–648 (1992)

U. Berner, *Project Opalinus Clay: Radionuclide Concentration Limits in the Cementitious Near-Field of an ILW Repository* (PSI Bericht, 2002) pp. 02–26

I. Bonhoure, E. Wieland, A.M. Scheidegger, M. Ochs, D. Kunz, EXAFS study of Sn(IV) immobilization by hardened cement paste and calcium silicate hydrates. Environ. Sci. Technol. **37**, 2184–2191 (2003)

M.H. Bradbury, L.R. Van Loon, *Cementitious Near-Field Sorption Data Bases for Performance Assessment of a L/ILW Disposal Facility in a Palfris Marl Host Rock*. CEM-94: Update I, June 1997, (PSI Bericht Nr., 1998) pp. 98–01

N.D.M. Evans, Binding mechanisms of radionuclides to cement. Cem. Concr. Res. **38**, 543–553 (2008)

T.G. Heath, D.J. Ilett, C.J. Tweed, Thermodynamic modelling of the sorption of radioelements onto cementitious materials. Mat. Res. Soc. Symp. Proc. **412**, 443–449 (1996)

D. Jacques, L. Wang, E. Martens, D. Mallants, Time dependency of the geochemical boundary conditions for the cementitious engineered barriers of the Belgian surface disposal facility, project near surface disposal of category: a waste at Dessel. NIRAS-MP5 DATA-LT(NF) Version 1, NIROND-TR 2008-24 E (2008)

B. Lothenbach, M. Ochs, D. Hager, Thermodynamic data for the solubility of tin(IV) in aqueous cementitious environments. Radiochim. Acta **88**, 521–526 (2000)

M. Ochs, B. Lothenbach, C. Talerico, *Support of Kd Models and Datasets for the Retention of Radionuclides in Cementitious Repositories*. Andra 2005 Report C.RP.0BMG.01-001, Andra 2005, France (2001)

M. Ochs, C. Talerico, Development of models and datasets for radionuclide retention by cementitious materials, Andra 2005 report 2006, C.RP.0BMG.06.0001A (2006)

M. Ochs, B. Lothenbach, D. Hager, A. Helfer, B. Wierczinski, G. Skarnemark, Solubility Limits and Adsorption Reactions. Experimental and Theoretical Investigation on the Behaviour of Sn, Ni, Eu (Am), Pb, Re (Tc), Th, Sr and Cs in Cementitious Systems, Andra 2005 Technical Note C NT 0BMG 97-001, Paris, France (1997)

M. Ochs, D. Hager, S. Helfer, B. Lothenbach, Solubility of radionuclides in fresh and leached cementitious systems at 22 & #xB0;C and 50 & #xB0;C. Mat. Res. Soc. Symp. Proc. **506**, 773–780 (1998)

N.J. Pilkington, N.S. Stone, The solubility and sorption of nickel and niobium under high pH conditions, NSS/R 186 (1990)

N.J. Pilkington, P.J. Shadbolt, J.D. Wilkins, Experimental measurements of the solubilities of selected long-lived fission products, activation products and actinide daughters under high pH conditions, NSS/R116, ILWRP/87/P7 (1988)

F. Séby, M. Potin-Gautier, E. Giffault, O.F.X. Donard, A critical review of thermodynamic data for inorganic tin species. Geochim. Cosmochim. Acta **65**, 3041–3053 (2001)

C. Talerico, M. Ochs, E. Giffaut, Solubility of niobium(V) under cementitious conditions: Importance of Ca-niobate. Mat. Res. Soc. Symp. Proc. **842**, 443–448 (2004)

U.S. Departement of Energy (USDOE), National low-level waste management program radionuclide report series, vol. 11: Niobium-94, DOE/LLW-127 (1995)

E. Wieland, L. Van Loon, Cementitious near-field sorption data base for performance assessment of an ILW repository in Opalinus Clay (PSI Bericht Nr., 2002), pp. 03–06

Chapter 11
Sorption Values for Hydrogen and Beryllium

Abstract Tritium (^{3}H or T) is a radioactive isotope of hydrogen occurring in radioactive waste in the form of gas or tritiated water (HTO). Tritium also has been and is being released into the environment as a result of military weapons testing and nuclear power generation. Radioactive waste may contain different beryllium isotopes. For both hydrogen and beryllium isotopes, there is some indication as well as chemical reasoning that sorption or isotope exchange may occur and retard transport. However, the lack of clear experimental data does not allow to assign any non-zero sorption value to either tritium or beryllium with sufficient confidence.

11.1 Hydrogen (Tritium)

11.1.1 Chemical Form, Speciation, and Solubility

Three possible hydrogen isotopes exist: ^{1}H, ^{2}H, and ^{3}H. The most abundant and lightest isotope of hydrogen has a mass number of one and is represented as ^{1}H or simply H. Approximately 99.85 % of all naturally occurring isotopes of hydrogen (present on Earth) consist of the light hydrogen (^{1}H) isotope. The next heaviest isotope of hydrogen has a mass number of two and is represented by the chemical symbols ^{2}H or D (deuterium). Both ^{1}H and ^{2}H are non-radioactive. The heaviest isotope, ^{3}H or tritium, has a mass number of three and is radioactive (half-life 12.3 years). Tritium is naturally produced in very small quantities by the interaction of cosmic rays with atoms and molecules of the upper atmosphere. Since the beginning of the atomic age, large quantities of tritium have entered the environment from man-made sources, mainly atmospheric testing of thermonuclear weapons (e.g. hydrogen bombs). Furthermore, increasing amounts of tritium are being released as the result of the normal operation of nuclear power reactors and fuel reprocessing operations. Small quantities of tritium are produced in the fuel and coolant of a nuclear reactor. For example, tritium is produced as a result of the

© Springer International Publishing Switzerland 2016

M. Ochs et al., *Radionuclide and Metal Sorption on Cement and Concrete*,
Topics in Safety, Risk, Reliability and Quality 29,
DOI 10.1007/978-3-319-23651-3_11

fission process itself and as activation of boron contained in the coolant of pressurised water reactors. Significant quantities of tritium can also be generated from activation of boron used in control rods. However, most of this material is trapped inside the rods. Tritium in LILW will be present as dissolved gas or as molecular water (i.e. tritiated water) or as hydrated proton H^+.

11.1.2 Sorption Values from the Literature for the Benchmark Cement

Tritium may prevail as dissolved gas or tritiated water in the pore solution of cement (Bradbury and Sarott 1995). Tritium in the dissolved gaseous form, if present, is unlikely to be retarded by cement to a large extent and is out of the scope of this review. Tritiated water (HTO) may be retained by cement through isotope exchange with water bound to cement. Although cement "hydration" may bind considerable amounts of water, e.g. by forming CSH phases, the question remains as to what proportion of this bound water is accessible for exchange with tritium. For this reason, Bradbury and Sarott conservatively assigned a zero R_d for tritium (Bradbury and Sarott 1995).

Tits et al. (2003) determined R_d for HTO by batch experiments on HCP and compared it with diffusion tests carried out by Jakob et al. (1999). Excellent agreement was found between the two experiments resulting in a non-zero R_d of 0.8 L/kg. In addition, the authors demonstrated that isotope exchange alone, even taking 100 % of bound water as accessible, cannot account for the observed sorption of HTO. Other mechanisms such as diffusion into dead-end pores in cement might be involved. Wieland and Van Loon (2002) reviewed literature and found lower R_d values (<0.1 L/kg), e.g. in the work of Holgersson et al. (1998). These differences in R_d for HTO might be due to different water to cement ratios used in HCP preparation. There was an indication that higher R_d values were generally found in cements prepared with higher water to cement ratios.

No summary graphs and tables were produced given the limited amount of data.

11.1.3 Sorption Mechanisms and Selected Sorption Values

Although tritium (HTO) is characterised by very low to modest sorption, comparison of different diffusion tests reveals sensitivity to water/cement ratio, i.e. higher water/cement ratios result in higher R_d values (Wieland and Van Loon 2002). It is suggested (E. Giffaut, personal communication) that the fresh cement state, where some partially hydrated phases may exist, might influence the retardation of tritium. For both cases, R_d may depend on cement formula because different cement may develop quite different pore structures in terms of dead-end pores and the degree of hydration.

Table 11.1 Selected best estimate, upper and lower limit R_d values for H

pH state	Best estimate (L/kg)	Upper limit (L/kg)	Lower limit (L/kg)
State I	0	0	0
State II	0	0	0
State III	0	0	0
State IV	0	0	0

11.1.3.1 Sorption Mechanisms

Tritiated water can undergo isotopic exchange reactions with hydrogen (bound protons, OH^- ions, and water) on cement. Other mechanisms such as diffusion into dead-end pores in cement have also been reported as possible uptake mechanism (Tits et al. 2003).

11.1.3.2 Sorption at States I, II, III, and IV

Due to an extreme lack of sorption data (two sets only and no potential analogues), the experts felt unable to assign any R_d values formally. The experts agreed that they could say that there is some evidence of weak retardation, but could not come up with any best estimates or upper/lower bounds. As a default, a value of 0 has been proposed. In older studies of cement, it was found that cements are not good for immobilising tritium, as it exchanges with the surroundings too readily (Table 11.1).

11.2 Beryllium

11.2.1 Chemical Form, Speciation, and Solubility

Beryllium is a relatively rare element in the Earth's crust. It is found naturally with other elements combined in minerals; it is found in coal, soil, and volcanic dust (ATSDR 2002). The beryllium concentration of the Earth's surface rocks is ca. 4–6 ppm. The free element is a steel-grey, strong, lightweight brittle alkaline earth metal which is primarily used as a hardening agent in alloys (e.g. beryllium copper) (Behrens et al. 2003). In its chemistry, beryllium exhibits the +II oxidation state.

Although beryllium (Be) has multiple isotopes, only ^{9}Be is stable. The other isotopes are short-lived apart from ^{10}Be. Cosmogenic ^{10}Be is produced in the atmosphere through spallation of oxygen and nitrogen. This ^{10}Be production depends on the intensity of high energy cosmic rays and is influenced by the solar wind. ^{10}Be accumulates at the soil surface and is present in common rocks and minerals, where its relatively long half-life [1.6×10^6 years (NEA 2006)] permits a long residence time before decaying to ^{10}B (Audi et al. 2003; Wieser 2006).

It can also be formed by nuclear explosions, through the reaction of fast neutrons with $^{13}CO_2$ in the air. In this way, it is one of the historical indicators of past activity of nuclear bomb testing. ^{10}Be and its daughter product are extremely useful to examine different soil formation processes, soil erosion, and the age of ice cores (Whitehead et al. 2008). Yet another naturally occurring beryllium isotope is ^{7}Be (half-life = 53.3 days); as with ^{10}Be, it is a natural cosmogenic radionuclide produced in the upper atmosphere by cosmic ray spallation of nitrogen and oxygen. It is used for investigating soil erosion processes occurring over short timescales, particularly individual storm events or short periods of heavy rainfall (Mabit et al. 2008). LILW may contain the beryllium radionuclides ^{7}Be and ^{10}Be.

In the absence of data specific for Be, a chemical analogue was considered, for instance with aluminium. However, since aluminium is present in large quantities in cement, it would complicate the analysis as some isotopic exchange mechanism would need to be assumed. Since considerable uncertainties exist about potential Al isotope distribution mechanisms (for example, will the presence of small amounts of Al results in formation of new phases?), the analogy with Al is currently not pursued although it has considerable potential.

No speciation plot is produced for Be since the Thermochimie 7b database does not contain data for Be. Other databases with Be data could be used, but for reasons of consistency this was not implemented.

11.2.2 Sorption Values from the Literature for the Benchmark Cement

No reliable sorption values for Be on cementitious materials could be found. Based on the hydrolysis characteristics of Be^{2+} (e.g. Baes and Mesmer 1986), a general tendency towards strong sorption can be expected. Wieland and Van Loon (2002) show an interesting plot relating the charge/size ratio (z/d) of various ions to sorption on HCP. In this plot, Be would be positioned very roughly in a region of $R_d \approx 1000$ L/kg. However, even though strong sorption would be expected following expert opinion, the absence of experimental data prevents the assignment of nominal values for Be.

11.2.3 Sorption Mechanisms, Selected Sorption Values, and Supplemental Values

There is insufficient evidence to derive sorption values for beryllium. Similarly, no supplemental values for assessment calculations can be provided, but only qualitative arguments for general guidance can be given. It is recognised that zero sorption would be overly conservative, not warranted and unlikely. Strong

Table 11.2 Selected best estimate, upper and lower limit R_d values for total beryllium

pH state	Best estimate (L/kg)	Upper limit (L/kg)	Lower limit (L/kg)
State I	i.d.[a]	i.d.	i.d.
State II	i.d.	i.d.	i.d.
State III	i.d.	i.d.	i.d.
State IV	i.d.	i.d.	i.d.

[a]i.d. = insufficient data

sorption could be expected in the form of substitution for Al in cement phases. On this basis and considering the charge/size ratio of the Be^{2+} ion as well as the relation of this value to sorption (Wieland and Van Loon 2002), strong sorption in the order of 1000 L/kg may be expected (with an upper limit certainly smaller than 10,000 L/kg). However, to date this cannot be supported by any measurements. Therefore, only a nominal supplemental value different from zero could be proposed for the lower limit (Table 11.2).

References

Agency for Toxic Substances and Disease Registry (ATSDR), *Toxicological Profile for Beryllium* (U.S. Department of Health and Human Services, Public Health Service, Atlanta, 2002)

G. Audi, A.H. Wapstra, C. Thibault, J. Blachot, O. Bersillon, Isotope masses from AME2003 atomic mass evaluation. Nucl Phys **A729** (2003)

C.F. Baes, R.E. Mesmer, *The Hydrolysis of Cations*, 2nd edn. ed. by R.E. Krieger (1986)

V. Behrens, in *11 Beryllium*, ed. P. Beiss, Landolt-Börnstein—Group VIII Advanced Materials and Technologies: Powder Metallurgy Data. Refractory, Hard and Intermetallic Materials, vol 2A1 (Springer , Berlin, 2003), pp. 1–11

M.H. Bradbury, F. Sarott, *Sorption Databases for the Cementitious Near-Field of a L/ILW Repository for Performance Assessment* (PSI Bericht, 1995), pp. 95–06

S. Holgersson, Y. Albinsson, B. Allard, H. Boren, I. Pavasars, I. Engkvist, Effects of Gluco-isosaccharinate on Cs, Ni, Pm, and Th sorption onto, and diffusion into cement. Radiochim. Acta. **82**, 393–398 (1998)

A. Jakob, F. Sarott, P. Spieler, Diffusion and sorption on hardened cement pastes—experimental and modelling results. Nagra technical report 99-06, August 1999

L. Mabit, M. Benmansour, D.E. Wallling, Comparative advantages and limitations of the fall-out radionuclides 137Cs, 210Pbex and 7Be for assessing soil erosion and sedimentation. J. Environ. Radioact. **99**, 1799–1807 (2008)

Nuclear Energy Agency (NEA-OECD), The JEFF-3.1 nuclear data library. JEFF report 21, OECD/NEA, Paris, France, 2006

J. Tits, A. Jakob, E. Wieland, P. Spieler, Diffusion of tritiated water and $^{22}Na^{+}$ through non-degraded hardened cement pastes. J. Contam. Hydrol. **61**, 45–62 (2003)

E. Wieland, L. Van Loon, *Cementitious Near-Field Sorption Data Base for Performance Assessment of an ILW Repository in Opalinus Clay* (PSI Bericht Nr., 2002), pp. 03–06

N. Whitehead, S. Endo, K. Tanaka, T. Takatsuji, M. Hoshi, S. Fukutani, R. Ditchburn, A. Zondervan, A preliminary study on the use of (10)Be in forensic radioecology of nuclear explosion sites. J. Environ. Radioact. **99**(2), 260–270 (2008)

M.E. Wieser, Atomic weights of the elements 2005 (IUPAC Technical Report). Pure Appl. Chem. **78**(11), 2051–2066 (2006)

Chapter 12
Sorption Values for Zirconium

Abstract Zirconium (Zr) is used in nuclear reactors (in the form of zircaloys) because of its low thermal neutron capture cross section and high resistance to corrosion. In aqueous solutions, zirconium exists exclusively in the tetravalent oxidation state. Zr(IV) hydrolyses strongly with $Zr(OH)_4(aq)$, and $Zr(OH)_6^{2-}$ being the only relevant species in cementitious environments (and low zirconium concentration). Very high sorption of zirconium has been observed in all cementitious materials investigated to date (hydrated cement pastes, CSH phases). Sorption appears to increase with the degree of cement degradation, in particular from a C/S ratio of 1.3 to 1.0. While the actual sorption mechanisms for zirconium are not known, the available evidence suggests that mainly CSH phases are responsible for zirconium sorption on cementitious materials.

12.1 Chemical Form, Speciation, and Solubility

Zirconium is a strong transition metal that resembles titanium. Zirconium is in oxidation number +IV in nearly all of its compounds. However, also the valences +I, +II, and +III exist (Wailes and Weigold 1971), although they are not stable in aqueous solution. Zirconium is generally used as an alloying agent due to its high resistance to corrosion (Lide 2007). It forms both inorganic and organometallic compounds such as zirconium dioxide and zirconocene dichloride, respectively. Ninety per cent of all zirconium produced is used in nuclear reactors (in the form of zircaloys) because of its low capture cross section for thermal neutrons and resistance to corrosion (Lide 2007). It is frequently used as cladding of fuel rods in nuclear reactors.

Naturally occurring zirconium is composed of five isotopes. ^{90}Zr (most common; i.e. 51.45 %), ^{91}Zr and ^{92}Zr are stable, whereas ^{94}Zr [half-life of 6×10^{15} years (NEA 2006)] and ^{96}Zr [half-life 3.9×10^{19} years (NEA 2006) are radioactive (Audi 2003)].

Furthermore, 28 artificial isotopes of zirconium have been synthesised. ^{93}Zr is the longest lived artificial isotope, with a half-life of 1.53×10^6 years (NEA 2006). It is formed by neutron activation of components in nuclear reactors or by

© Springer International Publishing Switzerland 2016

M. Ochs et al., *Radionuclide and Metal Sorption on Cement and Concrete*,
Topics in Safety, Risk, Reliability and Quality 29,
DOI 10.1007/978-3-319-23651-3_12

nuclear fission (Peterson et al. 2007). The heaviest isotope of zirconium ^{110}Zr has an estimated half-life of only 30 ms (NEA 2006). Radioactive isotopes at or above mass number 93 display beta-decay, whereas those at or below 89 decay by beta+. The only exception is ^{88}Zr, which decays by electron capture (Audi 2003). LILW may contain the following radionuclides: ^{93}Zr (half-life 1.53×10^6 years) and ^{95}Zr (half-life 0.175 years).

Data on the probable speciation of zirconium in cement are scarce. To facilitate understanding, calculations have been undertaken of the speciation state in respect of water.

Zirconium is not redox sensitive; therefore, Zr(IV) is the only oxidation state and the most important species at pH above 8 are shown in Fig. 12.1. In a cement system, only two hydrolysis species are important at a low activity level (10^{-8}): $Zr(OH)_4(aq)$ and $Zr(OH)_6^{2-}$.

In a cement system where pH is high, relevant solubility-controlling phases for Zr are hydroxides differing in crystallinity. The current database ThermoChimie 7b includes three Zr oxi- and hydroxides, namely ZnO_2(mono), $Zr(OH)_4$(am, aged), and $Zr(OH)_4$(am, fresh). Note that the data for the $Zr(OH)_4$(am, aged) were recalculated from some experimental data discussed in the NEA Zr review (Brown 2005). The review, however, did not select the phase $Zr(OH)_4$(am, aged) because of uncertainty.

Amorphous $Zr(OH)_4$(am) is the most soluble among the three phases with solubility around 10^{-4} mol/kg in equilibrium with the polynuclear species $Zr_4(OH)_{16}$ (Fig. 12.2). Based on the inventory concentration (Sect. 3.8.1) of Zr (around 10^{-5} mol/kg), Zr solubility controlled by amorphous $Zr(OH)_4$ cannot be reached; therefore, the phase is not relevant in the context of Zr solubility assessment. The more aged amorphous $Zr(OH)_4$ and the crystalline ZrO_2 have lower solubilities at about 10^{-8} and 10^{-9} mol/kg, respectively (Figs. 12.3 and 12.4).

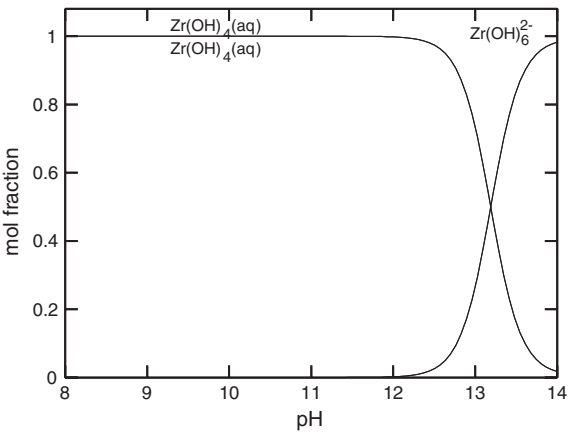

Fig. 12.1 Dissolved zirconium speciation as mol fraction versus pH (Zr concentration is 10^{-8} mol/L). Thermodynamic database: ThermoChimie 7b

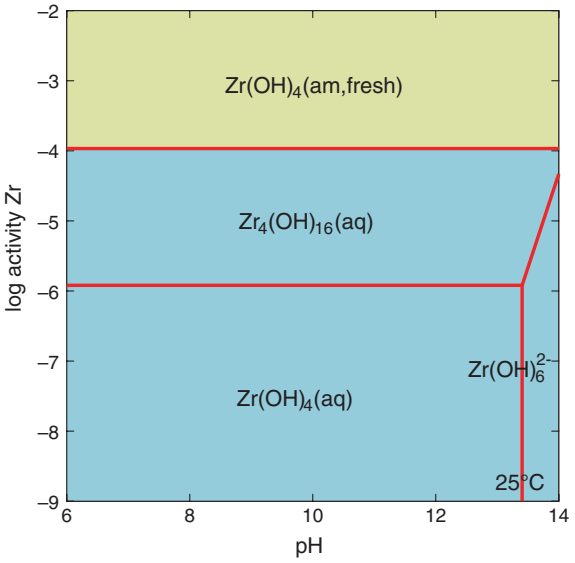

Fig. 12.2 Solubility of $Zr(OH)_4$ (am, fresh) in a Zr–H_2O system. Thermodynamic database: ThermoChimie 7b

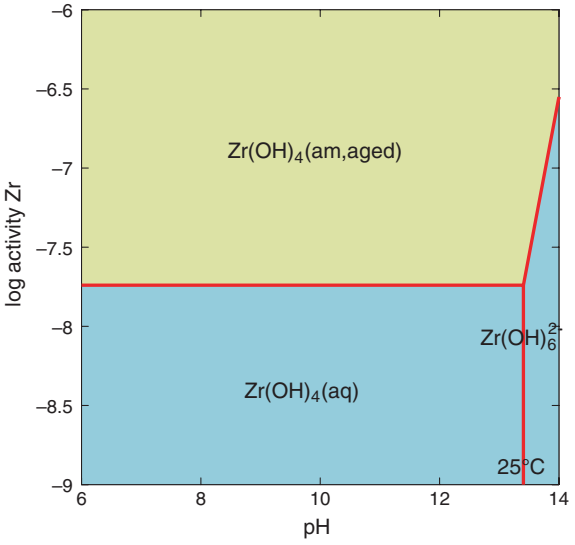

Fig. 12.3 Solubility of $Zr(OH)_4$ (am, aged) in a Zr–H_2O system. Thermodynamic database: ThermoChimie 7b

In summary, the calculated Zr solubility in a cement system is likely to be in a range of 10^{-9} to 10^{-8} mol/kg controlled by the solubility of either amorphous Zr hydroxide or crystalline Zr oxide.

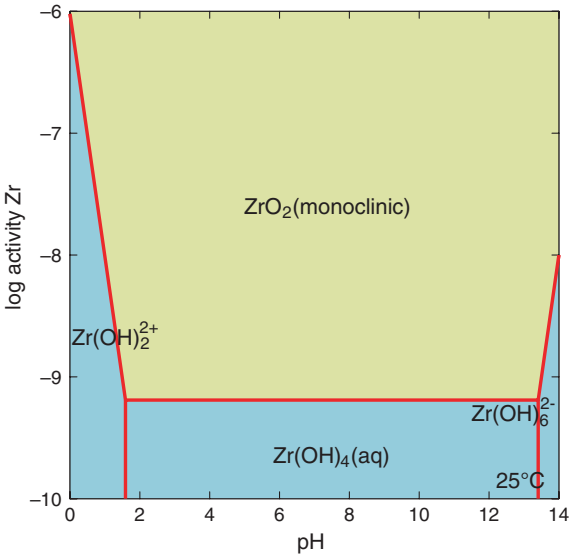

Fig. 12.4 Solubility of ZrO_2 (monoclinic) in a Zr–H_2O system. Thermodynamic database: ThermoChimie 7b

12.2 Sorption Values from the Literature for the Benchmark Cement

Only one reliable and relevant study was found (Pointeau et al. 2004). To our knowledge, no other reliable sorption data are available in the literature. Kulmala and Hakanen (1993) studied the sorption of Zr on HCP for reaction times up to 7 months. However, the initial Zr concentrations in their experiments were above or at the same level as the solubility limit of Zr measured under the same conditions (the solubility limit lies close to the detection limit, see above).

With respect to potential effects of colloid formation on the chemistry of Zr in solution, it is believed that at trace concentrations, the colloid problem should not be dominating. Most studies are done carefully in this respect, because researchers are generally aware of possible colloid problems in experiments with HCP. The sorption data were screened to ensure that investigators were aware of this possibility and took adequate precautions and sufficient characterisation to ensure that colloids were not present or, if present, were excluded from analysis.

Reviewed R_d values for zirconium in a cementitious system are presented in Fig. 12.5 and Table A.19 based largely on Pointeau et al. (2004). For their sorption experiments, they used the following cementitious materials:

- Hydrated cement pastes of CEM I and CEM V were prepared to correspond to different C/S ratios, as follows: CEM I 1.3; CEM I 1.0; CEM I 0.7; CEM V 1.3; CEM V 1.0; and CEM V 0.7.
- CSH phases were synthesised to correspond to C/S ratios of 0.7, 0.9, 1.0, and 1.3.

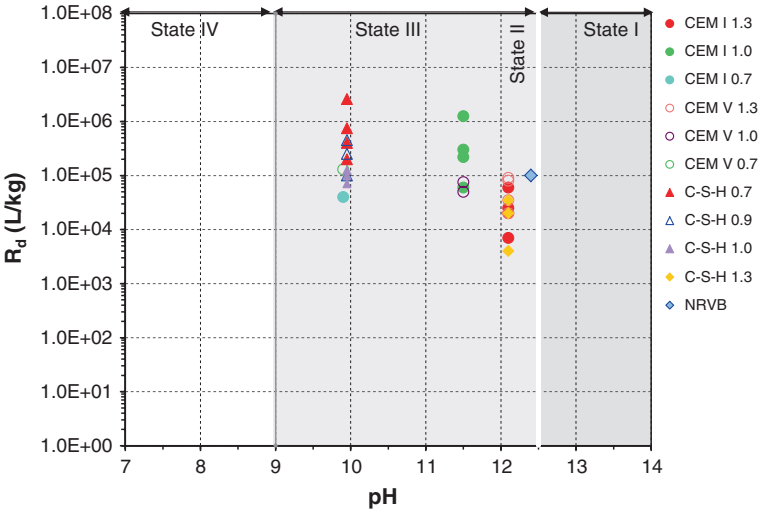

Fig. 12.5 Distribution ratio (R_d) of zirconium in cementitious systems as a function of pH. The data point for NRVB is from Brownsword et al. (2002), and all other data are from Pointeau et al. (2004)

- CEM I and CEM V had been hydrated for 4 years and then used as basis materials (hydration carried out in a saturated portlandite solution in order to avoid carbonation). The first two altered states were obtained using degradation by pure water. For the highest degraded state, an accelerated degradation was carried out using 0.5 mol/L ammonium nitrate solution, followed by filtration, washing, and subjection to final degradation with water. Finally, the solid phases were characterised by X-ray spectroscopy and analysis of the corresponding equilibrium solutions.
- Sorption experiments were performed using solid/liquid ratios from 2.5 to 4 kg/L. As tracer for the sorption experiments, ^{95}Zr with varying initial concentrations $<1 \times 10^{-10}$ mol/L was used. Equilibration time was 9 days.
- An additional value by Brownsword et al. (2002) is available for Zr sorption on HCP (NRVB, pH 12.4), which agrees well with the data by Pointeau et al. (2004).

12.3 Sorption Mechanisms and Selected Sorption Values

According to the data shown in Fig. 12.5, very high sorption of Zr ($R_d \gg 1000$ L/kg) can be observed on all cementitious materials investigated. No systematic difference between CEM I, CEM V, and CSH phases can be observed within each degradation state.

On the other hand, sorption increases with the degree of degradation, in particular from C/S 1.3 to C/S 1.0. This tendency appears to be more pronounced for CEM I and CSH phases than for CEM V. The value for NRVB at 12.4 corresponds very closely to the upper end of the data range for CEM V and CEM I at C/S 1.3.

The agreement between sorption on HCP samples and that on CSH is suggesting that CSH phases may be largely responsible for Zr sorption. At the same time, it can be seen that sorption increases with decreasing C/S ratio, as changing pH causes changes in Zr hydrolysis.

Pointeau et al. (2004) further observed that R_d decreases with increasing (equilibrium) concentration of Zr and offered progressive site saturation as a possible explanation.

12.3.1 Sorption Mechanisms

The data by Pointeau et al. (2004) suggest that mainly CSH phases may be responsible for Zr sorption on cementitious materials, but the actual sorption mechanisms for Zr are not known. According to Sect. 6.1.1, the speciation of Zr at trace levels is similar to Th at pH $\leq$ 12.5, i.e. for States II–III (and IV). Analogy with Th would also support the importance of CSH phases for Zr sorption (cf. Sect. 4.8 in Wang et al. 2009).

Whether the observed increase in Zr sorption from pH $\approx$ 12.1 (C/S 1.3) to pH $\approx$ 11.5 (C/S 0.7) is mainly due to a change in the structure of CSH phases or due to changes in the Zr speciation cannot be concluded on the basis of the available data. However, the very small changes in terms of predominance of $Zr(OH)_4$ over $Zr(OH)_6^{2-}$ between pH 12.1 and 11.5 and a comparison with similar data for Th (see Fig. 44 in Wang et al. 2009) would suggest that changes in the properties of the solid phase are at least partly responsible.

The proposed site saturation effect would be in line with work by Wieland et al. (1998) and Tits et al. (2000) who observed kinetically fast (completed within 2 days) sorption of Th which is indicative of adsorption rather than incorporation. This appears to be in contrast to Sn(IV), where slower sorption kinetics are observed (see Sect. 10.2.2).

12.3.2 Sorption at State I

The data shown in Fig. 12.5 are directly relevant for State III (as defined in Fig. 2.2) only. No direct measurements are available for State I (nor for State II in the strict sense, see below). Taking pH $\approx$ 13.2 as being representative for State I, the Zr species $Zr(OH)_4$ and $Zr(OH)_6^{2-}$ are about equally important. Thus, direct analogy with Th does not seem to be warranted. Analogy with Sn(IV) also needs

Table 12.1 Selected best estimate, upper and lower limit R_d values for zirconium

pH state	Best estimate (L/kg)	Upper limit (L/kg)	Lower limit (L/kg)
State I	i.d.[a]	i.d.	i.d.
State II	1×10^4	1×10^5	1×10^2
State III	1×10^5	5×10^6	1×10^3
State IV	i.d.	i.d.	i.d.

[a]*i.d.* insufficient data

to be taken with care, based on the charge-to-size ratio of the +4 ions (Baes and Mesmer 1986; Wieland and van Loon 2002) and on hydrolysis behaviour. Based on the above arguments, neither best estimate nor upper/lower limits were derived for State I (Table 12.1).

12.3.3 Sorption at State II

No direct measurements are available for State II, and the analogy with Th becomes more difficult as the formation of higher (negatively charged) hydrolytic Zr species becomes more important.

Data for State II are selected on the basis of the State III data for CEM V and CEM I at C/S 1.3 and for NRVB. Due to the lack of data corresponding to State II in the strict sense, the trend of the State III data for C/S 1.0 to C/S 1.3 (Fig. 12.5) is extended into State II. As best estimate, a value of 1×10^4 L/kg is then proposed for State II, with 1×10^5 L/kg as upper limit. As lower limit, 1×10^2 L/kg is proposed. This is a factor of 10 lower than the lower limit proposed for State III with respect to the indicated trend from State III to State II.

12.3.4 Sorption at State III

The data of Pointeau et al. (2004) (see Fig. 12.5) are directly applicable to State III. According to Fig. 2.2, it is considered that all data in Fig. 12.5 fall within State III. On this basis, a best estimate R_d value of 1×10^5 L/kg is selected for State III. Lower and upper limits are selected as 1×10^3 and 5×10^6 L/kg, respectively (Table 12.1).

These values are slightly higher than the corresponding values for Th, which are not unreasonable in view of the apparently stronger hydrolysis of Zr (onset of hydrolysis at lower pH, which would also indicate a higher tendency towards the formation of surface complexes; compare Fig. 12.1 with Fig. 39 in Wang et al. (2009).

12.3.5 Sorption at State IV

In the absence of data for Zr at State IV, no recommended value could be proposed.

12.4 Supplemental Values for Safety Assessment Calculations

12.4.1 Supplemental Values for State I

Supplemental values for State I are selected on the basis of the available data shown in Fig. 12.5. Further extrapolating the trend of the data for C/S 1.3 and C/S 1.0 considered for State II (see selected values) into State I does not seem reasonable in view of the mineralogical evolution of HCP depicted in Fig. 2.2. Following the hypothesis that Zr sorption is largely related to mineralogical properties, the relations shown in this figure would be consistent with a change in sorption when HCP evolves from State II to State III. On the other hand, no major mineralogical changes are depicted between State II and State I.

Therefore, upper (1×10^5 L/kg) and lower limits (1×10^2 L/kg) from State II were accepted as supplemental values. In comparison with the recommended values selected for Sn and Th, these values are conservative. No best estimate can be suggested based on the available data or analogies. We note again that these supplemental data are of lesser quality than the best estimates.

12.4.2 Supplemental Values for State IV

Based on the identical speciation at pH < 10, and the similar size/charge characteristics (Baes and Mesmer 1986), the values selected for Th sorption on calcite in Wang et al. (2009) are accepted as supplemental values for the upper limit (Table 12.1). The lower limit supplemental values are based on analogy with Sn. This would produce a maximum range reflecting the large uncertainty due to lack of data. No best estimate can be suggested based on the available data or analogies (Table 12.2).

Table 12.2 Selected supplemental R_d values for zirconium

pH state	Best estimate (L/kg)	Upper limit (L/kg)	Lower limit (L/kg)
State I	n.v.p.[a]	1×10^5	1×10^2
State IV	n.v.p.	1×10^6	0.3

[a]no value provided

References

G. Audi, A.H. Wapstra, C. Thibault, J. Blachot, O. Bersillon, Isotope masses from AME2003 atomic mass evaluation. Nucl. Phys. A **729** (2003)

C.F. Baes, R.E. Mesmer, *The Hydrolysis of Cations*, 2nd edn (Robert E. Krieger, New York, 1986)

P.L. Brown, in *Chemical Thermodynamics of Zirconium*, vol. 8, ed. by OECD Nuclear Energy Agency (Elsevier, North Holland, 2005)

M. Brownsword, M.C. Manning, N.J. Pilkington, S.J. Williams, The effect of cellulose degradation products on the solubility and sorption of zirconium and the sorption of lead under cementitious repository conditions. Report AEAT/ENV/0549, Jan 2002

S. Kulmala, M. Hakanen, The solubility of Zr, Nb and Ni in groundwater and concrete water, and sorption on crushed rock and cement. YJT report no. YJT-93-21, 1993

D.R. Lide, in *Zirconium*. CRC Handbook of Chemistry and Physics, vol. 4 (CRC Press, New York, 2007), p. 42

Nuclear Energy Agency (NEA-OECD), The JEFF-3.1 nuclear data library. JEFF report 21, OECD/NEA, Paris, France, 2006

J. Peterson, M. MacDonell, L. Haroun, F. Monette, R.D. Hildebrand, A. Taboas, Radiological and chemical fact sheets to support health risk analyses for contaminated areas. Argonne National Laboratory—Environmental Science Division in collaboration with U.S. Department of Energy, March 2007—http://www.ead.anl.gov/pub/doc/ANL_ContaminantFactSheets_All_070418.pdf

I. Pointeau, C. Landesman, N. Coreau, C. Moisan, P. Reiller, Etude de la rétention chimique des radionucléides Cs(I), Am(III), Zr(IV), Pu(IV), Nb(V), U(VI) et Tc(IV) par les matériaux cimentaires dégradés. CEA report 2004, RT DPC/SECR 03-037 indice A, 2004b

J. Tits, E. Wieland, M.H. Bradbury, J.-P. Dobler, The uptake of Eu(III) and Th(IV) by cement-type minerals in the alkaline disturbed zone of a nuclear waste repository, in *Applied Mineralogy in Research, Economy, Technology, Ecology and Culture*, ed. by D. Rammlmair, J. Mederer, T. Oberthür, R.B. Heimann, H. Pentinghaus (Rotterdam, Balkema, 2000)

P.C. Wailes, H. Weigold, Preparation of low oxidation state cyclopentadienyl complexes of titanium and zirconium. I. Compounds of zirconium. J. Organomet. Chem. **28**(1), 91–95 (1971)

L Wang, E. Martens, D. Jacques, P. De Canniere, J. Berry, D. Mallants, Review of sorption values for the cementitious near field of a near surface radioactive waste disposal facility, NIROND-TR 2008-23E, April 2009

E. Wieland, L. Van Loon, Cementitious near-field sorption data base for performance assessment of an ILW repository in Opalinus Clay, PSI Bericht Nr. 03-06, 2002

E. Wieland, J. Tits, P. Spieler, J.-P. Dobler, Interaction of Eu(III) and Th(IV) with sulphate-resisting Portland cement, in *Materials Research Society Symposium Proceedings*, vol. 506 (1998), pp. 573–578

Annex
Summary Tables with Sorption Data

Chlorine

See Table A.1.

© Springer International Publishing Switzerland 2016

M. Ochs et al., *Radionuclide and Metal Sorption on Cement and Concrete*,
Topics in Safety, Risk, Reliability and Quality 29,
DOI 10.1007/978-3-319-23651-3

Table A.1 Reviewed sorption values for chloride with indication of experimental conditions

Reference	Experimental conditions						
	Cementitious material	S/L (kg/L)	Initial concentration (M)	Contact solution	pH	Equilibration time	R_d (L/kg)
Baker et al. (1994)[a]	NRVB	0.02	5×10^{-8} to 0.5	Equilibrated water	12–13.5	Weeks	1–30
Bayliss et al. (1996)[a]	NRVB	0.02	5×10^{-8} to 0.5	Equilibrated water	12.5	49–58 days	1–30
Nielsen et al. (2005)	White and grey cement (low and high Fe content)	0.66	0.01–1	NaOH solution 250 and 550 mM	13.2–13.5	6 months	0.3–5
Aggarwal et al. (2000)	Cements and NRVB	0.02	5.6×10^{-4}	Artificial cement water	11.8–12.7	100 days	<0.7–4
Aggarwal et al. (2000)	CSH_0.83 to _3.0	0.02	5.6×10^{-4}	Artificial cement water	12.5	100 days	<0.7–1.3
Aggarwal et al. (2000)	Hydrotalcite	0.02	5.6×10^{-4}	Artificial cement water	12.5	100 days	32
Pointeau et al. (2008)	CEM I	0.001–0.007	7×10^{-8} ^{36}Cl in 10^{-5} to 3×10^{-4} mol/L total Cl	CEM I-contacted waters	12–13.2	1 month	10–240
Jakob et al. (1999)	SRPC	HCP cylinders (diffusion)	2.8×10^{-5}	Artificial cement water	13.3	~180 days	37–48.4
Sarott et al. (1992)	SRPC	HCP cylinders (diffusion)	2.9×10^{-5}	Artificial cement water	13.3	~167 days	30

[a]data sets are not independent

Iodine

See Table A.2.

Table A.2 Summary of the reviewed R_d for iodide (I^-) on cementitious materials with indication of experimental conditions

Reference	Experimental conditions						
	Cementitious material	S/L (kg/L)	Initial concentration (M)	Contact solution	pH	Equilibration time	R_d (L/kg)
Holland and Lee (1992)	OPC	0.02	1.9×10^{-12}	Equilibrated water	12.5	28 days	69
Allard et al. (1984)	SPB	0.02	1.9×10^{-10}	Artificial cement water	<13.4	6 h to 6 months	126
Andersson et al. (1983)	Cement	0.01–0.02	10^{-8}	Alkali water	13.4	1–14 days	13–20
Baker et al. (2002)	NRVB	0.02	2×10^{-10} to 2×10^{-4}	Artificial cement water	12.5	105–175 days	9–400
Hoglund et al. (1985)	SPB and concretes	0.02	1.9×10^{-9}	Alkali water	12.4–13.4	6 h to 3 months	20–100
Bayliss et al. (1996)	NRVB	0.02	10^{-8} to 10^{-6}	Cement water	12.5	68, 114 days	10–100
Aggarwal et al. (2000)	NRVB	0.02	8.6×10^{-8}	Artificial cement water	12.2	7–57 days	150
Aggarwal et al. (2000)	Cements	0.02	8.6×10^{-8}	Artificial cement water	11.4–12.3	7–57 days	1.9–4.2
Aggarwal et al. (2000)	CSH_0.9 to _3.0	0.02	8.6×10^{-8}	Artificial cement water	11.3–12.9	7–57 days	52–86
Aggarwal et al. (2000)	Ettringite	0.02	8.6×10^{-8}	Artificial cement water	11	7–57 days	5
Andra (2005)	CSH						<0.01
Noshita et al. (2001)	CSH_0.83 to _1.5	0.1	10^{-6}	NaOH and $Ca(OH)_2$ solutions	12.6 (initial)	7 days	5–580
Noshita et al. (2001)	AFm and AFt	0.1	10^{-6}	NaOH and $Ca(OH)_2$ solutions	12.6 (initial)	7 days	4–30
Hietanen et al. (1984)	Crushed concretes	0.1	10^{-6}	Concrete + saline groundwater	9.5–12.6	30 days	2.5–7.7

(continued)

Table A.2 (continued)

Reference	Experimental conditions						
	Cementitious material	S/L (kg/L)	Initial concentration (M)	Contact solution	pH	Equilibration time	R_d (L/kg)
Pointeau et al. (2008)	CEM I	n.a.	1.4×10^{-8}	CEM I-contacted waters	12–13.2	1 month	200–700
Bonhoure et al. (2002)	HCP	0.025	10^{-9} to 5×10^{-4} isotherm	ACW	13.3	7 days	20–150
Sarott et al. (1992)	SRPC	HCP cylinders (diffusion)	3.9×10^{-8}	Artificial cement water	13.3	~167 days	1

Caesium

See Table A.3.

Table A.3 Reviewed sorption values for Cs with indication of experimental conditions

Reference	Experimental conditions						
	Cementitious material	S/L (kg/L)	Initial concentration (M)	Contact solution	pH	Equilibration time (days)	R_d (L/kg)
Allard et al. (1984)	Concretes (a) Portland cement + quartz sand (b) Fly ash + Portland cement + quartz sand (c) Aged concrete from Porjus, Sweden (d) Aged concrete from Trollhättan, Sweden (e) Blast furnace slag cement (f) SRPC (g) Silica cement (h) High alumina cement	0.02	4.3×10^{-10}	(a–e) PW1 (f–g) PW2 (h) PW3	(a) 12.9 and 13.1 (b) 13.1 (c) 13.0 (d) 13.0 (e) 13.1 (f) 12.5 (g) 12.1 (h) 12.9	100	(a) 1 (b) 1.26 (c) 1.26–3.98 (d) 2.5 (e) 1.26 (f) 1 (g) 5 (h) 1.26
Andersson et al. (1983)	(a) Portland cement (b) Portland cement with sand ballast	0.011–0.02	1×10^{-8}	(a1) Artificial groundwater (a2) Artificial Baltic water (a3) Artificial sea water (a4) Pore water (b1) Artificial groundwater (b2) Artificial Baltic water (b3) Artificial sea water	(a1) 12.2 (a2) 10.7 (a3) 9.6 (a4) 13.5 (b1) 11.6 (b2) 9.4 (b3) 9.3	7	(a1) 0–4.8 (a2) 1.77 (a3) 0 (a4) 0–7.5 (b1) 245–850 (b2) 20.5 (b3) 13.2

(continued)

Table A.3 (continued)

Reference	Experimental conditions						
	Cementitious material	S/L (kg/L)	Initial concentration (M)	Contact solution	pH	Equilibration time (days)	R_d (L/kg)
Heitanen et al. (1984)	(a) Portland cement with sand ballast (b) LH cement with sand ballast	0.1	5×10^{-8}	(a) Loviisa groundwater equilibrated with cement water (b) Olkiluoto groundwater equilibrated with concrete	(a) 9.5 and 12.6 (b) 12.6	30	(a) 1.5–840 (b) 2.2–395
Hietanen et al. (1985)	Concrete	0.1	$<1 \times 10^{-7}$	Concrete-equilibrated water	12.5	7	150–390
Idemitsu et al. (1991)	Concrete	0.033	3×10^{-10}	NaOH, HNO_3	7	7	0.72–9.58
Aggarwal et al. (2000)	Cement pastes (a) 3:1 BFS/OPC (b) 9:1 BFS/OPC (c) 3:1 PFA/OPC (d) 10:1 PFA/OPC (e) 6:1 limestone/OPC CSH phases (f) CSH_0.83 (g) CSH_0.9 (h) CSH_1.5 (i) CSH_1.8	0.02	1.3×10^{-7}	(a–e) Cement-equilibrated water (f–i) $Ca(OH)_2$ -saturated water	(a) 12.5 (b) 12.3 (c) 12.2 (d) 11.8 (e) 12.7 (f–i) 12.5	7, 14 and 28	(a) 1 (b) 2.5 (c) 31 (d) 12.3 (e) 5.6 (f) 52 (g) 27 (h) 1 (i) 2
Atkinson and Nickerson (1988)	Cement paste	(a) 0.178 (b) 0.064 (c) 0.053 (d) 0.018 (e) 0.005	1×10^{-4}	Cement-equilibrated water	12.5	147	(a) 0.106 (b) 0.638 (c) 0.691 (d) 1.4 (e) 7.8

(continued)

Table A.3 (continued)

Reference	Experimental conditions						
	Cementitious material	S/L (kg/L)	Initial concentration (M)	Contact solution	pH	Equilibration time (days)	R_d (L/kg)
Holland and Lee (1992)	Cement pastes (a) BFS/SRPC 9:1 (b) PFA/SRPC 9:1 (c) HAC (d) OPC (e) SRPC 9:1	0.02	7.1×10^{-11}	Water	High pH	28	(a) 0 (b) 1.4 (c) 5.2 (d) 11 (e) 17
Iwaida et al. (2001)	CSH_0.8	0.01	1×10^{-2}	CsOH solution	12	7	11
Jakubick et al. (1987)	Concretes	>3.33	6.4×10^{-7} to 1×10^{-3}	Standard Canadian Shield saline solution	8.6–11.5	7	2.3–26.5
Noshita et al. (2001)	(a) CSH phases (b) Pure cement phases	0.1	1×10^{-7}	(a1) NaOH (a2) $Ca(OH)_2$ (b1) NaOH (b2) $Ca(OH)_2$	12.6	7	(a1) 7–3000 (a2) 8–6900 (b1) 0–1600 (b2) 0–34,000
Ochs et al. (2006)	Cement pastes (CEM I, V)	Low	Tracer	Pre-equilibrated pure water	9.6		15,000–30,000
Ochs et al. (2006)	Cement pastes (V/A)	High	Stable Cs	Pre-equilibrated artificial groundwater solution	12.2/12		1/4
Ochs et al. (2006)	Cement pastes (V/C)	High	Stable Cs	Pre-equilibrated artificial groundwater solution	9.4/8.2		100/200
Ochs et al. (2006)	Concrete (V/A)	High	Stable Cs	Pre-equilibrated artificial groundwater solution	11.6/9		1.5/3
Ochs et al. (2006)	CSH	Low	Tracer	Pre-equilibrated pure water	9.9/11.7 /12.1		300/200/150

(continued)

Table A.3 (continued)

Reference	Experimental conditions						
	Cementitious material	S/L (kg/L)	Initial concentration (M)	Contact solution	pH	Equilibration time (days)	R_d (L/kg)
Wieland et al. (2004)	CSH_1.2	0.014	3.8×10^{-9}	ACW	13.3	7–37	2.5
Viallis-Therrisse (2000)	CSH phases	0.05	1×10^{-6}; 1×10^{-4}; 1×10^{-2}; 1×10^{0}	Equilibrated solution	n.a.	10	9.3–411.7
Pointeau (2000)	CSH phases (a) C/S 0.83 (b) C/S 1 (c) C/S 1.25	(a) 0.005, 0.01 (b) 0.01 (c) 0.01	(a) 1.7×10^{-6} to 5.2×10^{-4} (b) 3.4×10^{-6} to 8.5×10^{-4} (c) 3.4×10^{-6} to 8.5×10^{-4}	Equilibrated solution	(a) 11.3 (b) 12.0 (c) 12.25	2	(a) 11–139 (b) 2.8–36 (c) 0.8–32

Strontium

See Table A.4.

Table A.4 Reviewed sorption values for Sr with indication of experimental conditions (contact solutions with $NaClO_4$ are indicated in italic)

Reference	Experimental conditions						
	Cementitious material	S/L (kg/L)	Initial concentration (M)	Contact solution	pH	Equilibration time	R_d (L/kg)
Wieland et al. (2008)	SRPC	2.5×10^{-3} to 0.13	2×10^{-9}	ACW	13.3	30 days	80–110
Wieland et al. (2008)	CSH	10^{-3} to 0.02	10^{-4}	ACW and equilibrated water	13.3 and 12.5	14 days	300 and 40
Tits et al. (2004)	CSH_0.6 to _1.82	0.02	10^{-4} to 10^{-5}	ACW	13.3	Up to ~200 days	100–4000
Ewart et al. (1985)	Cement and concrete	0.2	10^{-6} to 0.016	Equilibrated waters	12.3–12.6	n.a.	1.4–4.6
Hietanen et al. (1985)	Concrete	0.1	$<10^{-7}$	Equilibrated waters	10.5–12.5	7 days	1–5
Hietanen et al. (1984)	Concrete	0.1			9.5–12.6	30 days	1–4
Atkinson and Nickerson (1988)	SRPC	0.01–0.3	10^{-6} to 0.01	State II water	12.5	Up to 147 days	~5
Sugiyama and Fujita (1999)	OPC/BFS	0.02	2.23×10^{-3}	Equilibrated waters	10.8–12.3	35 days	5–170
Sugiyama and Fujita (1999)	CSH_0.9, _1.2, _1.8	0.02	2.23×10^{-3}	Equilibrated waters	9–11	35 days	50–2500
Iwaida et al. (2001)	CSH_0.8 to _1.8	0.01	10^{-3}	Pure water	11–12.4	20 days	25–700
Johnston and Wilmot (1992)	SRPC	0.1	$\sim 10^{-3}$	Saline water	12.5	n.a.	0.15
Zachara et al. (1991)	Calcite	0.025	10^{-7}	$CaCO_3 + NaClO_4$	8.3	1 day	~1

Radium

See Table A.5.

Table A.5 Reviewed sorption values for Ra with indication of experimental conditions (contact solutions with $NaClO_4$ are indicated in italic)

Reference	Experimental conditions						
	Cementitious material	S/L (kg/L)	Initial concentration (M)	Contact solution	pH	Equilibration time	R_d (L/kg)
Holland and Lee (1992)	OPC and SRPC	0.02	1.2×10^{-7}	Equilibrated waters	12.4–12.6	28 days	37–50
Bayliss et al. (2000)	Cements	0.002–0.2	10^{-7} to 10^{-11}	Equilibrated water	11.8–12.4	118–160 days	50–900
Tits et al. (2006a)	HCP-CEM I	10^{-4} to 0.02	~10^{-8}	ACW	12.5–13.3	1–60 days	140–400
Tits et al. (2006a)	CSH (0.64–1.19)	10^{-4} to 0.02	~10^{-8}	ACW	13.3	1−30 days	800–20,000
Tits et al. (2006a)	CSH (0.96–1.6)	10^{-4} to 0.02	~10^{-8}	CSH-equilibrated waters	11.5–12.5	1–30 days	100–2000
Berry et al. (2001)	Calcite	0.02	~10^{-8}	Saline groundwater	7	80 days	<7
Zachara et al. (1991)	Calcite	0.025	10^{-7}	$CaCO_3 + NaClO_4$	8.3	1 day	~1

Nickel

See Table A.6.

Table A.6 Reviewed sorption values for nickel with indication of experimental conditions (contact solutions with $NaClO_4$ are indicated in italic)

Reference	Experimental conditions						
	Cementitious material	S/L (kg/L)	Initial concentration (M)	Contact solution	pH	Equilibration time	R_d (L/kg)
Wieland et al. (2006a)	HCP	10^{-6} to 0.1	10^{-6} to 0.05	Alkali water	13.3	7–28 days	150
Wieland et al. (2000)	SRPC	0.025	10^{-9}	Alkali water	13.3	42 days	70–200
Holgersson et al. (1998)	Cement	0.05	Not available	Alkali water	13.4	1–60 days	10–40
Pilkington and Stone (1990)	HCP	~0.02	10^{-9} to 10^{-6}	State II water	12.3–12.7	21–42 days	100
Noshita et al. (2001)	CSH_1.5	0.1	10^{-8}	$Ca(OH)_2$ solution	12.6	7 days	1200
Noshita et al. (2001)	Portlandite	0.1	10^{-8}	$Ca(OH)_2$ solution	12.6	7 days	3600
Noshita et al. (2001)	Afwillite	0.1	10^{-8}	$Ca(OH)_2$ solution	12.6	7 days	7200
Noshita et al. (2001)	Tobermorite	0.1	10^{-8}	$Ca(OH)_2$ solution	12.6	7 days	7900
Noshita et al. (2001)	Brucite	0.1	10^{-8}	$Ca(OH)_2$ solution	12.6	7 days	3300
Aggarwal et al. (2000)	Cement	0.02	6.7×10^{-9}	Cement-equilibrated water	11.2–12.8	28 days	120–8200
Aggarwal et al. (2000)	CSH_0.9 to _3.0	0.02	6.7×10^{-9}	Cement-equilibrated water	12.3–12.9	28 days	220–470
Aggarwal et al. (2000)	Impure C_3S	0.02	6.7×10^{-9}	Cement-equilibrated water	11.8–12.8	28 days	280–560

(continued)

Table A.6 (continued)

Reference	Experimental conditions						
	Cementitious material	S/L (kg/L)	Initial concentration (M)	Contact solution	pH	Equilibration time	R_d (L/kg)
Cowper et al. (2005)	CSH_2.0	0.02	3×10^{-9}	CSH-equilibrated waters	12.6	30 days	170
Hietanen et al. (1984)	Crushed concretes	0.1	10^{-6}	Concrete + saline groundwater	9.5–12.6	30 days	560–5000
Andra (2005)	CSH_1.65	0.01	~1.5×10^{-7} M; 4.5×10^{-8}	Waters equilibrated with CSH	12.5	27 days	38; 70
Andra (2005)	Ettringite	0.01	~1.5×10^{-7} M; 4.5×10^{-8}	Waters equilibrated with ettringite	12.4	27 days	200; 600
Andra (2005)	Hydrotalcite	0.01	~1.5×10^{-7} M; 4.5×10^{-8}	Waters equilibrated with hydrotalcite	12.5	27 days	800; 1600
Lakshtanov et al. (2000)	Calcite	0.05–0.25	10^{-7} to 10^{-6}	$NaClO_4$	8.3	1 day	5
Zachara et al. (1991)	Calcite	0.025	10^{-7}	$Calcite + NaClO_4$	8.3	1 day	10

Carbon

See Table A.7.

Table A.7 Reviewed sorption values for inorganic C with indication of experimental conditions

Reference	Experimental conditions						
	Cementitious material	S/L (kg/L)	Initial concentration (M)	Contact solution	pH	Equilibration time (days)	R_d (L/kg)
Allard et al. (1981)	(a) Calcite (b) Concrete (c) Cement paste	0.020	Trace concentration	Artificial groundwater	8.1 (initial)	(a) 3–180 (b–c) 7–35	(a) 3.5–83 (b–c) 1600–10,000
Bayliss et al. (1988)	(a) SRPC (b) OPC/BFS	0.1–0.01	1.47×10^{-9}; 9.54×10^{-7}; 9.54×10^{-8}	Cement-equilibrated water	12.4 11.8	100	(a) 6000 (b) 600–3000
Hietanen et al. (1985)	Crushed concrete	0.1	$<10^{-7}$	Groundwater	12.5	7	1850
Matsumoto et al. (1995)	Mortar grain	0.033	7.4×10^{-8}	Distilled water	12.5	160	30,000
Noshita et al. (1988)	OPC (0 % BFS)	0.1	n.a.	Deionised water	12.5	7	2000
Noshita et al. (2001)	CSH_0.83–1.5 phases	0.033	10^{-6}	$Ca(OH)_2$ solution	12.6	7	1800–3900
Pointeau et al. (2008)	CEM I OPC	n.a.	10^{-7}	CEM I-contacted waters	11.5–13.3	30	670–7400

Thorium

See Table A.8.

Table A.8 Reviewed sorption values for thorium with indication of experimental conditions (contact solutions with brine are indicated in italic)

Reference	Experimental conditions						
	Cementitious material	S/L (kg/L)	Initial concentration (M)	Contact solution	pH	Equilibration time	R_d (L/kg)
Hoglund et al. (1985)	OPC and weathered concrete	0.02	2×10^{-6}	Alkali water	13.4	6 h to 3 months	4500
Allard et al. (1984)	Concretes	0.02	2×10^{-10}	Artificial cement water	11.2–13.2	6 h to 6 months	5000
Baker et al. (2002)	Carbonated NRVB	0.02	2×10^{-11}	$Ca(OH)_2$ -dominated cement water	12.5	50 days	3000
Holgersson et al. (1998)	Cement	0.05	n.a.	Alkali cement water	13.4	1 day to 3 months	from >1000 to >10,000
Wieland et al. (1998)	SRPC	10^{-5}	10^{-10}	Artificial cement water	13.3	14 days	5×10^{6}
Wieland and Van Loon (2002)	SRPC	10^{-4}	10^{-10}	Artificial cement water	13.3	14 days	3.5×10^{5}; 6×10^{6}
Wierczinski et al. (1998)	CEM I 42.5 HS	5×10^{-4}	1.1×10^{-11}	Cement-contacted artificial groundwater	12.5; 13.2	480 h	83,310; 19,500
Wierzinski et al. (1998)	CEM I 42.5 HS	5×10^{-3}	1.1×10^{-11}	Cement-contacted artificial groundwater	12.5; 13.2	480 h	>48,000; >3420
Wierzinski et al. (1998)	CEM I 42.5 HS	5×10^{-2}	1.1×10^{-11}	Cement-contacted artificial groundwater	12.5; 13.2	480 h	>4800; >342
Andra (2005)	CEM I	5×10^{-4}	n.a.	Cement-leached solutions	12.3; 11.6; 9.9	4 months	40,000; 40,000; 23,000

(continued)

Table A.8 (continued)

Reference	Experimental conditions						
	Cementitious material	S/L (kg/L)	Initial concentration (M)	Contact solution	pH	Equilibration time	R_d (L/kg)
Andra (2005)	CEM V	5×10^{-4}	n.a.	Cement-leached solutions	12.3; 11.6; 9.9	4 months	50,000; 13,000; 9000
Tits et al. (2000)	CSH_1.09	10^{-4} to 10^{-3}	10^{-10}	Artificial cement water	13.3	3 days	300,000
Greenfield et al. (1997)	NRVB	0.05	10^{-10}	NRVB-equilibrated water	12	1 month	3000
Tits et al. (2008)	CSH_0.65 to _1.82	5×10^{-4} to 1.6×10^{-3}	10^{-11}	ACW- and CSH-equilibrated waters	10.1–13.3	Up to 120 days	10^5 to 10^7
Cowper et al. (2006)	OPC	0.01	10^{-11}	Deionised water	12.9	7 days	64,000
Cowper et al. (2006)	DOPC	0.01	10^{-11}	Deionised water	11.6	7 days	10^6
Tits et al. (2005)	Calcite (Merck)	4×10^{-4} to 0.01	10^{-11}	Artificial cement water	13.3	3 days	30,000
Geibert and Usbeck (2004)	Calcite	5×10^{-7}	~10^{-12}	*Sea water*	8.3	2–120 h	>6×10^5
Maiti et al. (1989)	Calcite-dominated geologic material	0.02	10^{-5} (6 ppm)	*Synthetic brine (2 mol/L $MgCl_2$ and 1 mol/L NaCl)*	6.97	7 days	15,000

Uranium

See Table A.9.

Table A.9 Reviewed sorption values for U(VI) with indication of experimental conditions. Some data for U(IV) also included (italic cells)

Reference	Experimental conditions						
	Cementitious material	S/L (kg/L)	Initial concentration (M)	Contact solution	pH	Equilibration time	R_d (L/kg)
Baker et al. (2002)	Leached NRVB	0.02	1.22×10^{-7}	Water + leached NRVB 1 year	12.2	56 days	5000
Baker et al. (2002)	Leached and heated NRVB	0.02	1.2×10^{-7}	Water + leached and heated NRVB 1 year	11.5	56 days	6000
Baker et al. (2002)	Carbonated NRVB	0.02	4.8×10^{-8}	Artificial saline water	12.5	50 days	2000
Baker et al. (2002)	CSH_1.0	0.02	10^{-7}	Water + CSH 1 month	11.8	64 days	5000
Baker et al. (2002)	Brucite	0.02	6.7×10^{-8}	Water + brucite 1 month	10.3	69 days	5000
Baker et al. (2002)	Ettringite	0.02	6.7×10^{-8}	Water + ettringite 1 month	11	69 days	10,000
Bayliss et al. (1996)	NRVB	0.02	7.3×10^{-8}	Artificial State II water	12.5	106 days	6000
Bayliss et al. (1996)	NRVB	0.02	8.1×10^{-8}	Artificial saline water	12.5	100 days	5000
Berry et al. (2000)	Calcite	0.02	2×10^{-7}	0.1 N $NaNO_3$ solution	8.3–8.4	90 days	~50

(continued)

Table A.9 (continued)

Reference	Experimental conditions						
	Cementitious material	S/L (kg/L)	Initial concentration (M)	Contact solution	pH	Equilibration time	R_d (L/kg)
Pointeau et al. (2004)	CEM I and V	0.001	2×10^{-10} to 3.5×10^{-9}	Leached cement waters	9.8–12.2	3, 9, and 21 days	30,000–150,000
Pointeau et al. (2008)	CEM I	0.001	2×10^{-10} to 3.5×10^{-9}	Leached cement waters	11.5–13.3	15 days	1000–200,000
Sutton et al. (2003)	OPC/PFA grout	1×10^{-4} to 0.025	2×10^{-6}	Leached grout water	11.8	14 days	1500 and 3600
Tits et al. (2008)	CSH_0.64	8×10^{-4} to 5×10^{-3}	2×10^{-8} to 10^{-4}	Artificial cement water	13.3	30 days	500–4200
Tits et al. (2008)	CSH_1.1	8×10^{-4} to 5×10^{-3}	2×10^{-8} to 10^{-4}	Artificial cement water	13.3	30 days	1000–180,000
Tits et al. (2008)	CSH_0.73	8×10^{-4} to 5×10^{-3}	2×10^{-8} to 10^{-4}	Alkali-free pore water	12	30 days	14,000–4×10^5
Tits et al. (2008)	CSH_1.04	8×10^{-4} to 5×10^{-3}	2×10^{-8} to 10^{-4}	Alkali-free pore water	12	30 days	70,000–10^6
Tits et al. (2008)	CSH_0.73 to _1.04	9×10^{-4} to 5×10^{-3}	2×10^{-8} to 10^{-4}	Alkali-free pore water	11.4	1–120 days (kinetic experiment)	300,000–10^6
Tits et al. (2008)	CSH_0.73 to _1.04	9×10^{-4} to 5×10^{-3}	2×10^{-8} to 10^{-4}	Alkali-free pore water	12.1	1–120 days (kinetic experiment)	180,000–670,000

(continued)

Table A.9 (continued)

Reference	Experimental conditions						
	Cementitious material	S/L (kg/L)	Initial concentration (M)	Contact solution	pH	Equilibration time	R_d (L/kg)
Tits et al. (2008)	CSH_0.73 to _1.04	9×10^{-4} to 5×10^{-3}	2×10^{-8} to 10^{-4}	Alkali-free pore water	12.3	1–120 days (kinetic experiment)	150,000–630,000
Tits et al. (2008)	CSH_0.73 to _1.04	9×10^{-4} to 5×10^{-3}	2×10^{-8} to 10^{-4}	Alkali-free pore water	12.5	1–120 days (kinetic experiment)	60,000–260,000
Bayliss et al. (1996)	*NRVB*	*0.02*	*9.9×10^{-9}*	*Artificial State II water*	*12.5*	*136* day	*8000 U(IV)*
Bayliss et al. (1996)	*NRVB*	*0.02*	*9.4×10^{-9}*	*Artificial saline water*	*12.5*	*135* day	*6000 U(IV)*

Plutonium

See Table A.10.

Table A.10 Reviewed sorption values ffor Pu(IV) with indication of experimental conditions (contact solutions with sea water are indicated in italic)

Reference	Experimental conditions						
	Cementitious material	S/L (kg/L)	Initial concentration (M)	Contact solution	pH	Equilibration time	R_d (L/kg)
Allard et al. (1984)	Crushed concretes	0.02	2×10^{-10}	Artificial pore waters	12.3–13.2	6 h to 6 months	1000–10,000 presented as Pu(IV)
Hoglund et al. (1985)	Cements	0.02	1.2×10^{-9}	Artificial pore waters	12.5–13.4	6 h to 3 months	1000–4000 Pu(IV) assumed
Bayliss et al. (2000)	BFS/OPC	0.0025–0.025	$\sim 10^{-12}$	Equilibrated water	12.4	23–27 days	10,000 Pu(IV) assumed
Bayliss et al. (1996)	NRVB	0.02	$\sim 10^{-11}$	Equilibrated water	12.5	41–174 days	1000–70,000 Pu(IV) assumed
Baston et al. (1995)	Concrete and mortars	0.02	$\sim 10^{-12}$	Cement water	12.2–12.5	n.a.	$>10^6$ Pu(IV) assumed
Aggarwal et al. (2000)	Cements and NRVB	0.02	2×10^{-10}	Equilibrated waters	11.8–12.5	28 days	5000 to 10^5 Pu(IV) considered
Baker et al. (2002)	NRVB leached	0.02	1.1×10^{-10}	Artificial cement water	12.2	69 days	40,000 Pu(IV) assumed
Baker et al. (2002)	NRVB leached and heated	0.02	1.1×10^{-10}	Artificial cement water	11.5	69 days	40,000 Pu(IV) assumed
Baker et al. (2002)	CSH_1.0	0.02	1.1×10^{-10}	Artificial cement water	11.8	69 days	40,000 Pu(IV) assumed

(continued)

Table A.10 (continued)

Reference	Experimental conditions						
	Cementitious material	S/L (kg/L)	Initial concentration (M)	Contact solution	pH	Equilibration time	R_d (L/kg)
Baker et al. (2002)	Brucite	0.02	1.1×10^{-10}	Artificial cement water	10.3	69 days	30,000 Pu(IV) assumed
Baker et al. (2002)	Ettringite	0.02	1.1×10^{-10}	Artificial cement water	11	69 days	30,000 Pu(IV) assumed
Andra (2005)	CEM I and V	n.a.	n.a.	n.a.	10–12.2	n.a.	10^4 to 10^5 Pu(Iv)
Berry et al. (2000)	Calcite	0.02	7×10^{-11}	$NaNO_3$ 0.1 N	8.3	90 days	~300 Pu(IV)
Higgo and Rees (1986)	Calcite	0.04	2×10^{-10}	*Sea water*	8.2	100 days	100–400 Pu in reduced form
Higgo and Rees (1986)	Calcite	0.003	2×10^{-10}	*Sea water*	8.2	100 days	>10,000 Pu in oxidised from

Neptunium

See Table A.11.

Table A.11 Reviewed sorption values for Np(IV, V) with indication of experimental conditions

Reference	Experimental conditions						
	Cementitious material	S/L (kg/L)	Initial concentration (M)	Contact solution	pH	Equilibration time	R_d (L/kg)
Allard et al. (1984)	Crushed concretes	0.02	1.9×10^{-7} as Np(V)	Artificial pore waters	12–13.6	100 days	2000–30,000 Np(V)
Hoglund et al. (1985)	Cements	0.02	1.9×10^{-7} as Np(V)	Artificial pore waters	12.5–13.4	6 h to 3 months	300–20,000 Np(V)
Bayliss et al. (2000)	BFS/OPC	0.02	10^{-9} as Np(V)	Equilibrated water (reducing)	11.8–12.2	1–68 days	5300 to $>10^6$ Np(IV)
Bayliss et al. (2000)	BFS/OPC	0.02	10^{-9} as Np(V)	Equilibrated water (aerobic)	11.8–12.2	1–28 days	9000–140,000 Np(IV, V)
Bayliss et al. (1996)	NRVB	0.02	2.5×10^{-10} as Np(IV)	NRVB-equilibrated water	12.5	23 days	60,000 Np(IV, V)
Bayliss et al. (1996)	NRVB	0.02	2.5×10^{-10} as Np(IV)	NRVB-equilibrated saline water	12.5	23 days	200,000 Np(IV, V)

Data from crushed concrete are retained because the R_d values are not higher than others and are therefore judged as not affected by crushing and generation of additional sorption surfaces from aggregates

Protactinium

See Table A.12.

Table A.12 Reviewed sorption values for Pa(V) with indication of experimental conditions

Reference	Experimental conditions						
	Cementitious material	S/L (kg/L)	Initial concentration (M)	Contact solution	pH	Equilibration time	R_d (L/kg)
Berry et al. (1988)	SRPC and OPC/BFS cement	0.02	10^{-11} to 10^{-13}	Cement-equilibrated waters	13.0	Several days	500 to $>10^5$ after 0.45-μm filtration $>3 \times 10^3$ after 30,000 MWCO filtration
Geibert and Usbeck (2004)	Calcite	5×10^{-7}	~10^{-14}	Sea water	8.3	2–120 h	$0.03–0.34 \times 10^6$

Americium

See Table A.13.

Table A.13 Reviewed sorption values for americium and europium (italic cells) with indication of experimental conditions

Reference	Experimental conditions						
	Cementitious material	S/L (kg/L)	Initial concentration (M)	Contact solution	pH	Equilibration time	R_d (L/kg)
Pointeau et al. (2004b)	CEM I (degraded)[a]	5×10^{-4}	n.a.[b]	Equilibrated water	9.8–12.2	7–37 days	$40–150 \times 10^3$
Pointeau et al. (2004b)	CEM V (degraded)[a]	5×10^{-4}	n.a.[b]	Equilibrated water	9.8–12.2	7–37 days	$3–95 \times 10^3$
Pointeau et al. (2004b)	CSH (1.3, 1.0, 0.7)	5×10^{-4}	n.a.[b]	Equilibrated water	9.8–12.2	7–37 days	$86–200 \times 10^3$
Tits et al. (2002)	Calcite	10^{-4} and 10^{-3}	10^{-10} to 10^{-9}	ACW	13.3	Up to 30 days	10^5 and 10^4
Cowper et al. (2006)	OPC	0.01	10^{-12} and 10^{-11}	Distilled water	12.8–12.9	7 days	3000–6000
Cowper et al. (2006)	Degraded OPC	0.01	10^{-12} and 10^{-11}	Distilled water	11.6	7 days	$>10^5$
Baston et al. (1995)	Concrete	0.02 and 0.2	~10^{-11}	Equilibrated water	12.4	n.a.	~10^5
Baston et al. (1995)	Mortar	0.02 and 0.2	~10^{-11}	Equilibrated water	12.2	n.a.	10^4 and 10^5
Baston et al. (1995)	Sandstone	0.02 and 0.2	~10^{-11}	Syn groundwater	~8	n.a.	$3–6 \times 10^4$
Bayliss et al. (2000)	OPC	0.017 and 0.2	10^{-12} to 10^{-11}	Equilibrated water	~12	19–45 days	~10^4
Bayliss et al. (1996)	NRVB	0.02	~10^{-12}	Equilibrated water	12.5	144 days	1000

(continued)

Table A.13 (continued)

Reference	Experimental conditions						
	Cementitious material	S/L (kg/L)	Initial concentration (M)	Contact solution	pH	Equilibration time	R_d (L/kg)
Allard (1984)	Calcite	$6–15 \times 10^{-3}$	$1.8–5 \times 10^{-9}$	Artificial groundwater ($NaHCO_3$)	7–9	5 days	10,000–25,000
Allard et al. (1984)	Crushed concrete	0.02	10^{-9}	Artificial cement water	12.5–13.4	100 days	$100–10^5$
Wieland et al. (1998)	*SRPC*	*10^{-5}*	*10^{-10}*	*ACW*	*13.3*	*Up to 130 days*	*$3–40 \times 10^5$ Eu*
Wieland and Van Loon (2002)	*HTS cement*	*10^{-5} to 10^{-3}*	*10^{-10}*	*ACW*	*13.3*	*7 days*	*$3–7 \times 10^5$ Eu*
Tits et al. (2000)	*CSH_1.09*	*5×10^{-4}*	*10^{-9}*	*ACW*	*13.3*	*Up to 90 days*	*10^5 to 10^6 Eu*
Tits et al. (2003a)	*CSH_1.09* syn CSH_1.0	*3.8×10^{-4}, 5.4×10^{-3}*	*2×10^{-9}*	*ACW*	*13.3*	*1–90 days*	*6×10^5 Eu*

[a]Cement leached by water progressively to result in portlandite-free paste with C/S 1.3, 1.0, and 0.7
[b]Claimed to be below an operational solubility value measured before sorption test

Selenium

See Table A.14.

Table A.14 Reviewed sorption values for selenium with indication of experimental conditions

Reference	Experimental conditions						
	Cementitious material	S/L (kg/L)	Initial concentration (mol/L)	Contact solution	pH	Equilibration time	R_d (L/kg)
Se(IV)							
Ochs and Talerico (2006)	CSH 0.83	5×10^{-3}	1×10^{-5}	Synthetic pore water (pre-equilibrated)	12.4	2 weeks	–
Ochs and Talerico (2006)	CSH 0.83	5×10^{-3}	1×10^{-5}	Synthetic pore water (pre-equilibrated)	12.4	3 months	4
Ochs and Talerico (2006)	CSH 0.83	5×10^{-3}	1×10^{-5}	Synthetic pore water (pre-equilibrated)	12.4	5 months	9
Ochs and Talerico (2006)	CSH 1.0	5×10^{-3}	1×10^{-5}	Synthetic pore water (pre-equilibrated)	12.4	2 weeks	5
Ochs and Talerico (2006)	CSH 1.0	5×10^{-3}	1×10^{-5}	Synthetic pore water (pre-equilibrated)	12.4	3 months	16
Ochs and Talerico (2006)	CSH 1.2	5×10^{-3}	1×10^{-5}	Synthetic pore water (pre-equilibrated)	12.5	2 weeks	11
Ochs and Talerico (2006)	CSH 1.2	5×10^{-3}	1×10^{-5}	Synthetic pore water (pre-equilibrated)	12.5	3 months	146
Ochs and Talerico (2006)	CSH 1.2	5×10^{-3}	1×10^{-5}	Synthetic pore water (pre-equilibrated)	12.5	5 months	96
Ochs and Talerico (2006)	CSH 1.65	5×10^{-3}	1×10^{-5}	Synthetic pore water (pre-equilibrated)	12.6	2 weeks	14
Ochs and Talerico (2006)	CSH 1.65	5×10^{-3}	1×10^{-5}	Synthetic pore water (pre-equilibrated)	12.6	3 months	125
Ochs and Talerico (2006)	CSH 1.65	5×10^{-3}	1×10^{-5}	Synthetic pore water (pre-equilibrated)	12.6	5 months	100
Ochs and Talerico (2006)	Portlandite ($Ca(OH)_2$)	53×10^{-3}	1×10^{-5}	Synthetic pore water (pre-equilibrated)	12.6	2 weeks	290
Ochs and Talerico (2006)	Portlandite ($Ca(OH)_2$)	50×10^{-3}	1×10^{-5}	Synthetic pore water (pre-equilibrated)	12.6	3 months	280
Ochs and Talerico (2006)	Portlandite ($Ca(OH)_2$)	50×10^{-3}	1×10^{-5}	Synthetic pore water (pre-equilibrated)	12.6	9 months	210

(continued)

Table A.14 (continued)

Reference	Experimental conditions						
	Cementitious material	S/L (kg/L)	Initial concentration (mol/L)	Contact solution	pH	Equilibration time	R_d (L/kg)
Ochs and Talerico (2006)	Hydrotalcite	5×10^{-3}	1×10^{-5}	Synthetic pore water (pre-equilibrated)	12.2	2 weeks	22.8
Ochs and Talerico (2006)	Hydrotalcite	5×10^{-3}	1×10^{-5}	Synthetic pore water (pre-equilibrated)	12.2	3 months	–
Ochs and Talerico (2006)	Hydrotalcite	5×10^{-3}	1×10^{-5}	Synthetic pore water (pre-equilibrated)	12.2	9 months	–
Ochs and Talerico (2006)	Calcite ($CaCO_3$)	46×10^{-3}	1×10^{-5}	Synthetic pore water (pre-equilibrated)	12.6	2 weeks	1.5
Ochs and Talerico (2006)	Calcite ($CaCO_3$)	51×10^{-3}	1×10^{-5}	Synthetic pore water (pre-equilibrated)	12.6	3 months	4.8
Ochs and Talerico (2006)	Calcite ($CaCO_3$)	50×10^{-3}	1×10^{-5}	Synthetic pore water (pre-equilibrated)	12.6	9 months	436
Ochs and Talerico (2006)	Hydrogarnet	5×10^{-3}	1×10^{-5}	Synthetic pore water (pre-equilibrated)	12.4	2 weeks	200
Ochs and Talerico (2006)	Hydrogarnet	5×10^{-3}	1×10^{-5}	Synthetic pore water (pre-equilibrated)	12.4	3 months	350×10^3
Ochs and Talerico (2006)	Hydrogarnet	5×10^{-3}	1×10^{-5}	Synthetic pore water (pre-equilibrated)	12.4	5 months	76.1×10^3
Baur and Johnson (2002)	Ettringite	1.9×10^{-3} 3.8×10^{-3} 19×10^{-3}	0.3×10^{-6} to 4.5×10^{-3} 0.3×10^{-6} to 4.5×10^{-3} 0.3×10^{-6} to 4.5×10^{-3}	Prostrated solution	11.0	7 days	180 70 90
Baur and Johnson (2002)	Monosulphate	1.9×10^{-3}	0.3×10^{-6} to 4.5×10^{-3}	Presaturated solution	11.7	7 days	380
Baur et al. (2002)	CSH 1.0	1.9×10^{-3}	0.3×10^{-6} to 4.5×10^{-3}	Presaturated solution	11.8	7 days	210
Ochs and Talerico (2006)	HCP-CEM V/A	1×10^{-3}	4.5×10^{-7} 1.0×10^{-6}	Synthetic pore water (pre-equilibrated)	12.2	2 weeks	4.1×10^3 0.3×10^3

(continued)

Table A.14 (continued)

Reference	Experimental conditions						
	Cementitious material	S/L (kg/L)	Initial concentration (mol/L)	Contact solution	pH	Equilibration time	R_d (L/kg)
Ochs and Talerico (2006)	HCP-CEM V/A	10×10^{-3}	4.5×10^{-7} 1.0×10^{-6}	Synthetic pore water (pre-equilibrated)	12.2	2 weeks	2.1×10^{3} 1.4×10^{3}
Ochs and Talerico (2006)	HCP-CEM V/A	1×10^{-3}	4.5×10^{-7} 1.0×10^{-6}	Synthetic pore water (pre-equilibrated)	12.2	9 months	3.5×10^{3} 5.25×10^{3}
Ochs and Talerico (2006)	HCP-CEM V/A	10×10^{-3}	4.5×10^{-7} 1.0×10^{-6}	Synthetic pore water (pre-equilibrated)	12.1	9 months	1.7×10^{3} 2.1×10^{3}
Ochs and Talerico (2006)	HCP-CON V/A	1×10^{-3}	4.5×10^{-7} 1.0×10^{-6}	Synthetic pore water (pre-equilibrated)	11.7	2 weeks	1.3×10^{3} 0.7×10^{3}
Ochs and Talerico (2006)	HCP-CON V/A	10×10^{-3}	4.5×10^{-7} 1.0×10^{-6}	Synthetic pore water (pre-equilibrated)	11.7	2 weeks	1.0×10^{3} 0.96×10^{3}
Ochs and Talerico (2006)	HCP-CON V/A	1×10^{-3}	4.5×10^{-7} 1.0×10^{-6}	Synthetic pore water (pre-equilibrated)	11.5	9 months	13.1×10^{3} 17.9×10^{3}
Ochs and Talerico (2006)	HCP-CON V/A	10×10^{-3}	4.5×10^{-7} 1.0×10^{-6}	Synthetic pore water (pre-equilibrated)	11.2	9 months	1.7×10^{3} 3.02×10^{3}
Ochs and Talerico (2006)	HCP-CEM V/C	1×10^{-3}	4.5×10^{-7} 1.0×10^{-6}	Synthetic pore water (pre-equilibrated)	9.4	2 weeks	0.12×10^{3} 0.14×10^{3}
Ochs and Talerico (2006)	HCP-CEM V/C	10×10^{-3}	4.5×10^{-7} 1.0×10^{-6}	Synthetic pore water (pre-equilibrated)	9.4	2 weeks	0.12×10^{3} 0.12×10^{3}
Ochs and Talerico (2006)	HCP-CEM V/C	1×10^{-3}	4.5×10^{-7} 1.0×10^{-6}	Synthetic pore water (pre-equilibrated)	8.3	9 months	0.29×10^{3} 0.32×10^{3}
Ochs and Talerico (2006)	HCP-CEM V/C	10×10^{-3}	4.5×10^{-7} 1.0×10^{-6}	Synthetic pore water (pre-equilibrated)	8.4	9 months	0.50×10^{3} 0.28×10^{3}
Lothenbach et al. (1999)	Ettringite	2.5×10^{-3}	1×10^{-4}	Na_2SO_4 solution	11	41 days	100
Cowan et al. (1990)	$CaCO_3$	0.1	1×10^{-7}	$CaCO_3$ (aq)	7.0	24 h	10

(continued)

Table A.14 (continued)

Reference	Experimental conditions						
	Cementitious material	S/L (kg/L)	Initial concentration (mol/L)	Contact solution	pH	Equilibration time	R_d (L/kg)
Cowan et al. (1990)	$CaCO_3$	0.1	1×10^{-7}	$CaCO_3$ (aq)	7.85	24 h	2.12–2.50
Cowan et al. (1990)	$CaCO_3$	0.1	1×10^{-7}	$CaCO_3$ (aq)	9.15	24 h	0.25
Cowan et al. (1990)	$CaCO_3$	0.1	1×10^{-7}	$CaCO_3$ (aq)/$CaSO_4$ (aq)	7.0	24 h	5.38
Cowan et al. (1990)	$CaCO_3$	0.1	1×10^{-7}	$CaCO_3$ (aq) $CaSO_4$ (aq)	7.5	24 h	1.76–2.90
Ticknor et al. (1988)	Calcite	4.0×10^{-2}	ca. 4–9 $\times 10^{-11}$	Standard Canadian Shield saline solution (different salinity levels)	7.5–8	14 days	1.3–7.5
Johnson et al. (2000)	HCP-CEM V	33×10^{-3}	7×10^{-7}	NaOH solution	12.4	7 days	890
Johnson et al. (2000)	HCP-CEM V	33×10^{-3}	7×10^{-7}	NaOH solution	12.4	7 days	570
Johnson et al. (2000)	HCP-CEM V	33×10^{-3}	7×10^{-7}	NaOH solution	12.4	7 days	930
Pointeau et al. (2008)	HCP-CEM I	–	2.2×10^{-8}	Assumed to be the same as Mace et al. (2007)	11.9	3 days 7 days 17 days 25 days 35 days 180 days	300 300 600 700 800 1000
Pointeau et al. (2008)	HCP-CEM I	–	2.2×10^{-8}	Assumed to be the same as Mace et al. (2007)	12.4	1 day 10 days 20 days 30 days 50 days 100 days 150 days	2000 2100 3000 3800 4000 5000 5500

(continued)

Table A.14 (continued)

Reference	Experimental conditions						
	Cementitious material	S/L (kg/L)	Initial concentration (mol/L)	Contact solution	pH	Equilibration time	R_d (L/kg)
Pointeau et al. (2008)	HCP-CEM I	–	2.2×10^{-8}	NaOH solution in deionised water	11.9	–	800
Mace et al. (2007)	HCP/20-20_alt20	n.r.	8.1×10^{-8}	Pre-equilibrated Millipore solution	12.5	90 days 100 days	3250 4800
Mace et al. (2007)	HCP/20-20_alt20	n.r.	1.8×10^{-7}	Pre-equilibrated Millipore solution	12.5	135 days	5700
Mace et al. (2007)	HCP/70-20_alt20	n.r.	8.9×10^{-8}	Pre-equilibrated Millipore solution	12.3	90 days	4700
Mace et al. (2007)	HCP/70-20_alt20	n.r.	1.7×10^{-7}	Pre-equilibrated Millipore solution	12.3	135 days	5300
Pointeau et al. (2006)	HCP fresh	7.4×10^{-3}	2.2×10^{-8}	Mineralised water	13.2	2 days 15 days 25 days 170 days	76 90 95 116
Pointeau et al. (2006a)	HCP deg	7.4×10^{-3}	2.2×10^{-8}	Mineralised water	11.9	2 days 15 days 25 days 170 days	300 540 680 960
Sugiyama and Fujita (1999)	OPC	2×10^{-2}	1.9×10^{-4}	Synthetic groundwater	12.2	35 days	500
Sugiyama and Fujita (1999)	OPC	2×10^{-2}	1.9×10^{-4}	Distilled water	12.1	35 days	1600
Sugiyama and Fujita (1999)	OPC/BFS	2×10^{-2}	1.9×10^{-4}	Synthetic groundwater	11.8	35 days	425

(continued)

Table A.14 (continued)

Reference	Experimental conditions						
	Cementitious material	S/L (kg/L)	Initial concentration (mol/L)	Contact solution	pH	Equilibration time	R_d (L/kg)
Sugiyama and Fujita (1999)	Altered CSH gel (Ca/Si = 0.9)	2×10^{-2}	1.9×10^{-4}	Distilled water	12.4	35 days	150
Sugiyama and Fujita (1999)	Altered CSH gel (Ca/Si = 1.2)	2×10^{-2}	1.9×10^{-4}	Distilled water	12.5	35 days	525
Kato et al. (2002)	HCP (OPC)	0.1–0.01	1.4×10^{-6} to 2.5×10^{-4}	Pre-equilibrated water	ca. 12.5	14 days	75–462
Se(VI)							
Su and Suarez (2000)	Am–$Fe(OH)_3$	4×10^{-3}	1×10^{-3}	NaCl solution	10.2	1 day	41
Su and Suarez (2000)	Am–$Fe(OH)_3$	4×10^{-3}	1×10^{-3}	NaCl solution	10.5	1 day	34
Su and Suarez (2000)	Am–$Fe(OH)_3$	4×10^{-3}	1×10^{-3}	NaCl solution	11	1 day	16
Staudt et al. (1994)	$CaCO_3$	4×10^{-3}	2×10^{-5}	$CaCO_3$ solution	7.5	5 days	0.1 0.3
Lothenbach et al. (1999)	Ettringite	2.5×10^{-3}	1×10^{-4}	Na_2SO_4 solution	11.0	325 days	70
Lothenbach et al. (1999)	Ettringite	2.5×10^{-3}	1×10^{-4}	Na_2SO_4 solution	11.0	552 days	50
Lothenbach et al. (1999)	Fresh CEM HS	5×10^{-3}	8×10^{-5}	Pore water after equilibration	13.2	56 days	3
Lothenbach et al. (1999)	Fresh CEM HS	50×10^{-3}	8×10^{-5}	Pore water after equilibration	13.2	56 days	4
Lothenbach et al. (1999)	Fresh CEM HS	5×10^{-3}	8×10^{-5}	Pore water after equilibration	13.1	5 days	12
Lothenbach et al. (1999)	Fresh CEM HS	5×10^{-3}	8×10^{-5}	Pore water after equilibration	13.1	24 days	18

(continued)

Table A.14 (continued)

Reference	Experimental conditions						
	Cementitious material	S/L (kg/L)	Initial concentration (mol/L)	Contact solution	pH	Equilibration time	R_d (L/kg)
Lothenbach et al. (1999)	Fresh CEM HS	50×10^{-3}	8×10^{-5}	Pore water after equilibration	13.1	5 days	3
Lothenbach et al. (1999)	Fresh CEM HS	50×10^{-3}	8×10^{-5}	Pore water after equilibration	13.1	24 days	3
Lothenbach et al. (1999)	Aged CEM HS	5×10^{-3}	8×10^{-5}	Pore water after equilibration	12.6	56 days	2
Lothenbach et al. (1999)	Aged CEM HS	50×10^{-3}	8×10^{-5}	Pore water after equilibration	12.6	56 days	4
Lothenbach et al. (1999)	Aged CEM HS	5×10^{-3}	8×10^{-5}	Pore water after equilibration	12.5	5 days	0
Lothenbach et al. (1999)	Aged CEM HS	5×10^{-3}	8×10^{-5}	Pore water after equilibration	12.5	24 days	9
Lothenbach et al. (1999)	Aged CEM HS	50×10^{-3}	8×10^{-5}	Pore water after equilibration	12.5	5 days	3
Lothenbach et al. (1999)	Aged CEM HS	50×10^{-3}	8×10^{-5}	Pore water after equilibration	12.5	24 days	1
Lothenbach et al. (1999)	Fresh S71	5×10^{-3}	8×10^{-5}	Pore water after equilibration	12.8	56 days	200
Lothenbach et al. (1999)	Fresh S71	50×10^{-3}	8×10^{-5}	Pore water after equilibration	12.8	56 days	650
Lothenbach et al. (1999)	Fresh S71	5×10^{-3}	8×10^{-5}	Pore water after equilibration	12.0	56 days	22
Lothenbach et al. (1999)	Fresh S71	5×10^{-3}	8×10^{-5}	Pore water after equilibration	12.8	4 days	80
Lothenbach et al. (1999)	Fresh S71	5×10^{-3}	8×10^{-5}	Pore water after equilibration	12.8	21 days	170
Lothenbach et al. (1999)	Fresh S71	50×10^{-3}	8×10^{-5}	Pore water after equilibration	12.8	4 days	80
Lothenbach et al. (1999)	Fresh S71	50×10^{-3}	8×10^{-5}	Pore water after equilibration	12.8	21 days	360
Lothenbach et al. (1999)	Aged S71	5×10^{-3}	8×10^{-5}	Pore water after equilibration	12.0	4 days	4
Lothenbach et al. (1999)	Aged S71	5×10^{-3}	8×10^{-5}	Pore water after equilibration	12.0	21 days	4
Lothenbach et al. (1999)	Aged S71	5×10^{-3}	8×10^{-5}	Pore water after equilibration	12.0	57 days	22

(continued)

Table A.14 (continued)

Reference	Experimental conditions						
	Cementitious material	S/L (kg/L)	Initial concentration (mol/L)	Contact solution	pH	Equilibration time	R_d (L/kg)
Lothenbach et al. (1999)	Aged S71	50×10^{-3}	8×10^{-5}	Pore water after equilibration	12.0	4 days	6
Lothenbach et al. (1999)	Aged S71	50×10^{-3}	8×10^{-5}	Pore water after equilibration	12.0	21 days	7
Lothenbach et al. (1999)	Aged S71	50×10^{-3}	8×10^{-5}	Pore water after equilibration	12.0	57 days	29
Lothenbach et al. (1999)	Fresh CFL/5°	5×10^{-3}	8×10^{-5}	Pore water after equilibration	12.7	56 days	960
Lothenbach et al. (1999)	Fresh CFL/5°	50×10^{-3}	8×10^{-5}	Pore water after equilibration	12.7	56 days	1041
Lothenbach et al. (1999)	Fresh CFL/5°	5×10^{-3}	8×10^{-5}	Pore water after equilibration	12.7	4 days	640
Lothenbach et al. (1999)	Fresh CFL/5°	5×10^{-3}	8×10^{-5}	Pore water after equilibration	12.7	21 days	1380
Lothenbach et al. (1999)	Fresh CFL/5°	50×10^{-3}	8×10^{-5}	Pore water after equilibration	12.7	4 days	250
Lothenbach et al. (1999)	Fresh CFL/5°	50×10^{-3}	8×10^{-5}	Pore water after equilibration	12.7	21 days	1080
Lothenbach et al. (1999)	Aged CFL/5°	5×10^{-3}	8×10^{-5}	Pore water after equilibration	10.4	56 days	23
Lothenbach et al. (1999)	Aged CFL/5°	50×10^{-3}	8×10^{-5}	Pore water after equilibration	10.4	56 days	17
Lothenbach et al. (1999)	Aged CFL/5°	5×10^{-3}	8×10^{-5}	Pore water after equilibration	10.4	4 days	4
Lothenbach et al. (1999)	Aged CFL/5°	5×10^{-3}	8×10^{-5}	Pore water after equilibration	10.4	21 days	4
Lothenbach et al. (1999)	Aged CFL/5°	50×10^{-3}	8×10^{-5}	Pore water after equilibration	10.4	4 days	10
Lothenbach et al. (1999)	Aged CFL/5°	50×10^{-3}	8×10^{-5}	Pore water after equilibration	10.4	21 days	10
Lothenbach et al. (1999)	Aged CFL/50°	5×10^{-3}	8×10^{-5}	Pore water after equilibration	11.1	4 days	25
Lothenbach et al. (1999)	Aged CFL/50°	5×10^{-3}	8×10^{-5}	Pore water after equilibration	11.1	21 days	20
Lothenbach et al. (1999)	Aged CFL/50°	5×10^{-3}	8×10^{-5}	Pore water after equilibration	11.1	57 days	12

(continued)

Table A.14 (continued)

Reference	Experimental conditions						
	Cementitious material	S/L (kg/L)	Initial concentration (mol/L)	Contact solution	pH	Equilibration time	R_d (L/kg)
Lothenbach et al. (1999)	Aged CFL/50°	50×10^{-3}	8×10^{-5}	Pore water after equilibration	11.1	4 days	3
Lothenbach et al. (1999)	Aged CFL/50°	50×10^{-3}	8×10^{-5}	Pore water after equilibration	11.1	21 days	9
Lothenbach et al. (1999)	Aged CFL/50°	50×10^{-3}	8×10^{-5}	Pore water after equilibration	11.1	57 days	4
Baur and Johnson (2003)	Ettringite	1.9×10^{-3}	0.3×10^{-6} to 4.5×10^{-3}	Presaturated solution	11.0	7 days	30
Baur and Johnson (2003)	Monosulphate	1.9×10^{-3}	0.3×10^{-6} to 4.5×10^{-3}	Presaturated solution	11.7	7 days	2060

Molybdenum

See Table A.15.

Table A.15 Reviewed sorption values for molybdenum with indication of experimental conditions

Reference	Experimental conditions						
	Cementitious material	S/L (kg/L)	Initial concentration (mol/L)	Contact solution	pH	Equilibration time	R_d (L/kg)
Kato et al. (2002)	HCP (OPC)	0.1; 0.45 μm	5.55×10^{-5}	Pre-equilibrated water	12.64	14 days	214; 232
Kato et al. (2002)	HCP (OPC)	0.1; 0.45 μm	4.25×10^{-6}	Pre-equilibrated water	12.55	14 days	106; 101
Kato et al. (2002)	HCP (OPC)	0.1; 0.45 μm	5.37×10^{-7}	Pre-equilibrated water	12.54	14 days	21.8; 19.5
Kato et al. (2002)	HCP (OPC)	0.1; MWCO10.000	5.21×10^{-5}	Pre-equilibrated water	12.64	14 days	55.6; 113
Kato et al. (2002)	HCP (OPC)	0.1; MWCO10.000	6.20×10^{-6}	Pre-equilibrated water	12.55	14 days	110; 58.8
Kato et al. (2002)	HCP (OPC)	0.1; MWCO10.000	7.43×10^{-7}	Pre-equilibrated water	12.54	14 days	9.64; 3.78
Kato et al. (2002)	HCP (OPC)	0.01; 0.45 μm	6.05×10^{-5}	Pre-equilibrated water	12.56	14 days	81.0; 82.1
Kato et al. (2002)	HCP (OPC)	0.01; 0.45 μm	3.69×10^{-6}	Pre-equilibrated water	12.43	14 days	141; 171
Kato et al. (2002)	HCP (OPC)	0.01, 0.45 μm	4.81×10^{-7}	Pre-equilibrated water	12.41	14 days	60.2; 64.0
Kato et al. (2002)	HCP (OPC)	0.01; MWCO10.000	6.06×10^{-5}	Pre-equilibrated water	12.56	14 days	860; 743
Kato et al. (2002)	HCP (OPC)	0.01; MWCO10.000	6.40×10^{-6}	Pre-equilibrated water	12.43	14 days	98.6; 212
Kato et al. (2002)	HCP (OPC)	0.01; MWCO10.000	7.50×10^{-7}	Pre-equilibrated water	12.41	14 days	56.3; 79.4

Technetium

See Table A.16.

Table A.16 Reviewed sorption values for Tc(IV) and Tc(VII) with indication of experimental condition

Reference	Experimental conditions						
	Cementitious material	S/L (kg/L)	Initial concentration (M)	Contact solution	pH	Equilibration time	R_d (L/kg)
Bayliss et al. (1992)	NRVB	0.02	10^{-10}	Equilibrated water (non-saline)	13.1	49 days	6000 Tc(IV)
Bayliss et al. (1996)	NRVB	0.02	10^{-11}	Equilibrated water (saline)	13.1	49 days	1000 Tc(IV)
Andra (2005)	CEM I/V and CSH	n.a.	n.a.	n.a.	9.9–12.1	n.a.	750–3700 Tc(IV)
Baker et al. (2004)	NRVB	0.1	8×10^{-7} to 8×10^{-9}	Equilibrated water	12.8	3 months	<1 Tc(VII)
Swanton and Mayatt (2004)	Calcite	0.11	10^{-7}	Equilibrated water	8–9	115 days	0.7–3.5 Tc(VII)

Niobium

See Table A.17.

Table A.17 Reviewed sorption values for niobium (Nb(IV)) with indication of experimental conditions

Reference	Experimental conditions						
	Cementitious material	S/L (kg/L)	Initial concentration (M)	Contact solution	pH	Equilibration time	R_d (L/kg)
Pilkington and Stone (1990)	HCP (PFA/OPC)	0.005–0.04	5.3×10^{-3}	Equilibrated water	11.8	1–2 months	500–80,000
Baker et al. (1994)	NRVB	0.02	4.5×10^{-13}	NaCl 0.5 M	12.2	Weeks	35,000–41,000
Andra (2005)	CEM I and V (pastes and CSH)	>Solubility limit	6.5×10^{-8}	CEM I-contacted waters	12–13.2	25 days	26,000–350,000

Tin

See Table A.18.

Table A.18 Reviewed sorption values for tin with indication of experimental conditions

Reference	Experimental conditions						
	Cementitious material	S/L (kg/L)	Initial concentration (mol/L)	Contact solution	pH	Equilibration time	R_d (L/kg)
Bonhoure et al. (2003)	HCP	2.5×10^{-2}	1.06×10^{-8}	Synthetic pore water	13.3	30 days	18.0×10^{3}
Bonhoure et al. (2003)	HCP	2.5×10^{-2}	3.61×10^{-8}	Synthetic pore water	13.3	30 days	18.0×10^{3}
Bonhoure et al. (2003)	HCP	2.5×10^{-2}	7.64×10^{-8}	Synthetic pore water	13.3	30 days	30.8×10^{3}
Bonhoure et al. (2003)	HCP	2.5×10^{-2}	2.29×10^{-7}	Synthetic pore water	13.3	30 days	50.0×10^{3}
Bonhoure et al. (2003)	HCP	2.5×10^{-2}	4.63×10^{-7}	Synthetic pore water	13.3	30 days	55.6×10^{3}
Baker et al. (1994)	Nirex reference vault backfill (NRVB)	2×10^{-2}	5.8×10^{-8}	Backfill-equilibrated water (non-saline water, 15–25 °C)	12.8	Several weeks	$1–3 \times 10^{5}$
Baker et al. (1994)	Nirex reference vault backfill (NRVB)	2×10^{-2}	5.8×10^{-8}	Backfill-equilibrated water (non-saline water, 72–82 °C)	12.8	Several weeks	$>2 \times 10^{5}$
Heath et al. (1996)	Nirex reference vault backfill (NRVB)	n.r.	n.r.	Water (I = 0.05 M)	12.5	n.r.	$>93 \times 10^{3}$
Bayliss et al. (1989)	Sulphate-resisting Portland cement (SRPC)	n.r.	1×10^{-6}	SRPC-equilibrated water	12.5	21 days (filtration)	9.7×10^{3}
Bayliss et al. (1989)	Sulphate-resisting Portland cement (SRPC)	n.r.	1×10^{-6}	SRPC-equilibrated water	12.5	56 days (filtration)	40×10^{3}

(continued)

Table A.18 (continued)

Reference	Experimental conditions						
	Cementitious material	S/L (kg/L)	Initial concentration (mol/L)	Contact solution	pH	Equilibration time	R_d (L/kg)
Ochs and Talerico (2006)	CSH 1.65	1×10^{-3}	1.3×10^{-6}	Pre-equilibrated solution, pH ≈ 12.5	12.6	2 weeks	1×10^{3}
Ochs and Talerico (2006)	CSH 1.65	1×10^{-3}	1.3×10^{-6}	Pre-equilibrated solution, pH adjusted	12.6	3 months	135×10^{3}
Ochs and Talerico (2006)	CSH 1.2	5×10^{-3}	1.3×10^{-6}	Pre-equilibrated solution, pH adjusted	12.5	2 weeks	22×10^{3}
Ochs and Talerico (2006)	CSH 1.2	5×10^{-3}	1.3×10^{-6}	Pre-equilibrated solution, pH adjusted	12.5	3 months	189×10^{3}
Ochs and Talerico (2006)	CSH 1.0	1×10^{-3}	1.3×10^{-6}	Pre-equilibrated solution, pH adjusted	12.4	2 weeks	23×10^{3}
Ochs and Talerico (2006)	CSH 1.0	1×10^{-3}	1.3×10^{-6}	Pre-equilibrated solution, pH adjusted	12.4	3 months	214×10^{3}
Ochs and Talerico (2006)	CSH 0.83	5×10^{-3}	1.3×10^{-6}	Pre-equilibrated solution, pH adjusted	12.4	2 weeks	1×10^{3}
Ochs and Talerico (2006)	CSH 0.83	5×10^{-3}	1.3×10^{-6}	Pre-equilibrated solution, pH adjusted	12.4	3 months	135×10^{3}
Ochs and Talerico (2006)	Ettringite	1×10^{-3}	1.3×10^{-6}	Pre-equilibrated solution, pH adjusted	12.5	2 weeks	17.1×10^{3}
Ochs and Talerico (2006)	Ettringite	1×10^{-3}	1.3×10^{-6}	Pre-equilibrated solution, pH adjusted	12.5	3 months	22.6×10^{3}
Ochs and Talerico (2006)	Calcite ($CaCO_3$)	5×10^{-3}	1.3×10^{-6}	Pre-equilibrated solution, pH adjusted	12.6	2 weeks	2.5
Ochs and Talerico (2006)	Calcite ($CaCO_3$)	5×10^{-3}	1.3×10^{-6}	Pre-equilibrated solution, pH adjusted	12.6	3 months	3

(continued)

Table A.18 (continued)

Reference	Experimental conditions						
	Cementitious material	S/L (kg/L)	Initial concentration (mol/L)	Contact solution	pH	Equilibration time	R_d (L/kg)
Ochs and Talerico (2006)	Hydrotalcite	1×10^{-3}	1.3×10^{-6}	Pre-equilibrated solution, pH adjusted	12.2	2 weeks	5.3×10^{2}
Ochs and Talerico (2006)	Hydrotalcite	1×10^{-3}	1.3×10^{-6}	Pre-equilibrated solution, pH adjusted	12.2	3 months	7.2×10^{2}
Ochs and Talerico (2006)	Hydrogarnet	5×10^{-3}	1.3×10^{-6}	Pre-equilibrated solution, pH adjusted	12.4	2 weeks	87
Ochs and Talerico (2006)	Hydrogarnet	5×10^{-3}	1.3×10^{-6}	Pre-equilibrated solution, pH adjusted	12.4	3 months	3×10^{3}

Zirconium

See Table A.19.

Table A.19 Reviewed sorption values for zirconium with indication of experimental condition

Reference	Experimental conditions						
	Cementitious material	S/L (kg/L)	Initial concentration (mol/L)	Contact solution	pH	Equilibration time	R_d (L/kg)
Pointeau et al. (2004b)	CEM I 1.3	2.5×10^{-3} to 4×10^{-3}	1×10^{-6}	?	12.1	9 days	25×10^3 20×10^3 7×10^3 60×10^3
Pointeau et al. (2004b)	CEM I 1.0	2.5×10^{-3} to 4×10^{-3}	1×10^{-6}	?	11.5	9 days	1250×10^3 300×10^3 220×10^3 60×10^3
Pointeau et al. (2004b)	CEM I 0.7	2.5×10^{-3} to 4×10^{-3}	1×10^{-6}	?	9.9	9 days	400×10^3
Pointeau et al. (2004b)	CEM V 1.3	2.5×10^{-3} to 4×10^{-3}	1×10^{-6}	?	12.1	9 days	80×10^3 90×10^3 35×10^3 20×10^3
Pointeau et al. (2004b)	CEM V 1.0	2.5×10^{-3} to 4×10^{-3}	1×10^{-6}	?	11.5	9 days	75×10^3 50×10^3
Pointeau et al. (2004b)	CEM V 0.7	2.5×10^{-3} to 4×10^{-3}	1×10^{-6}	?	9.9	9 days	130×10^3
Pointeau et al. (2004b)	CSH 0.7	2.5×10^{-3} to 4×10^{-3}	1×10^{-6}	?	9.95	9 days	2600×10^3 750×10^3 400×10^3 200×10^3

(continued)

Table A.19 (continued)

Reference	Experimental conditions						
	Cementitious material	S/L (kg/L)	Initial concentration (mol/L)	Contact solution	pH	Equilibration time	R_d (L/kg)
Pointeau et al. (2004b)	CSH 0.9	2.5×10^{-3} to 4×10^{-3}	1×10^{-6}	?	9.95	9 days	450×10^3 250×10^3 100×10^3
Pointeau et al. (2004b)	CSH 1.0	2.5×10^{-3} to 4×10^{-3}	1×10^{-6}	?	9.95	9 days	125×10^3 100×10^3 70×10^3
Pointeau et al. (2004b)	CSH 1.3	2.5×10^{-3} to 4×10^{-3}	1×10^{-6}	?	12.1	9 days	35×10^3 20×10^3 4×10^3
Brownsword et al. (2002)	NRVB	0.02	2.3×10^{-11}	NRVB-equilibrated water	12.4	38 days	1×10^5

Bibliography

B. Allard, *Radionuclide sorption on concrete* (NAGRA NTB 85-21, NAGRA, Baden, 1985)

K. Andersson, B. Allard, M. Bengtsson, B. Magnusson, Chemical composition of cement pore solutions. Cem. Concr. Res. **19**, 327–332 (1989)

A. Atkinson, N.M. Everitt, R. Guppy, Evolution of pH in a radwaste repository: Internal reactions between concrete constituents: part 2, DOE/RW/89/025 (1989)

A. Atkinson, S.J. Williams, S.J. Wisbey, NSARP reference document: the near field—January 1992. UK Nirex Ltd Report NSS/G117 (1993)

G. Audi, Nubase 2003 evaluation of nuclear and decay properties. Nucl. Phys. A (Atomic Mass Data Center) **729**, 3–128 (2003)

B. Baeyens, M.H. Bradbury, A quantitative mechanistic description of Ni, Zn, and Ca sorption on Na-montmorillonite. Part II: sorption measurements, PSI Bericht Nr. 95–11 (1995)

Ya. Bashilov, P.S. Kindyakov, Calcium molybdate, Tsvet. Metal. 879 (1931)

BELGATOM, Container types, Modified drawing, 30/01/2008, Project number 94815005 (2008)

Belgoprocess, Nota 2004-00248 (2004)

P. Biddle, B.F. Greenfield, N.J. Pilkington, M.W. Spindler, Further studies on the effects of the products from the anaerobic degradation of cellulosic wastes in the near field, AEAT/ERRA-0154 (2000)

P. Biddle, B.F. Greenfield, B.J. Myatt, G.P. Robertson, M.W. Spindler, The effects of the degradation of some organic polymers and ion-exchange resins on plutonium solubility in the near field, AEAT/ERRA-0355 (2002)

D.J. Blackwood, J.L. Gould, C.C. Naish, F.M. Porter, A.P. Rance, S.M. Sharland, N.R. Smart, M.I. Thomas, T. Yates, The localised corrosion of carbon steel and stainless steel in simulated repository environments, Report AEAT-ERRA-0318 (2002)

I. Bonhoure, I. Baur, E. Wieland, C.A. Johnson, A.M. Scheidegger, Se(IV/VI) immobilization by cementitious systems: an X-ray absorption study. Cem. Concr. Res. **36**, 91–98, (2006)

X. Bourbon, P. Toulhoat, Influence of organic degradation products on the solubilisation of radionuclides in intermediate and low level radioactive wastes. Radiochim. Acta **74**, 315–319 (1996)

M.H. Bradbury, B. Baeyens, A mechanistic description of Ni and Zn sorption on Na-montmorillonite, 2: modelling. J. Contam. Hydrol. **27**, 223–248 (1997)

M.H. Bradbury, B. Baeyens, Sorption of Eu on Na- and Ca-montmorillonites: experimental investigations and modelling with cation exchange and surface complexation. Geochim. Cosmochim. Acta **63**, 325–336 (2007)

P. Brown, Jr. J. Bothe, The system $CaO–Al_2O_3–CaCl_2–H_2O$ at 23 ± 2 °C and the mechanisms of chloride binding in concrete, Cem. Concr. Res. **34**, 1549–1553 (2004)

P.L. Brown, *Chemical Thermodynamics of Zirconium*, vol 8 (OECD Nuclear Energy Agency, Elsevier, 2005)

© Springer International Publishing Switzerland 2016

M. Ochs et al., *Radionuclide and Metal Sorption on Cement and Concrete*,
Topics in Safety, Risk, Reliability and Quality 29,
DOI 10.1007/978-3-319-23651-3

J. Bruno, D. Bosbach, D. Kulik, A. Navrotsky, *Chemical thermodynamics of solid solutions of interest in nuclear waste management* (OECD Nuclear Energy Agency, Data Bank, France, 2007)

V. Chambers, S.J. Williams, S.J. Wisbey, Nirex safety assessment research programme—nirex near field research: report on current status in 1994, Nirex report S/95/011 (1995)

A.V. Chambers, S.J. Williams, S.J. Wisbey, Science report—nirex safety assessment research programme. Nirex Near Field Research: Report on the Current Status in 1994, Report No. S/95/011, Nirex, Harwell, UK (1995)

R. Choppin, E.N. Rizkalla, in *Handbook on the physics and chemistry of rare earths*, ed. by Jr. K.A. Gschneidner, L. Eyring, G.R. Choppin, G.H. Lander, Solution chemistry of actinides and lanthanides (Elsevier, Amsterdam, 1994)

COMSOL, Multi-physics Users Guide Version 3.3 (2007)

Ch. Cosemans, R. Verbeke, Inventaire des volumes de déchets radioactifs, ondraf/niras note 96-4777 (4 Jan 1997)

Cosemans, Inventaris van het radioactief afval: chemische samenstelling van het referentievolume geconditioneerd afval, NIRAS/ONDRAF note 2004-0975 (2004)

A. Davis, Molecular scale observation and models of sorption reactions, in *Radionuclide Retention in Geologic Media, Workshop Proceedings*, Oskarshamn, Sweden, 7–9 May 2001

A. Davis, J.A. Coston, D.B. Kent, C.C. Fuller, Application of the surface complexation concept to complex mineral assemblages. Environ. Sci. Technol. **32**, 2820–2828 (1998)

R. Dayal, E.J. Reardon, Carbon-14 behaviour in a cement-dominated environment: implications for spent candu resin waste disposal. Waste Manage. **14**, 457–466 (1994)

B. Deng, T.J. Campbell, D.R. Burris, Hydrocarbon formation in metallic iron/water systems. Environ. Sci. Technol. **31**, 1185–1190 (1997)

M.V. Di Giandomenico, D. Trubert, C. Le Naour, Sulphate complexation of protactinium (V) at 25 °C. Radiochim. Acta **95**, 617–623 (2007)

M.-A. Elrashidi, D.C. Adriano, S.M. Workman, W.L. Lindsay, Chemical equilibria of selenium in soils: a theoretical development. Soil Sci. **144**, 141–152 (1987)

EN-197:2000, Cement. Composition, specifications and conformity criteria for low heat common cements (2000)

EPA, Understanding Variation in Partition Coefficient, Kd, Values, Volume I, The Kd model, methods of measurement, and application of chemical reaction codes, EPA 402-R-99-004A (1999)

M.E. Essington, Estimation of the standard free energy of formation of metal arsenates, selenates, and selenites. Soil Sci. Soc. Am. J. **52**, 1574–1579 (1988)

M.E. Essington, Calcium molybdate solubility in spent oil shale and a preliminary evaluation of the association constants for the formation of CaMoO40(aq), KMoO4–(aq), and NaMoO4–(aq). Envi. Sci. Technol. **24**, 214–220 (1990)

European Commission, Commission recommendation of 15 September 1999 on a classification system for solid radioactive waste (1999/699/EC, Euratom), Official Journal of the European Communities, L 265 Volume 42, 13 October 1999

B. Fourest, J. Perrone, P. Tarapcik, E. Giffaut, The hydrolysis of Protactinium(V) studied by capillary diffusion. J. Sol. Chem. **33**, 953–973 (2004)

M. Fuhrmann, P. Colombo, Radionuclide release from cement waste forms in seawater, Radioactive Waste Manage. Nucl. Fuel Cycle **11**, 365–380 (1989)

S. Gamble, M. Schnitzer, H. Kerndorff, C.H. Langford, Multiple metal ion exchange equilibria with humic acid. Geochim. Cosmochim. Acta **47**(7), 1311–1323 (1983)

García-Gutierrez, U. Alonso de los Rios, T. Missana, M. Mingarro, N., Granizo, M. Grivé, X. Gaona, E. Colàs, L. Duro, J. Bruno, Estudio bibliográfico sobre sorción y difusión de radionucleidos en cementos, hormigones y productos de corrosión en presencia de cementos. Enresa technical report PT-02/07, 180 (2007)

G.K. Glass, N.R. Buenfeld, Chloride-induced corrosion of steel in concrete. Prog. Struct. Engng. Mater. **2**, 448–458 (2000)

P. Glasser, K. Luke, M.J. Angus, Modification of cement pore fluid compositions by pozzolanic additives. Cem. Concr. Res. **18**, 165–178 (1988)

M.A. Glaus, L.R. Van Loon, S. Achatz, A. Chodura, K. Fischer, Degradation of celllulosic materials under the alkaline conditions of a cementious disposal facility for low and intermediate level radioactive waste, part I: identification of degradation products. Analytica Chimica Acta **398**, 111–122 (1999)

M. Glaus, L. Van Loon, A generic procedure for the assessment of the effect of concrete admixtures on the retention behaviour of cement for radionuclides: concept and case studies, PSI Bericht Nr. 04–02, Paul Scherrer Institut, Villingen, Switzerland (2004)

M.A. Glaus, L. Van Loon, Degradation of cellulose under alkaline conditions: new insights from a 12 years degradation study. Environ. Sci. Technol. **42**, 2906–2911 (2008)

B.F. Greenfield, B.J. Myatt, G.P. Robertson, M.W. Spindler, D.R. Woodwark, The effects of chemical and radiation degradation of organic materials on radioelement chemistry in the near field, AEAT/ERRA-0074 (2007)

F. Greenfield, G.J. Holtom, M.H. Hurdus, N. O'Kelly, N.J. Pilkington, A. Rosevear, M.W. Spindler, S.J. Williams, The identification and degradation of isosaccharinic acid, a cellulose degradation product. Mater. Res. Soc. Symp. Proc. **353**, 1151–1158 (1995)

F. Greenfield, A.D. Moreton, M.W. Spindler, S.J. Williams, D.R. Woodwark, The effects of the degradation of organic materials in the near-field of a radioactive waste disposal facility. Mater. Res. Soc. Symp. Proc. **257**, 299–306 (1992)

J.M. Gruhlke, J. Neiheisel, L. Battist, Estimates on the quantities, form, and transport of carbon-14 in low-level radioactive waste. EPA-520/1-86-019 (1986)

A. Haworth, S.M. Sharland, The evolution of the Eh in the pore water of a radioactive waste repository, NSS/R308 (1995)

B. Huet, V. L'Hostis, F. Miserque, H. Idrissi, Electrochemical behavior of mild steel in concrete: influence of pH and carbonate content of concrete pore solution. Electrochim. Acta **51**, 172–180 (2005)

W. Hummel, in *Solubility of Solids in Radioactive Waste Repositories*, ed. by T.M. Letcher. Development and applications in solubility (RSC Publishing, UK, 2007)

M.H. Hurdus, N.J. Pilkington, The solubility and sorption of 2-C-(hydroxymethyl)-3-deoxy-D-pentonic acid in the presence of nirex reference vault backfill and its degradation under alkaline conditions, AEAT/ERRA-0153 (2000)

International Atomic Energy Agency (IAEA), Classification of radioactive waste, IAEA Safety Series No. 111-G-1.1, Vienna, May 1994

International Atomic Energy Agency (IAEA), Application of ion exchange processes for the treatment of radioactive waste and management of spent ion exchangers, Technical Reports Series no. 408, Vienna, June 2002

International Atomic Energy Agency (IAEA), Draft Safety Requirements: Disposal of radioactive waste, iaea Safety Standards Series DS 354 Draft 4, Vienna, 17 October 2006

International Atomic Energy Agency (IAEA), Draft Safety Guide: Classification of radioactive waste, iaea Safety Standards Series DS 390 Draft, Vienna, 3 July 2006

L. Jefferies, The evolution of carbon-14 and tritium containing gases in a radioactive waste repository. Nirex Report NSS/R198 (1990)

A. Jenne, In *Adsorption of Metals by Geomedia*, ed. by E.A. Jenne. Adsorption of metals by geomedia: data analysis, modelling, controlling factors, and related issues (Academic Press: San Diego, 1998)

L. Johnson, B. Schwyn, Behaviour of 14C in the safety assessment of a repository for spent fuel, high-level waste and long-lived intermediate level waste in Opalinus Clay. In *Proceedings of a Workshop on the Release and Transport of C-14 in a Repository Environment* (NAGRA Nagra Internal Report, Nagra, Wettingen, Switzerland, 2004), pp. 1–7

W.A. Jury, W.R. Gardner, W.H. Gardner, *Soil physics* (Wiley, New York, 1991)

M. Khalaf, Effect of the fractionation and immobilization on the sorption properties of humic acid, Von der Fakultät für Mathematik, Informatik und Naturwissenschaften der

Rheinisch-Westfälischen Technischen Hochschule Aachen zur Erlangung des akademischen Grades eines Doktors der Naturwissenschaften (2003)

B. Kienzler, V. Metz, M. Kelm, C. Nebelung, L. Baraniak, Interactions of carbon in a repository environment. In *Proceedings of a Workshop on the Release and Transport of C-14 in a Repository Environment* (NAGRA Nagra Internal Report, Nagra, Wettingen, Switzerland, 2004), pp. 73–79

Kingdom of Belgium, Koninklijk Besluit van 16 oktober 1991 houdende wijziging van het Koninklijk Besluit van 30 maart 1981 houdende bepaling van de opdrachten en de werkingsmodaliteiten van de Openbare Instelling voor het beheer van radioactief afval en splijtstoffen / Arrêté Royal du 16 octobre 1991 modifiant l'Arrêté Royal du 30 mars 1981 déterminant les missions et fixant les modalités de fonctionnement de l'Organisme public de gestion des déchets radioactifs et des matières fissiles, Belgisch Staatsblad / Moniteur Belge, 22 November 1991

J. Kissel, A. Pourbaix, Les effets combinés de la teneur en chlorure et de l'alcalinité des bétons sur la corrosion de l'acier, Rapports Techniques, Vol. 165, RT.315 (ISSN 0528-4325), CEBELCOR (1996)

N. Kogawa, Migration of C-14 in activated metal under anaerobic alkaline conditions. In *Proceedings of a Workshop on the Release and Transport of C-14 in a Repository Environment* (NAGRA Nagra Internal Report, Nagra, Wettingen, Switzerland, 2004), pp. 101–107

P. Kreis, Hydrogen evolution from corrosion of iron and steel in low/intermediate-level waste repositories. Nagra Technical Report NTB 91–21, Nagra, Wettingen, Switzerland, (1991)

D.A. Kulik, GEMS-PSI 2.2, PSI-Villigen, Switzerland (2007), available at http://gems.web.psi.ch/

C. Kunz, Carbon-14 discharge at three light-water reactors. Health Phys. **49**(1), 25–35 (1985)

D. Langmuir, *Aqueous Environmental Geochemistry* (Prentice Hall, New Jersey, 1997)

C. Le Naour, D. Trubert, C. Jaussaud, Hydrolysis of Protactinium(V). II equilibrium constants at 40 and 60 °C: a solvent extraction study with TTA in the aqueous system Pa(V)/H2O/H +/Na +/ClO4-. J. Sol. Chem. **32**, 489–504 (2003)

C. Le Naour, D. Trubert, M.V. Di Giandomenico, C. Fillaux, C. Den Auwer, P. Moisy, C. Hennig, First structural characterization of a Protactinium(V) single oxo bond in aqueous media, Inorganic Chemistry **44**, 9542–9546 (2005)

D.R. Lide, *CRC Handbook of Chemistry and Physics*. Zirconium, 4 (CRC Press, New York, 2007), p. 42

R.D. Lindberg, D.D. Runnels, Ground water redox reactions: an analysis of equilibrium state applied to Eh measurements and geochemical modelling. Science **225**, 925–927 (1984)

B. Lothenbach, E. Wieland, A thermodynamic approach to the hydration of sulphate resisting Portland cement. Waste Manag **26**, 706–719 (2006)

B. Lothenbach, T. Matschei, G. Möschner, F.P. Glasser, Thermodynamic modelling of the effect of temperature on the hydration and porosity of Portland cement. Cem. Concr. Res. **38**, 1–18 (2008)

D. Mallants, G. Volckaert, S. Labat, Parameter values used in the performance assessment of the disposal of low level radioactive waste at the nuclear zone Mol-Dessel, volume 2: annexes to the data collection forms for engineered barriers, SCK•CEN-R-3521 rev.1, December, 2003, Mol, Belgium (2003)

F. Mansfeld, J.V. Kenkel, Electrochemical monitoring of atmospheric corrosion phenomena. Corros. Sci. **16**, 111–118 (1976)

E. Martens, D. Jacques, T. Van Gerven, L. Wang, D. Mallants, PHREEQC Modelling of Leaching of Major Elements and Heavy Metals from Cementitious Waste Forms. In: Scientific Basis for Nuclear Waste Management XXXI, Sheffield, United Kingdom, 17–23 September 2007/Materials Research Society, Warrendale, United States, Materials Research Society, 2008, p. 475–482, (2007)

E. Martens, D. Jacques, T. Van Gerven, L. Wang and D. Mallants, PHREEQC Modelling of Leaching of Major Elements and Heavy Metals from Cementitious Waste Forms.- In:

Scientific Basis for Nuclear Waste Management XXXI, Sheffield, United Kingdom, 17–23 September 2007 / Materials Research Society, Warrendale, United States, Materials Research Society, 2008, p. 475-482 (2007)
E. Martin, Carbon-14 in low-level radioactive wastes from two nuclear power plants. Health Phys. **50**, 57–64 (1986)
T. Matschei, B. Lothenbach, F. Glasser, Thermodynamic properties of Portland cement hydrates in the system CaO-Al2O3-SiO2-CaSO4-CaCO3-H2O. Cem. Concr. Res. **37**, 1379–1410 (2007)
T. Matschei, B. Lothenbach, F. Glasser, The Afm phase in Portland cement. Cem. Concr. Res. **73**, 118–130 (2007)
J. Matsumoto, T. Banba, S. Muraoka, Adsorption of C-14 on mortar. Mat Res. Soc. Symp. Proc. **353**, 1029–1035 (1995)
P. McKinley, E.A. Jenne, Experimental investigation and review of the "solids concentration" effect in adsorption studies. Environ. Sci. Technol. **25**, 2082–2087 (1991)
G. Mckinley, W.R. Alexander, Constraints on the applicability of 'in-situ distribution coefficient' values, J. Environ. Radioact. **15**, 19–34 (1992)
L. Means, D.A. Crerar, Migration of radioactive wastes: radionuclide mobilization by complexing agents. Science **200**, 1477–1481 (1978)
S. Mindess, J.F. Young, *Concrete* (Prentice-Hall, Inc., Englewood Cliffs, N.J., 1981)
D. Moreton, Thermodynamic modelling of the effect of hydroxycarboxylic acids on the solubility of plutonium at high pH. Mat. Res. Soc. Symp. Proc. **294**, 753–758 (1993)
N.A.A. Mumallah, W.J. Popiel, Calcium-selective electrode measurements of calcium molybdate solubilities in water. Anal. Chem. **46**, 2055–2056 (1974)
D.J. Nancarrow, T.J. Sumerling, J. Ashton, Preliminary radiological assessments of low-level waste repositories, DOE, Rep. DOE/RW/88.084, London, UK (1988)
Nuclear Energy Agency (NEA-OECD), Sorption modelling and measurement for nuclear waste disposal studies, RWM-4, OECD-NEA, Paris (1983)
Nuclear Energy Agency (NEA-OECD), NEA Sorption Project Phase II: Interpretation and prediction of radionuclide sorption onto substrates relevant for radioactive waste disposal using thermodynamic sorption models, Radioactive Waste Management, Nuclear Energy Agency, OECD 2004
A.M. Neville, Properties of concrete, 4th edn. (Prentice Hall, London, 2000)
M. Niemeyer, U. Noseck, D. Becker, A. Rübel, J. Wollrath, Treatment of 14C release and transport in the long-term safety assessment in the final repository in Morsleben. In *Proceedings of a Workshop on the Release and Transport of C-14 in a Repository Environment* (NAGRA Nagra Internal Report, Nagra, Wettingen, Switzerland, 2004), pp. 9–19
M. Ochs, B. Brüschweiler, A. Häner, D. Oehler, R. Gälli, ANACAD—analysis and fate of concrete admixtures in wastewaters. BMG Engineering Ltd, February 2000, Final report EU Project ENV4-CT97-0474, Part B (2000)
ONDRAF/NIRAS, ACRIA DC-LAGAT-HEC-151, 2000-4220 (herziening 0) (2000)
ONDRAF/NIRAS, Functional rationale of the system and its environment, niras-mp3-02, nirond-tr 2007-04 e, September 2007
D.L. Parkhurst, C.A.J. Apello, User's guide to PHREEQC (version 2)—a computer program for speciation, batch-reaction, one-dimensional transport, and inverse geochemical calculations. *Water-Resources Investigation Report 99-4259*, Denver, Colorado (1999)
Pavasars, *Characterisation of organic substances in waste materials under alkaline conditions, Linkoping Studies in Arts and Science, 196* (University Linkoping, Sweden, 1999)
J. Peterson, M. MacDonell, L. Haroun, F. Monette, R.D. Hildebrand, A. Taboas, Radiological and chemical fact sheets to support health risk analyses for contaminated areas, in *Argonne National Laboratory—Environmental Science Division in collaboration with U.S.* Department of Energy, March 2007—http://www.ead.anl.gov/pub/doc/ANL_ContaminantFactSheets_All_070418.pdf
I. Pointeau, N. Coreau, D., Hainos and P. Reiller, Effet des produits de dégradation de composés organiques présents dans les déchets B, vis-à-vis du comportement chimique des RN dans les milieux cimentaires. Rapport final, RT DPC-SECR 05-061 indice A (2006b)

M.A. Pouchon, E. Curti, C. Degueldre, L. Tobler, The influence of carbonate complexes on the solubility of zirconia: new experimental data. Prog. Nucl. Energy **3–4**, 443 (2001)

D. Rai, R.G. Strickert, D.A. Moore, J.L. Ryan, Am(III) hydrolysis constants and solubility of Am(III) hydroxide. Radiochim. Acta **33**, 201–206 (1983)

T.Y. Reich, S. Amayri, J. Drebert, J., N.L. Banik, R.A. Buda, J.V. Kratz, N. Trautmann, Application of XAFS spectroscopy to actinide environmental science. In *13th International Conference on X-Ray absorption Fine Structure* (XAFS13), pp. 179–183 (2007)

E. Revertégat, C. Richet, F. Adenot, Synthèse des études concernant la dégradation des ciments: processus physiques et chimiques—Modélisation. Influence sur les transferts de matière. Perspectives, 1ère partie: dégradation en eau naturelles peu chargée en sels, Note technique CEA, NT SCS 93.103 (1993)

C. Richet, Etude de la migration des radioéléments dans les liants hydrauliques: influence du vieillissement des liants sur les mécanismes et la cinétique des transferts, thése de l'Université d'Orsay (1992)

C. Richet, C. Galle, P. Le Bescop, H. Peycelon, S. Bejaoui, I. Tovena, I. Pointeau, V. L'Hostis and P. Lovera, Synthèse des connaissances sur le comportement à long terme des bétons applications aux colis cimentés, Rapport CEA-R-6050 (2004)

J. Rose, A. Bénard, S. El. Mrabet, A. Masion, I. Moulin, V. Briois, L. Oliv, J.-Y. Bottero, Evolution of iron speciation during hydration of C4AF. Waste Manage. **26**, 720–724 (2006)

M. Scheidegger, D.L. Sparks, A critical assessment of sorption-desorption mechanisms at the soil mineral/water interface. Soil Sci. **161**, 813–831 (1996)

M. Scheidegger, M. Vespa, D. Grolimund, E. Wieland, M. Harfouche, I. Bonhoure, R. Dahn, The use of (micro)-X-ray absorption spectroscopy in cement research. Waste Manage. **26**, 699–705 (2006)

H.M. Selim, M.C. Amacher, *Reactivity and Transport of Heavy Metals in Soils* (Lewis Publishers, New York, 1997)

Serco, *Record of Expert Panel Meetings for Category a Waste Disposal*. Report to ONDRAF/NIRAS (2008)

S.M. Sharland, P.W. Tasker, C.J. Tweed, The coupling of chemical and transport processes in near field modelling. MRS Symposium Proceedings (Boston), vol. 84 (MRS, Pittsburg, PA, 1987), p. 683

S. Sharmasarkar, K.J. Reddy, G.F. Vance, Preliminary quantification of metal selenite solubility in aqueous solutions. Chem. Geol. **132**, 165–170 (1996)

N.R. Smart et al., The anaerobic corrosion of carbon and stainless steel in simulated cementitious repository environments: a summary review of Nirex research, AEAT/ERRA-0313 (2004)

Soil Science Society of America, *Glossary of Soil Science Terms* (Madison, WI, 1996)

V.I. Spitsyn, I.A. Savich, The solubility of calcium molybdate. J. Gen. Chem. **22**, 1323–1325 (1952)

K. Stenström, A. Magnusson, Methods for measuring 14C on spent ion exchange resins—a review. In *Proceedings of a Workshop on the Release and Transport of C-14 in a Repository Environment* (NAGRA Nagra Internal Report, Nagra, Wettingen, Switzerland, 2004), pp. 25–41

S.W. Swanton, B.J. Myatt, The behaviour of technetium in the far field—a report produced for United Kingdom Nirex Limited, SA/ENV-0598 (2004)

P. Tarapcik, B. Fourest, E. Giffaut, Comparative approach of the solubility of protactinium oxy/hydroxides. Radiochim. Acta **93**, 27–33 (2007)

H.P. Thomason, S.J. Williams, Near-field solubility studies, Harwell Laboratory UKAEA, Nirex report NSS/R128, UKAEA report AEA-DandR-0068 (1992)

B. Torstenfelt, Reducering av 14C-utsläpp fran karnkraftverk. SSI-P 877.95 (1996)

Trubert, C. Le Naour and C. Jaussaud, Hydrolysis of Protactinium(V). I. Equilibrium constants at 25 °C: a solvent extraction study with TTA in the aqueous system Pa(V)/H2O/H+/Na+/ClO4-. J. Sol. Chem. **32**, 489–504 (2002)

D. Trubert, C. Le Naour, C. Jaussaud, O. Mrad, Hydrolysis of protactinium(V). III determination of standard thermodynamic data. J. Sol. Chem., 32: 505–517, 2003

N. Vance, J.E. Cline, D.E. Robertson, Characterization of Carbon-14 generated by the nuclear power industry. EPRI TR-105715, EPRI, Palo Alto (1995)

Van Cotthem, Demonstration of the supercontainer design for spent fuel waste disposal, Stage 2—Concrete characterization—Adaptation and large scale tests, Belgatom Report, to be published

L.R. Van Loon, M.A. Glaus, Experimental and theoretical studies on alkaline degradation of cellulose and its impact on the sorption of radionuclides (PSI bericht nr. 98–07, Paul Scherrer Institue, Villigen, Switzerland, 1998)

R. Van Loon, M.A. Glaus, Review of the kinetics of alkaline degradation of cellulose in view of its relevance for safety assessment of radioactive waste repositories. J. Environ. Polym. Degrad. **5**(2), 97–109 (1997)

R. Van Loon, W. Hummel, The degradation of strong basic anion exchange resins and mixed-bed ion-exchange resins: effect of degradation products on radionuclide speciation. Nucl. Technol. **128**, 388–401 (1999)

K. Vercammen, *Complexation of Calcium, Thorium and Europium by a-Isosaccharinic Acid under Alkaline Conditions*, Ph.D. thesis (Swiss Federal Institute of Technology Zurich, 2000)

S. Vines, S. Norris, A. Harris, Application of a new gas generation model to develop the source-term of Carbon-14 bearing gases in radioactive waste disposal. In *Proceedings of a workshop on the release and transport of C-14 in a repository environment* (NAGRA Nagra Internal Report, Nagra, Wettingen, Switzerland, 2004), pp. 121–129

T. Vieno, H. Nordman, *Safety Analysis of the VLJ Repository (in Finnish)* (Nuclear Waste Commission of Finnish Power Companies rep. YJT-91–11, Helsinki, Finland, 1991)

P.C. Wailes, H. Weigold, Preparation of low oxidation state cyclopentadienyl complexes of titanium and zirconium I. Compounds of zirconium. J. Organomet. Chem. **28**(1), 91–95 (1971)

L. Wang, Near-field chemistry of a HLW/SF repository in boom clay—scoping calculations relevant to the supercontainer design. External report of the Belgian Nuclear Research Centre. Mol, Belgium, SCK-CEN-ER-17 (2006)

P. Warwick, N. Evans, T. Hall, S. Vines, Complexation of Ni(II) by α-isosaccharinic acid and gluconic acid from pH 7 to pH 13. Radiochim. Acta **91**, 233–240 (2003)

P. Wersin, L.H. Johnson, B. Schwyn, U. Berner, E. Curti, *Redox Conditions in the Near Field of a Repository for SF/HLW and ILW in Opalinus Clay* (Nagra Technical Report 02–13, March 2003)

S.M. Wickham, M.B. Crawford, D.G. Bennett, *Belgian Supercontainer Design for HLW and Spent Fuel Disposal, Evaluation of the Reference Design.* Galson Sciences report 0460-5 Version 1.0 (June 2005), 2005

T.J. Wolery, EQ3/EQ6 a software package for geochemical modelling of aqueous systems, package overview and installation guide (version 7.0). Lawrence Livermore National Laboratory Report UCRL-MA-110662. Data from the thermodynamic database Thermo.dat. datafile 0.3245R46 (1992)

A.N. Zelikman, T.E. Prosenkova, Solubility of molybdates of calcium, copper, zinc, iron, and lead in water and dilute ammoniacal solutions. Russ. J. Inorg. Chem. **6**, 212–215 (1961)

A.P. Zhidikova, I.L. Khodakovskii, Powellite activity product at 25 °C, Geokhimia 427–432 (1971)

P. Zuloaga, M. Ordonez, Concrete characterization programme, Disposal facility of C.A. El Cabril (LILW), (presentation to ONDRAF/NIRAS visitors) (2007)